Advancing Understanding of the Bacteriophage Lambda T4RII Exclusion (REX) Phenotype

by

Hibah Yaseen Alattas

A thesis
presented to the University of Waterloo
in fulfillment of the
thesis requirement for the degree of
Doctor of Philosophy
in
Pharmacy

Waterloo, Ontario, Canada, 2025

© Hibah Yaseen Alattas 2025

Examining Committee Membership

The following served on the Examining Committee for this thesis. The decision of the Examining Committee is by majority vote.

External Examiner	DR. SUSAN GOTTESMAN Chief, Laboratory of Molecular Biology, Center for Cancer Research, NCI, and NIH Distinguished Investigator
Supervisor	DR. RODERICK SLAVCEV Associate Professor School of Pharmacy University of Waterloo
Internal Member	DR. SHAWN WETTIG Professor School of Pharmacy University of Waterloo
Internal Member	DR. MARC AUCOIN Professor Department of Chemical Engineering University of Waterloo
Internal-external Member	DR. TREVOR CHARLES Professor Department of Biology University of Waterloo

Author's Declaration

This thesis consists of material all of which I authored or co-authored: see Statement of Contributions included in the thesis. This is a true copy of the thesis, including any required final revisions, as accepted by my examiners.

I understand that my thesis may be made electronically available to the public.

Statement of Contributions

The work described in this thesis was carried out solely by Hibah Alattas under the supervision of Dr. Roderick Slavcev, with the following clarifications:

- Portions of this thesis are from publications based on work both presented here and from my Master's thesis. The content has been adopted with permission from the respective publishers. Documentation of copyright permissions is included in the Letters of Copyright Permissions section. These publications include contributions from co-authors Dr. Shirley Wong and Dr. Roderick Slavcev (supervision); Dr. Shirley Wong contributed to drafting the manuscripts and designing the figures and graphs in both of the following publications:
    1. Alattas, H., Wong, S., & Slavcev, R. (2020). Identification of *Escherichia coli* Host Genes That Influence the Bacteriophage Lambda (λ) T4*rII* Exclusion (Rex) Phenotype. *Genetics*, *216*(4), 1087–1102. https://doi.org/10.1534/genetics.120.303643
    2. Wong, S., Alattas, H. & Slavcev, R. (2021). A Snapshot of the λ T4*rII* Exclusion (Rex) Phenotype in *Escherichia coli*. *Curr Genet* **67**, 739–745. https://doi.org/10.1007/s00294-021-01183-2
    3. Alattas, H. (2015). Isolation and Characterization of Host Mutations that Suppress the Bacteriophage Lambda (λ) Rex Phenotype (master's thesis). Retrieved from UWSpace: http://hdl.handle.net/10012/9638

Abstract

The Bacteriophage Lambda (λ) T4**r***II* **ex**clusion (Rex) system is a finely tuned antiviral defense mechanism in *Escherichia coli* (*E. coli*) lysogens that prevents the propagation of T4*rII* mutant bacteriophage. This exclusion phenotype is defined as the inability of T4*rII* mutant bacteriophage to propagate within λ-lysogenized *E. coli* cells. This phenomenon is encoded by two genes of λ (*rexA and rexB*), whose expression is primarily regulated and driven by the λ P_M promoter under the regulation of the λ *cI* repressor gene. The T4*rII* infection of Rex^+ lysogen triggers the onset of the Rex phenotype. It is characterized by a harsh cascade of cellular responses, including rapid membrane depolarization and the induction of a stress environment that mimics the physiology of the stationary phase. In addition, the disruption of the RexA:RexB balance, particularly the overexpression of *rexA* relative to *rexB*, can lead to the same manifestations without infection, indicating that the stoichiometry of RexA:RexB is relevant. Rex "activation" results in significant cell death and has been proposed to serve as an altruistic cell death system to protect the species. In contrast, despite some cell killing, infected lysogens do, to an extent, recover from Rex activation. As such, the phenotype may additionally serve as a mutualistic mechanism that protects both the λ prophage and its stability, as well as its host, by limiting superinfection. For a long time, researchers have hypothesized that *E. coli* host proteins are involved in this pleiotropic phenotype and identifying them has been a key goal in elucidating the Rex mechanism.

Notably, Rex activation depends not only on gene expression and the stoichiometry of RexA to RexB but also on an optimal monovalent cationic environment, underscoring the importance of membrane ion channels and transport systems. Identifying all host mutations that attenuate or abrogate Rex will help in understanding the role of individual components, directly or indirectly, in triggering and

inducing the cellular (physiological) manifestations of the Rex phenotype. While many *E. coli* membrane proteins control the passage of solutes and ions through the membranes, mutations in these proteins may disrupt the ionic environment, thereby resulting in the attenuation or abrogation of Rex. This finding was observed and confirmed by the deletion of several outer membrane proteins, including *ompW*, *ompX, ompA*, and *ompF* (Alattas et al., 2020). Beyond these membrane-associated proteins, the ability of additional genetic and regulatory components to modulate and influence Rex and Rex escape to varying degrees was demonstrated, including *tolA, mglC,* and *rpoS* (σ^S). Several of the identified genes play a critical role in cellular osmotic balance and are governed by the stationary phase sigma factor (σ^S) or envelope stress sigma factor (σ^E) as part of the stationary phase and/or envelope distress regulons, under the control of many non-coding regulatory small RNAs. The impact of mutations in these regulatory proteins on Rex activity was examined following superinfection by T4 and T4*rII*, and the role of the σ^S regulatory proteins, including RssB and IraD, in the Rex and Rex escape mechanisms was reported for the first time. However, the mechanism by which this occurs remains unclear.

The impact of fluorescence fusions on colony morphology and texture was investigated, showing variations in colony size among fusion sites and Rex types. These experiments suggested that the fusion site and the expression status of the partner significantly affect Rex activity**,** likely by interfering with proper protein folding, complex formation, or the stoichiometric balance of RexA to RexB. N-terminal fusions severely attenuated Rex activity, while dual N-terminal tagging almost entirely abolished it. In contrast, C-terminal fusions only partially affected Rex activity, with dual C-terminal fusions showing minimal impact on exclusion capability.

Together, these findings highlight the Rex system as a multifactorial, tightly regulated antiviral mechanism that integrates gene stoichiometry, membrane composition, sigma factor regulation and its RNA-mediated control. This work adopts a genetic approach to enhance and refine the existing model of Rex-mediated T4*rII* exclusion, leading to a new model of Rex that offers new insights into its

underlying molecular determinants and paves the way for further exploration of bacteriophage-host dynamics, superinfection exclusion strategies, and programmed cell death in prokaryotes.

Acknowledgements

My sincerest gratitude goes to Allah Almighty for granting me the strength, patience, and perseverance to complete this journey. His mercy and guidance have been my light through every challenge, and I am forever indebted to His grace.

My deepest gratitude goes to our beloved Prophet, my grandfather, Mohammad (PBUH), whose teachings and example continue to guide me in all aspects of life. His legacy inspires me to strive for excellence with humility and compassion.

I would like to express my heartfelt appreciation to my supervisor, Dr. Roderick Slavcev, for his ongoing support, mentorship, and faith in my potential. His guidance has been a cornerstone of my academic growth, and I am genuinely grateful for the opportunity to work under his supervision.

Special thanks to my advisory committee members, Dr. Shawn Wettig and Dr. Trevor Charles, for their valuable insights, thoughtful feedback, and encouragement throughout my research. Their expertise has significantly contributed to shaping this thesis in meaningful ways.

I am also deeply thankful to my examiners, Dr. Marc Aucoin and Dr. Susan Gottesman, for their time, careful review, and constructive critique. Their thoughtful questions and suggestions have contributed significantly to the refinement of this work. I would like to extend my sincere thanks to Dr. Monica Tudorancea for her invaluable assistance with the School of Pharmacy Core Research Facility equipment. I am also grateful to Dr. Emmanuel Ho and Dr. Michael Beazely for their generosity in sharing their laboratory instruments, which greatly supported my experimental work.

To my parents, Yaseen and Mayadah, and my siblings—thank you for your unconditional love, prayers, and unwavering support. I owe every achievement to your faith in me. Your encouragement has been my strength, and your sacrifices have made this journey possible.

I extend my thanks to my extended family and dear friends, whose kindness, patience, and encouragement have helped me overcome many challenges along the way. Your presence in my life has been a source of comfort and joy.

I am deeply thankful to Taibah University and the Saudi Cultural Bureau in Canada for their generous financial support throughout my graduate studies. Their commitment to education and research has empowered me to pursue this academic journey with confidence, purpose, and pride. The work presented in this thesis was also made possible through the support of the Natural Sciences and Engineering Research Council of Canada, the Ontario Graduate Scholarship program, and the School of Pharmacy at the University of Waterloo, whose contributions have been instrumental in bringing this research to life.

Finally, I am grateful to all the colleagues, lab mates, and collaborators who have shared this journey with me. Your support, friendship, and scientific insight have made this experience both enriching and memorable.

Dedication

To Allah Almighty, the source of all strength, wisdom, and mercy—this work is a reflection of the blessings You have bestowed upon me.

To our beloved Prophet, my grandfather, Mohammad (PBUH), whose teachings continue to guide my heart and actions.

To my parents, Yaseen and Mayadah, whose love, prayers, and sacrifices have carried me through every step of this journey.

And to everyone who believed in me when I needed it most—this thesis is for you.

Table of Contents

Author's Declaration iii
Statement of Contributions iv
Abstract v
Acknowledgements viii
Dedication x
List of Figures xv
List of Tables xviii
List of Abbreviations, Definitions and Genetic Usage xix
Chapter 1 Introduction 1
1.1 Introduction to the Lambda T4*rII* Exclusion (Rex) Phenotype 1
1.1.1 The Foundation and Characterization of the Rex Phenotype 1
1.1.2 The Bacteriophage Lambda *rex* Genes and Immunity Regulator 3
1.1.3 The Physiological Manifestations of the Rex Activation 12
1.2. The *rII* Genes of Lytic Bacteriophage T4 43
1.2.1. Bacteriophage T4 and the *rII* Genes 43
1.2.2. Types of the Rapid Lysis "*r*" Mutations 46
1.2.3. The *motA* Gene of Bacteriophage T4 49
Chapter 2 Project Hypothesis and Objectives 52
2.1 The Current Model and Rationale 52
2.2 Hypothesis 56
2.3 Objectives 57
Chapter 3 Materials and Methods 59
3.1 Strains and Plasmids 59
3.2 Plasmid Maps 66
3.3 Phage Lysate Preparation and Purification 70
3.4 Plate Overlay Phage Titration and Efficiency of Plating (EOP) Assay 71
3.5 Assessing Rex and T4*rII* Activity 72

3.6 *E. coli* K-12 Host Transformation 72
3.7 Calcium Chloride Heat Shock Transformation 73
3.8 Polymerase Chain Reaction Assay (PCR) 73
3.8.1 Colony PCR 73
3.8.2 Preparation of Knock-Out Gene PCR Products 74
3.8.3 Inverse PCR and Mutant Identification 75
3.9 Plasmid Extractions, Digestions and Purifications for Ligation 77
3.9.1 Plasmid Extraction and Purification 77
3.9.2 Plasmid Digestion and DNA Purification 77
3.9.3 DNA Extraction and Purification 78
3.9.4 DNA Ligation 78
3.9.5 DNA Cloning 78
3.10 Cell Viability Assay 81
3.11 Infective Center Assay 81
3.12 Assessing the Effect of Deletion Mutations on Rex Activity 82
3.13 Phage λ (*rex*$^+$) Lysogenization of *E. coli* Cells 83
3.14 Lambda Immunity Assay 83
3.15 Plasmid Curing 84
3.16 GFP Tag Plasmid Preparation and Imaging 84
Chapter 4 Results 86
4.1 Identification of Host Genes Involved in the Rex$^-$ Phenotype 86
4.1.1 Confirmation of Mutants as Phenotypically Rex$^-$ and Genotypically *rex*$^+$ 86
4.1.2 Plasmid Curing and Rex$^-$ Mutants 89
4.1.3 Inverse PCR and Identification of Rex$^-$ Mutant 89
4.2 Screening for Susceptible Host Proteins Influences Rex/ RII Activity 93
4.2.1 Assessing the effect of glucose transporter membrane proteins on Rex activity 94
4.2.2 Assessing the effect of Sigma factors and other membrane proteins on Rex activity 97
4.2.3 Assessing the Effect of Stationary Phase Regulators on Rex Activity 101

4.2.4 T4*rII* Infective Center Assay for Host Genes Activity with Natural *rex* Gene Dosage 104
4.2.5 Complementation of Identified Host Genes Influencing the Rex Phenotype 106
4.3 Developing a Rex Protein Visualization System Using GFP Fusions 110
Chapter 5 Discussion 144
5.1 Identification of the Interrupted Genes Responsible for the Rex⁻ Phenotype 144
5.1.1 Inverse PCR and Identification of Rex⁻ Mutant: 146
5.2 Screening for Susceptible Host Proteins Involved in Rex/ RII Activity 148
5.2.1 Assessing Rex Activity in Mutants of Glucose Transporter Membrane Proteins Suspected to be Involved in T4*rII* Exclusion 152
5.2.2 Assessing Rex Activity of Other Membrane Proteins that May Influence Rex Activity 153
5.2.3 Assessing the Effect of Sigma Factors and Their Regulatory Elements Mutations on Rex Activity 157
5.2.4 Complementation of Deletion Mutants Restores the Rex Phenotype 160
5.3 Development of a Visualization System of Rex Proteins Using Fluorescent Tagging 163
5.4 A proposed Model for Rex and RII Suppression of Rex 175
T4 infection activates host stress responses: 177
Rex onset increases *tol* and *rpoE* expression but reduces *rpoS* expression: 178
Rex manifestation is a stationary-like phase: 179
RII attenuates Rex exclusion: 180
Chapter 6 182
Conclusion and Future Directions 182
6.1 Conclusion 182
6.2 Future Directions 184
Letters of Copyright Permission 193
References 199
Appendix A 230
Solutions and Buffers 230

Appendix B 236
Supplementary DNA data 236
Appendix C 237
Plasmid Maps of GFP-Rex Constructs 237
Appendix D 255
Tap Tagging and Rex proteins 255

List of Figures

Figure 1-1. Lambda T4*rII* Exclusion Phenotype. 1

Figure 1-2. Replication Cycles of Bacteriophage λ.. 4

Figure 1-3. Immunity Region of Phage λ and Maintenance of Lysogeny. 5

Figure 1-4. Portion of the Immunity Region from Phage λ. 6

Figure 1-5. Morphological Changes in Rex$^+$ *E. coli* Following T4*rII* Phage Infection. 14

Figure 1-6. RexA/RexB Activation Model in Response to T4*rII* Infection.. 16

Figure 1-7. The σ^E Signalling Pathway and Its Activation Mechanism.. 22

Figure 1-8. Stabilization, Activation, and Degradation of σ^S in *E. coli.*. 25

Figure 1-9. Components of the *E. coli* Cell Envelope. 27

Figure 1-10. The Tol-Pal Complex System in the *E. coli* Cell Envelope.. 33

Figure 1-11. Proteins and Regulatory Components of the *E. coli* D-Galactose Transport System. 38

Figure 1-12. Plaque Morphology of Wild-Type T4 and T4*rII* Mutants on *E. coli* B and K-12 λ Lysogens Demonstrating the Rex Exclusion Phenotype.. 45

Figure 2-1. Proposed Model of Rex System Activation Involving Outer Membrane Proteins.. 55

Figure 3-1. Plasmid pHA1 Map.. 66

Figure 3-2. The pHA2 pRex Suicide Construct for Rex Operon Chromosomal Integration.. 67

Figure 3-3. pPL451 Vector Map for Conditional Expression of *rex::egfp* Cassettes. 68

Figure 3-4. Plasmid Map of pUC19 Used in Complementation Assays. 69

Figure 3-5. Plasmid Map of pBR322 Used in Complementation Assays. 70

Figure 3-6. PCR Mapping of Tn*10* Insertions in the *E. coli* Chromosome Using Four Designed Primers. 76

Figure 3-7. Step One in Construct Generation for Complementation Assay. 79

Figure 3-8. Step Two in Construct Generation for Complementation Assay. 80

Figure 4-1. Agarose Gel Electrophoresis of Rex$^-$ Isolate Plasmids. 88

Figure 4-2. PCR Amplification of Target DNA Fragments. 91

Figure 4-3. Snapshot of BLAST Results. 92

Figure 4-4. Influence of *mgl* and *gal* gene Deletions on Rex Activity. 96

Figure 4-5. Deletions of *tolA* and Other Membrane Proteins Influence Rex Activity.. 99

Figure 4-6. Interaction of Regulatory sRNAs and Sigma Factors with Rex Activity.. 103

Figure 4-7. Agarose Gel Electrophoresis of the *ompF* Fragment Digested with Restriction Enzymes. 107

Figure 4-8. Colony Morphology of *E. coli* BW25113 [pPL451-*rex*] Lysogens at 30 °C.. ... 124

Figure 4-9. Colony Morphology of *E. coli* BW25113 [pPL451-*rex*] lysogens at 37 °C.. 127

Figure 4-10. Colony Morphology Consistency of *E. coli* BW25113 [pPL451-*rex*] lysogens at 37 °C. 130

Figure 4-11. Fluorescence Microscopy of *E. coli* BW25113 lysogen harbouring [pPL451 *rex::egfp*] plasmids (single expression). 135

Figure 4-12. Fluorescence Microscopy of *E. coli* BW25113 lysogens harbouring [pPL451 *rex::egfp*] plasmids (Dual expression).. 139

Figure 5-1. Role of Outer Membrane Proteins in Modulating Rex Activity.. 149

Figure 5-2. Rex Activity Assay.. 162

Figure 5-3. Model of T4 and T4*rII* Infection in a *rex*$^+$ *E. coli* Cell (The Rex Mechanism). 177

Figure C-1. Plasmid Maps of eGFP::RexA Constructs with and without Linker. 238

Figure C-2. Plasmid Maps of eGFP::RexB Constructs with and without Linker. 239

Figure C-3. Plasmid Maps of eGFP::RexA-RexB Constructs with and without Linker.. 240

Figure C-4. Plasmid Maps of RexA-eGFP::RexB Constructs with and without Linker. 241

Figure C-5. Plasmid Maps of Dual-Tagged Rex Constructs: eGFP::RexA-RFP::RexB and eGFP::RexA-RexB::RFP. 242

Figure C-6. Plasmid Maps of Dual-Tagged Rex Constructs: eGFP::RexA-RFP::RexB and eGFP::RexA-RexB::RFP with linker. 243

Figure C-7. Plasmid Maps of RexA::eGFP Constructs with and without Linker. 245

Figure C-8. Plasmid Maps of RexB::eGFP Constructs with and without Linker. 246

Figure C-9. Plasmid Maps of RexA::eGFP-RexB Constructs with and without Linker. 247

Figure C-10. Plasmid Maps of RexA-RexB::eGFP Constructs with and without Linker. ... 248

Figure C-11. Plasmid Maps of Dual-Tagged Rex Constructs with and without linker: RexA::eGFP-RexB::RFP..... 249

Figure D-1. Plasmid Map Featuring C- terminal TAP Tagging Cassette..... 255

Figure D-2. Plasmid Maps of Rex Constructs with C-terminal TAP Tags. 256

Figure D-3. Overview of the Two-Step Tandem Affinity Purification (TAP) Process.. 257

Figure D-4. Plasmid Maps of TAP-Tagged Rex Constructs using the pPL451 Expression Vector. 259

List of Tables

Table 3-1: Bacterial strains, phage, plasmids, and primers used in this study 59

Table 4-1. Isolated integrant mutants attenuated for Rex activity. 87

Table 4-2. The effect of the membrane galactose transporter on Rex Activity. 94

Table 4-3. The impact of the membrane protein deletions on Rex activity. 97

Table 4-4. The stationary phase sRNAs and regulators are required for Rex activity and superinfection exclusion. 102

Table 4-5. Influence of Stress-response regulators on Rex-mediated T4*rII* exclusion 105

Table 4-6. Rex activity after plasmid complementation of host mutations. 108

Table 4-7. The fusion site of GFP significantly affects the activity of RexA and RexB across various incubation temperatures. 112

Table 4-8. Assessing the Relative Transformation Efficiency of GFP-*rex* Combination Constructs at Various Temperatures. 118

Table 4-9. Summary of fluorescent cell counts and expression rates in λ lysogen *E. coli* BW25113 harbouring *rex::egfp* constructs. 142

Table A-1. Solutions and Buffers 230

List of Abbreviations, Definitions and Genetic Usage

Bacteriophage	A virus that infects and replicates specifically within bacterial cells; also called phage
Gene	A DNA sequence encoding a functional product (protein or RNA). Written in italics, lowercase (e.g., *rexA*)
Lysogen	A bacterial cell containing an integrated prophage within its genome, in a dormant state
Protein	The expressed functional product of a gene; typically, a polypeptide performing biological roles and written capitalized and non-italic (e.g., RexA)
Prophage	Latent form of a bacteriophage genome integrated into the bacterial chromosome or maintained episomally
λ	Bacteriophage lambda
λimmF	λ immunity region forward sequence primer
λimmR	λ immunity region reverse sequence primer
λF7	*λDam15imm21cIts* derivative with defective (suppressible) *D* gene and the immunity region (*imm*) of phage 21
λCI857	λCI[Ts]857; temperature-inducible a prophage; higher temperatures are indicated by a reduction in repressor activity and expression of the downstream *rex* genes
λ*cI*[Ts]*rex*$^+$	λ*cI*857; temperature-sensitive repressor encoding *cI*[Ts]-*rexA*-*rexB* genes
σ^E	Subunit of RNA holoenzyme encoded by *rpo*E gene; activated in response to stressful environments such as hyperosmotic shock, metal ion exposure, and changes in outer membrane lipopolysaccharide structure, governs transcriptional activation of many downstream genes including the periplasmic folding proteins and degrading factors

σ^S	Subunit of RNA holoenzyme encoded by *rpoS* gene; a 37.8 kD protein. *rpoS* is transcribed in late exponential phase, and RpoS is the primary regulator of stationary phase genes. RpoS is a central regulator of the general stress response and operates in both a retroactive and a proactive manner: it not only allows the cell to survive environmental challenges, but it also prepares the cell for subsequent stresses
a.a.	Amino acid; organic molecules that serve as the building blocks of proteins
ABC transporter	ATP-binding cassette transporters; a large family of proteins that use ATP hydrolysis to transport various substrates across cellular membranes
Ap^R	Ampicillin antibiotic resistance marker (β-lactamase); cells grow in the presence of ampicillin antibiotic
Ap^S	Ampicillin-sensitive phenotype; cells cannot grow in the presence of ampicillin antibiotic
asRNA	Antisense RNA; single-stranded RNA complementary to messenger RNA (mRNA), inhibits translation, or promotes degradation
ATP	Adenosine triphosphate; primary energy carrier in cells
bp	Base pair; unit of DNA length
C-terminal	End of a protein or polypeptide chain with a free carboxyl group (-COOH); last part synthesized during translation
cAMP	Cyclic AMP; second messenger derived from ATP in many biological processes. It is involved in transmitting signal transduction
cfu	Colony forming unit; number of viable cells per unit volume
CI	λ repressor protein, allows phage to reside in a lysogenic state
cI	λ gene encoding CI repressor
CII	λ transcriptional activator; stimulates of high-level transcription from λ P_E promoter
Cro	λ repressor protein binding O_R and O_L operator sequences; inhibits CI stimulation of P_M transcription

clpP	Hsp100 protease subunit requiring ClpX or ClpA for substrate recognition
ClpXP	ATP-dependent protease complex consists of two components, ClpX, an ATPase that belongs to the AAA+ (ATPases Associated with diverse cellular Activities); and ClpP, the proteolytic subunit that degrades the misfolded proteins
cro	λ gene encoding Cro protein; binds to O_R and O_L operator sequences and inhibits CI stimulation of P_M transcription
Da	Dalton; atomic mass unit
DNA	Deoxyribonucleic acid; genetic material of most organisms
dsRed	Red fluorescent protein derived from *Discosoma coral*
DegS	*E. coli* protease activating stress response σ^E during envelope stress
E	T4 endolysin protein encoded by the *e* gene of T4; degrades peptidoglycan to lyse the host cell
EnvZ	Sensor histidine kinase in the EnvZ/OmpR two-component regulatory system in *E. coli*.; regulates porin expression (OmpF and OmpC) in response to osmolarity.
EOP	Efficiency of plating; relative viability of phage sample in comparison to a positive control
ExbBD	Inner membrane proteins in TonB-dependant energy transduction system to transport energy into the bacterial cell in nutrient limitation
F^+ plasmids	Conjugative plasmid enabling DNA transfer in *E. coli*.; also called fertility or F factor.
FepA	Outer membrane protein Ferric enterobactin transporter; TonB-ExbBD dependent
FhuA	Outer membrane proteins Ferrichrome transporter; TonB-ExbBD dependent
galE	Epimerase in *gal* operon; responsible for the metabolism of D-galactose

galK	Galactokinase in *gal* operon; responsible for the metabolism of D-galactose
galR	*galR* gene encoding the Gal repressor protein (GalR); regulates the *gal* operon
galS	Gene encoding the GalS repressor protein; similar to GalR
galT	Galactose transferase in *gal* operon
Gene l	Bacteriophage T5 gene; mutants sensitive to Rex-mediated exclusion
Gene 20	T7 gene; mutants in gene *20* cannot grow on rex^+ λ lysogens; Gene *20* works as *rII* genes of T4 to grow on λ lysogen
GFP/eGFP	Green fluorescent protein / enhanced green fluorescent protein
gpE	λ gene product E; major structural protein in the λ phage capsid head
gp5	T4 phage late sigma factor; this enzyme (glycoside hydrolases) degrades the periplasmic peptidoglycan layer of host cell, leads to broken host cell wall within 5 min of infection. Has a homology with sigma S and sigma E factors of *E. coli*
h	Hour unit
Hfq	Protein encoded by the *hfq* gene that mediates or helps with sRNA-based regulation (chaperone for sRNAs). May act as a repressor of mRNA translation
λimm	Immunity region of bacteriophage P_M-*cI*-*rexA*-*rexB*-t_{imm}
IGRs	Intergenic Regions; non-coding DNA sequences between genes on the genome. While they don't code for proteins, they play several important regulatory and structural roles
IraD	Anti-adaptor protein binds to RssB; stabilizing RpoS by inhibiting RssB-mediated degradation by the ClpXP protease
IraM	Anti-adaptor protein binds to RssB; IraM stabilizes RpoS**,** allowing it to accumulate and activate the transcription of stress response genes

IraP	Anti-adaptor protein binds to RssB; IraP prevents RpoS degradation, thereby stabilizing RpoS levels during stress conditions
IPTG	Isopropyl β-D-1-thiogalactopyranoside; inducer of *lac* operon
IS10	Insertion sequence element in Tn*10* transposon
IU	International unit
K	Kilo unit; 1000 times
Km^R	Kanamycin antibiotic resistance marker. Cells are not inhibited by the presence of kanamycin antibiotic
Km^S	Kanamycin-sensitive phenotype; cells cannot grow in the presence of kanamycin antibiotic
Lac	*E. coli* operon comprised of l*ac*Z-Y-A genes and required for cellular metabolism of lactose
LacZ	β-galactosidase; hydrolyses lactose
LamB	Maltoporin, a type of outer membrane protein primarily found in Gram-negative bacteria like *E. coli*.
LIN	T4 lysis inhibition phenotype; phage inhibition of host lysis in response to adsorption of secondary T-even phage
Lpp	Lipoproteins, crucial components of the bacterial cell envelope, especially in Gram-positive and Gram-negative bacteria
LPS	Lipopolysaccharide
MazF	Stable toxin functioning as an mRNA endoribonuclease; cleaves mRNA at ACA sites, halting protein synthesis and leading to cell death
MazE	Labile antitoxin that binds to and neutralizes MazF under normal conditions; rapidly degraded under stress, allowing MazF to act
MCS	Multiple cloning site; a short DNA segment in plasmids containing numerous restriction sites for molecular cloning or sub-cloning procedures

MeGal permease	Methyl-Galactoside permease enzyme required for galactose and galactoside transport
***micA* (MicA RNA)**	Small RNA besides *rybB,* regulated by σ^E; downregulates *ompA*, *ompC* and *ompW*
MicF	Small non-coding RNA in *E. coli* and other Gram-negative bacteria; regulates gene expression post-transcriptionally in response to environmental stress
MglABC	β-Methyl-Galactoside Transport System; includes ATP-binding proteins (MglA), two integral transmembrane proteins (MglC), and solute-binding protein (MglB)
motA	T4 transcription modulation gene that also called *rim* gene (Rex Immunity gene); mutation in the *motA* gene reverses Rex exclusion
MOI	Multiplicity of infection; ratio of infective phage per bacterial cell
N-terminal	The end of a polypeptide with a free amino group ($-NH_2$); synthesized first during translation
mRNA	Messenger RNA; carries genetic information from DNA to ribosomes for protein synthesis
MW	Molecular weight unit (in Daltons); pure atomic weight
N	λ anti-terminator protein; binds to *nutR* and *nutL* sites to bypass transcription terminators.
NADH	Nicotinamide adenine dinucleotide (reduced form); key coenzyme in cellular energy metabolism, especially in energy production
NDH-1	NADH dehydrogenase I; multi-subunit enzyme in the aerobic respiratory chain
ncRNAs	Non-protein coding RNAs; RNA molecules not translated into proteins
O	λ replication initiator protein; O binds iteron (*int*[4]) sequences at *ori*
O/N	Overnight
Omp	Outer membrane protein in Gram-negative bacteria; regulate cellular osmolarity and nutrient uptake

OmpA	Outer membrane protein in Gram-negative bacteria; multifunctional structural protein found in the outer membrane
OmpC	Outer membrane porin protein in bacteria; upregulated in high osmolarity and facilitates passive diffusion of small hydrophilic molecules (e.g., sugars, ions)
OmpF	Outer membrane porin protein in bacteria; upregulated in low osmolarity and facilitates passive diffusion of small hydrophilic molecules (e.g., sugars, ions)
OmpR	Response regulator protein, along with the sensor kinase KnvZ, in a two-component system; controls expression of *ompF* and *ompC*
OmpW	Outer membrane protein involved in transport of small hydrophobic molecules
OmpX	Outer membrane protein involved in adhesion, biofilm formation, and host interaction
O_L	λ leftward promoter; regulates the strong promoter, P_L
O_R	λ rightward operator; regulates the strong promoter, P_R
P_E	λ establishment promoter; stimulated by CII
oop	λ functional RNA that attenuates Rex exclusion when expressed from multicopy plasmid
ori	Origin of replication
Pal	peptidoglycan-associated lipoprotein
PCR	polymerase chain reaction; amplifies DNA sequences
***phoA* fusion**	Alkaline phosphatase is encoded by the *phoA* gene in *E. coli*. The *phoA* gene has a signal-sequence allowing export of alkaline phosphatase into the periplasm where it is active; due to the highly reducing environment, alkaline phosphatase is not active in the cytoplasm
pfu	Plaque forming unit; single immobilized phage that grows to form a plaque on an agar cell lawn. A means to calculate lysate titer and EOPs
P_L	λ leftward promoter; repressed by CI binding at O_L operator

P_{Lit}	λ late immunity transcription promoter; located within the C-terminal of *rexA* and transcribes *rexB*
P_M	λ low-level maintenance promoter; stimulated by CI in a repressed prophage
P_R	λ right-ward promoter; repressed by CI binding at O_R operator
PFA	Paraformaldehyde (4%) for fixation, preserves GFP fluorescence well
PBS	Phosphate-Buffered Saline, buffer solution to wash and remove any debris from bacterial cultures before fluorescence exams and imaging. It maintains osmotic balance.
R6K	Antibiotic-resistance plasmid in *E. coli,* requires π replication protein for initiation of plasmid replication
r^+	Wild type *r* loci
RdgC	Recombination-associated DNA-binding protein C; involved in regulation of homologous recombination, DNA repair, and replication fork repair and stability.
Red	λ general recombination genes *(exo, bet)*
ren	λ Rex suppressor gene
RFP	Red fluorescent protein
Rex phenotype	Exclusion of T4*rII* mutants by λ rex^+ lysogen
rexA-rexB	λ genes conferring exclusion of T4*rII* by a λ lysogen
Rex-centric mutualism	Ability of *rex* genes to protect λ lysogens from T4*rII* infection
rho	*E. coli* mRNA helicase (hexameric); dislodges RNA polymerase from DNA and mRNA, required for efficient termination transcription at Rho-dependent sites.
RI	T4 periplasmic protein that inhibiting T holin activity; essential for establishment of lysis inhibition
rII (rIIA-rIIB)	T4 genes enabling escape from Rex exclusion by a λ lysogen

rIII	T4 gene hypothesized to stabilize lysis inhibition by influencing interactions between *rI* and *T* genes
rIV	T4 gene aiding infection by repairing membrane damage during T4 adsorption and DNA injection
r-type plaque	Rapid lysis plaque morphology; large, sharp-edged plaques from T4 *r* mutants lacking lysis inhibition
RT	Room temperature
RPM	Revolutions per minute
RNAP	RNA polymerase (RNAP); essential enzyme responsible for transcribing genetic information stored in DNA into RNA
RNA	Ribonucleic acid
RNAs (sRNAs)	Small non-coding RNA molecules that regulate gene expression in prokaryotes and eukaryotes
rpoE	RNA polymerase sigma factor (σ^E) in *E. coli*, activated in response to envelope stress (e.g., hyperosmotic shock, metal ion, and outer membrane LPS changes)
rpoS	RNA polymerase sigma factor σ^S; master regulator of general stress response and stationary phase gene expression in bacteria
RseA	Anti-sigma factor that inhibits σ^E (RpoE), the sigma factor responsible for the envelope stress response
RseP	Intramembrane site-2 protease; cleaves RseA to activate σ^E (RpoE) in *E. coli*
RssA	Putative patatin-like phospholipase in *E. coli*
RssB	Response regulator-like adaptor protein; targets RpoS (σ^S) for degradation via ClpXP protease
rybB	Small RNAs, like *micA*, regulated by σ^E, down-regulates *ompA*, *ompC* and *ompW*
rV, t	T4 holin gene; forms inner membrane lesions for endolysin egress

S	λ holin gene; accumulates in host inner membrane and enables λ endolysin egress to the periplasm
Sec/YidC	Membrane protein insertion machinery in *E. coli,* essential for inserting and folding membrane proteins into the inner membrane. The system is critical for cell viability
SraD RNA (MicA)	Small non-coding RNA; expression inhibited in stationary phase; binds Hfq protein and regulates gene expression via antisense mechanism
Tc^R	Tetracycline antibiotic resistance marker; enables growth in tetracycline-containing media
Tc^S	Tetracycline-sensitive phenotype; cells cannot grow in tetracycline-containing media
t, rV	T4 holin gene; accumulates in inner membrane an enables T4 endolysin egress to the periplasm
T4	Bacteriophage T4
T5	Bacteriophage T5
T7	Bacteriophage T7
T-even	Family of phages with similar characteristics, including T2, T4, and T6
t_{imm}	λ transcription terminator in early region; halts transcription unless overridden by N-mediated antitermination
Tn*10*	Transposon with IS10 insertion elements; confers tetracycline resistance to recipients
TN	Tris-NaCl buffer
Tol	Bacterial protein that maintains outer membrane integrity and supports cell division
TolB	periplasmic protein plays a role in bacterial outer membrane integrity and cell division

TolQRA	Inner membrane protein complex in Gram-negative bacteria and is involved in outer membrane integrity and helps with cell division
TonB	Energy transducer protein; works with ExbB and ExbD to harness proton motive force (PMF)
tRNA	Transfer RNA in *E. coli*; delivers specific amino acids to the ribosome during translation
Ts	Temperature-sensitive phenotype
tsp	Tail-specific protease; periplasmic endoprotease that recognizes hydrophobic C-terminal residues of periplasmic proteins
unc	*E. coli* genes encoding ATPase
UV	Ultraviolet light
wt	Wild type

Chapter 1

Introduction

1.1 Introduction to the Lambda T4*rII* Exclusion (Rex) Phenotype

1.1.1 The Foundation and Characterization of the Rex Phenotype

The Lambda T4***r**II* **ex**clusion phenotype, also known as the **Rex** phenotype, is defined as the ability of *rex* genes (*rexA, rexB)* of bacteriophage lambda (λ) to prevent plaque formation by the mutant lytic bacteriophage T4*rII* on *Escherichia coli* lysogenized by λ (λ lysogen) (Figure 1-1; Benzer 1955).

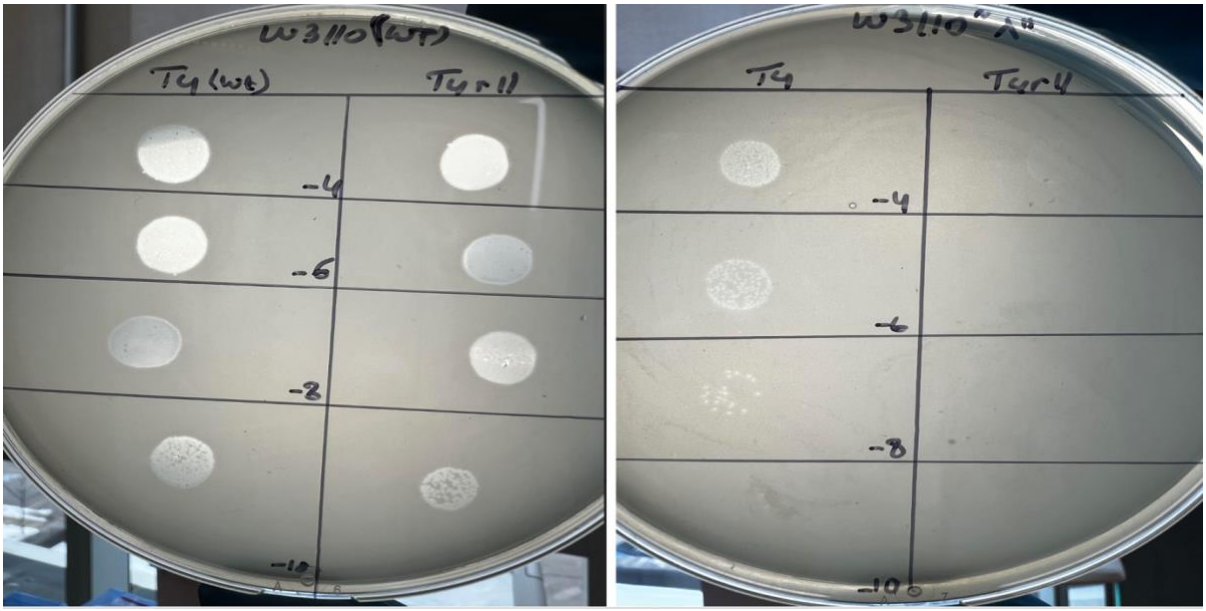


Figure 1-1. Lambda T4*rII* Exclusion Phenotype. Wild-type T4 phage can successfully infect and form plaques on both wild-type and λ lysogen lawns with nearly the same efficiency of plating (EOP~ 1), so plaques are visible even at very high dilutions of the stock (up to 10^{-10}). In contrast, the T4*rII* mutant can form plaques on wild-type *E. coli* lawns but fails to produce plaques on λ lysogen lawns, even at undiluted or at very low dilutions (e.g., 10^{-2}), reflecting strong Rex-mediated exclusion.

The Rex phenotype was discovered in the mid-twentieth century by Seymour Benzer, who noted that while the wild-type lytic T4 bacteriophage was able to replicate and generate plaques on a lawn of *E. coli* λ lysogens, the mutant T4*rII* phage, which is missing the *rII* gene, exclusively could not (Benzer 1955). Benzer successfully mapped the *rIIA* and *rIIB* genes of bacteriophage T4 by employing a genetic selection method based on plaque morphology. Mutations at the *r* loci led to a different plaque morphology (large with sharp edges) relative to the wild-type r^+ morphology (small, fuzzy edges; Benzer 1959; 1962). This selection technique played a crucial role in establishing our current understanding of the central concept of homologous recombination and in revealing the triplet nature of the genetic codon and the principles of genetic analysis (Benzer 1959, 1962). Applying this unique exclusion phenotype system, thousands of T4*rII* mutants (both point mutation and deletion) were isolated and mapped by complementation and recombination experiments that examined the frequency of rII^+ recombinant formation. While the Rex system has sufficiently demonstrated its ability to exclude *rII* mutants with a genetic reversion frequency of $\leq 10^{-8}$, some of the isolated *rII* mutants were able to form very small plaques (r^+ like morphology) on *E. coli* lysogens. Benzer proposed that these "leaky" mutants retained some residual RII function, enabling them to behave like wild-type bacteriophage T4rII^+ (Benzer 1959; 1962). As infection of λ lysogens by the T4*rII* mutant was associated with a significant level of cell death, Benzer concluded his observations by proposing the Rex system as a cell-killing mechanism (Benzer 1959; 1962).

Parma et al. (1992), aligning with Benzer's original discoveries, proposed the Rex system as a mechanism for altruistic cell death. They theorized that Rex-mediated death would be "triggered" upon superinfection of the lysogenic host by a Rex-sensitive phage like T4*rII*. A "superinfecting" phage refers to a second phage infecting a bacterium already carrying a prophage. In this model, Rex serves as a defense mechanism for the population, guiding the prophage to eliminate its host. This suggests that the λ prophage prefers self-destruction over allowing a competing phage to thrive within its infected host population. In essence,

triggering Rex leads to the death of the prophage, superinfecting phage, and the infected bacterial host (Maclean et al.,1974). This Rex-mediated death/altruistic cell death model proposed by Parma et al. (1992) provided the sole mechanistic and phenomenological explanation model for the Rex system mechanism up until later refinements.

Slavcev et al. (2001; 2003) later proposed another possible mechanism of Rex, based on the observed physiological manifestations associated with Rex activation on the host cell. This model suggested that the Rex system shunts cells into a stationary phase-like state. This cellular environment is harsh but reversible. It is associated with some cell death; however, it crucially prevents the spread of the superinfecting phage.

1.1.2 The Bacteriophage Lambda *rex* Genes and Immunity Regulator

Lambda bacteriophage, also known as Enterobacteria phage λ, has a double-stranded DNA genome that is approximately 48,502 base pairs long and specifically infects the *E. coli* bacterium (Lederberg and Lederberg 1953; Casjens and Hendrix 2015). Upon infection, lambda can undergo either lytic or lysogenic life cycles, and the decision to choose one pathway over the other depends on the environmental conditions and the physiological status of the host cell (Hoess et al., 1980; Van Duyne and Landy 2024). In the lytic phase, λ phage DNA replicates using the host's machinery and all phage genes are transcribed and translated to produce new phage proteins. When sufficient proteins are made, all phage particles are assembled within the host cell. Later, when new phages are ready to leave the cell, the host cell is lysed to release new progeny and is ready to infect other *E. coli* cells and start a new lytic cycle (Lee et al., 2018; Van Duyne and Landy 2024). However, if the environmental conditions are favourable, the λ phage would enter the lysogenic cycle by integrating its own DNA into the host bacterial chromosome. The integrated phage DNA, known as a prophage, is replicated along with the host cell DNA and remains dormant for several generations until the environment changes. Under certain stress conditions, the prophage can be

excised from the host genome and enter the lytic cycle (Figure 1-2; Groth and Calos 2004; Court et al., 2007; Van Duyne and Landy 2024).

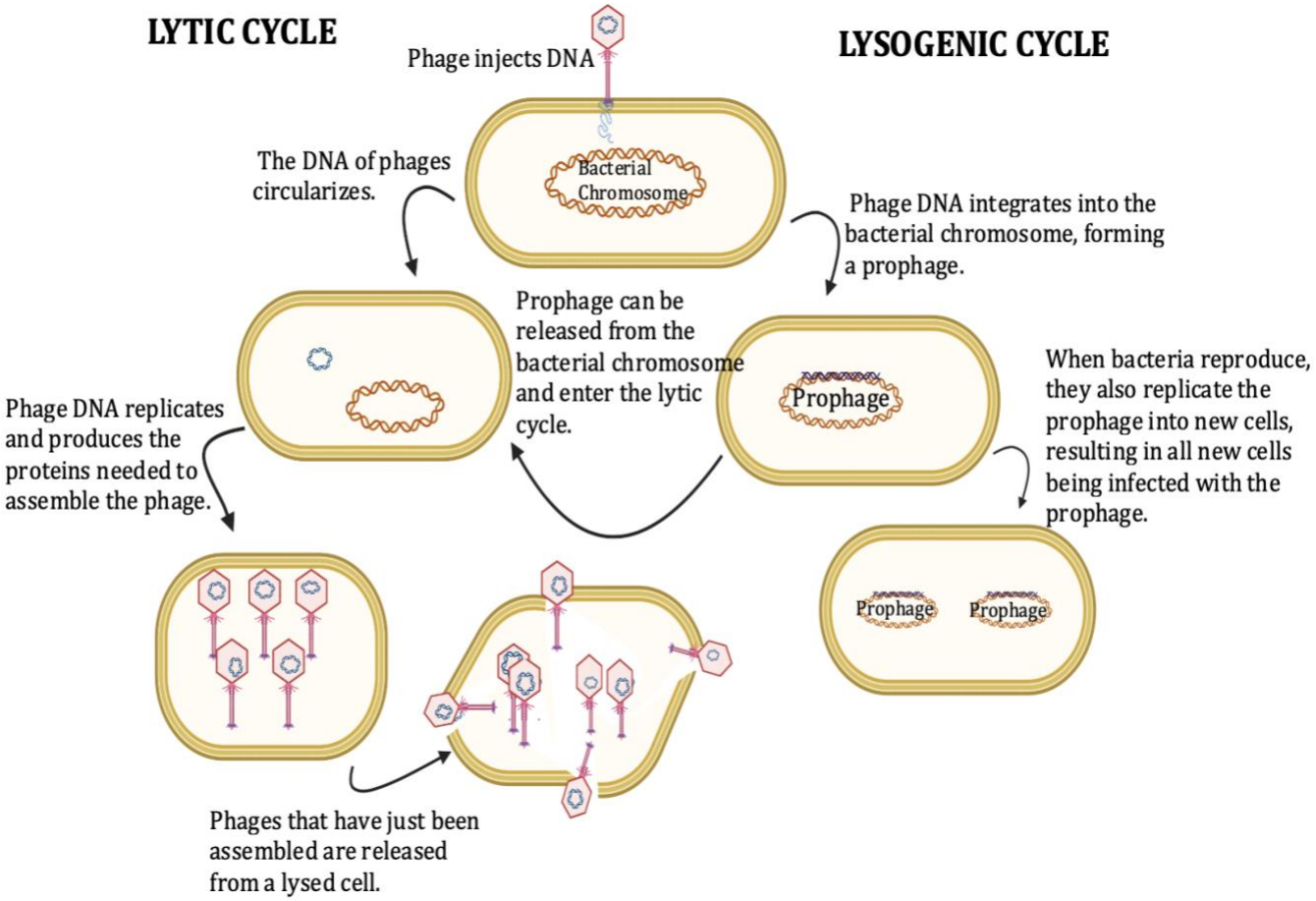


Figure 1-2. Replication Cycles of Bacteriophage λ. Upon infecting an *E. coli* cell, the bacteriophage λ infects the cell and injects its DNA into the host cell. In the lysogenic cycle, the phage DNA integrates into the bacterial genome, forming a prophage that is passively replicated as the host cell divides. Under stress conditions, the prophage may excise from the bacterial genome and enter the lytic cycle. In the lytic cycle, the phage DNA is actively replicated, and phage proteins are synthesized and assembled into new virions. The host cell is eventually lysed, releasing the newly formed phage.

***Lambda rex Genes*:** The Rex system, which governs the exclusion phenotype, is encoded by the phage λ immunity region (λ*imm*), which determines the infective "lifestyle" of the phage. This immunity operon consists of the λ *cI* repressor and *rexA-rexB* genes flanked by the leftward and the rightward operators (O_L, O_R). These operators connect to the regulator λ CI repressor and control both rightward (O_R) and leftward (O_L) expression of all remaining λ genes. Operators O_L and O_R selectively block the strong leftward (P_L) and rightward (P_R) promoters, respectively, during the λ lifecycle (Figure 1-3; Heinemann and Spiegelman 1970; Echols and Green 1971; Meyer et al., 1980; Li and Susskind 1994; Thomason et al., 2021).

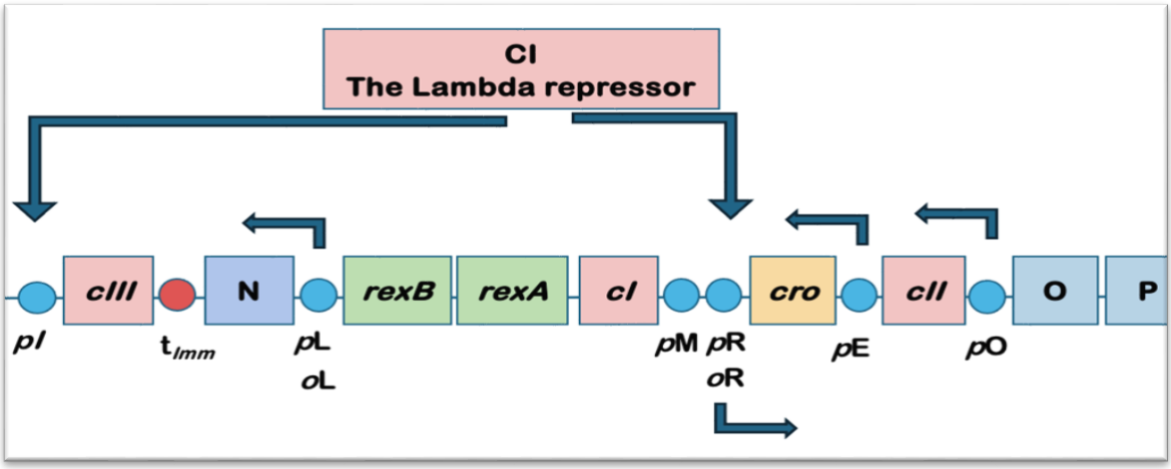


Figure 1-3. Immunity Region of Phage λ and Maintenance of Lysogeny. The λ repressor CI maintains lysogeny by binding to operator sites O_L and O_R, which overlap the promoters P_L and P_R, respectively. The P_E promoter, located upstream of the *cI* gene and activated by CII, initiates transcription for repressor establishment. The P_M, the promoter for repressor maintenance, overlaps O_R and maintains low-level *cI-rexA-rexB* transcription during lysogeny. CI binds to O_R repressor transcription from P_R and stimulates transcription from P_M, ensuring the continued expression of *cI*. The genes *rexA* and *rexB* are co-transcribed with *cI*. Figure key: Red circles: Terminators, Blue circles: Promoters.

The λ P_M-*cI*-*rexA*-*rexB*-t_{imm} operon is a 2,112 bp locus from 37,940 to 35,828 bp of the 48,512 bp λ genome. Promoter P_M is located at λ 37,940 bp and overlaps O_R, where the transcription of *rex* genes along *cI* repressor in a repressed λ prophage progresses from P_M through the terminator t_{imm} at 35,804 bp (Figure 1-4; Hayes and Szybalski, 1973; Daniels et al., 1983).

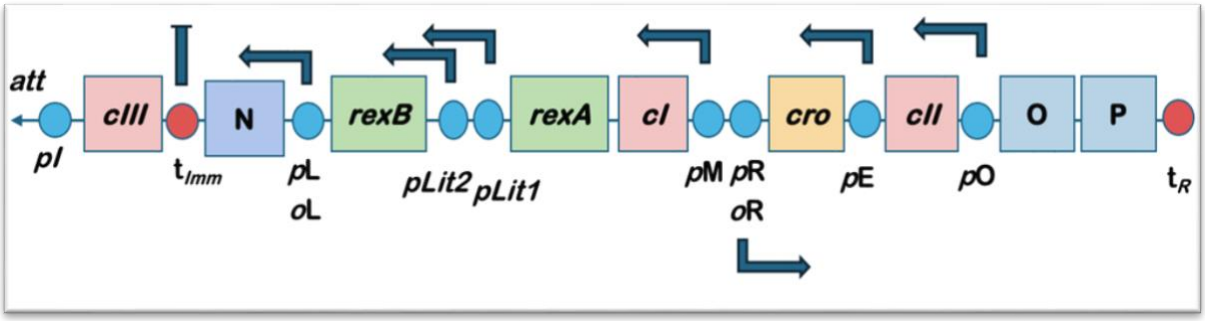


Figure 1-4. Portion of the Immunity Region from Phage λ. The Operator sites O_L and O_R are critical regulatory elements that, when bound by the CI repressor, inhibit transcription from the leftward (P_L) and the rightward (P_R) promoters, respectively to maintain lysogeny. The terminator t_{imm} halts transcription initiated from the P_{Lit} promoters, which drive expression of *rexB*, as well as transcription from the maintenance promoter P_M and the strong establishment promoter P_E, which transcribes the *cI*-*rexA*-*rexB* operon.

***Rex and the Lysogenic State*:** Bacteriophage λ is a temperate phage capable of executing both lysogenic and lytic replication cycles when it infects *E. coli*. The λ immunity region controls lysogeny proteins in addition to "deciding" which cycle is established and (in the case of lysogeny) maintained. Once an uninfected *E. coli* host is infected by λ, the λ phage DNA is delivered through the attachment site, LamB protein, triggering the immediate activation of P_R and resulting in *cII* expression. The CII protein, although unstable, is a potent transcriptional activator of the gene expression under the control of the lysogenic **E**stablishment promoter (P_E), leading to a surge in *cI-rexA-rexB* transcript production (Echols and Green 1971). This mRNA surge promotes lysogeny and is crucial for the lysis-lysogeny decision, also known as the "genetic switch", during phage infection (Echols and Green 1971; Thomason et al., 2021). The expression of the *cII* gene is necessary for establishing the lysogenic state, whereas *cI* represses *cII* during the maintenance of the lysogenic state (Echols and Green 1971). Thus, the CI repressor is crucial for maintaining the λ lysogenic state, but does not alone determine the lytic-lysogenic decision.

λ prophage confers lysogeny and maintains this state as long as the repressor maintenance promoter (P_M) is stimulated. The repressor CI binds to the operator O_R at a low transcript level (lysogeny "maintenance" level) through the P_M-*cI-rexA-rexB*-t_{imm} operon and is autoregulated by binding Cl to O_R, conferring repressor production and a Rex^+ "ready" state (Heinemann and Spiegelman 1970; Meyer et al., 1980). Accordingly, the expression of *rexB-rexA* in a λ lysogen depends on transcription initiated from P_M, which is modulated by the autoregulatory effect of CI at P_M (Echols and Green 1971; Thomason et al., 2021). Therefore, the CI repressor's binding to O_R fulfills two key roles: 1) it represses the expression of all lytic genes during lysogeny (Meyer et al., 1980; Ptashne 1986, 2004, 2006; Thomason et al., 2021); 2) the CI repressor's expression continues to sustain a lysogenic state (Meyer et al., 1980; Ptashne 1986, 2004, 2006; Thomason et al., 2021).

***Rex and λ Late Immunity Transcripts* (LIT):** The Rex operon is positively regulated and maintained in the lysogenic state under the autoregulation of the CI repressor at P_M. When encountering harmful signals, such as the presence of a mutagen or other stressors, the repressor CI is cleaved as part of the cellular SOS response, resulting in its loss of ability to repress transcription from the strong promoters P_R and P_L (Fix 1993). The transcription from P_R is stimulated and, in turn, initiates transcription of the "lysis-inducing gene" *cro* (a co-repressor). The prophage is then derepressed, and the cell leaves lysogeny to enter the lytic phase (Fix 1993; Thomason et al., 2021). Within the λ P_M-*cI*-*rexA*-*rexB*-t_{imm} operon, an extra promoter exists downstream of RexA that directs λ **L**ate **I**mmunity **T**ranscription (*LIT;* Figure 1-4). *LIT* is governed by two promoters (P_{lit1} and P_{lit2}) and upon activation during λ prophage de-repression, P_{lit1} initiates transcription from the *rexB* gene and leads to the high expression level of *rexB* gene (*rexB*-biased) in the absence of the *rexA* or *cI* genes (Hayes et al., 1997; 2003). This scenario may clarify how λ can evade its own exclusion mechanism and persist thanks to the favoured disproportionate ratio of RexB to RexA (discussed in detail in Section 1.1.3.1). The first promoter, P_{lit1}, is strong, influential, and inducible, whereas the second promoter, $P_{lit2,}$ is weaker and constitutive. Another λ gene, *oop*, may also support and protect the λ prophage by surviving its own exclusion system, stimulating the P_{lit1} promoter (Hayes et al., 1997). The *oop* gene encodes a functional RNA that acts as an antisense RNA to downregulate CII (Krinke et al., 1991). Overexpression of *rexB* in the absence of *rexA* (e.g., from a strong promoter, such as P_{lit1}) leads to the abrogation of Rex. It permits the superinfecting phage to propagate, conferring the Rex$^-$ phenotype (Hayes et al., 1997).

While *cI* stimulates its own expression and the expression of *rexA* and *rexB* genes, the CI repressor is not essential for Rex function. For instance, transformed cells carrying plasmids co-expressing the *rexA* and *rexB* genes without *cI* have been demonstrated to confer the Rex phenotype during subsequent infections by T4*rII* phage (Shinedling et al., 1987; Snyder and McWilliams 1989). The Rex phenotype requires both

RexA and RexB gene products to confer the phenotype and exclude T4*rII* from plating; mutation of either gene leads to the loss of the exclusionary phenotype, allowing the T4*rII* mutant to restore its plating capacity (Matz et al., 1982).

Properties of RexB*:** The RexB gene product is a 16 KDa polytopic transmembrane protein that may act as an ion channel on the host cell's membrane (Landsmann et al., 1982). The topology of the RexB protein was first analyzed through **a**lkaline **pho**sphatase fusion analysis (phoA*** fusion; Parma et al., 1992). This ***phoA*** fusion analysis took advantage of the requirement for alkaline phosphatase to be translocated through the periplasmic membrane for activation (Hoffman and Wright 1985; San Millan et al., 1989). Parma et al. (1992) found that in RexB::PhoA fusions spanning the *rexB* gene, the phosphatase enzyme domain exhibits its highest activity when the fusion is directed into the periplasmic space. On the other hand, the phosphatase enzyme was inactive if the fusion was directed into the cytoplasm. By applying this fusion strategy, RexB was observed to cross the cytoplasmic membrane at least four times, with the hydrophilic, positively charged regions adhering to the "plus inside (cytoplasm) rule" (Von Heijne 1986). In addition to its essential role in generating the Rex phenotype, RexB also plays a distinct role in safeguarding the λ O protein from degradation. This protein is necessary for initiating phage DNA replication. RexB inhibits the ATP-dependent cellular protease ClpXP, which is responsible for degrading λ O. Therefore, it leads to stabilizing λ O and ensuring successful phage replication, although the exact mechanism—whether through direct interaction or indirect modulation—remains to be fully elucidated (Schoulaker-Schwarz et al., 1991; Engelberg-Kulka et al., 1998). ClpPA and ClpXP are ATP-dependent proteases in *E. coli* that degrade misfolded or regulatory proteins to maintain cellular homeostasis (Gottesman et al., 1998). ClpPA targets unstable regulatory proteins, such as MazE (an antitoxin). The MazEF toxin-antitoxin system comprises a stable toxin, MazF, which acts as an endoribonuclease that cleaves mRNA, thereby disrupting protein synthesis and leading to cell death. MazE, the unstable antitoxin, neutralizes the toxic effect of MazF and

is degraded by ClpPA. During amino acid starvation, MazE is not synthesized and is degraded, thereby activating MazF and ultimately causing cell death (Gottesman et al., 1998; Kolodkin-Gal and Engelberg-Kulka 2006). RexB has been shown to inhibit ClpPA-mediated degradation of MazE, thereby indirectly limiting MazF-dependent mRNA cleavage and cell death (Aizenman et al., 1996; Gottesman et al., 1998; Kolodkin-Gal and Engelberg-Kulka 2006; Engelberg-Kulka and Kumar 2015). While this supports cell survival during stress, there is no direct evidence connecting RexB to the inhibition of the SOS response or ClpXP-mediated degradation of MazF. This implies that RexB's inhibition of ClpPA, thereby stabilizing MazE and preventing MazF-induced cell death (Engelberg-Kulka et al., 1998), could play further roles related to Rex. Currently, the only established link between Rex exclusion and ClpPA/ClpXP proteases is that Rex activation leads to a depletion of intracellular ATP, which is a critical cofactor required for the proteolytic activity of both ClpPA and ClpXP complexes.

Properties of RexA: The RexA protein (31.5 KDa) is predominantly hydrophilic and is postulated to localize in the cytoplasm (Belfort 1978; Parma et al., 1992). In RexA overexpression studies, Slavcev and Hayes (2003) found that cells overexpressing *rexA* form a strange “sticky cell” morphology. Based on this observation, it was suggested that RexA might be an outer membrane protein or located in the cytoplasm; however, this has never been validated. Although the function of RexA remains unknown, RexA is still believed to act as a “sensor” that activates or regulates the pore-forming RexB at some point, following a Rex-sensitive phage superinfection (Parma et al., 1992; Slavcev and Hayes 2003). Recently, the structure of RexA was revealed by X-ray crystallography at a 2.05Å resolution to be a two-domain architecture consisting of a split globular (DNA-binding) domain and a dimerization domain connected by flexible linkers. These domains correspond to the central and base domains of the recombination-associated DNA-binding protein C (RdgC), respectively, revealing unexpected structural similarities to this bacterial recombination-associated protein (Adams et al., 2024). The dimerization domains of each of these proteins form continuous eight-stranded anti-parallel β-sheet platforms stabilized by extensive hydrophobic

interactions and hydrogen bonds. RexA also exhibits an extensive bare patch across the surface of the globular domains at the dimer interface, conferring electrostatic surface properties, which may be involved in DNA binding (Adams et al., 2024). This structural similarity suggests that both RexA and RdgC may have evolved from a common ancestor and have conserved mechanisms for DNA binding. However, they have diverged to perform distinct biological roles in phage biology and regulation of recombination, respectively (Adams et al., 2024). RexA binds to DNA through a DNA-dependent conformational change (Adams et al., 2024). In its crystallized form, RexA adopts a closed conformation; however, modelling and experimental data suggest that it can transition to an open conformation, allowing DNA to interact (Adams et al., 2024). Additionally, a study using Electrophoretic Mobility Shift Assays (EMSA) demonstrated that RexA binds DNA in a non-specific manner, and mutations that disrupt the conformational flexibility or key residues involved in DNA interaction can impair DNA binding (Adams et al., 2024). RexA exhibits DNA-binding activity, functioning as a molecular sensor for abnormal DNA structures during phage infection or under stress conditions in bacterial cells (Thomason et al., 2021; Adams et al., 2024). This activity is essential for its role in the RexAB system, which safeguards the bacterial population by disrupting phage replication or triggering programmed cell death in infected cells (Thomason et al., 2021; Adams et al., 2024). Alongside its critical role in the Rex T4*rII* exclusion, recent studies have highlighted the significant function of RexA in aiding the transition of λ from lysogeny to the lytic cycle (Thomason et al., 2021) through its binding to the CI repressor. Once the lytic cycle is initiated, if the bistable switch reverts toward the lysogenic 'immune' state, RexA reduces the likelihood of maintaining that state. RexA stabilizes the lytic phase by directly or indirectly interfering with CI repressor activity, thereby preventing CI from repressing the lytic P_L and P_R promoters. When CI repression is relieved, these lytic promoters, P_L and P_R, are active and drive the expression of genes required for the lytic cycle. RexA's influence on these promoters indicates that it acts as a molecular switch to promote the lytic phase when specific conditions are met, such as stress or phage activation signals. Although RexB plays a role in modulating the effects of RexA and

may assist in establishing phage DNA replication during lytic growth, only RexA is essential for maintaining the lytic state and decreasing the likelihood of reverting to the immune state (Thomason et al., 2021). Thomason's observation could shed light on the enduring hypothesis proposed by Paddison et al. (1998) regarding the similarity between P2 prophage exclusion and λ Rex exclusion. They proposed that the swift lysis of T4*rII* in P2 lysogens might be associated with the Rex exclusion seen in λ lysogenic cells. Their hypothesis suggested that P2 may have a basic and less practical version of the Rex system, which initiates early lysis of T4*rII*-infected lysogens. It is proposed that Rex exclusion could work similarly, but with greater efficiency, lysing the infected cell before the phage matures. RexA may induce cell lysis when the Rex system is activated. In other words, RexA might be the leading cause of cell lysis in the Rex phenotype because it induces the transition to the lytic cycle (Paddison et al., 1998; Slavcev and Hayes 2002; Thomason et al., 2021).

1.1.3 The Physiological Manifestations of the Rex Activation

1.1.3.1 The Stoichiometry of RexA to RexB

Upon infection by a superinfecting phage, the Rex system is triggered. It imparts a severe cellular environment resulting in shutting down of total cellular macromolecular synthesis (Snyder and McWilliams 1989), alterations and depolarization of the periplasmic membrane, severe drop of the cellular ATP energy, reduction of the cellular respiration, and death of most of the infected population (Parma et al., 1992; Slavcev and Hayes 2002). This severe cessation of production affects super-infecting phage and cellular DNA, RNA, and proteins. Activation of Rex can occur through infection by Rex-sensitive phage or, in the absence of superinfection, by overexpressing *rexA* relative to *rexB* from a multicopy plasmid (Snyder and McWilliams 1989; Slavcev and Hayes 2003). The stoichiometry of RexA to RexB is crucial for Rex onset

or the abrogation of the exclusion phenotype. For instance, the Rex phenotype is not observed when either *rexA* or *rexB* is overexpressed in the absence of the other, or when *rexB* is overexpressed in the presence of *rexA* (Snyder and McWilliams 1989; Slavcev and Hayes 2002; 2003).

Interestingly, the enhanced co-expression of *rexA-rexB* from a multicopy plasmid not only prepares the cell for exclusion but can also exclude both T4 (RII^+) and T4*rII*, along with phages T5 and T7, though it does not affect λ (Snyder and McWilliams 1989; Slavcev and Hayes 2003). Even when using rex^+ λ lysogenic cells, the cells can be affected by disturbances to the stoichiometry of *rexA* to *rexB*, resulting in an altered Rex phenotype. Slavcev and Hayes (2003) noted that when rex^+ λ lysogens are transformed with a low-copy plasmid that expresses *rexA* constitutively, there is only a minor decrease in the Rex exclusion phenotype. Nevertheless, cells altered with a constitutive or inducible multicopy plasmid that expresses *rexA* or *rexB* completely eliminated the Rex exclusion phenotype. Conversely, using low-copy or multicopy plasmids with *rexA-rexB* co-expression or rex^- variants did not remove Rex exclusion in a rex^+ context (Slavcev and Hayes 2003).

These contrasting outcomes suggest that the Rex phenotype highly depends on the quantitative relationship between *rexA* and *rexB* (a "gene dosage relationship"). The Rex phenotype occurs if *rexA* is overexpressed relative to *rexB* (Snyder and McWilliams 1987; Slavcev and Hayes 2003). However, the Rex system is not activated upon overexpression of *rexB* compared to *rexA*. In this case, T4*rII* phage and lambdoid Rex-sensitive mutants will be capable of propagating and lysing the infected host cell (Parma et al., 1992; Slavcev and Hayes 2003). Interestingly, Slavcev and Hayes (2003) discovered that, akin to the Rex^+ cell population during T4*rII* infection, overexpressing *rexA* relative to *rexB* activates Rex, leading to significant host cell death; however, at least 10% of the infected cells survive. Moreover, these infected cells were morphologically similar to those observed during the stationary phase (Figure 1-5).

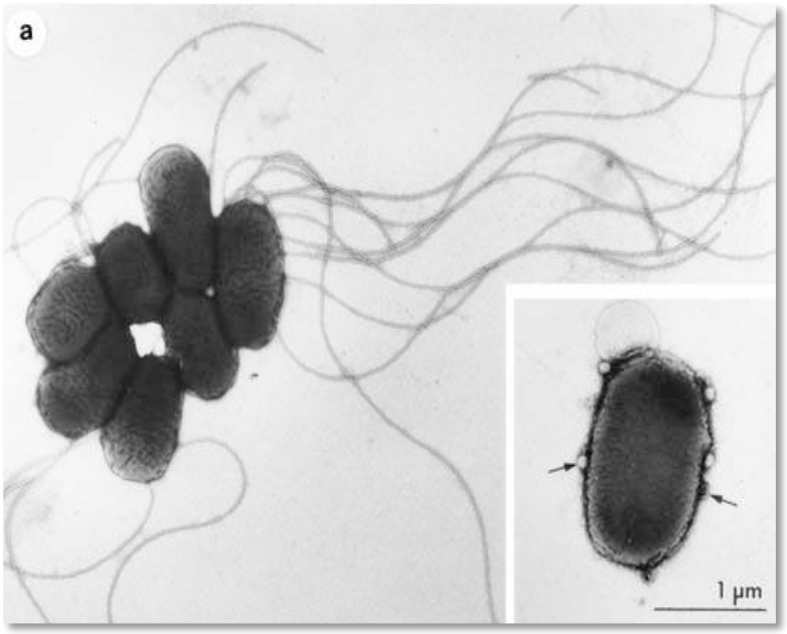


Figure 1-5. Morphological Changes in Rex$^+$ *E. coli* Following T4*rII* Phage Infection. Infection of Rex$^+$ *E. coli* cells by T4*rII* phage induces distinct morphological changes, including the loss of flagella and transition to a spherical cell shape. These alterations resemble a quiescent or stationary phase phenotype, likely resulting from a metabolic shift triggered by Rex activation. *Source: Slavcev and Hayes (2003).*

This harsh, quiescent-like state was characterized by alterations in cellular state, including a spherical cellular morphology, loss of flagellar production, and a decline in the proton motive force within the cell. Based on these physiological manifestations, Slavcev and Hayes (2002) proposed a model whereby Rex imparts an osmotic imbalance that stimulates the stationary phase and cellular shutdown. In this metabolic-like state, the propagation of many Rex-sensitive super-infecting phages, including T4, is not permissive. These observations suggested that Rex may not be a cell death system but rather a protective mechanism established to protect at least some λ lysogens against superinfection (Slavcev and Hayes 2002).

An explanatory mechanism for Rex was suggested by Parma et al. (1992), describing the status of Rex proteins in λ lysogens and upon superinfection. RexA and RexB proteins are present at a balanced ratio in λ lysogens “primed” and “ready to trigger”, where the ratio of RexA to RexB somehow increases upon

infection by T4*rII*, resulting in the activation of the Rex system (Figure 1-6). This model proposes that RexA functions as a sensor to activate the Rex system by triggering the pore-formation activity of RexB, much like a phage holin in the inner membrane. Upon superinfection, levels of RexA increase compared to those of RexB, leading to two (or more) RexA proteins for each RexB. This state results in RexB pore activation and the onset of Rex. In the scenario where RexB is overproduced, the ratio of RexA to RexB is disturbed, whereby the possibility of RexB subunits interacting with several RexA subunits declines, resulting in the loss of the exclusion phenotype (Parma et al., 1992; Slavcev et al., 2003).

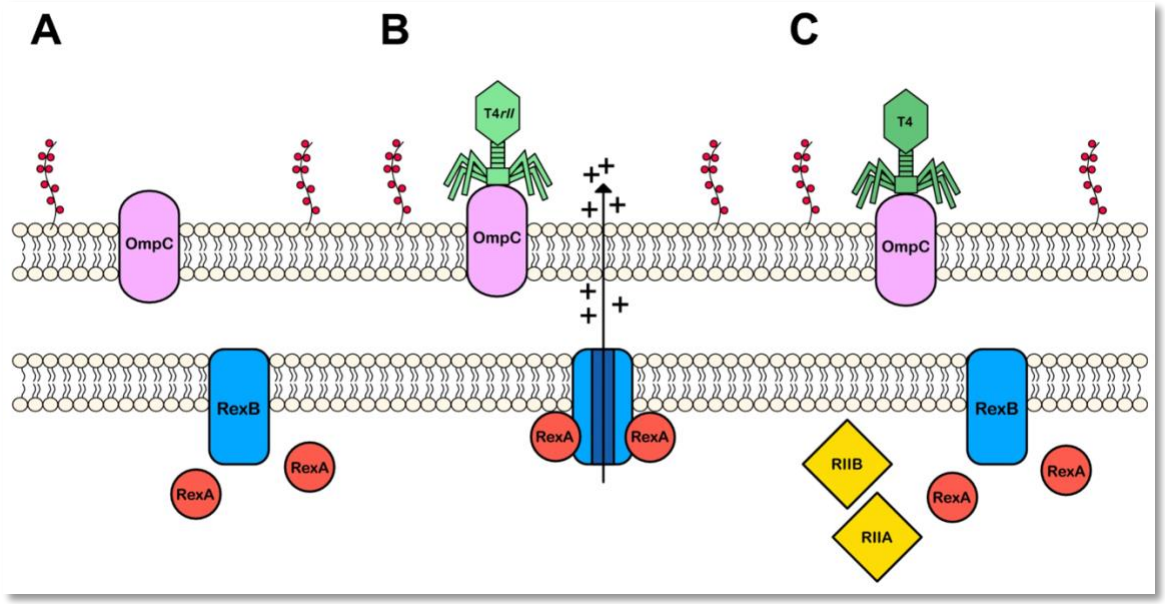


Figure 1-6. RexA/RexB Activation Model in Response to T4*rII* Infection. RexB functions as an ion channel and forms a 1:1 complex with RexA, even in the absence of external stimuli. Upon infection by T4*rII*, RexA is hypothesized to accumulate relative to RexB, triggering the activation of the RexB channel. This leads to ion efflux, depolarization of the cell membrane, and a loss of membrane potential. **A.** shows the inactive state of Rex, RexA, and RexB are present but not interacting functionally. **B.** illustrates the activated state, T4*rII* infection induces RexA-mediated activation of RexB, resulting in ion efflux. **C.** demonstrates infection by T4 (wt), which bypasses Rex-mediated exclusion and successfully kills the host cell. *Source: Wong et al., 2021.*

The Rex system was observed to terminate with only temporary abortion of macromolecular synthesis upon alteration in the cellular physiological states, such as nutrient limitation or osmotic imbalance (Sauerbier et al., 1969; Campbell and Rolfe 1977). Snyder and McWilliams (1989) demonstrated that cellular macromolecular synthesis could be halted without infection, specifically through the overexpression of *rexA* compared to *rexB* from a multicopy plasmid. Importantly, this effect was absent in the co-expressed *rexA* and *rexB* and the solo expression of either *rexA* or *rexB*. These results emphasize the importance of

the Rex proteins' stoichiometry, indicating that a surplus of RexA is essential for activating the Rex phenotype and causing a metabolic "shutdown" in the cell.

E. coli λ lysogen cellular growth has been noted to carry on for 10 minutes upon infection by T4*rII* phage (Colowick and Colowick 1983; Parma et al., 1992), which is interestingly also the time needed for superinfecting T4 phage to produce the RII proteins and suppress Rex (Sauerbier et al., 1969; Parma et al., 1992). Rex is then activated, and all the associated cellular (physiological) manifestations become noticeable, leading to the cessation of cellular metabolic systems (Sauerbier et al., 1969; Parma et al., 1992). The infected lysogen loses the cellular membrane potential and proton motive force at ten minutes (Parma et al., 1992), rapidly losing cellular ATP energy (Colowick and Colowick 1983). Although the majority of T4*rII* DNA transcription and mRNA synthesis in the host stops around the 13-minute point, the transcription within both the host cell and the prophage has been observed to persist in surviving cells afterwards (Sauerbier et al., 1969). This finding supports the model that infected lysogens encounter a sudden osmotic shift, which shunts them into a temporarily inactive state, helping the lysogen escape competing invading DNA; some of which survive the process. In many scenarios, only 10% of the super-infected population survives the environmental lethality; however, viability is over 10^5 times greater than that observed following T4*rII* infection of a Rex^- lysogen (Slavcev and Hayes 2002; Alattas et al., 2020). Infected with the mutant T4*rII*, λ Rex^+ lysogens exhibited significant delays in colony formation, which persisted for up to 48 hours. This lag is probably due to the activation of the Rex system, which impacts cellular physiology during and after infection (Slavcev and Hayes 2002). The activation of any trigger in the Rex system significantly disrupts macromolecular synthesis, resulting in profound physiological changes within the targeted cells (Garen 1961; Sekiguchi 1966).

1.1.3.2 Rex and the Cellular Environment

While the stoichiometric balance between RexA and RexB proteins is essential and influential in precisely modulating the Rex system's function, any deviations can lead to altered ion channel activity and potential cytotoxic effects. Equally critical is the cellular environment, which plays a vital role in regulating Rex activity. These environmental cues may act as physiological switches that fine-tune Rex-mediated responses to other phage infections or cellular stresses.

1.1.3.2.1 Rex and the Ionic Environment

The exclusionary phenotype can be established in the presence of monovalent cations like H^+, Na^+, K^+, or Cs^+ in the cellular culture (Garen 1961; Sekiguchi 1966) but is attenuated in the presence of divalent cations such as Ca_2^+, Mg_2^+, polyamines, arginine or sucrose in external culture (Garen 1961; Ames and Ames 1965; Brock 1965). These findings suggest that RexB, a non-specific ion exchanger, lacks discrimination between ion types or sizes and may be regulated solely by ion concentration. RexB may contribute to forming a lesion in the host membrane, which would disrupt the ionic gradient across the cytoplasmic membrane when Rex is activated (Buller and Astrachan 1968; Slavcev and Hayes 2003). The presence of divalent cations in culture during the first ten minutes following the infection of λ *rex*$^+$ lysogen by superinfecting T4*rII* phage can prevent the onset of Rex. It was noted by Buller and Astrachan (1968) that during the sixth minute of T4*rII* infection, phage exclusion can be reversed; however, the reversal of the Rex phenotype is greatly diminished after that point. These cellular manifestations, following infection, result in the rapid loss of cellular ATP, membrane potential, and proton motive force. Consequently, this leads to the lysogen's inability to properly uptake divalent cations into the cellular medium after the six-minute mark (Buller and Astrachan 1968).

1.1.3.2.2 Rex and Cellular Energy

Rex activation results in a significant cellular energy depletion, but this seems unrelated to the Rex exclusion phenotype on its own. It was noted that *unc* (ATPase) mutants were unable to hydrolyze ATP compared to the wild type (Colowick and Colowick 1983; McCarthy 1988). The *unc* genes or (*atp* operon) encode eight ATPase subunits essential for the proton-translocating ATP synthase (H^+-ATPase). A complete mutation of *unc* genes leads to defects in H^+-ATPase synthesis and conduction, resulting in cellular dysfunction (Colowick and Colowick 1983; McCarthy 1988). The cellular energy of the λ *unc* mutant lysogens remains stable after being infected by T4*rII*; this is because the superinfecting T4*rII* phage cannot initiate its own DNA replication (Colowick and Colowick 1983). While the significant decrease in ATP levels seen in λ lysogenic cells after T4*rII* infection does not directly correlate with exclusion, functional cellular ATPase activity still appears critical for managing the energy crisis induced by Rex activation (Colowick and Colowick 1983). In a Rex-activated cell, the system responds to a stressful or challenging situation, such as phage infection or DNA damage, by triggering a defence mechanism where energy is required to restore the proton motive force, resulting in the depletion of intracellular ATP. Colowick and Colowick (1983) noted that infection of λ lysogens with wild-type T4 phages caused a swift depletion of cellular ATP, which could be reversed by halting the infection source. On the other hand, infection of λ lysogens by T4*rII* mutants resulted in a swift and irreversible drop in cellular energy (Colowick and Colowick 1983).

1.1.3.2.3 Rex and Sigma Factors

Sigma Factors: Bacterial cells encounter various non-optimal conditions and stresses throughout their growth and development. General stress can impact cells at multiple stages, including gene replication, transcription, translation and DNA synthesis. To cope with these stresses, cells activate internal cellular responses that enable them to adapt and survive under various stress conditions (Zeman and Cimprich 2014; Hsu et al., 2021). The activation of the Rex system has revealed specific phenotypes, including a shift to a stationary phase-like morphology, which may protect host cells against T4*rII* superinfection and cell killing (Slavcev and Hayes 2003). Sigma factors in *E. coli* are small protein subunits (σ) that bind to the core RNA polymerase (RNAP), directing transcription at their specific cognate promoter sequences on the DNA to initiate bacterial transcription at the right place (Ranquet and Gottesman 2007; Feklístov et al., 2014; Handler and Kirkpatrick 2024). Each sigma factor can recognize different sets of promoters. As a result, they are essential in regulating and managing sets of gene expression, enabling cells to adapt to varying environmental signals or conditions (Ranquet and Gottesman 2007; Feklístov et al., 2014). This type of disturbed environment can significantly impact Rex activity; hence, the sigma factors can directly or indirectly affect Rex and the Rex mechanism.

Non-coding RNAs: Phenotypic diversity and the ability to respond to environmental signals are closely linked to proteins across all domains of life, as seen in phenotypic plasticity (Sommer 2020). However, the discovery of non-protein-coding RNAs (ncRNAs) that bind with proteins, DNA and/or mRNAs has changed our understanding of gene regulation. In bacteria, post-transcriptional regulation of gene expression is carried out by small RNAs (sRNA). These sRNAs are typically 50 to 500 nucleotides in length and are encoded in the intergenic regions (IGRs) of the bacterial genome. Another important class of bacterial ncRNAs is the anti-sense RNA (asRNA). These asRNAs are transcribed from the opposite strand

of their target protein-coding genes (Georg and Hess 2011; Saberi et al., 2016) and are located in the untranslated regions (UTRs) of specific mRNAs (Breaker 2011; Kortmann and Narberhaus 2012; Saberi et al., 2016). However, intragenic intraRNAs originate within protein-coding genes (Miyakoshi et al., 2015; Agostini et al., 2021).

The sigma E factor (σ-24, σ^E), a subunit of RNA holoenzyme encoded by the *rpoE* gene, is a minor sigma subunit of the *E. coli* response element. The σ^E factor, also known as the envelope or extra-cytoplasmic stress factor, is activated in response to stressful environments, including hyperosmotic shock, exposure to metal ions, and changes in outer membrane lipopolysaccharide structure. (Ades et al., 2003; Valentin-Hansen et al., 2007). Under-growth and non-stress conditions, σ^E is negatively regulated by the inner-membrane protein subunit of RseA, which functions in the antisense regulation of σ^E expression. (Missiakas et al., 1997; Nagamitsu et al., 2013; Kosaka et al., 2017).

During envelope stress, the anti-sigma factor RseA is sequentially degraded by the proteases DegS, RseP, and ClpXP (Flynn et al., 2004; Nagamitsu et al., 2013; Gottesman 2019; Kosaka et al., 2017), leading to the activation of σ^E. The level of σ^E expression depends on the extent of stress exposure from the extra-cytoplasmic compartment of *E. coli*, and the expression level persists until the cell once again reaches homeostasis (Ades et al., 2003). Activation of σ^E triggers the transcriptional activation of a wide array of downstream genes. These genes are essential for the periplasmic folding proteins and degrading factors (Murata et al., 2012; Rangarajan 2022). It is involved in a pathway that directs cell lysis through a cascade of events. This cascade involves the σ^E-regulated expression of small RNAs *micA* and *rybB*, which in turn downregulate the production of outer membrane proteins (Omps; detailed in the next section), ultimately leading to the disintegration of the bacterial outer membrane (Figure 1-7; Gogol et al., 2011; Murata et al., 2012).

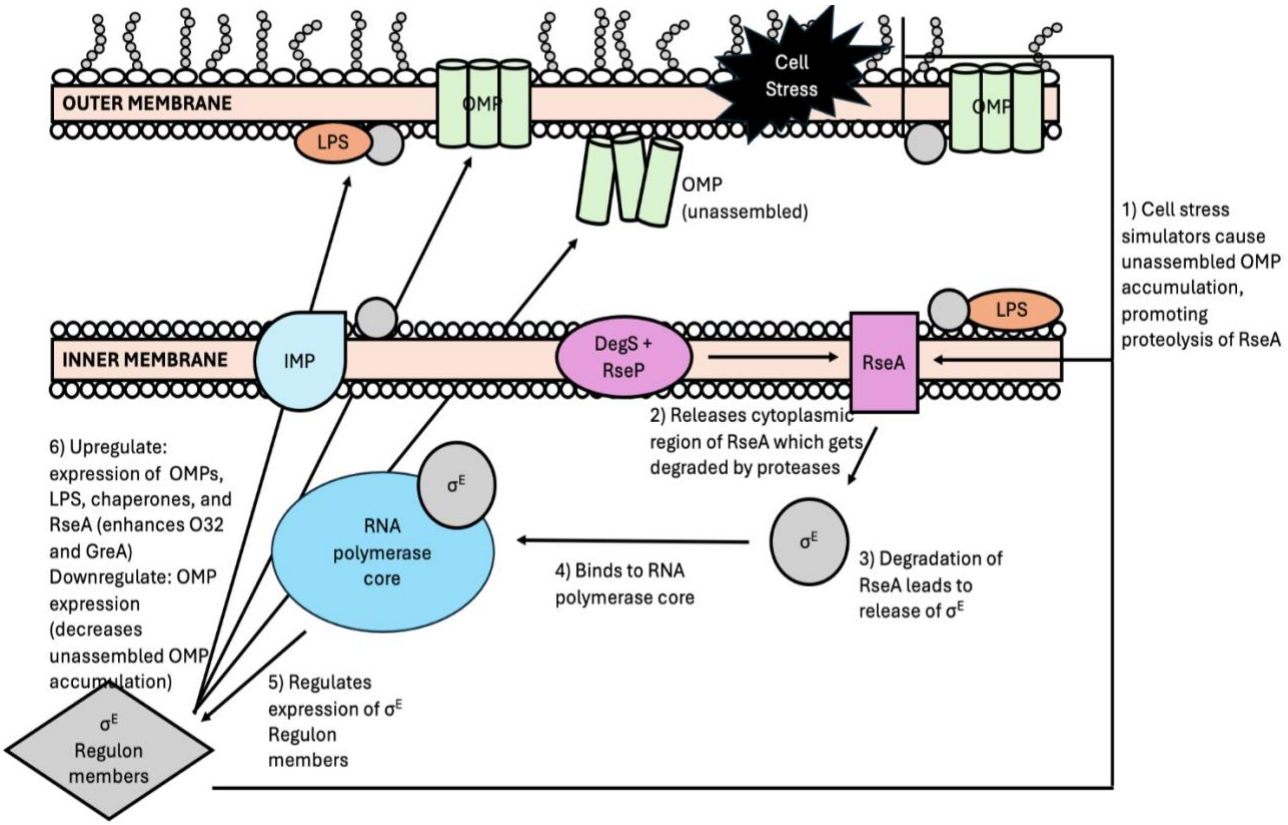


Figure 1-7. The σ^E Signalling Pathway and Its Activation Mechanism. The anti-sigma factor RseA binds and sequesters σ^E, keeping it inactive. This inhibition is regulated by two types of molecules: outer membrane proteins (Omps) and lipopolysaccharides (LPSs). The inner membrane protease DegS is activated upon binding to misfolded Omps, while RseB, which stabilizes RseA, is displaced by LPS. These events allow DegS to initiate the proteolytic cleavage of RseA. Subsequently, RseP completes the degradation of RseA, releasing σ^E into the cytoplasm. However, σ^E remains bound to RseA fragments until ClpXP and other ATP-dependent proteases degrade RseA, fully liberating σ^E. The active σ^E then promotes the transcription of genes involved in the synthesis and assembly of LPS and Omps.

Sigma S factor (σ-38, σ^S), encoded by *rpoS*, is expressed in the stationary phase and is necessary for expressing and regulating more than 10 % of *E. coli* genes to maintain cell viability during this phase. The *rpoS* product is a general stress response regulator and is considered an essential gene during the stationary phase when cells become more resistant to various external stresses (Suh et al., 1999; Weber et al., 2005). Any mutation to *rpoS* may also affect the stability and function of other sigma factors (Battesti et al., 2011; Bouillet et al., 2023, 2024). For example, the absence of the σ^S factor triggers an extracellular stress response that results in the elevation of *rpoE* expression, as well as the degradation of Omps, ultimately causing cell lysis (σ^E-dependent cell lysis; Lima et al., 2013; Nagamitsu et al., 2013; Kosaka et al., 2017). Various small RNAs (sRNAs) regulate *RpoS*/σ^S at the transcriptional, translational and post-translational levels (Schweder et al., 1996; Battesti et al., 2015). RpoS stability is primarily controlled post-translationally by the adaptor RssB and the ClpXP protease, while anti-adaptors (IraD, IraM, IraP) prevent RpoS degradation under stress (Gottesman 2019).

Interestingly, OmpF is one of the proteins that is indirectly negatively regulated by the induction of *rpoS*. The expression of the *ompF* gene is regulated by the small RNA MicF and potentially negatively influenced by the σ^S factor. The anti-sense RNA MicF binds to the *ompF* mRNA and prevents its translation, resulting in a reduction in the levels of OmpF protein (Pratt and Silhavy 1996; Suzuki et al., 1996; Patten et al., 2004). The permeability of the bacterial outer membrane is limited when the expression of *rpoS* is stimulated, but is dramatically increased in *rpoS* mutants (Notley-McRobb and Ferenci 1999; Mitchell et al., 2016). In several studies, the expression of *ompF* was significantly higher in *rpoS* mutants, but no effect was observed on the *ompC* expression (Pratt and Silhavy 1996; Darcan and Özkanca 2008).

Other studies have noted that the high-affinity galactose transport system, *mglABC*, which is regulated by the *galS* repressor, shows noticeable induction in *rpoS* mutants compared to *rpoS*$^+$ (wild-type) cells in response to suboptimal conditions (Notley-McRobb and Ferenci 1999).

During the log phase of growth, *rpoS* gene expression is rapidly degraded by the protease complex ClpXP, which binds to the *rpoS* transcript adaptor protein RssB. On the other hand, the anti-adaptors IraD, IraM, and IraP stabilize RpoS by preventing its delivery to ClpXP via RssB during stress (Figure 1-8; Schweder et al., 1996; Gottesman et al.,1998; Gottesman 2019; Battesti et al., 2015). These anti-adaptors are generated in response to various stress conditions: IraD is induced in response to DNA damage and during the transition from log to stationary phase; IraM is induced under magnesium starvation conditions; and IraP is induced under phosphate deficiency conditions (Battesti et al., 2013; Hryckowian et al., 2014). RssA is an sRNA within the RssB operon and is involved in the σ^S degradation process; however, the mechanism by which it controls σ^S levels is still poorly understood (Muffler et al., 1996). It was noted that RssA does not appear to regulate σ^S or its cellular levels, as disruption of the *rssA* gene has not been demonstrated to alter σ^S levels (Ruiz et al., 2001).

Another factor that can affect σ^S is the SsrA-tagging system, also known as the tmRNA system. This system serves as a critical quality control mechanism, rescuing stalled ribosomes and ensuring the degradation of incomplete or aberrant proteins (Karzai et al., 2000). When translation stalls on defective mRNA, the system appends a short peptide tag to the incomplete proteins, thus marking them for degradation by ClpXP or ClpAP proteases. This process not only maintains protein quality but also indirectly supports the translation of RpoS by preserving ribosome availability and reducing competition from faulty transcripts (Müller et al., 2021; D'Urso et al., 2023; Rodriguez-Aliaga et al., 2023). In the absence of SsrA, RpoS levels decline, resulting in impaired stress responses. During the stationary phase, ClpXP enhances the expression of *rpoE,* thereby stimulating the σ^E response. ClpXP contributes to this regulation by degrading specific negative regulators or modulating the stability of transcriptional repressors that otherwise inhibit *rpoE* expression. As a result, ClpXP activity indirectly stimulates the σ^E regulon, enabling the cell to respond to envelope stress conditions that are common during the stationary phase (Rizzolo et al., 2021). This activation causes changes in Omp stability, subsequently altering the bacterial cell morphology. In the

ΔrpoS mutant, the lack of *rpoS* transcripts allows ClpXP to elevate the σ^E factor expression (Smith et al., 2014). RexB may inhibit ClpXP activity and function as an antisense RNA during the stationary phase, or perhaps by linking membrane stress signals to the SsrA-RpoS axis. This might indirectly stabilize σ^S in this phase, allowing RexB to support or initiate the stationary phase upon Rex activation (Gottesman et al.,1998; Engelberg-Kulka and Glaser 1999).

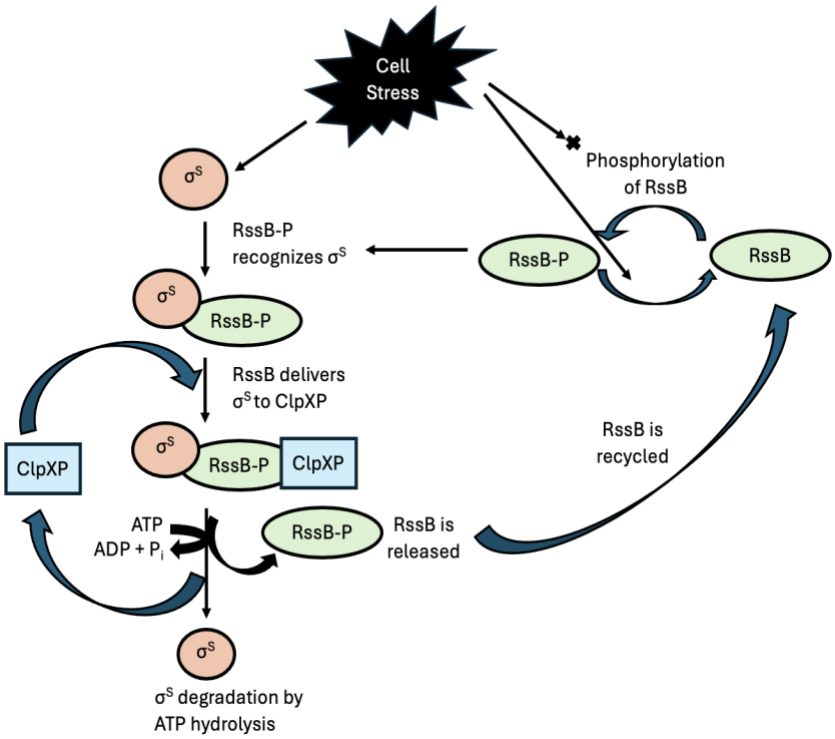


Figure 1-8. **Stabilization, Activation, and Degradation of σ^S in *E. coli.*** The adaptor protein RssB plays a central role in regulating the stability of the σ^S (RpoS) sigma factor. When phosphorylated, RssB binds to σ^S, forming a complex that targets σ^S for degradation by the ClpXP protease. Within ClpXP, σ^S is unfolded and completely degraded, while RssB is released for reuse. During the stationary phase or stress conditions, phosphorylation of RssB is modulated, allowing σ^S to accumulate and activate stress response genes.

1.1.3.3 Rex and *E. coli* Membrane Proteins

Slavcev (2005) predicted that *ompF* mutants could attenuate Rex activity. The *ompF* gene encodes a porin protein that polyamines can inhibit, resulting in decreased membrane permeability (Delcour and Vega 1996; Vinson et al., 2010). It has already been known that polyamines and divalent cations dramatically compromise Rex activity (Garen 1968). Furthermore, overexpression of RexA was also observed to result in sticky cells (Slavcev 2005), supporting the idea that outer membrane proteins may play a role in initiating specific physiological manifestations of Rex. Mutants of the tolerance membrane protein TolA displayed similar cellular characteristics. The *tolA* mutants exhibit spherical cell shapes and are highly permeable, thereby increasing cell permeability and sensitivity to external stresses, including phage infections (Lazzaroni et al., 2002; Li et al., 2022). This could help in understanding the results from Rolfe and Campbell's (1977) studies, where *tolB* mutant λ *rex*$^{+}$ lysogens exhibited full plating of T4*rII* and near complete abrogation of Rex. Considering our current understanding that Rex activity is influenced by monovalent ions and is inhibited by divalent cations and polyamines (Garen 1968), investigating how various mutations in membrane proteins affect Rex activity could offer valuable insights.

The Outer Membrane Proteins (Omps): The outer membrane (OM) of Gram-negative bacteria is a complex structure comprised of a lipopolysaccharide (LPS) decorated phospholipid membrane, scattered with an array of proteins (DiRienzo et al., 1978; Koebnik et al., 2000; Wexler 2002; May et al., 2015). The outer membrane is a crucial barrier surrounding the cytoplasmic membrane, playing a vital role in bacterial survival, adaptation, and protection from harsh external conditions (Koebnik et al., 2000; Ghai 2023). The OM enables crucial cellular functions by facilitating the uptake of nutrients and solutes through translocation via pore-like structures known as porins, which are typically composed of Omp homotrimers (Koebnik et al., 2000; Nikaido 2003). Omp porins make up over 50% of the outer membrane density; however, only a limited number have been structurally and functionally characterized to date (Figure 1-9;

Koebnik et al., 2000; Nikaido 2003; Belousov et al., 2023). The Omps control the influx and efflux of solutes across the membrane and are crucial for maintaining the stability and functionality of the bacterial cell (DiRienzo et al., 1978; Wexler 2002; Nikaido 2003). The proteins exposed on the outer membrane also determine the bacteriophage host range by acting as attachment sites for phage adsorption or as receptors for superinfecting signals against superinfecting phage (Koebnik et al., 2000; Wang and Lin 2001).

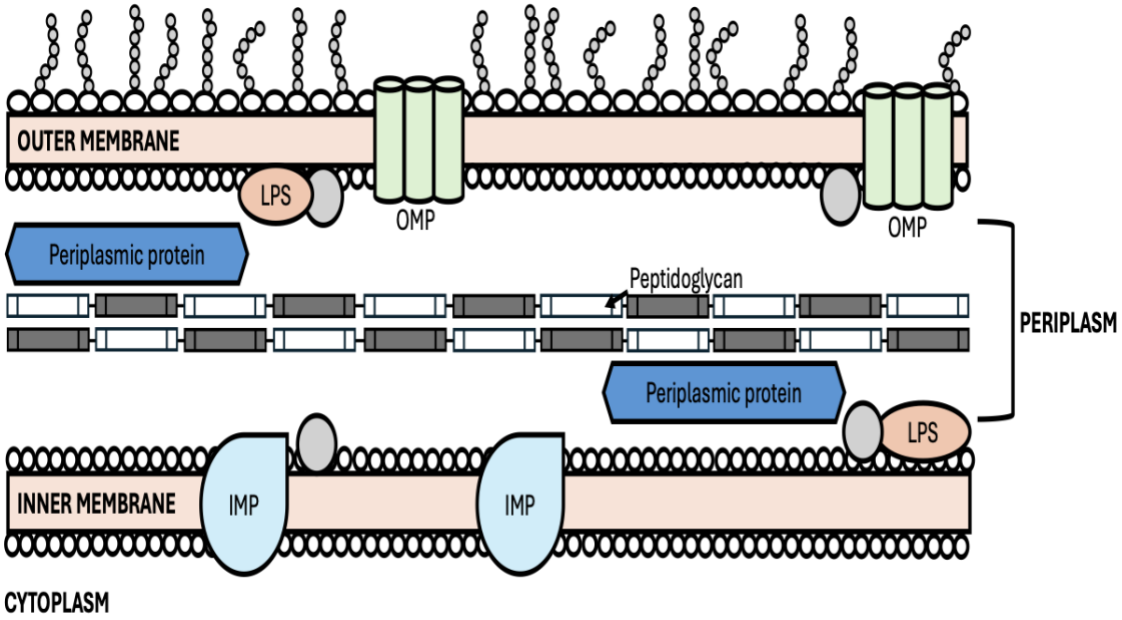


Figure 1-9. Components of the *E. coli* Cell Envelope. The *E. coli* cell envelope is a multilayered structure composed of: Outer membrane, asymmetrical in composition, with lipopolysaccharide (LPS) in the outer leaflet and phospholipid in the inner leaflet. It also contains porins, which serve as diffusion channels for small molecules; Periplasmic space, located between the outer- an inner- membranes, it includes the periplasm and a thin layer of peptidoglycan, which provides structural support; Inner (plasma) membrane, a phospholipid bilayer that maintains the proton motive force and membrane potential, essential for energy production and transport processes.

OmpA: OmpA has been extensively studied and is recognized as vital for maintaining the *E. coli* outer membrane structure and stability. It also acts as a receptor for bacterial conjugation and DNA transformation (Ried and Henning 1987; Sun et al., 2013). OmpA acts as a nonspecific diffusion channel for small solutes (Sugawara and Nikaido 1992) that can affect the development of its pores, thus shielding the bacterial cells from osmotic stress (Hong et al., 2006). OmpA also serves as a primary defense mechanism against environmental stressors; *ompA* null mutations make the cell more susceptible and less resistant to viral infections (Wang and Lin 2001; Nie et al., 2020). Modifications in the cell membrane structure render cells more vulnerable and sensitive to superinfecting phages like T4 (Wang and Lin 2001). This is quite intriguing in light of our previous findings that *ompA* mutants with a high-copy *rex*$^{+}$ plasmid not only exhibit complete Rex activity but also decrease T4 (RII^{+}) plating by more than 10^{3}-fold (Alattas et al., 2020).

Additionally, stress exposure in Δ*ompA* cells has also been found to induce phenotypic changes in *E. coli*, transforming the cells into spherical shapes, similar to those in the stationary phase (Wang 2002). This may suggest these mutants are more susceptible to entering the stationary state phase. The stability of the *ompA* mRNA transcript declines as the bacterial growth rate increases and is contingent on the cellular growth stage (Vytvytska et al., 1998; Rasmussen et al., 2005). Quiescent cells with stable *ompA* exhibit a turnover of over 15 minutes in log-phase cells but only about 4 minutes in stationary-phase cells (Rasmussen et al., 2005). Regulation of the *ompA* transcript is influenced by its 5'-untranslated region that contains cleavage sites for RNase E. The stability and decay of the *ompA* mRNA depend on another factor, RNA chaperone Hfq, which binds to this region.

Alongside Hfq, the short SraD RNA (highly conserved among Enterobacteriaceae and known as MicA) binds to the *ompA* mRNA region near its ribosome binding site during the transition from rapid growth to the stationary phase (Rasmussen et al., 2005). This interaction blocks ribosome entry and promotes RNase E-mediated cleavage, leading to degradation of the transcript after translation, and reduced OmpA levels in

these stationary-phase cells (Rasmussen et al., 2005; Udekwu et al., 2005). The increased Rex activity noted in the *ompA* mutants may occur because these host cells are prone to experiencing osmotic irregularities and entering a "stationary-like" phase (Alattas et al., 2020). In the context of Rex activation, the *ompA* mutation causes additional osmotic and structural instability; therefore, the cell's osmotic balance and membrane potential recovery may be irreversible. This would account for the abrogation of the Rex-centric mutualism phenotype and the significantly lower viability of *rex*$^{+}$ *ompA* mutants, as previously observed (Alattas et al., 2020).

Alternatively, the *ompA* mutant's failure to efficiently transfer and expel invading DNA during the Rex onset would expose the cell to the deadly effects of superinfection DNA (Wang and Lin 2001; Alattas et al., 2020). In both instances, the irreversible metabolic state of Rex activation within the *ompA* mutant would also account for the consequential Rex-dependent exclusion of T4*rII* and T4 (*rII*$^{+}$) alike (Snyder and McWilliams 1989; Slavcev and Hayes 2003), as the stationary phase prohibits the propagation of all T-even species (Bryan et al., 2016). The potent inhibition of plating seen for the *ompA rex*$^{+}$ mutant was Rex-dependent, as it was not seen in the *rex*$^{-}$ mutant (in its ability to reduce T4 plating efficiency) and could not wholly abrogate T4 plating efficiency (Alattas et al., 2020). These results indicate that OmpA could be a potential target for inactivation by Rex protein(s) and RII proteins. Alternatively, RII may compete with this activity, as it requires interaction with OmpA to inhibit Rex. These data imply that *ompA* is not the sole host gene involved and may need direct interaction with other targets to achieve the superinfection exclusion phenotype.

OmpX: Similar to OmpA, OmpX has been implicated in the cell's defense against bacterial virulence (Vogt and Schulz 1999). OmpX has been proven crucial for *E. coli's* cell adhesion and biofilm development, although the exact mechanism of action is not fully understood (Vogt and Schulz 1999; Otto and Hermansson 2004). Deletion of the *ompX* gene in *E. coli* results in mutants being more susceptible to stressful environments, infection and, ultimately, sensitivity to death (Otto and Hermansson 2004; Dupont

et al., 2007). Deleting the *ompX* gene compromises the integrity of the outer membrane, altering the affected cell surface hydrophobicity and increasing the negative charge on the cell surface, which may enhance bacterial cell-target surface interaction and infection (Otto and Hermansson 2004; Dupont et al., 2007).

The *ompX* gene exhibits over-expression in λ lysogens, suggesting that it acts as a host defense-response neutralizer when faced with any stress (Heffernan et al., 1994; Koebnik et al., 2000). OmpX overproduction relates to the overexpression of *rpoE* in *E. coli* (Sigma E factor; σ^E) and is associated with the increase in σ^E activity (Mecsas et al., 1993; Ades et al., 2003; Dupont et al., 2007). The expression of *ompX* is regulated by σ^E-dependent small RNAs MicA and RybB (Valentin-Hansen et al., 2007). Deletion *of* Δ*ompX* was able to attenuate T4*rII* exclusion by more than 10^3-fold (Alattas et al., 2020) when *rex*$^+$ was expressed from a high-copy plasmid, which may be related to its influence on the σ^E factor, as the underproduction of OmpX has been noted to reduce σ^E activity in *E. coli* (Mecsas et al., 1993; Dupont et al., 2007). Additionally, Alattas et al. (2020) previously noted that Δ*ompX* exhibited a more than 100-fold reduction in viability on T4*rII*-infected cells carrying the *rex*$^+$ plasmid compared to the *rex*$^+$ control, likely due to compromised T4*rII* exclusion in these *rex*$^+$ mutants.

OmpF and OmpC: The *ompF* and *ompC* genes are differentially expressed based on changes in extracellular medium osmolarity, as sensed by the membrane-bound EnvZ sensor. As a two-component system, EnvZ-OmpR, the EnvZ sensor undergoes autophosphorylation and transfers the phosphate to the cytoplasmic osmoregulation transcriptional regulator OmpR. This phosphorylated OmpR can bind to the promoters of *the ompF* and *ompC* genes, leading to the inverse regulation of *ompF* and *ompC* expression under different osmolarity conditions (Lan and Igo 1998; Srividhya and Krishnaswamy 2004).

OmpF forms a channel that is 10 times wider than OmpC, making it a more general passaging route preferentially expressed under low osmolarity medium conditions, as expected during the stationary phase (Benz 1988). Conversely, OmpC proteins favourably decorate the outer membrane under high osmolarity conditions, requiring a lower solute passaging level (Benz 1988). Both OmpF and OmpC function as cation-

charge-selective diffusion channels for the passive membrane diffusion and pore formation for small molecules (Cowan et al., 1992; Apirakaramwong et al., 1998; Lan and Igo 1998). OmpC also serves as the primary adsorption receptor for T4, the deletion of which prevents T4 adsorption and infection (Yu and Mizushima 1982; Washizaki et al., 2016; Alattas et al., 2020). Interestingly, the overproduction of either OmpC or OmpF increases σ^E activity, triggering a stress response that may lead to cell lysis. Simultaneously, lower levels of OmpC and OmpF inhibit σ^E activity (Mecsas et al., 1993; Noor 2015).

Due to the prohibitive nature of *ompC* mutants toward T4 plating, the involvement of OmpC in Rex activity could not be directly tested (Alattas et al., 2020). However, potential scenarios can be envisioned for OmpC involvement based on a combination of current and previous observations, along with our current understanding of osmotic regulation. For instance, firstly, given that OmpC serves as the binding site for T4, it is a sensible target for Rex activation or a sensor that responds to later T4 super-infection. Secondly, the deletion of *ompF* attenuated Rex activity by more than 10^2-fold (Alattas et al., 2020) but was unable to entirely abrogate the phenotype, suggesting that while it influences Rex, its contribution could be less direct, possibly through osmotic imbalance and triggering of a dormant phase-like state. Also, OmpR regulates the transcription levels of both *ompF* and *ompC* and as the mutation of the *ompR* gene significantly inhibits T4 plating efficiency in a Rex-dependent context (Alattas et al., 2020), insignificant T4 infectivity could be partially attributed to the low *ompC* expression level that again, is required for T4 adsorption. Moreover, OmpR controls the transcription of the MicC sRNA, which promotes the degradation of *ompC* mRNA transcripts, thereby inhibiting the expression of OmpC in an OmpR-deprived environment (documented in Δ*ompR* mutants; Alattas et al., 2020) (Guillier et al., 2006). In addition, sucrose can stimulate ompC gene expression independently of OmpR through a unique mechanism; hence, sucrose is known to powerfully suppress Rex activity (Schnaitman and McDonald 1984; Batchelor et al., 2005). OmpR regulates the expression of OmpC and OmpF in response to varying osmolarity conditions. Even in an *ompF* mutant, unphosphorylated OmpR can still promote *ompC* transcription, although the reaction to OmpR

phosphorylation is impaired (Srividhya and Krishnaswamy 2004). Lastly, during the stationary phase, the expression of *ompC* is downregulated, which aligns with the cellular state observed during the onset of Rex (Alattas et al., 2020).

OmpW: The OmpW protein in the *E. coli* outer membrane forms porins that create long, narrow hydrophobic channels, which act as ion channels transporting small hydrophobic molecules across the membrane (Hong et al., 2006). OmpW was noted to protect *E. coli* cells against any environmental stressors, especially against super-infection (Wu. et al., 2013). Deletion of *ompW* conferred a significant reduction in Rex activity by approximately 10^3-fold. Also, T4*rII*-infected Δ*ompW* mutants showed 10^2-fold reduced viability when carrying the *rex*$^+$ plasmid. These findings suggest that OmpW may be a potential trigger for Rex by acting in conjunction with OmpA and OmpF (Alattas et al., 2020). An interesting similar scenario occurs when *E. coli* cells enter the stationary phase, where active σ^E decreases the transcription and production of OmpA, OmpC, and OmpW (Kabir et al., 2005). The *micA* and *rybB* transcripts further downregulate *ompA* and *ompC* translation (Valentin-Hansen et al., 2007). Disruption in forming these Omps causes increased cell lysis during the early stationary phase, as indicated by high protein density in the culture medium (Kabir et al., 2005; Kosaka et al., 2017).

The Tolerance (Tol) Membrane Proteins: Along with outer membrane proteins (Omps), the Tol system also plays a vital role in maintaining the stability, integrity, and maintenance of the *E. coli* cell membrane (Lazzaroni et al., 1999; Lloubès et al., 2001). Tol proteins also import and export micro- and macromolecules through the cell membrane. The Tol system, specifically TolQRAB, is the primary system by which bacterial toxins, such as colicins, are imported into the cell (Meury and Devilliers 1999; Lloubès et al., 2001; Lazzaroni et al., 2002). In Gram-negative bacteria, the TolA, Q, and R proteins are located in the cytoplasmic membrane, while TolB is located in the periplasm. Together, they form a complex system that functionally links with the membrane protein Pal (peptidoglycan-associated lipoprotein), which

anchors to the outer membrane through its N-terminus and strongly interacts with the peptidoglycan layer through its C-terminal region (Cascales *et al.* 2002). The Pal protein increases cell envelope complexity and serves to maintain cell integrity (Figure 1-10; Lazzaroni and Portalier 1992; Bouveret et al., 1995; Lazzaroni et al., 1995; Clavel et al., 1998; Germon et al., 1998). TolC is an outer membrane protein considered to be a part of the bacterial cell export system in addition to the ABC transporter to efflux proteins and other toxins outside cells (Bernadac et al., 1998; Andersen et al., 2000; Lloubès et al., 2001).

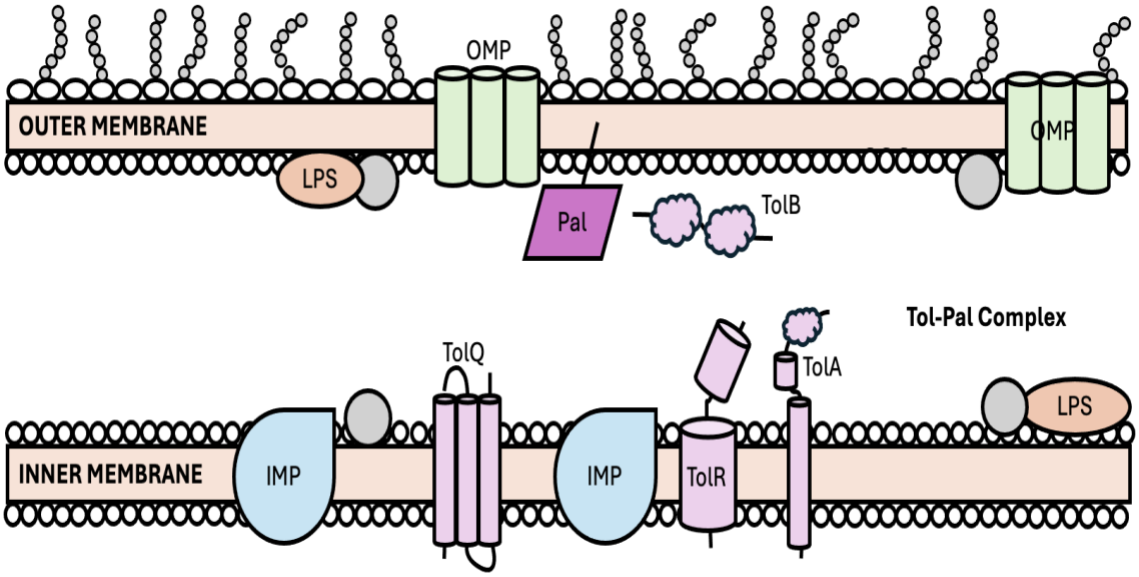


Figure 1-10. **The Tol-Pal Complex System in the *E. coli* Cell Envelope.** The Tol-Pal system is a multi-protein complex that spans the *E. coli* cell envelope, playing a crucial role in maintaining outer membrane integrity and coordinating cell division. It includes the inner membrane proteins TolA, TolR, and TolQ, the periplasmic protein TolB, and the outer membrane-anchored Pal protein. Together, these components form a trans-envelope network that physically links the inner membrane, periplasm, and outer membrane, ensuring structural cohesion and dynamic coordination during envelope constriction.

TolA: TolA is a 421 amino-acid cytoplasmic membrane protein that has three domains that extend to the outer membrane, where the interactions between outer- and inner-membrane proteins occur (Levengood-Freyermuth et al., 1993; Derouiche et al., 1996). TolA, specifically its periplasmic C-terminal functional domains, is required for transporting filamentous phage, chromosomal DNA materials, and colicins into the cell. Colicins are protein toxins produced by certain strains of *E. coli* bacteria and are harmful to neighbouring related bacteria. These molecules require the TolQRAB complex and the membrane-pore-forming OmpF and OmpC proteins, in addition to OmpA, to translocate into the cells, where the outer membrane proteins serve either as receptors or translocators for the toxins (Meury and Devilliers 1999; Lazzaroni et al., 2002; Lloubès et al., 2001).

Mutations in any of the *tol-pal* genes may result in 1) release of periplasmic content; 2) an increase in sensitivity to many antimicrobial agents and/or some chelating agents**;** 3) loss of outer membrane integrity; 4) increased formation of membrane blebs; and 5) changes in cell morphology (Yem and Wu 1977; Fung et al., 1978). It was noted in one study that mutation of any of the *tolA, tolB,* or *tolP* genes results in the allowance of T4*rII* to plate on λ *rex*$^{+}$ lysogens fully*,* i.e. results in abrogation of the T4*rII* exclusion phenotype (Rolfe and Campbell 1977), but Alattas et al. (2020) could not replicate the finding. Mutation of *tolC* was observed to be combined with many phenotypic changes, including an extreme reduction in OmpF protein synthesis (to an untraceable level in the membrane) and a simultaneous increase in the level of OmpC protein; the effect was found to be through the activation of the sRNA *micF,* which inhibits the translation of *ompF* mRNA (Misra and Reeves 1987; Fralick and Burns-Keliher 1994; Bernadac et al., 1998). Mutations in *tolA* alter cell shape, rendering bacterial cells highly permeable and susceptible to external stresses, including infections, while maintaining resistance to colicins (Meury and Devilliers 1999; Lazzaroni et al., 2002; Lloubès et al., 2001). Although no direct interactions between TolA and OmpA have been found yet, TolA is also heavily involved in the assembly and integrity of outer membrane porins. Any mutations may affect LPS synthesis and the functionality of porins. TolA may influence the regulation of

OmpF and OmpC, indirectly increasing the *ompF* expression level by negatively controlling *ompC* expression. The *ompF* expression was found to be downregulated in *tolA* mutant cells (Lazzaroni et al., 1986; Derouiche et al., 1996).

Lpp: Alongside the Tol-Pal complex, Lpp serves as a key prolipoprotein on the inner surface of the outer membrane, playing a crucial role in safeguarding and preserving the structural and functional integrity of the cell membrane (Ozawa and Mizushima 1983; Asmar and Collet 2018). Lpp maintains the connection between the outer membrane and the peptidoglycan layer. Similar to other membrane proteins, the transcription of the *lpp* gene is regulated by σ^E, highlighting its significance in stress responses (Rhodius et al., 2006). Mutations in the *lpp* gene disrupt the structural connection between the outer and inner membranes of the envelope. As a result, periplasmic proteins enter the medium and form vesicles, which are phenotypically similar to those caused by mutations in *tol-pal* (Bernadac et al., 1998; Mathelié-Guinlet et al., 2020). Additionally, mutations in *lpp* have no impact on the expression of Tol-Pal; however, *tolA* mutations inhibit *lpp* expression (Cascales et al*.,* 2000). As part of the T4's strategy to seize the host's cellular machinery after infection, *lpp* transcripts are rapidly degraded (Qi et al*.,* 2015). Lpp could serve as a crucial connection between TolA and Omps. While a direct interaction between TolA and OmpA has not been identified so far, TolA does engage indirectly with a complex consisting of TolB, Pal, Lpp, and OmpA, alongside the other Omps (Lloubès et al., 2001).

LamB: Also known as a maltoporin, LamB is a trimeric protein in the outer membrane of *E. coli.* LamB's primary function is to facilitate the uptake of maltose by forming a channel in the cell membrane, but it also serves as a receptor for λ adsorption (Randall Hazelbauer and Schwartz 1973; Gibbs et al*.,* 2004; Chatterjee and Rothenberg 2012). Like OmpA, its expression is regulated by σ^E through the small RNA MicA. During the stationary phase, *lamB* can be upregulated by σ^S, along with the *mal* operon (Hengge-Aronis 2002). Mutations in the *lamB* gene are detrimental to the *E. coli* cell, causing significant defects in the inner membrane that disrupt the proton motive force and unfold Omps. It was also noted that LamB expression

levels were inhibited in *tolA* mutants, resulting in the activation of cell stress responses (Derouiche et al., 1996).

The TonB system: TonB, ExbB, and ExbD, encoded by the *exb* operon, are inner membrane proteins that are part of TonB-dependant energy transduction system to transport energy into the bacterial cell in nutrient limitation (Bernadac et al., 1998; Held and Postle 2002). The TonB system is crucial for the active transport of iron chelates, siderophores, and vitamin $B_{12,}$ as well as for establishing a connection between the inner and outer membranes. However, the system cannot function independently without ExbB and ExbD, where TonB cannot respond to the cytoplasmic membrane proton motive force in their absence (Bernadac et al., 1998; Held and Postle 2002; Noinaj et al., 2010; Lill et al., 2016). All the TonB, ExbB, and ExbD proteins are in the inner membrane. Both TonB and ExbB proteins are predicted to be anchored in the cytoplasm, spanning the cytoplasmic membrane three times, with the hydrophobic N-terminus localized to the periplasm. The ExbD protein is expected to anchor at the N-terminus within the inner membrane, with the bulk of the protein in the periplasm (Kampfenkel and Braun 1992,1993; Braun 1995; Lill et al., 2016).
TonB, ExbB, and ExbD are homologues of TolA, TolQ, and TolR, respectively. Additionally, it was discovered that the *exb* operon function can be partially (~10%) replaceable by the *tol* operon. However, outer membrane defects and phenotypic changes accompanied by mutations in the *tol-pal* system are not similarly observed in *tonB* system mutants (Eick-Helmerich and Braun, 1989; Bernadac et al., 1998; Held and Postle 2002). Ferrichrome transporter (FhuA) and Ferric enterobactin transporter (FepA) proteins are also part of the TonB-dependent transporter system, both of which specifically target and bind metal chelators at the extracellular side of the bacterial cell membrane and interact with the TonB-ExbBD system at the periplasmic side of the outer membrane (Ferguson et al., 1998,2000; Eisenhauer et al., 2005; Noinaj et al., 2010). FhuA and FepA are *E. coli* outer membrane proteins. In addition to their function in energizing cells, they also serve as adsorption receptors for many phages, such as T1 and T5, as well as several colicins

such as colicin M, B, and D. Any mutation of either gene would increase the susceptibility of the bacterial cell to phage infections and make it sensitive to several antibiotics and colicins (Günter and Braun 1990; Liu et al., 1993; Braun 1994; Killmann and Braun 1995).

The β-Methyl-Galactoside Transport System (Mgl): The MglABC is another group of Gram-negative bacterial cell membrane protein members that belong to the superfamily of ATP-Binding Cassette (ABC) systems (Harayama et al., 1983; Hogg et al., 1991; Saurin et al., 1999). This ABC transporter complex constitutes one of the most prominent protein families of all living microorganisms. Approximately 5% of the entire *E. coli* genome encodes ABC transporter components with various physiological functions (Dassa and Bouige 2001; Higgins 2001). Studies have shown a correlation between the functional characterization of the ABC transporter cassette and its phylogenetic classification (Saurin et al., 1999; Dassa and Bouige 2001). The primary distinction between these systems is related to the polarity of the ABC transporter, which can be either an exporter or an importer. More than 50 subfamilies have been described based on phylogenetic and functional classifications (Saurin et al., 1999; Dassa and Bouige 2001; Higgins 2001). The transporter complex MglABC is an example of an ABC importer system involved in the influx of galactose and/or β-methyl-galactoside (Lengeler et al., 1971; Death and Ferenci 1993, 1994). The complex is composed of two peripheral ATP-binding proteins (MglA), two integral transmembrane proteins (MglC) and a periplasmic recognition solute-binding protein (MglB) (Harayama et al., 1983; Rotman and Guzman, 1982; Hogg et al., 1991). This system was found to be regulated by two Gal repressors, GalS and GalR; the Gal operon encodes galactose and β-Methyl-Galactoside permease (MeGal permease) enzymes necessary for galactose and galactoside transport and metabolism (Boos 1969; Lengeler et al., 1971; Boos and Sarvac 1970; Weickert and Adhya 1992, 1993). MeGal permease mutants exhibit low-to-no galactose uptake (Boos et al., 1988, 1996; Boos and Sarvac 1970; Weickert and Adhya 1992, 1993). The g*al* operon consists of *galS* and *galR* repressors, overlapping promoters P_1 and P_2, external O_E and internal O_I operators, cyclic

AMP receptor protein (CRP), and three enzymatic genes *galE* (epimerase), *galT* (galactose transferase), and *galK* (galactokinase) (Figure 1-11; Hua and Markovitz 1975; Queen and Rosenberg 1981; Adams et al., 1987; Horvath et al., 2010; Lewis and Adhya 2015).

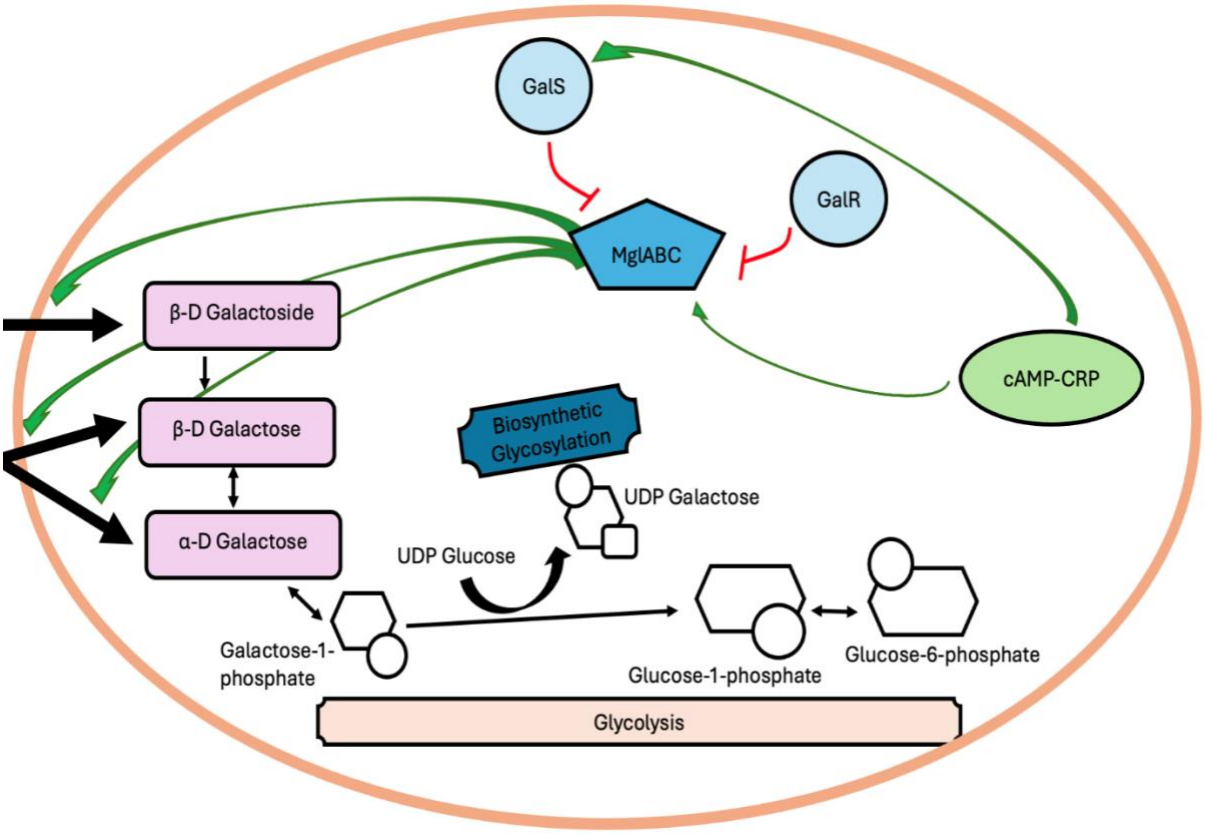


Figure 1-11. Proteins and Regulatory Components of the *E. coli* D-Galactose Transport System. The D-galactose transport and metabolic system in *E. coli* involves approximately 12 genes, including both protein-coding genes and small RNAs, as identified through bioinformatics analysis. Central to this system is the MglABC transporter complex, which facilitates the uptake of galactose. Its expression is tightly regulated by the transcriptional repressors GalS and GalR. Regulatory interactions are depicted with red lines indicating repression and green lines indicating activation.

Under glucose-limited conditions, transcription and induction of the *mgl* operon are regulated by the *galS* repressor, where GalS can control transcription even in the absence of GalR. GalS is negatively regulated by the galactose inducers and positively regulated by the cAMP receptor protein, while *galR* is constitutively expressed (Lengeler et al., 1971; Weickert and Adhya 1992; Death and Ferenci 1993; Weickert and Adhya 1993; Horvath et al., 2010). The hydrophilic MglA protein is closely linked to the cytoplasmic membrane, spans the membrane, and probably supplies the transport system with ATP (Hogg et al., 1991; Mimura et al., 1991). This complex system provides a pathway for the passage of water-soluble substrates through the hydrophobic barrier and directly interacts with the solute-binding protein MglB located on the periplasmic side of the membrane (Rotman and Guzman 1982; Hogg et al., 1991; Mimura et al., 1991). MglC is a 336-amino-acid hydrophobic protein likely situated on the internal face of the cytoplasmic membrane, where its localization has been estimated based on its direct interaction with the cytoplasmic domain of MglA (Harayama et al., 1983; Hogg et al., 1991). A null mutation of one or all of the *mgl-A, -B,* or *-C* genes would result in deficient galactose uptake, while the mutation of the *galS* repressor would increase the *mgl* expression in the cell (Lengeler et al., 1971; Notley-McRobb and Ferenci 1999).

Additional *rex*-dependent Phenotypes

Several other noteworthy Rex-related phenotypes have been noted in conjunction with the central mystery of T4*rII* exclusion. These phenotypes are not directly related to the exclusion itself but rather are associated with the physiological manifestations of the *rex* genes and the activation of Rex. For example, when there is no infection and cells are exposed to UV light, the DNA photolyase enzyme is amplified, where the activity or the expression of this enzyme is increased (the gene product of the *phr* gene). This enzyme attaches to DNA pyrimidine dimers to fix the DNA damage caused by UV light exposure (Li et al., 1992; Fix 1993). In the presence of the *rexA* and *rexB* genes, this protein-DNA interaction activates Rex, leading to the cessation of cellular metabolism. (Li et al., 1992). The authors propose that the interaction between photolyase and DNA acts as a "trigger" for the activation of Rex. Conversely, Li et al. (1992) performed experiments assessing the expression of *lacZ* in the presence of amplified photolyase. The results revealed that rex^+ λ lysogenic cells showed increased gene inactivation following ultraviolet (UV) exposure compared to rex^- λ lysogens or non-lysogens. They discovered that either *rexA* or *rexB* mutations could reverse the Rex exclusion. This suggests that the interaction of UV-induced pyrimidine dimers with photolyase serves as a trigger for Rex activation, resulting in the cessation of macromolecular synthesis in *E. coli* cells.

Additionally, when λ lysogens are exposed to low doses of UV light, the substitution of the *rexA* or *rexB* genes with a green fluorescent protein (GFP) reporter results in reduced induction compared to lysogens retaining the intact *rexA* and *rexB* genes, suggesting that one or both Rex proteins contribute to prophage induction (Baek et al., 2003). This finding indicates that both RexA and RexB, or at least one of them, may be involved in enhancing the λ prophage induction. This supports the theory that *rex* genes play a role in the genetic switch from lysogeny to the lytic phase (Thomason et al., 2021). The *rex* genes have been associated with modifying cellular responses to DNA damage induced by UV light and alkylating agents,

indicating an increased sensitivity (Fix 1993; Thomason et al., 2021). To put it differently, the combined expression of *rexA* and *rexB* can enhance the UV sensitivity of *E. coli*, while the degree of sensitivity is regulated by the ratio of RexA to RexB (Parma et al., 1992; Li et al., 1992; Fix 1993). The extent of energetic dysfunction depends on the ratio of RexA to RexB; the higher the RexA, the greater the damage. However, the presence of RexA without RexB does not exert a toxic effect (Parma et al., 1992; Li et al., 1992; Fix 1993). This could be due to a defect in the P_{LIT} promoter, resulting in a reduction of RexB level. RexB is also produced from a second promoter, P_{LIT}, which is embedded within the *rexA* gene (Fix 1993; Thomason et al., 2019). Cells exposed to MNU (N-methyl-N-nitrosourea) exhibited sensitization attributed to the expression of *rexA-rexB* from either a prophage or a low-copy plasmid, even without stimulation for mutagenesis. Fix (1993) suggested that the inhibition of repair for DNA damage caused by UV and alkylating agents may arise from DNA-protein interactions during the repair process, potentially signalling Rex exclusion. In this context, SOS responses may represent a form of "self-exclusion" in λ lysogens. Fix (1993) did not analyze the individual effects of RexA or RexB, suggesting that Rex's influence on DNA damage sensitivity might represent a broader consequence of the overall Rex exclusion phenotype.

The λ *red* (*exo* and *bet*) genes encode the λ generalized recombination system, Red, and act at the replication fork to enhance the phage replication system (Toothman and Herskowitz 1980). The *ren* gene is adjacent to the λ DNA replication genes *O* and *P* and plays a role in λ DNA replication and repair (Thomason and Court 2022). Both λ *red* and λ *ren* circumvent Rex during λ infection and replication (Toothman and Herskowitz 1980; Thomason and Court 2022). Evidence suggests that deleting either the *ren* or *red* genes heightens λ sensitivity to Rex. (Toothman and Herskowitz 1980; Thomason and Court 2022). Without the Red system, phage DNA is more likely to be recognized as abnormal, triggering RexA sensing and subsequent the activation of RexB. Deleting either *ren* or *red* disrupts the phage's ability to maintain normal DNA replication and repair or effectively transition to lysis. This leaves the phage more exposed to RexAB-mediated defenses, which sense and respond to these molecular abnormalities. The Red recombination

proteins may protect λ from Rex exclusion by addressing the molecular triggers that activate Rex or restoring the damaged DNA caused by the Rex phenotype (Daniels et al., 1983). Recently, Thomason and Court (2022) found that the *ren* gene can rescue UV sensitivity and correct the Rex-mediated lysis phenotype caused by the expression of RexA and RexB. RexA and RexB may interfere with the NADH dehydrogenase I (NDH-1) complex, leading to NAD^+ limitation and reduced DNA ligase activity, which in turn causes replication and recombination defects. However, Ren expression may counteract the effects of RexA and RexB by promoting lysine transfer RNA (tRNA) thiolation, which helps maintain a balanced redox state in the cell and the λ phage's ability to modulate the host's cellular environment for its benefit (Thomason and Court 2022).

Gene *l* of bacteriophage T5 is essential in facilitating the bacteriophage's transfer of its DNA into host cells and subsequent degradation of host DNA (Zivanovic et al., 2014). Jacquemin-Sablon and Lanni (1973) found that T*5l* mutant phages were excluded from λ lysogenic cells. T7 20 mutant phages were also found to be eliminated from λ *rex*$^+$ lysogens, where gene 20 exhibits significant sequence similarity to *rII* of bacteriophage T4, which is essential for suppressing Rex. This Rex-dependent interference likely happens later in the lytic cycle, particularly during DNA packaging (Pao and Speyer 1975).

1.2. The *rII* Genes of Lytic Bacteriophage T4

1.2.1. Bacteriophage T4 and the *rII* Genes

The Enterobacteriaceae phage T4 is a member of the T-even coliphage family that infects the bacterium *E. coli*. It is exceptionally distinguished by its capability to undergo only a lytic replication lifecycle. T4 encapsulates a linear double-stranded DNA genome of 168,903 base pairs within its icosahedral head (Carlson et al., 1994; Kutter et al., 1995; Miller et al., 2003). The lytic T4 is one of the largest known phages and has been thoroughly studied in bacterial molecular genetics, contributing to many important discoveries in the history of genetics. The **r**apid lysis (***rII***) genes of lytic phage T4 suppress the Rex phenotype. Following the discovery of the exclusion phenotype, the *rIIA* and *rIIB* genes have been thoroughly studied to understand their characteristics and uncover the mechanism of Rex (Benzer, 1955, 1959). While the *rIIA* and *rIIB* genes (*rII* locus) are the most studied and mapped to date, their exact functions are still unknown (Benzer 1955).

The T4 and other T-even phages are known for their ability to control the timing of lysis in host cells (Paddison et al., 1998; Abedon et al., 2003). Simultaneously, they can utilize all available host resources in the environment to enhance phage propagation. At an optimal temperature of 37 $^{\circ}$C, wild-type T4 infects bacterial host cells and lyses them in approximately 25 to 30 minutes, releasing between 100 and 200 progeny per cell (Abedon et al., 2003). During the first three minutes of initial infection, if other external "superinfecting" T-even phages are present in the culture, the lysis timing can be postponed for several hours (Doermann 1948; Abedon et al., 2003). The onset of the lytic cycle is influenced by the multiplicity of infection (MOI), where the infecting phage replicates and grows within the host cell for hours, ultimately releasing up to 10^3 new progeny per cell (Doermann 1948; Abedon et al., 2003).

The **L**ysis **In**hibition phenotype (LIN) refers to the T4 phage's ability to delay its entry into the lytic cycle and postpone the lysis timing. This leads to a dramatic increase in the number of progenies released, increasing the burst size compared to regular lysis. (Hershey 1946; Benzer 1955). It was observed that LIN can be easily isolated and identified from rapid lysis mutants on plates seeded with *E. coli* B; the *rII* genes (*rIIA*-*rIIB*) are necessary for establishing LIN in *E. coli* B strains but not K strains (Hershey 1946; Doermann 1948; Benzer 1955). The classical wild-type T4 phage generates small, fuzzy-edged plaques, whereas the T4 *r* mutants, which cannot establish the LIN phenotype, form large, sharp-edged plaques as a result of rapid lysis (Figure 1-12; Hershey 1946; Benzer 1955).

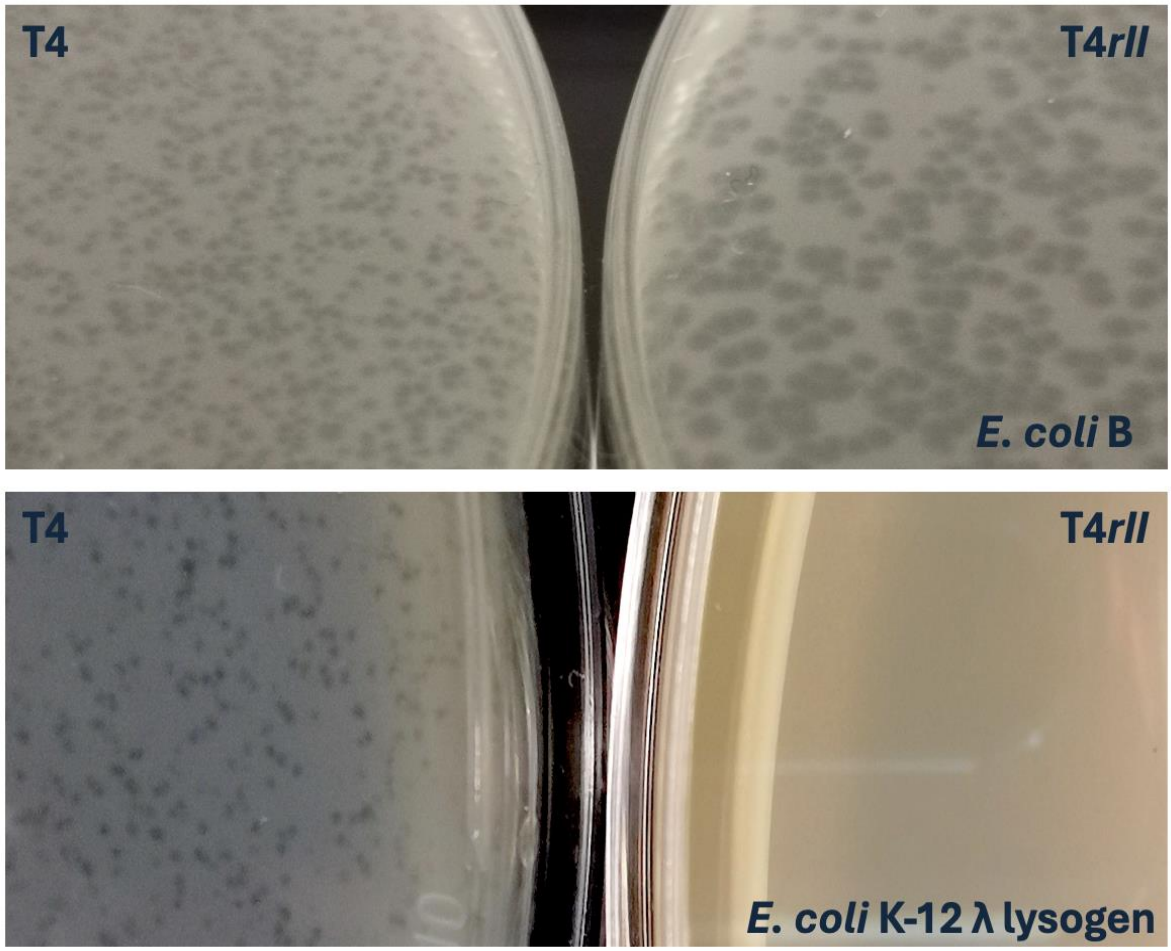


Figure 1-12. Plaque Morphology of Wild-Type T4 and T4*rII* Mutants on *E. coli* B and K-12 λ Lysogens Demonstrating the Rex Exclusion Phenotype. On *E. coli* B, wild-type T4 phage forms small plaques with diffuse, fuzzy edges, while T4*rII* mutants produce larger plaques with sharply defined edges. In contrast, on *E. coli* K-12 λ lysogens, wild-type T4 continues to form small plaques, but T4*rII* mutants are unable to form plaques, indicating complete exclusion. This inability to form plaques on λ lysogens is characteristic of the Rex exclusion phenotype, mediated by the RexA/RexB system.

Hershey (1946) and Benzer (1955) utilized the LIN phenotype to identify and map the first three rapid lysis loci of bacteriophage T4: *rI* gene, an anti-holin; the *rII* genes *rII*A and *rII*B, which are both needed to establish LIN; and the *rIII* gene, whose function has yet to be identified. Interestingly, the expression of *rexB* alone**,** whether from a multicopy plasmid or a *rexA-rexB*$^{+}$ phage, can suppress LIN in *E. coli* K strains infected by the T4*rII* phage (Slavcev and Hayes 2002)**.** This suggests that RexB can function independently of RexA to modify the host-phage interaction, possibly by disrupting the mechanism that T4 uses to induce delayed lysis. The suppression of LIN by RexB suggests that the RexB protein interferes with the signalling or membrane integrity processes necessary for lysis inhibition, effectively restoring the normal lytic cycle in which the bacterial cell rapidly lyses after infection and propagates more efficiently (Paddison et al., 1998; Slavcev and Hayes, 2002).

1.2.2. Types of the Rapid Lysis "*r*" Mutations

The discovery of T4 *r* mutants has been essential for understanding genetic recombination, the nature of the genetic code in T4 phage, and the method of point mutations at the nucleotide level. The T4 genomics analysis confirmed the location of five central *r* genes within the T4 genome map (Miller et al., 2003; Burch et al., 2011). The *rI* gene encodes the anti-holin periplasmic protein of bacteriophage T4, which is secreted into the periplasmic membrane and likely acts as a "sensor" to detect superinfection by other classical T-even phages (Paddison et al., 1998). If superinfection occurs, the release of anti-holin protein RI inhibits the T holin protein of T4 (RV) to form pores in the host cell membrane (Paddison et al., 1998).

So far, the *rIII* gene product has no clearly recognized function. However, it was suggested that RIII may enhance the interaction between RI and T-holin during LIN by providing a stabilizing effect (Ramanculov and Young 2001). The RIV protein was hypothesized to localize in the periplasm and is suggested to play a role in fixing the damaged membrane during T4 attachment and DNA injection (Abedon et al., 2003; Kai et al., 1999). The RV (T holin) is an essential protein encoded by dsDNA phages. It serves a function very

similar to that of the λ *S* holin function, even replacing it during *in vivo* λ infection (Lu and Henning 1992). Notably, the overexpression of RexB can also suppress the T4 *t* and λ *S* mutations (Slavcev and Hayes 2005). RV accumulates in the host's inner membrane, strategically timed during infection, to control the establishment of the lytic cycle and facilitate the release of new T4 progeny (Young 1992). When the T4 lytic cycle begins, the T holin protein forms holes in the cytoplasmic membrane. This action directs the *gpE* muralytic endolysin enzyme (lysozyme) to its target in the periplasm, where it hydrolyzes peptide bonds in the peptidoglycan layer, thereby lysing the cell (Josslin 1971; Young 1992). Dressman and Drake (1999) suggested that the isolated *rV* mutants probably regained holin activity but lost sensitivity to suppression by RI. This indicates that although the *rV* mutants maintained their function in facilitating cell lysis, they were no longer controlled or inhibited by the RI protein, resulting in a loss of lysis inhibition. This finding provided valuable insights into the mechanisms of lysis and lysis inhibition in bacteriophage T4.

The lytic RII proteins of T4 consist of RIIA, approximately 82.9 kDa, and RIIB, approximately 35.5 kDa. Both RII proteins appear to be ATP-dependent proteins linked with the host's inner membrane (Weintraub and Frankel 1972; Ennis and Kievitt 1973; Takacs and Rosenbusch 1975; Huang 1975). The *rII* mutants cannot grow on *E. coli* lysogenized with λ, indicating that both genes are essential for T4*rII*$^{+}$ viability (Huang 1975; Takacs and Rosenbusch 1975). The RII proteins are not critical for T4 growth on *rex*$^{+}$ lysogenic cells until 10 minutes post-infection. Before the 10-minute post-infection mark, the *rll* mutant behaves similarly to the wild-type T4*rII*$^{+}$ phage in terms of oxygen consumption and DNA and protein synthesis. After the ten-minute mark, host metabolism significantly decreases in T4*rll*-infected cells (Sauerbier et al., 1969; Parma et al., 1992; Miller et al., 2003).

However, the role of the *rII* genes in T4 replication and DNA recombination is poorly understood (Manoil et al., 1977). The RII proteins are hypothesized to localize in the inner membrane of *E. coli*, and the *rII* genes are expressed early in T4 host infection (Huang 1975; Takacs and Rosenbusch 1975). The RII membrane-associated proteins are suggested to play a structural role in linking the T4 efficient replication

complex to the host internal membrane (Mosig et al. 1984; Mosig 1987; Parma et al., 1992; Snyder and Kaufmann 1994; Paddison et al., 1998). It has been suggested that RIIA exhibits some DNA-binding activity, and when combined with RIIB, it helps stabilize the replication machinery and facilitates DNA synthesis (Huang and Buchanan 1974; Miller et al., 2003). Mutations in either *rIIA* or *rIIB* can suppress gene mutations essential for recombination, replication, and DNA packaging (Mosig et al., 1984; Mosig 1987). Reducing *rIIA* and *rIIB* levels has been linked to restoring T4 propagation in instances where the T4 ligase (gene 30) is missing or defective (Ebisuzaki and Campbell 1969; Berger and Kozinski 1969; Karam et al., 1979). Without T4 ligase activity, endonuclease nicking of T4 DNA remains unrepaired, leading to significant DNA degradation (Rossella et al., 1997; Edgell et al., 2010). This issue can be minimized through mutations in *rIIA* or *rIIB*, resulting in a similar effect to that of endonuclease II-ligase double mutants (Warner 1971). RIIA and RIIB were proposed to either enhance the activity of existing phage endonucleases or serve as endonucleases independently (Berger and Kozinski 1969). Later discoveries revealed that the RII rescue of phages lacking ligase functionality relied entirely on the presence of a host ligase (Gellert and Bullock 1970; Mosig and Breschkin 1975; Karam et al., 1979). This suggests that F products, typically involved in phage replication and assembly, may hinder the host ligase's ability to compensate for the T4 deficiency ligase (Altmann and Gennery 2016).

1.2.3. The *motA* Gene of Bacteriophage T4

Alongside the *rex* genes of bacteriophage λ and the *rII* genes of bacteriophage T4, the T4 *motA* (**mo**dulation of **t**ranscription) gene was also identified as an influencing factor on Rex. MotA, as a transcriptional activator that, together with AsiA, redirects host RNA polymerase to T4 middle promoters (mot boxes), enabling expression of middle genes (Mattson et al., 1974; Guild et al., 1988; Pande et al., 2002). Mutations in *motA* can suppress Rex-mediated exclusion, allowing T4, including *rII* mutants, to propagate in λ lysogens (Mattson et al., 1974; Shinedling et al., 1987). The onset of the Rex system activates MotA, leading to all the associated cellular manifestations of exclusionary (Johnson and Hall 1973; Mattson et al., 1974). The double mutation of *rII* and *motA* was found to bypass the Rex-mediated exclusion and was named the **R***ex* **Im**munity (*rim*) system (Mattson et al., 1974). As a result, T4 can infect and propagate regardless of the presence of Rex in the cell. Parma et al. (1992) also noted that *motA* mutants could also delay the drop in the membrane potential after T4*rII* infection of λ lysogens.

Summary

The Rex phenotype is a very complex and convoluted collection of phenotypes. Since Seymour Benzer discovered the Rex phenotype in 1955, he and other researchers have made many attempts to better understand the genomic sequence and protein locations of Rex, the mechanism of T4*rII* exclusion, RII-mediated suppression of Rex, and other peripherally connected phenotypes. It has long been believed that *E. coli* host proteins are involved in this pleiotropic phenotype, and their identification was sought as the "holy grail" to elucidate the Rex mechanism. It has been shown that the ionic environment is critically relevant to Rex activity, which can be inhibited by polyamines and divalent cations (Garen, 1968). Slavcev et al. (2003) noted that mutants of *ompF,* an outer membrane protein (Omp) that functions in osmoregulation, attenuated Rex activity. This observation was later confirmed by Alattas et al. (2020), who further uncovered the influence of OmpA, OmpW, OmpX, and OmpF in Rex activity and the attenuation of Rex in their absence, to varying severity. Additionally, a system was designed to isolate and characterize *E. coli* mutants that attenuate T4*rII* exclusion, providing essential insights into the functionality of Rex and the mechanism behind its activation. In this PhD project and upon application of the designed system, a host gene involved in Rex attenuation – the membrane protein MglC – was identified, supporting the hypothesis that Rex is a complex, multifactorial system.

In addition to the outer membrane proteins, many other membrane-associated systems, such as the Tol system, Pal, Mgl, and Gal, were investigated as potential contributors to the physiological manifestations of Rex. Given the intricate network of osmotic control and physiological states associated with Rex, sigma factors were also examined for their role in regulating gene expression during the transition from growth to stress phases. The mechanism underlying Rex exclusion has remained intricate and challenging to clarify, and the precise manner by which RII mediates the bypass of Rex remains mysterious. The data presented

here identify several novel host genes involved in Rex, leading to the proposal of a new mechanistic model to understand their interactions with RexA/B and RII.

Chapter 2

Project Hypothesis and Objectives

2.1 The Current Model and Rationale

In Alattas' MSc Thesis (2015), work, based on a mutagenesis of host genes approach, while retaining the *rex*$^{+}$ genotype, a Rex activity model involving some of the outer membrane proteins was developed. Since then, a comprehensive mutational analysis has been conducted, including many additional outer membrane protein genes related to Rex activity. While no single mutation completely abrogated the exclusion phenotype, it was postulated that the involvement of Omps would be either indirect or part of a complex signalling pathway stimulated by superinfection or Rex activation.

Δ*ompA* mutants carrying a high-copy *rex*$^{+}$ plasmid exhibited an enhanced Rex phenotype, "hyper-Rex", that conferred the ability to exclude not only T4*rII* but also T4. OmpA was suggested to may serve as a direct target for Rex proteins under natural exclusionary conditions. Upon the inhibition or targeting of OmpA, cells may undergo morphological changes, resembling a stationary phase state of arrest. Additionally, the Δ*ompA* mutants exhibited over a hundred-fold increased sensitivity to T4*rII* killing during infection, suggesting once more that Rex activity is heightened in these cells and is likely irreversible, leading to cell death at the onset of Rex. The heightened Rex phenotype observed with excessive expression of r*exA-rexB* genes may therefore be attributed to the more effective inhibition of OmpA, which is highly expressed and represented in the outer membrane. Given the reduced plating of T4 by Δ*ompA* mutants (*rex*$^{+}$), OmpA was proposed either as a direct target for inactivation by RexA and/or RexB, which may compete with RII proteins at that site to inhibit OmpA, or alternatively, RII may require interaction with OmpA to suppress Rex.

The membrane porin OmpW regulates the transport of various solutes across the outer membrane (OM). Mutation of *ompW* reduces Rex activity by more than 3×10^3-fold in a *rex*$^+$ context. Given the observed modulation of Rex activity by both OmpA and OmpW, along with their relationship to σ^E, it is quite enticing to postulate that σ^E, via *micA* and/or *rybB* expression, is directing the harsh physiological conditions associated with Rex due to the known osmotic imbalance related to membrane destabilization induced by Rex triggering, which may involve the reduction of OmpA in the outer membrane. The cell-killing effect associated with Rex may thus be directly linked to the σ^E-mediated OM destabilization arising from the down-regulated expression of *ompA* in the outer membrane, as explained in the introduction, Chapter One. Furthermore, underproduction of OmpX has also been noted to reduce σ^E activity in *E. coli* as a "strain-dependent" phenotype, which may further explain the reduction in Rex activity associated with this mutation in *rex*$^+$ cells. OmpX or OmpF, either in conjunction with OmpC, are viable candidates involved in Rex activity, based on their functions and what is known about the Rex proteins.

The ionic environment is crucial for the onset of the Rex phenotype – monovalent cations are essential for its initiation, while divalent cations attenuate the phenotype. Upon infection with T4*rII*, OmpX, as a virulence factor, can protect *E. coli* cells by maintaining the surface hydrophobicity and the negative charge on the cell surface. Puncturing the cell surface through T4*rII* phage adsorption would disrupt surface stability, activating Rex, which would allow OmpX to re-stabilize the surface hydrophobicity and send a signal to σ^E to initiate the stress response. This would influence subsequent cell adhesion and susceptibility to infection, as well as the stability of host cells. In the absence of OmpX, σ^E activation would not ensue. In contrast, OmpW, OmpF, and OmpC may be indirectly involved in triggering Rex by modulating osmotic stress, which includes activation of σ^S, potentially initiated by RexB-mediated disruption of the membrane potential. Deletion of one of these genes would decrease the rate and ability of cells to sense and correct osmolarity, and to enter the stationary phase before T4*rII* can replicate, thereby increasing the plating efficiency of T4*rII* in these *rex*$^+$ mutants.

T4*rII* adsorbs to OmpC on the outer surface of the host. OmpC and OmpF function as cation-charge channels but also play significant roles in influencing Rex activity, with OmpC, particularly the T4 adsorption site, being a key target candidate. OmpF and OmpC regulate cell osmolarity in response to changes in the growth medium's osmolarity. When cells grow in high osmotic medium, *ompC* is preferentially expressed; in contrast, in a low osmotic environment, *ompF* is expressed to stabilize cellular osmosis.

The penetration of a T4 phage's tail will lyse the peptidoglycan of both the outer membrane and the inner membrane, causing a disturbance in periplasmic and cytoplasmic osmolarity. In this scenario, the cytoplasm becomes more acidic than usual, resulting in the stimulation of the phosphatase enzyme via OmpR (EnvZ) and heightened *ompF* expression to restore cell osmolarity (K^+ efflux). This action could result in 1) increased diffusion of cation charge through OmpF ion channels outside cells; 2) the presence of monovalent cation charges in the medium that permit Rex 'activation'; and 3) production of free σ^S and σ^E factors to initiate a cellular 'stationary-like' phase. Deleting *ompF* might reduce Rex activity and slightly allow T4*rII* plating due to the inability of this mutant *rex*$^+$ lysogen to restore the normal osmotic state of monovalent cations inside the cell after infection, which is essential for initiating Rex (Figure 2-1; Alattas MSc. Thesis, 2015).

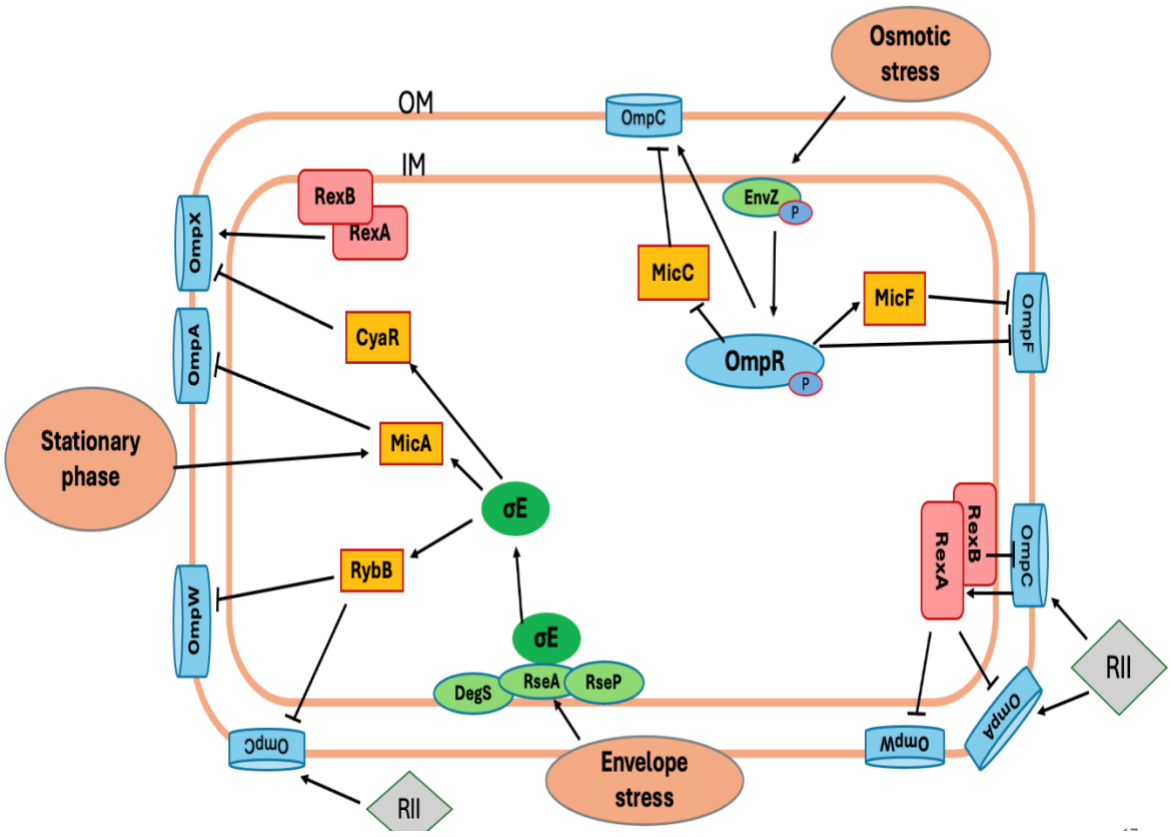


Figure 2-1. Proposed Model of Rex System Activation Involving Outer Membrane Proteins. Under stress conditions, *E. coli* increases the production of outer membrane proteins (Omp), resulting in elevated expression of the sigma factor σ^E and inducing a stationary phase-like physiological state. The Rex system may be activated either by general Omp activity or by specific Omps, triggering a shift in cellular metabolism. This model suggests a regulatory link between envelope stress responses and Rex-mediated exclusion. Figure key: Blue ovals/cylinders, outer membrane proteins (Omps); Gray diamonds, RII proteins of T4 phage; Red boxes, Rex proteins of λ; Yellow boxes, small RNAs regulating *omp* genes transcription and Omp expression; Green ovals, regulatory proteins controlling sigma factors expression; Blunted arrows indicate inhibition/downregulation/blocking expression; Regular arrows indicate stimulation/upregulation/initiation of expression; OM: outer membrane; IM: inner membrane.

Based on these leads, the following hypothesis is formulated, which will be evaluated through the ensuing objectives for the current work.

2.2 Hypothesis

The Rex-mediated establishment of a harsh, yet transient, cellular environment is dependent on the coordinated action of λ *rexA* and *rexB*, in conjunction with *E. coli* host stress response genes, to enact this complex yet reversible scenario. The onset of Rex represents the induction of a native membrane stress response in *E. coli*, as a physiological state that is aberrantly triggered by activation of the Rex system, thereby conferring transient immunity to superinfection.

The comprehensive and systematic analysis of host mutations that influence Rex may serve to identify the "puzzle pieces" involved directly and indirectly in "triggering" and inducing the cellular (physiological) manifestations of the Rex phenotype. Notably, this induced state mimics a naturally occurring membrane stress response in *E. coli* but is artificially triggered by the presence of phage elements associated with superinfection. Specifically, RexA acts as a sensor of foreign phage DNA or proteins. In contrast, RexB, a membrane-associated protein, modulates cellular ion homeostasis or membrane potential, resulting in a rapid but reversible physiological shift. This shift renders the host cell refractory to further phage infection by creating an intracellular environment incompatible with the injection, replication, or transcription of superinfecting phage DNA. Importantly, this response is non-lethal and reversible, allowing the host to recover normal physiological function once the threat of superinfection is resolved.

In combination with the current understanding of the vital effects of the ionic environment and how monovalent and divalent cations, as well as polyamines, influence Rex activity, I hypothesize that, in addition to σ^E-dependent stress response proteins, other sigma-dependent stress response proteins and their regulators may be involved in the Rex mechanism. As such, assessing the influence of various σ^S stationary phase-related genes on Rex activity is necessary to further understand the mechanism behind T4*rII*

exclusion. Moreover, since we know so little about RexA, RexB, and RII proteins, it would further prove beneficial to develop a system for easily probing Rex protein interactions and localizations upon Rex onset and in the 'primed' state.

The Rex phenotype is a very complex system; however, the information garnered from these experiments should further aid in our understanding of the Rex phenotype and the elucidation of this enigmatic exclusion mechanism.

2.3 Objectives

1. Identification of host genes influencing the Rex$^-$ phenotype via insertional mutagenesis.
    a. To screen and validate *rex*$^+$ *E. coli* mutants that exhibit a Rex$^-$ phenotype by assessing their sensitivity to T4*rII* phage plating. These mutants, although genotypically *rex*$^+$, display a phenotypic loss of Rex function. Enhanced T4 and T4*rII* plaque formation will serve as an indicator of disrupted host genes potentially involved in the Rex exclusion mechanism. This screening is performed as a result of an insertional mutation system, in which transposon insertions randomly disrupt host genes while simultaneously delivering a functional *rex*$^+$ allele into the host genome. The dual function enables the identification of host genes that are directly or indirectly required for Rex activity.
    b. To identify host genes disrupted by transposon insertion that attenuate or abrogate *rII* exclusion. Inverse PCR will be employed to amplify and sequence the genomic regions flanking the Tn*10* insertion sites. Functional annotation of these genes will elucidate their potential roles in the Rex pathway and provide mechanistic insights into host contributions to the exclusion phenotype.

2. Functional screening of *E. coli* host genes involved in Rex/ RII activity.
    a. To systematically evaluate candidate membrane-associated genes and their regulators hypothesized to influence Rex activity. Using the Keio collection of single-gene knockouts, each strain will be tested for altered sensitivity to T4 and T4*rII* using a plating assay. A loss or reduction of Rex-mediated exclusion will indicate the involvement of the deleted gene in the Rex exclusion mechanism.
    b. To confirm the role of candidate genes identified in the knockout screen by the complementation assay. Restoration of Rex activity upon reintroduction of the wild-type gene will validate its functional contribution to the Rex phenotype.
3. Development of a Rex protein visualization system and functional analysis using fluorescent tagging
    a. To construct Green and Red Fluorescent Proteins (GFP and RFP)-tagged RexA, RexB, and RexAB fusion proteins at both N- and C-terminal sites. These constructs will be used to study the expression dynamics of Rex proteins via fluorescence microscopy.
    b. To assess the impact of fluorescent tagging on Rex function by evaluating T4*rII* plating efficiency in strains expressing the tagged constructs. This will determine whether the fusion site or Rex protein type affects Rex-mediated exclusion.
    c. To evaluate Rex protein expression and stability by comparing fluorescence signal intensity and distribution under induced and non-induced conditions.
    d. To assess the physiological effects of expressing tagged Rex proteins in host cells by analyzing colony morphology, growth characteristics, and transformation efficiency in both wild-type and λ*cI* temperature-sensitive lysogens. This will help identify any deleterious effects associated with specific fusion constructs under varying genetic and environmental conditions.

Chapter 3

Materials and Methods

3.1 Strains and Plasmids

Table 3-1 lists and describes all the plasmids, bacterial strains and phage strains used in this study.

Table 3-1: Bacterial strains, phage, plasmids, and primers used in this study

Designation	Description	Source
Bacterial Strains		
DH5α	F-, Δ*(argF-lac)169, ϕ80dlacZ58(*M15*), ΔphoA8, glnV44(*AS*), λ-, deoR481, rfbC1, gyrA96(NalR), recA1, endA1, thi-1, hsdR17*	*E. coli* Genetic Stock Collection (CGSC) #12384
DH5α (λ*pir*)	DH5α lysogenized by phage λ434 (heteroimmune derivative) containing the *pir* gene	Gift from Dr. Charles lab, Biology department, UW (2009)
W3110	F-, λ-, *IN*(*rrnD-rrnE*)*1, rph-1*	CGSC# 4474
BW25113 wt	F-, *567*, *ΔlacZ4787*(::rrnB-3), λ^-, *rph-1*, *Δ(rhaD-rhaB)568*, *hsdR514*	CGSC# 7636
JW0427-1	Δ*clpP::km*^{R}, λ^-	CGSC# 8590
JW0727-1	BW25113 isogenic derivative: *ΔtolQ786:: km*^{R}	CGSC# 8793 (Baba et al., 2006; the Keio collection)
JW0728-1	BW25113 isogenic derivative: *ΔtolR787:: km*^{R}	CGSC# 8794 (Baba et al., 2006; the Keio collection)
JW0729-3	BW25113 isogenic derivative: *ΔtolA788:: km*^{R}	CGSC# 8795 (Baba et al., 2006; the Keio collection)

JW5100-1	BW25113 isogenic derivative: *ΔtolB789:: km^R*	CGSC# 11174 (Baba et al., 2006; the Keio collection)
JW5437-1	BW25113 isogenic derivative: *ΔrpoS746:: km^R*	CGSC# 11387 (Baba et al., 2006; the Keio collection)
UQ285	P90A5 isogenic derivative: *rpoD285*[ts]	CGSC# 6328 (Isaksson et al., 1977)
JW5503-1	BW25113 isogenic derivative: *ΔtolC732:: km^R*	CGSC# 11430 (Baba et al., 2006; the Keio collection)
JW0739-1	BW25113 isogenic derivative: *ΔgalM728:: km^R*	CGSC# 8802 (Baba et al., 2006; the Keio collection)
JW0740-3	BW25113 isogenic derivative: *ΔgalK729:: km^R*	CGSC# 8803 (Baba et al., 2006; the Keio collection)
JW0741-1	BW25113 isogenic derivative: *ΔgalT730:: km^R*	CGSC# 8804 (Baba et al., 2006; the Keio collection)
JW0742-1	BW25113 isogenic derivative: *ΔgalE740:: km^R*	CGSC# 8297 (Baba et al., 2006; the Keio collection)
JW1224-1	BW25113 isogenic derivative: *ΔgalU745:: km^R*	CGSC# 9110 (Baba et al., 2006; the Keio collection)
JW2027-2	BW25113 isogenic derivative: *ΔgalF731:: km^R*	CGSC# 9664 (Baba et al., 2006; the Keio collection)
JW2135-1	BW25113 isogenic derivative: *ΔmglC775:: km^R*	CGSC# 9730 (Baba et al., 2006; the Keio collection)
JW2136-1	BW25113 isogenic derivative: *ΔmglA776:: km^R*	CGSC# 9731 (Baba et al., 2006; the Keio collection)
JW2137-1	BW25113 isogenic derivative: *ΔmglB777:: km^R*	CGSC# 9732 (Baba et al., 2006; the Keio collection)
JW2138-1	BW25113 isogenic derivative: *ΔgalS778:: km^R*	CGSC# 9733 (Baba et al., 2006; the Keio collection)
JW2805-1	BW25113 isogenic derivative: *ΔgalR762:: km^R*	CGSC# 10192 (Baba et al., 2006; the Keio collection)
JW2910-2	BW25113 isogenic derivative: *ΔgalP789:: km^R*	CGSC# 10251 (Baba et al., 2006; the Keio collection)
JW3996-1	BW25113 isogenic derivative: *ΔlamB732:: km^R*	CGSC# 10877 (Baba et al., 2006; the Keio collection)
JW1667-5	BW25113 isogenic derivative: *Δlpp-752::km^R*	CGSC # 9417 (Baba et al. 2006; the Keio collection)
JW2974-1	BW25113 isogenic derivative: *ΔexbB779:: km^R*	CGSC# 10285 (Baba et al., 2006; the Keio collection)
JW2973-1	BW25113 isogenic derivative: *ΔexbD778:: km^R*	CGSC# 10284 (Baba et al., 2006; the Keio collection)

JW5195-1	BW25113 isogenic derivative: *ΔtonB760:: km^R*	CGSC# 11229 (Baba et al., 2006; the Keio collection)
JW0146-2	BW25113 isogenic derivative: *ΔfhuA766:: km^R*	CGSC# 8416 (Baba et al., 2006; the Keio collection)
JW5086-3	BW25113 isogenic derivative: *ΔfepA721:: km^R*	CGSC# 11165 (Baba et al., 2006; the Keio collection)
JW1223-1	BW25113 isogenic derivative: *ΔrssB744:: km^R*	CGSC# 9101 (Baba et al., 2006; the Keio collection)
JW1222-2	BW25113 isogenic derivative: *ΔrssA743:: km^R*	CGSC# 9108 (Baba et al., 2006; the Keio collection)
JW0373-4	BW25113 isogenic derivative: *ΔiraP747:: km^R*	CGSC# 8551 (Baba et al., 2006; the Keio collection)
JW1147-5	BW25113 isogenic derivative: *ΔelbA749:: km^R (ΔiraM)*	CGSC# 9066 (Baba et al., 2006; the Keio collection)
JW5782-2	BW25113 isogenic derivative: *ΔyjiD724:: km^R (ΔiraD)*	CGSC# 11574 (Baba et al., 2006; the Keio collection)

Phage

T*4D*	Wild type T4	Obtained from Mosig G (2009), Slavcev lab Freezer Pro # 23 phage box
T4*rII*Δ1586	Δ(*rIIA-rIIB*)	Obtained from Mosig G. (2009), Slavcev lab Freezer Pro # 24 phage box
λ (*cI*857)	*cI*[ts]*857,* (*rex*$^+$)	NBRP # ME6104 (2009)

Plasmids

pUC19	High copy number plasmid; MCS-*lacZ*α, Ap^R	NEB # N3041S, Whitby, Canada
pPL451	Mid copy number plasmid, Ap^R, driven by Lambda PR and PL promoters	Love CA, Lilley PE, Dixon NE. *Gene* 176 (1996): 49–53
pBR322	Ap^R, Tc^R	Bolivar et al., 1977
pBS1479	High copy number plasmid contains TAP tag: Protein A (IgG-binding) + TEV cleavage site + Calmodulin-binding peptide (CBP). For C-	Gift from Dr. Edyta Marcon Donnelly Centre, University of Toronto (2021)

	terminal tagging of proteins for tandem affinity purification (TAP)	Puig et al., *Methods* (2001); Kilchert et al., *Cell Reports* (2015)
pHA1	pUC19 [*cI-rexA-rexB*]; MCS- *lacZ*α, Ap^R, *pM-cI857-rexA-rexB-*t_{imm}	Alattas MSc Thesis, 2015; Alattas et al., 2020
pHA2 (pRex)	pBSL199 [*cI-rexA-rexB*]; IS10-Tc^R, *pM-cI857-rexA-rexB-*t_{imm}	Alattas MSc Thesis, 2015; Alattas et al., 2020
pPL451 -*egfp*	EGFP cloned into MCS of pPL451	This study
pPL451 (eGFP::RexA)	EGFP fused to the N-terminus of RexA in pPL451 plasmid	This study, made by GenScript
pPL451 (eGFP-linker-RexA)	EGFP fused to the N-terminus of RexA and separated by linker, Linker sequence p(TSGSGSGSGSGT)	This study, made by GenScript
pPL451 (RexA::eGFP)	EGFP fused to C-terminus of RexA	This study, made by GenScript
pPL451 (RexA-linker-eGFP)	EGFP fused to the C-terminus of RexA and separated by linker, Linker sequence p(TSGSGSGSGSGT)	This study, made by GenScript
pPL451 (eGFP::RexB)	EGFP fused to the N-terminus of RexB	This study, made by GenScript
pPL451 (eGFP-linker-RexB)	EGFP fused to the N-terminus of RexB and separated by linker, Linker sequence p(TSGSGSGSGSGT)	This study, made by GenScript
pPL451 (RexB::eGFP)	EGFP fused to the C-terminus of RexB	This study, made by GenScript
pPL451 (RexB-linker-eGFP)	EGFP fused to the C-terminus of RexB and separated by linker, Linker sequence p(TSGSGSGSGSGT)	This study, made by GenScript
pPL451 (eGFP::RexA-RexB)	EGFP fused to the N-terminus of RexA, RexB present on the same ORF and separated with 16 bp from RexA	This study, made by GenScript
pPL451 (eGFP-linker-RexA-RexB)	EGFP fused to the N-terminus of RexA and separated by linker, Linker sequence p(TSGSGSGSGSGT). RexB present on the same ORF	This study, made by GenScript

pPL451 (RexA::eGFP-RexB)	EGFP fused to the C-terminus of RexA. RexB present on the same ORF.	This study, made by GenScript
pPL451 (RexA-eGFP::RexB)	EGFP fused to the N-terminus of RexB, RexA present on the same ORF and separated with 16 bp from RexB	This study, made by GenScript
pPL451 (RexA-eGFP-linker-RexB)	EGFP fused to the N-terminus of RexB and separated by linker, Linker sequence p(TSGSGSGSGSGT). RexA present on the same ORF	This study, made by GenScript
pPL451 (RexA-RexB::eGFP)	EGFP fused to the C-terminus of RexB. RexA present on the same ORF	This study, made by GenScript
pPL451 (RexA-RexB-linker-eGFP)	EGFP fused to the C-terminus of RexB and separated by linker, Linker sequence p(TSGSGSGSGSGT). RexA present on the same ORF	This study, made by GenScript
pPL451 (eGFP::RexA-RFP::RexB)	EGFP fused to the N-terminus of RexA. RFP fused to the N-terminus of RexB. All present on the same ORF	This study, made by GenScript
pPL451 (eGFP-linker-RexA-RFP-linker-RexB)	EGFP fused to the N-terminus of RexA and separated by linker. RFP fused to the N-terminus of RexB and separated by linker. All present on the same ORF.	This study, made by GenScript
pPL451 (RexA::eGFP-RexB::RFP)	EGFP fused to the C-terminus of RexA. RFP fused to the C-terminus of RexB. All present on the same ORF.	This study, made by GenScript
pPL451 (RexA-linker-eGFP-RexB-linker-RFP)	EGFP fused to the C-terminus of RexA and separated by linker. RFP fused to the C-terminus of RexB and separated by linker. All present on the same ORF	This study, made by GenScript
pPL451 (eGFP::RexA-RexB::RFP)	EGFP fused to the N-terminus of RexA. RFP fused to the C-terminus of RexB. All present on the same ORF.	This study, made by GenScript
pPL451 (eGFP-RexA-RexB-linker-RFP)	EGFP fused to the N-terminus of RexA and separated by linker. RFP fused to the C-terminus and separated by linker. All present on the same ORF.	This study, made by GenScript

Primer* **	**Target gene**	**Sequence (5'- 3')**
IS10 -F	IS*10* transposon (for amplify flanking region)	CTTTGGTCACCAACGCTTTTCCCG
IS10 -R	IS*10* transposon (for amplify flanking region)	GGCCACGCGTCGACTAGTAC
Tn*10* Primer #1 -F	Tn*10* region (general amplification or sequencing of Tn*10* region)	TTGCTGCTTATAACAGGCACTGAG
Tn*10* Primer #2 -R	Tn*10* region (degenerate primer for inverse PCR, random hexamers)	GGCCACGCGTCGACTAGTACNNNNNNNNNNGCTGG
Tn*10* Primer #3 -F	IS10-specific primer (flanking region amplification)	CTTTGGTCACCAACGCTTTTCCCG
Tn*10* Primer #4 -R	Tn10 region (adaptor or linker primer for inverse PCR)	GGCCACGCGTCGACTAGTAC
rexA -F	*rexA*	AATTGAATTCATGAGTAAAGGAGAAGAACT
rexA -R	*rexA*	AATTGAGCTCAGTTCTTCTCCTTTACTCAT
rexB -F	*rexB*	AATTGAATTCATGGCTAGTGAAGAGGTTGT
rexB -R	*rexB*	AATTGAGCTCACAACCTCTTCACTAGCCAT
rexA-B -F	*rexA-rexB*	AATTGAATTCATGAGTAAAGGAGAAGAACT
rexA-B -R	*rexA-rexB*	AATTGAGCTCAGTTCTTCTCCTTTACTCAT
ompA -F **	*ompA*	CCGGTTTCAGGGTTGCTTTG
ompA -R**	*ompA*	AAAGGCAGCGTTGAAAACGG
ompF -F **	*ompF*	ATGGCGACATGACCTATGCC
ompF -R**	*ompF*	AAGTAGTAGGTTGCGCCCAC
ompW -F **	*ompW*	TCTCTCTGGCAGTGCCTTTG
ompW -R**	*ompW*	GCAGCTCCCCAGGAATCTTT
ompX -F **	*ompX*	GCATGTCTTTCAGCACTGGC
ompX -R**	*ompX*	TAACCAACACCGGCAATCCA
mglC -F **	*mglC*	CTCGGTGTGGCAGGGTTAAT
mglC -R**	*mglC*	TCAGTGAATCCAGCGCTACG
mglA -F **	*mglA*	CGTCCTCCGGGGAATACTTG
mglA -R**	*mglA*	ACGCAAGACGCAGAATTTCG
mglB -F **	*mglB*	TGGCCAGCATGTTATTCGGT
mglB -R**	*mglB*	CCTTTACCATCGGCCAGGTT
tolA -F **	*tolA*	GGTGCGGTAGTTGAGCAGTA

tolA -R**	*tolA*	AAGCATTGTTCCCTTTCGCC
lpp -F **	*lpp*	ATGGTTTCTGGTGCACTGGT
lpp -R**	*lpp*	AGTCAGCGCAGAATGGTGAA
tolQ -F **	*tolQ*	TCAATCGCATCTTGGGCCAT
tolQ -R**	*tolQ*	TTACCCCTTGTTGCTCTCGC
tolR -F **	*tolR*	GAGGTCGTCGCGATCTCAAG
tolR -R**	*tolR*	CCGATTTCACACCCGCACTA
lamB -F **	*lamB*	GCACGTTCCGGTATTGGTTG
lamB -R**	*lamB*	TGAAATCAGCAGGAACGGCT
rssA -F **	*rssA*	TGCGATCGATTATCTGCGCT
rssA -R**	*rssA*	ACCAACGGCAAAAGTTCGTC
rssB -F **	*rssB*	AGCAGGTATTTCGCTCGCTT
rssB -R**	*rssB*	GACAACATCAAGCGCAGTCG
rpoS -F **	*rpoS*	AACTGTTATCGCAGGGAGCC
rpoS -R**	*rpoS*	CCCTGCGTTTGCAGGATTTC
iraD -F **	*iraD*	TGCGACAATCACTTCAGGCT
iraD -R**	*iraD*	CCAACCGCCATTATCCCAGA

CGSC: Coli Genetics Stock Center NEB: New England Biolabs

**RE: Restriction enzyme, *Xba*l: TCTAGA, Overhang: 5′ CTAG.

** All genes included in the complementation assay

*** All primers were made by Sigma Aldrich, Oakville, Canada

3.2 Plasmid Maps

Maps of pHA1 and pHA2 (pRex) are shown in Figures 3-1 and 3-2. PHA1 was used to introduce the *rexA* and *rexB* genes of λ into the cell, thereby conferring the Rex phenotype. pHA2 was used to create Rex^{-} mutants through transpositional *E. coli* insertional inactivation mutations.

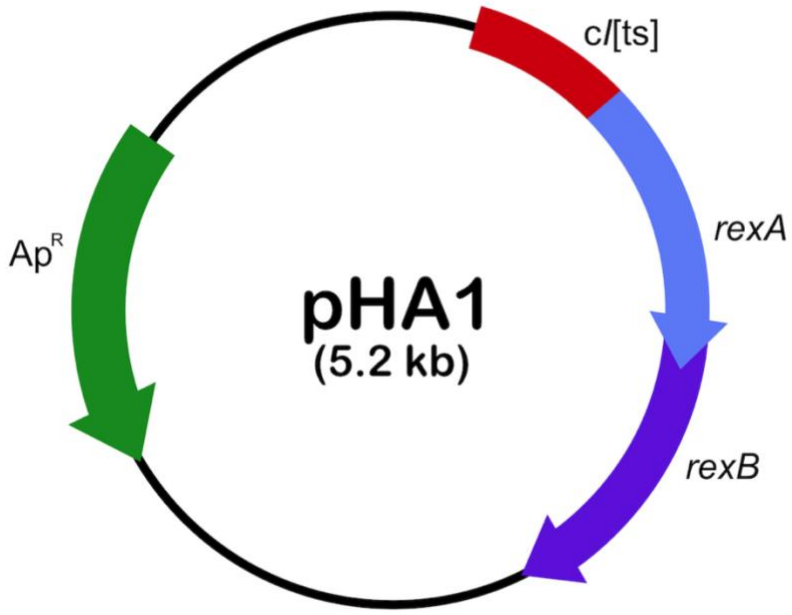


Figure 3-1. Plasmid pHA1 Map. Plasmid PHA1is a high-copy-number plasmid derived from pUC19, engineered to carry the *rexA* and *rexB* genes. Their expression is regulated by the temperature-sensitive *cI*[ts] repressor, enabling conditional control of Rex system activation through temperature shifts. *Source: Alattas MSc Thesis, 2015.*

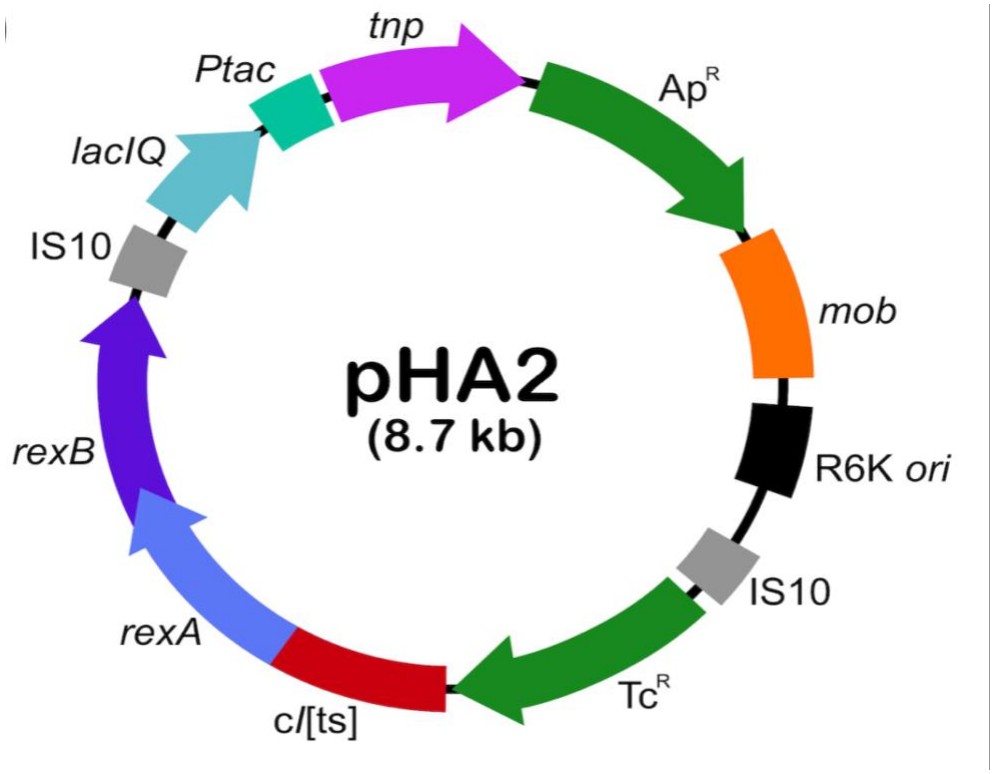


Figure 3-2. The pHA2 pRex Suicide Construct for Rex Operon Chromosomal Integration. The pHA2 construct is a suicide plasmid based on the R6K origin of replication, carried by the vector pBSL199, which cannot replicate in wild-type *E. coli* (*pir*$^{-}$). It contains a thermos-regulated P_M-*cI*857-*rexA*-*rexB*-t_{imm} cassette flanked by two IS10 elements. Upon induction of Tn*10* transposase expression, the mini-Tn*10* cassette, encoding the *rex* operon, can transpose into the host chromosome, generating a library of insertional mutants. All resulting clones are genotypically *rex*$^{+}$, ensuring that any isolated Rex^{-} phenotype arises from insertional inactivation of host genes involved in Rex function. This construct also encodes: *lac*I^{Q}: a mutant lac repressor that modulates *Lac*I expression; P_{tac}: an IPTG-inducible promoter controlling downstream gene expression; *tnp*: Encodes transposase enzyme, stimulates transposition of transposable element; *mob*: a mobilization gene enabling conjugative plasmid transfer between donor and recipient cells; Ap^{R}: ampicillin resistance marker on the plasmid backbone; Tc^{R}: tetracycline resistance marker within the transposable element. *Source: Alattas MSc. Thesis 2015.*

The plasmid pPL451 (Figure 3-3) was used as the backbone for generating a series of *rex::egfp* fusion constructs. The Rex proteins, RexA, RexB, and the combined RexA-RexB, were cloned individually or in combination into the MCS of pPL451, enabling either C-terminal or N-terminal fusion to GFP alone or both GFP and RFP. These constructs were designed to assess the expression, stability, and functional impact of fluorescently tagged Rex proteins. A comprehensive list of all generated constructs is provided in Table 3-1, and their corresponding plasmid maps are presented in Appendix C (Figures Appendix C1-11).

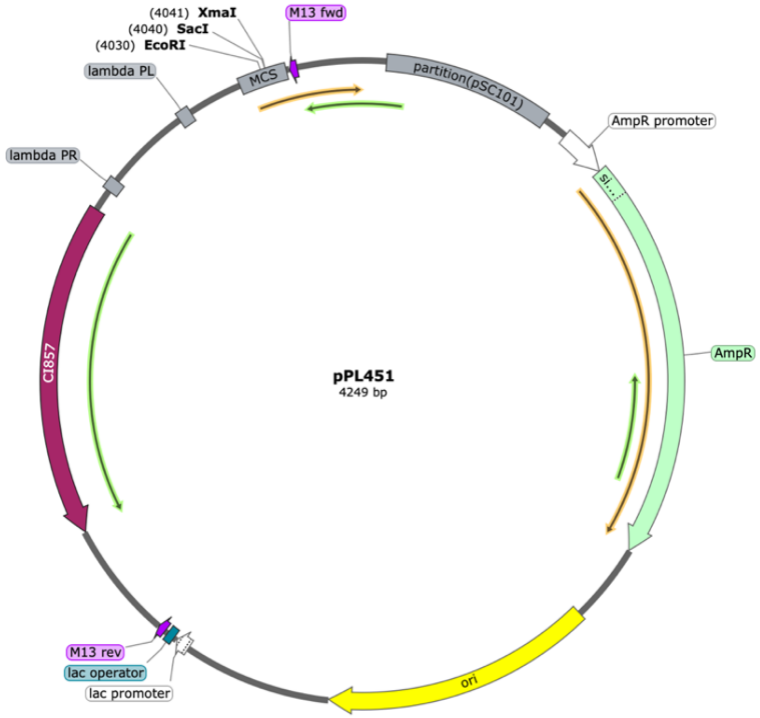


Figure 3-3. pPL451 Vector Map for Conditional Expression of *rex::egfp* Cassettes. This plasmid map illustrates the pPL451 vector, highlighting the multiple cloning site (MCS) where the *rex::egfp* fusion cassettes are inserted. The vector is designed for conditional gene expression, allowing controlled studies of Rex function and localization via eGFP tagging. *Created by SnapGene.*

The following maps of pUC19 and pBR322 were selected to facilitate the complementation assays. Both are well-characterized plasmids with features compatible with standard cloning techniques. pUC19 offers a versatile multiple cloning site (MCS) that supports flexible insertion of target genes. The pBR322 plasmid provides relevant restriction sites within the tetracycline resistance region, enabling the selection and expression of complementing alleles. The plasmid maps (Figures 3-4 and 3-5) illustrate the key restriction sites and structural features relevant to the cloning strategies used in the complementation assay.

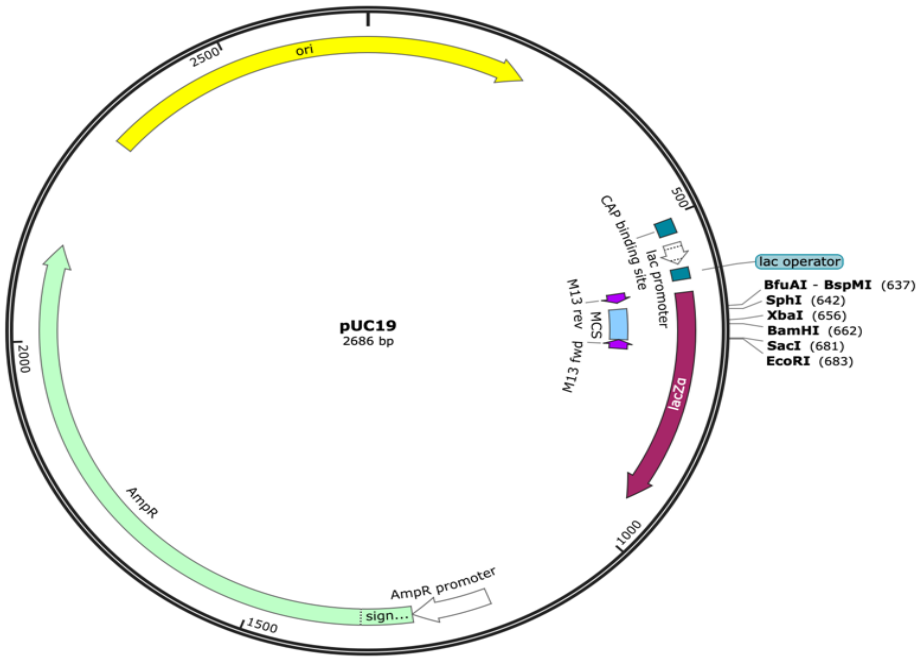


Figure 3-4. Plasmid Map of pUC19 Used in Complementation Assays. This vector features a high-copy origin of replication and a multiple cloning site (MCS) containing several restriction enzyme sites, allowing for flexible insertion of target genes. It's an ampicillin resistance marker that facilitates selection in *E. coli*. The map was generated using SnapGene.

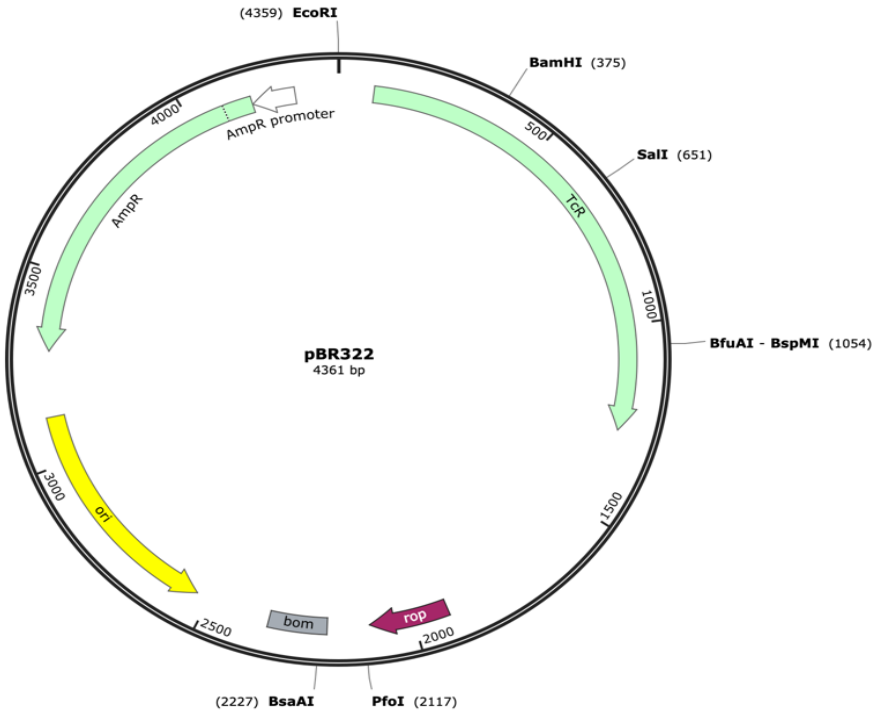


Figure 3-5. Plasmid Map of pBR322 Used in Complementation Assays. The pBR322 vector contains a tetracycline resistance gene (Tet) region interrupted by the insertion of target genes at specific restriction sites. It offers a medium-copy origin of replication and is widely used for stable maintenance of cloned sequences. The plasmid map was generated using SnapGene.

3.3 Phage Lysate Preparation and Purification

E. coli K-12 W3110 (wild-type host strain) was plated at 30 °C overnight (O/N). A culture was prepared at 30 °C while shaking at 225 RPM O/N. A subculture was prepared from the overnight culture at a 1:100 dilution and was grown to an optical density of $A_{600} = 0.4$ (Spectrophotometer, Fisher Bio-Scientific, Ottawa, Canada). Primary lysate serial dilutions were prepared in Tris-NaCl (TN) buffer pH 7.8 (Fisher Scientific, USA) in 1:10 increments to determine the optimal concentration before adding lysates to the bacterial stocks. Lysate dilutions of phage were added at a maximum volume of 300 µL to fresh cell cultures, along with 3 mL of top agar. The mixture was then immediately poured onto LB plates and incubated overnight

at 37 °C. The plates were then examined for consistent and productive lysis patterns the next day, and productive plates were used to prepare phage lysates, where one of the following techniques was performed:

1) Plate lysate preparation: Plates with productive lysis patterns were incubated at 4 °C for 4-24 h with 10 mL of TN buffer. The solutions and top agar were transferred into pre-chilled conical tubes, and 45 µL of chloroform ($CHCl_3$) was added. Lysates were incubated on ice for 20 min. To remove any cellular debris, the mixtures were centrifuged at 4 °C for 30 min and then filter-sterilized using a 0.45 µm polyether sulfone filter membrane (VWR, Mississauga, Canada). They were subsequently stored at 4 °C.

2) Liquid lysate preparation: A single plaque was isolated and incubated with 300 µL of fresh O/N culture of wild-type cells at 37 °C for 30 min. Next, 10 mL of pre-warmed LB was added to the culture and incubated at 37 °C while shaking at 260 RPM for 4-5 hours. The cultures were monitored for a pattern of turbidity followed by clearing, at approximately 4-5 h, to a final A_{600}= 0.05. The lysate was incubated on ice for 10 min, and 45 µL of $CHCl_3$ was added before further incubation for an additional 10 min. Mixtures were centrifuged at 4 °C for 30 min at 12,000 RPM to remove cell debris and filter-sterilized using a 0.45 µm polyether sulfone filter membrane (VWR, Mississauga, Canada). The filtrate was stored at 4 °C.

3.4 Plate Overlay Phage Titration and Efficiency of Plating (EOP) Assay

Lysate dilutions ranging from 10^{-2} to 10^{-8} phage/mL were prepared in TN buffer and added in 10 µL aliquots to 300 µL of fresh O/N W3110 culture. Top agar (3 mL) was added to the mixture and was immediately poured on LB plates. Each lysate dilution (10 µL) was dropped onto the solidified top agar and then incubated overnight at 30 °C. Plaque counts were calculated the following day relative to plating efficiency and Rex activity compared to the 100% control strain, W3110.

3.5 Assessing Rex and T4*rII* Activity

Cultures of W3110/BW25113 (wt) and W3110/ BW25113 (λ) were prepared in 5 mL aliquots at a 1:100 dilution. Cultures were then incubated while shaking O/N. The next day, 300 µL of culture was added to 3 mL of top agar and poured immediately onto pre-warmed LB plates and then left at room temperature to solidify. Serial dilutions of T4 (wt) and T4r*II* lysates were prepared in TN buffer with concentrations ranging from 10^{-2} to 10^{-8} phage/mL to quantify plating efficiency and Rex activity. Lysates were added in 10 µL drops onto W3110/ BW25113 (wt) and W3110/ BW25113 (λ) overlay plates. Plates were left to dry for 30 min, then incubated overnight at 30 °C. The following day, plates were assessed, and plaques (when evident) were quantified.

3.6 *E. coli* K-12 Host Transformation

E. coli strains and their resident plasmids are shown in Table 1. O/N cultures (5 mL) of host cells were prepared, shaking at 30 °C. Subcultures were prepared the following day at a dilution of 1:100 and grown for 3- 4 h (A_{600} = 0.4-0.6). Cells were incubated on ice for 10 min, then centrifuged at 4 °C RPM (Avanti J-E Centrifuge, Beckman Coulter, Mississauga, Canada) for 30 min. The supernatant was discarded, and the pellet was washed with 20 mL of pre-chilled, sterile deionized water (ddH2O) to remove any charged particles that could interfere with the electroporation process. Cells were centrifuged at 4000 RPM again for 10 min at 4 °C. The supernatant was discarded, and the pellet was washed with 10 mL of pre-chilled sterile ddH_2O. Cells were centrifuged at 4000 RPM for 10 min at 4 °C, and the pellet was resuspended to a final volume of 1.0-5.0 mL with pre-chilled sterile ddH_2O. Small aliquots (100 µL per tube) were prepared, and plasmid DNA with a concentration ranging from 0.5 µg to 1.0 µg was added and mixed with electro-competent cells. The mixture was then incubated on ice for 10 min. The mixture was added to the pre-chilled electroporation cuvettes and pulsed for 3 seconds at 1000 V using the Electroporator 2510 (Eppendorf, Mississauga, Canada). Cells were immediately resuspended in 1 mL of pre-warmed SOC medium and incubated at 37 °C, while shaking at 50 RPM for one hour. Aliquots of cells (200-250 µL)

were then plated on selection antibiotic plates and incubated overnight at 30 °C. Serial dilutions of electroporated cells were plated at various temperatures ranging from 23 °C, 30 °C, 35 °C, and 37 °C to assess the relative efficiency of transformation, where necessary.

3.7 Calcium Chloride Heat Shock Transformation

Calcium-competent *E. coli* cells (wild-type or mutants) were prepared (100 µL aliquots in microcentrifuge tubes) and left on ice for approximately 30 min to thaw. 100-200 ng of plasmid DNA was then added to the cells and left on ice for 30–45 minutes. Subsequently, the cells were placed in a 42 °C water bath for 90 seconds and then immediately transferred to ice for 3 min. LB broth (1000 uL) was then added to the cells, which were subsequently incubated at 37 °C while shaking at 250 RPM for one hour. Next, 150 µL of cells were plated on LB agar plates containing the appropriate antibiotic. The plates were inverted and incubated overnight at 37 °C (approximately 16 –18 h). Negative control samples (without added DNA) were also transformed into competent cells to verify the absence of contamination. The next day, the plates were observed for the growth of colonies.

3.8 Polymerase Chain Reaction Assay (PCR)

The PCR method was used to amplify specific sequences and confirm the presence of particular gene sequences, as well as to construct new constructs for testing. The following sections outline the different types of PCR employed for this study.

3.8.1 Colony PCR

A single colony was streaked onto an LB plate and incubated overnight at 30 °C. One colony from the fresh plate was picked and diluted in 100 µL of DNase/RNase-free molecular grade water (Hyclone, Ottawa, Canada).To begin, an initial heating step of the diluted colony was conducted at 94 °C for 10 min using a C1000 Touch™ Thermal Cycler **(**Bio-Rad, Mississauga, Canada). The forward and the reverse primers

were designed using Sigma Aldrich (Oakville, Canada) and diluted to small aliquots (1 mL/tube) to a final concentration of 1 IU/mL.

The PCR reaction was prepared with 5 µL of diluted pre-heated template mixed with 10 µL each of forward and reverse primers,10 µL of DNA polymerase enzyme (Phusion Flash High-Fidelity PCR Master Mix, Fisher Scientific, Ottawa, Canada), and sufficient DNase/RNase-free molecular grade water (Hyclone, Ottawa, Canada) for a final volume of 25 µL per reaction. A negative control without template DNA was also prepared. The reaction cycle included an initial denaturation step at 98 °C for 30 sec, a denaturation step at 98 °C for 10 sec, an annealing step at 72 °C +/- 5C for 10 sec, an extension step at 72 °C for 3 min, then finally, an additional extension step at 72 °C for 10 min. Cycles of denaturation, annealing, and extension were repeated 30 times. After passing through the final extension cycle, the thermal cycling reaction was cooled to 4 °C, at which point the PCR reaction was completed. Reactions were then collected, and gel electrophoresis was performed by running the samples on a 0.8 % agarose gel. DNA bands of interest were identified based on fragment size. The PCR fragment was gel extracted using a gel extraction kit (Omega Bio-Tek, Norcross, USA), purified using a PCR cycle-pure kit (Omega-Bio-Tek, Norcross, USA), digested by restriction enzymes (RE) (NEB, New England Biolabs, Whitby, Canada) and purified again using a miniprep kit (Plasmid Mini Kit I, Omega Bio-Tek, Norcross, USA). Finally, the DNA concentration was determined using the Nanodrop 2000 spectrophotometer at $A_{260/280}$ ratio (Thermo Fisher Scientific, Ottawa, Canada).

3.8.2 Preparation of Knock-Out Gene PCR Products

To identify the interrupted host gene, primers were designed, approximately 25 nucleotides in length, with the forward primer 5'- CTTTGGTCACCAACGCTTTTCCCG - 3' and the reverse primer 5'- GGCCACGCGTCGACTAGTAC - 3' (Sigma Aldrich, Oakville, Canada), targeting the terminal ends of the two IS*10* elements.

The colony PCR preparation and reaction were as follows: A single colony of each isolate was streaked on a Km plate (Km^R marker from Keio collection strains) and incubated O/N at 30 °C. One colony from the fresh plate was picked and diluted in 100 µL of DNase/RNase-free molecular grade water (Hyclone, Ottawa, Canada), and the PCR reaction began with heating (initial heating step) the diluted colony at 94 °C for 10 min (C1000 Touch™ Thermal Cycler**,** Bio-Rad, Mississauga, Canada). The forward and reverse primers were diluted to small aliquots (1 mL/ tube) to a final concentration of 1 IU/mL. Then, 5 µL of the diluted pre-heated template was mixed with 10 µL of each primer, 10 µL DNA polymerase enzyme (Phusion Flash High-Fidelity PCR Master Mix, Fisher Scientific, Ottawa, Canada) to a final volume of 25 µL per reaction with DNase/RNase-free molecular grade water (Hyclone, Ottawa, Canada). A negative control without template DNA was also prepared.

The cycling thermal reaction included an initial denaturation step at 98 °C for 30 sec, a denaturation step at 98 °C for 10 sec, an annealing step at 72 °C for 10 sec, an extension step at 72 °C for 3 min, and finally, an additional extension step at 72 °C for 10 min. Cycles of denaturation, annealing, and extension were repeated 30 times. After passing through the final extension cycle, the thermal cycling reaction was cooled to 4 °C, at which point the PCR reaction was completed. Reactions were then collected, and gel electrophoresis was performed by running the samples on a 0.8 % agarose gel. DNA bands of interest were identified based on fragment size. After several rounds of PCR to amplify the knocked-out gene product, the fragments were purified using a PCR Cycle-Pure Kit (Omega Bio-tek, Norcross, USA) and sent for sequencing (Bio Basic Inc., Markham, ON, CA).

3.8.3 Inverse PCR and Mutant Identification

Inverse PCR requires four critical primers to run two rounds of PCR. Using *the Taq* DNA polymerase enzyme (Fisher Scientific, Ottawa, Canada), inverse PCR can be performed according to the method described by Ochman et al. (1990) to amplify the Tn*10*-targeted fragment from the pRex plasmid (Figure

3-2). The primers were synthesized and designed from the Tn*10* sequence and in the opposite orientation to those generally employed for PCR (Figure 3-6). A typical PCR mixture and conditions were used, with some optimizations required to accommodate specific primer requirements. Primers used in the inverse PCR reactions are listed in Table 3-1. The cycling thermal reaction for the first round (Tn*10* primers 1 and 2; Table 3-1) included an initial denaturation step of 95 °C for 5 min, a denaturation step of 95 °C for 30 s, an annealing step of 30 °C for 1 min, an extension step 72 °C for 1 min, which was repeated 10x. Next, samples were heated to 95 °C for 30 s, 42 °C for 1 min, and 72 °C for 1 min, a process repeated 30 times. A 1:10 dilution of this first PCR reaction was used as a template for a second round, which included an initial denaturation step at 95 °C for 5 min, a denaturation step at 95 °C for 30 s, an annealing step of 50 °C for 45 s, and an extension step at 72 °C for 1 min, which was repeated 30x.

Reactions were separated by gel electrophoresis on a 0.8% agarose gel. The presenting band (approximately 800 bp) was extracted using the E.Z.N.A.® Gel Extraction Kit (Omega Bio-Tek). PCR fragments amplified from primers 3 and 4 were commercially sequenced (Bio-Basic Inc., Markham, CA).

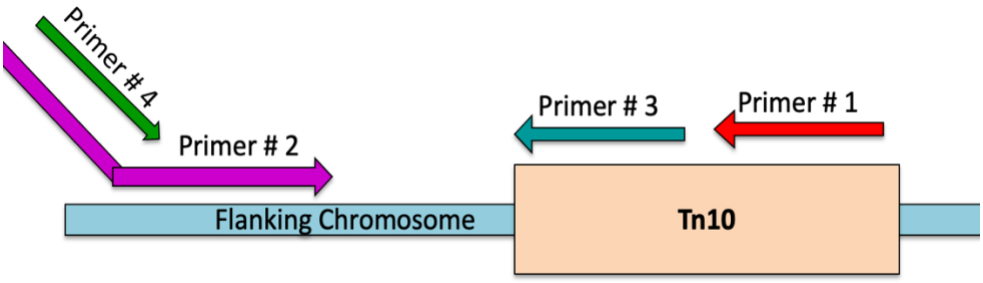


Figure 3-6. PCR Mapping of Tn*10* Insertions in the *E. coli* Chromosome Using Four Designed Primers. To identify the chromosomal location of Tn*10* insertions, four specific primers were designed: two flanking the insertion site within the host genome and two internal to the Tn*10* transposon. PCR amplification using various primer combinations allows for precise mapping of insertion sites. Successful amplification patterns indicate the orientation and position of the Tn*10* element relative to the host genome.

3.9 Plasmid Extractions, Digestions and Purifications for Ligation

This section outlines the steps taken to produce the vector and inserts for ligation, which are used in generating new constructs using the restriction enzyme cloning method. The process begins with initial plasmid extraction and concludes with the final ligation step.

3.9.1 Plasmid Extraction and Purification

A single colony isolated from a successful transformation plate was cultured in 10 mL of LB medium containing antibiotics overnight at 37 °C with shaking. Resident plasmid was extracted and purified using a mini-prep kit (Plasmid Mini Kit I, Omega Bio-Tek, Norcross, USA). The plasmid was then eluted in 50-100 µL of DNase/RNase-free molecular-grade water (Hyclone, Ottawa, Canada) and stored at 4 °C. The DNA concentration was determined using a Nanodrop 2000 spectrophotometer at $A_{260/280}$ (Thermo Fisher Scientific, Ottawa, Canada).

3.9.2 Plasmid Digestion and DNA Purification

Plasmids were digested using specific restriction enzymes (Res) (New England Biolabs, Whitby, Canada). In a 600 µL sterile microcentrifuge tube (Eppendorf, VWR, Mississauga, Canada), 1 µg of plasmid, 5 µL of 10X CutSmart NEB buffer, 1 IU of RE were mixed, and DNase/RNase-free molecular grade water (Hyclone, Ottawa, Canada) was added to a volume of 50 µL. In this study, *Bam*HI-HF, *X*baI, *Eco*RI, and other enzymes were used to cut plasmids at a specific site in the MCS, or double digests were performed to cut plasmids to prepare them for ligation.

The digestion reaction was then gently mixed and incubated at 37 °C for 1-2 h. Where required, the reaction was inactivated by heat shock at 64 °C for 10 min. The concentration of the DNA fragments was measured and assessed using a Nanodrop 2000 spectrophotometer at $A_{260/280}$ (Thermo Fisher Scientific, Ottawa, Canada).

3.9.3 DNA Extraction and Purification

The digested insert(s) and vector(s) fragments were separately mixed with 6X loading dye (New England Biolabs, Whitby, Canada) and electrophoresed on a 0.8% agarose gel at 100 V for 1 h or at 50 V for 3 h. The DNA bands were then visualized using a Spectroline UV Transilluminator (Thermo Fisher Scientific, Ottawa, Canada) and the vector and insert bands were recognized based on their sizes and compared to the 1 kb ladder. The correct bands were then cut, collected, and purified using a gel extraction kit (Omega-Bio-Tek, Norcross, USA). The vector/insert concentrations were measured using a Nanodrop 2000 spectrophotometer at $A_{260/280}$ (Thermo Fisher Scientific, Ottawa, Canada). Gel extraction was repeated as necessary to collect a concentrated volume of DNA required for subsequent manipulation.

3.9.4 DNA Ligation

A 1:3 or 1:5 ratio of vector: insert DNA was ligated using TV DNA ligase (NEB, Whitby, Canada). The ligation reaction contained the appropriate ng of vector and insert DNA, 1 IU of T4 DNA ligase enzyme (NEB, Whitby, Canada), and 10X T4 ligase buffer. DNase/RNase-free molecular grade water was added to a final volume of 25 µL. The negative control reactions contained insert only, vector only, and insert + vector without the ligase enzyme. Ligation reactions were mixed gently and incubated O/N at RT. The reactions were inactivated by heat shock at 64 °C for 10 min the next day and then kept on ice to proceed with transformation preparation as formerly described.

3.9.5 DNA Cloning

Following colony PCR and using designed primers to amplify the gene of interest, cassettes flanked by specific restriction sites are obtained. These are then digested with the same restriction enzyme and prepared for DNA ligation. The final step involves transforming the particular *E. coli* cells with the new constructs and preparing them for further experiments. All cloning steps are thoroughly described in the sections above. An example of successful cloning was conducted to create plasmids for a complementation assay,

as shown in the following diagrams. The first step is colony PCR to amplify the genes of interest and clone them into PUC19 in the MCS (Figures 3-4 and 3-7).

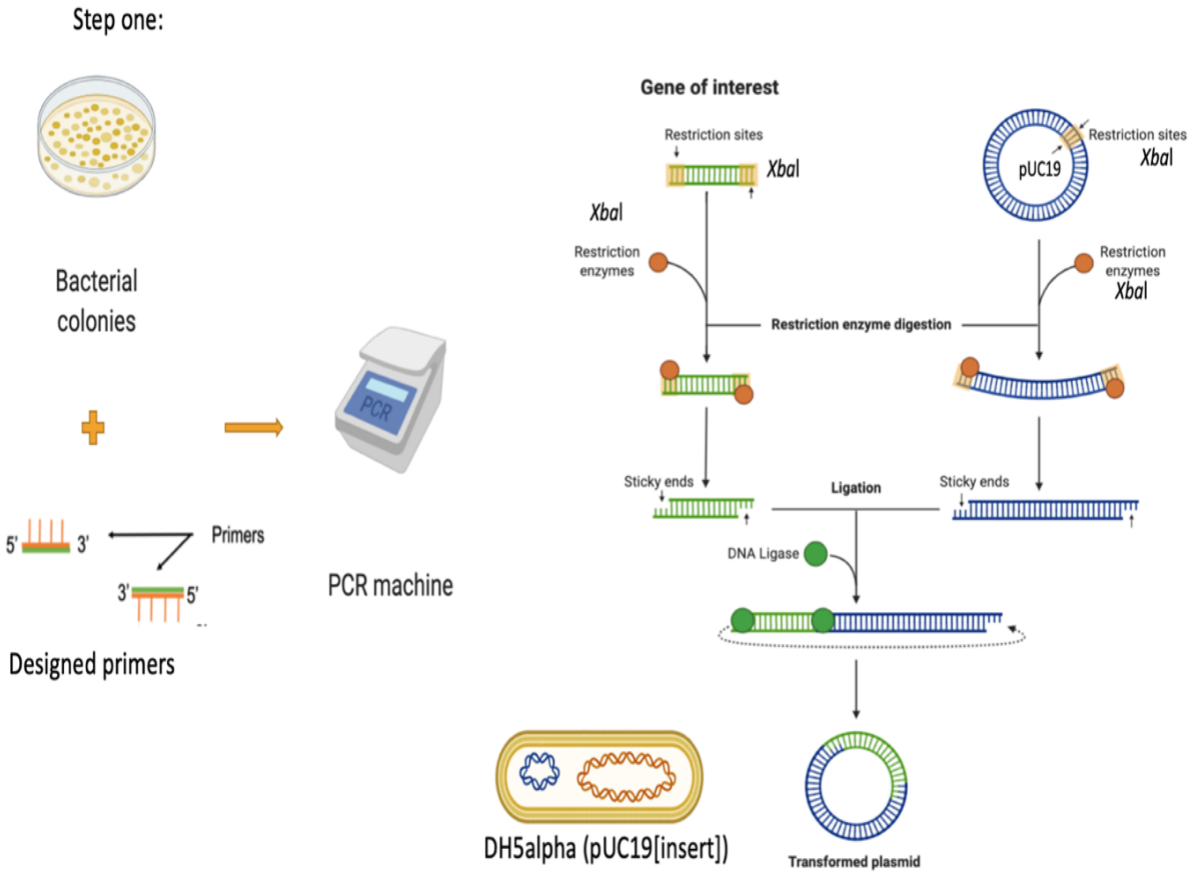


Figure 3-7. Step One in Construct Generation for Complementation Assay. In the first step of construct generation, colony PCR was performed using specifically designed primers to amplify the gene of interest, flanked by *Xba*I restriction sites. The amplified product and the pUC19 vector were both digested with *Xba*I, followed by ligation of the insert into the vector. This ligation product forms the initial construct used in subsequent cloning steps. *Created with Biorender.com.*

In the next step, plasmids created in Step One were used to digest and cut the cassettes encoding the genes of interest, and then they were cloned again into the final plasmid pBR322 to conduct the complementation assay (Figures 3-5 and 3-8).

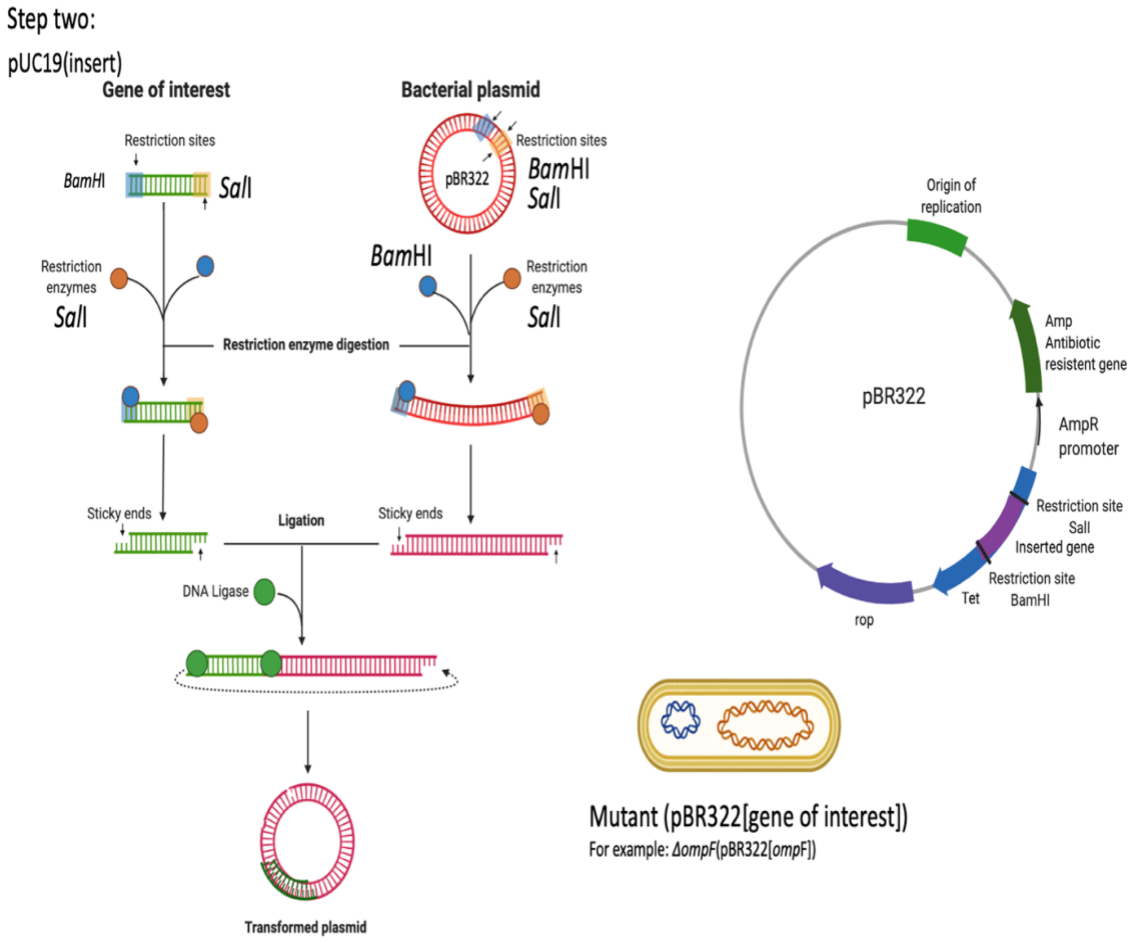


Figure 3-8. Step Two in Construct Generation for Complementation Assay. In the second step, constructs generated in Step One were digested with *BamH*I and *Sal*I to excise the insert containing the gene of interest. Simultaneously, the pBR322 plasmid was digested with the same restriction enzymes to serve as the recipient vector. The insert and vector were then ligated, and the resulting recombinant plasmid was used to transform the appropriate *E. coli* mutants. *Created with Biorender.com.*

3.10 Cell Viability Assay

Cultured cells of membrane protein gene mutants and other examined mutants containing high-copy *rex*$^{+}$ plasmid pHA1 (Figure 3-1) or pUC19 were assessed for cell viability. The parent strain, BW25113 [pHA1], was used as a positive control, and BW25113[pUC19] was used as a negative control for Rex. The Δ*ompC* mutant, which inhibits T4 attachment, was used as the negative control for infection. Cells were grown in LB + Ap and incubated at 30 °C while shaking at 225 RPM O/N. Subculture dilutions (1:100) of each were then prepared from the O/N cultures in LB + Ap and incubated at 30 °C while shaking at 225 RPM until an A_{600} of 0.8 was reached. The 1:100 subculture preparations were then prepared in TN buffer, and 200 µL aliquots were mixed with phage T4*rII* lysate at a multiplicity of infection (MOI) of 3. The mixture was gently mixed. The infected cells were incubated at 30 °C for 10- 15 min, then washed twice with 2 mL of TN buffer. Cells were resuspended to a final volume of 1 mL. The suspended cells were diluted again in 1:1000 TN buffer, and 100 µL aliquots were prepared to be mixed with 3 mL top agar before being poured onto pre-warmed LB + Ap plates. The preparations were incubated at 30 °C for 48 hours.

3.11 Infective Center Assay

The infective center assay was used to quantify the number of bacterial cells successfully infected by phage particles. This method involves allowing phages to adsorb to host cells, washing away unbound phages, and plating the infected cells to determine infective centers based on plaque formation. O/N cultures of mutant [pHA1] cells as experimental strains, the parent strain BW25113 wt [pHA1] as the positive control, and BW25113 [pUC19] and JW2203-1 Δ*ompC* [pHA1] as the negative controls, were grown in LB + Ap and incubated at 30 °C while shaking at 225 RPM. Subcultures (1:100 dilution) were then prepared in LB + Ap and incubated at 30 °C with shaking at 225 RPM until an A_{600} of 0.8 was reached. Approximately 2 mL of culture was then centrifuged at 10,000 RPM for 10 min, and the cells were resuspended in 1 mL of

$CaCl_2$. T4*rII* lysate was then added at an MOI of 3 and allowed to adsorb for 15-20 min. Infected cells were washed 3X in TN buffer and re-suspended in 100 µL TN buffer. 200 µL of the original O/N cultures were then added to the resuspended cells, mixed with 3 mL of top agar, and then poured onto pre-warmed LB + Ap plates. The plates were incubated O/N at 30 °C.

O/N cultures of selected mutants lysogenized with λ*cI*-857 cells as experimental strains, the parent strain BW25113 wt [λ*cI*-857] as the positive control, and BW25113 (wt) and Δ*ompC* as the negative controls, were grown in LB+ Km and incubated at 30 °C while shaking at 225 RPM. Subcultures (1:100 dilution) were then prepared in LB + Km and incubated at 30 °C with shaking at 225 RPM until an A_{600} of 0.8 was reached. Approximately 2 mL of culture was centrifuged at 10K RPM for 10 min, and the cells were resuspended in 1 mL of $CaCl_2$. T4*rII* lysate was then added at an MOI of 3 and allowed to be adsorbed for 15-20 min. Infected cells were washed 3X in TN buffer and re-suspended in 100 µL TN buffer. Next, 200 µL of the original overnight cultures were added to the resuspended cells, mixed with 3 mL of top agar, and poured onto pre-warmed LB + Km plates. The plates were then incubated overnight at 30 °C.

3.12 Assessing the Effect of Deletion Mutations on Rex Activity

Following the spot test of T4 and T4*rII* plating assay, the Rex activity of the deletion mutants was assessed. Cultures of Rex^- isolated mutants were prepared in 5 mL aliquots at a 1:100 dilution and incubated while O/N. Next, 300 µL of culture was added to 3 mL of top agar and poured immediately onto prewarmed LB plates, then left on the bench to solidify. Serial dilutions of T4 (wt) and T4r*II* lysates were prepared in TN buffer with concentrations ranging from 10^{-2} to 10^{-8} phage/mL to quantify plating efficiency and Rex activity. Lysates were added in 10 µL drops onto isolated Rex^- mutants overlay plates. Plates were left to dry for 30 min, then incubated overnight at 30 °C. The following day, plates were assessed, and plaques (when evident) were quantified.

3.13 Phage λ (*rex*$^{+}$) Lysogenization of *E. coli* Cells

Fresh O/N cultures were prepared from a single colony of each strain and mutants in LB at 30 °C. Overlay plates were prepared by mixing 300 µL of the cell cultures with 3 mL of top agar and plated on LB plates. The plates were allowed to dry and left on a bench for 20 min until the top agar solidified. Then, 10 µL of 10^{-4} fresh λ*cI*-857 and λ wt lysates in TN buffer were spotted onto the experimental plates. Phage spots were allowed to dry, and the plates were incubated O/N at 30 °C for λ*cI*857 lysogens and at 42 °C for λ wt lysogens. The following day, large turbid plaques were visualized and isolated using sterile toothpicks to confirm λ lysogeny by immunity assay.

For λ*cI*857 lysogens, colonies were grown at 30 °C and then shifted to 42 °C to inactivate the CI repressor, allowing any lysogens to undergo phage growth and lyse their resident cells, thereby killing the host. For λ wt lysogens, cells that were able to grow at both 30 °C and 42 °C were considered potential lysogens and tested to confirm the presence of λ wt lysogens. This was done by stabbing cells in the top agar of a λF7 overlay plating assay to test for λ immunity, thereby confirming lysogenization.

3.14 Lambda Immunity Assay

This assay was performed to confirm the presence of functional λ immunity in candidate lysogens. Lambda (wt) lysogens that grew at both temperatures (30 °C and 42 °C) were streaked out to test a single colony per lysogen. An O/N culture of heteroimmune lysogen W3899 (λF7) was prepared, and 300 µL of this fresh culture was mixed with 10 µL of 10^{-4} λF7 lysate diluted in TN buffer and added to 3 mL of top agar before being poured onto an LB plate. The experimental colonies were stabbed in the overlay top agar using sterile toothpicks and incubated O/N at 30 °C. Resistance to lysis indicated immunity to λF7 and confirmed successful Lysogenization.

3.15 Plasmid Curing

A single colony of each Rex$^-$ isolate was streaked on an LB agar plate and incubated overnight at 42 °C. Next, a single colony of each treated isolate was picked and streaked out on an LB agar master plate. In tandem, cells were streaked out on Ap plates, and all plates were incubated overnight at 30 °C to screen for cells that had been cured of the Tn*10-rex* plasmid. Cultures of the cured isolates that did not grow on Ap plates (indicating loss of the *rex*$^+$ plasmid) were prepared by inoculating a single colony into 5 mL LB broth and incubating overnight with aeration at 225 RPM at 30 °C. The next day, the overlay T4*rII* plaque assay was applied to test the cured isolate for loss of the Rex$^-$ phenotype associated with the Tn*10-rex* plasmid. Additionally, overnight cultures of all cured isolates were extracted and purified using a mini-prep kit (Plasmid Mini Kit I, Omega Bio-tek, Norcross, USA) and run on a 0.8% agarose gel to confirm that the cells were free of plasmid DNA.

3.16 GFP Tag Plasmid Preparation and Imaging

To prepare the Rex-GFP constructs, the Rex-GFP or RFP cassettes were inserted into the temperature-regulated pPL451 plasmid under the control of the *cI*857 promoter. The fluorescent fusion protein was used to measure the quality of fusions, where fluorescence, in conjunction with inhibition of T4*rII* plating (i.e., Rex phenotype), indicates a successful fusion configuration that does not impede Rex protein function. All GFP-tagged *rexAB* combinations were synthesized by polymerase chain reaction (PCR). First, reverse and forward primers for each cassette were designed to amplify *rex* genes *rexA, rexB*, and *rexA-rexB* from W3110(λ) lysogen, which feature endonuclease target sites for the restriction enzymes *Eco*RI and *Sac*I, compatible with the MCS of the pPL451 vector (Figure 3-3; Table 3-1).

The pPL451 vector was digested with the same restriction enzymes and prepared for ligation with the rex inserts. The GFP sequence was subsequently designed with compatible ends for insertion into the vector's

multiple cloning site (MCS). GenScript assembled the fragments into the final *rex::gfp* constructs (Table 3-1).

The *rex::gfp* plasmids were transformed by BW25113 (wt) cells, following the electroporation transformation protocol described previously. The transformation efficiency was calculated at various temperatures**:** 23 °C, 30 °C, 35 °C, and 37 **°**C using the following equation:

$$\text{Transformant cfu} = \text{No. of bacteria colonies x dilution ratio x } \frac{\text{original transformation volume}}{\text{plated volume}}$$

$$\text{Relative Transformation Efficiency (TE)} = \frac{\text{Number of colonies on LB + Amp}}{\text{Numbumbr of colonies on LB only}} \text{ x } 100\%$$

Each transformation was plated on both a control LB plate and an LB plate supplemented with Amp to confirm successful transformation. The grown colonies were compared to the 100% control, which was plated on LB for each construct.

The cells were imaged using fluorescence microscopy with an EVOS FL Auto imager (ThermoFisher Scientific, Canada). Cells were treated and then washed with 500 µL of PBS, followed by centrifugation at 500 × g for 5 min. The supernatant was discarded, and 500 µL of PBS was added to the cells, which were then centrifuged again at 500 × g for 5 min. The supernatant was discarded, and the cells were finally resuspended in 300 µL of PBS. Fixation of suspended cells was done using 4% paraformaldehyde (PFA) in PBS. After the final wash, 5-10 µL of each sample was dropped on a slide and covered with the coverslip. After drying, the slide was stored at 4 °C in the dark. Images were captured after adjusting the focus to the highest available magnification (60x) to observe cell details. Images were collected of all controls with no GFP expression, samples with GFP expression only, and samples with GFP/RFP co-expression.

Chapter 4

Results

4.1 Identification of Host Genes Involved in the Rex⁻ Phenotype

To identify host genes in *Escherichia coli* that could be involved in the exclusionary phenotype, a one-step insertional mutagenesis and isolation technique was employed. This approach used a customized pRex/pHA2 construct carrying *rexA* and *rexB* under the λ P_R promoter with *cI* [Ts] regulator, and a mini-Tn10 transposon for random chromosomal insertion. Integration was achieved by conjugative transfer into a Δ*clpP::kan* background, which facilitated Kanamycin selection; although *clpP* deletion can elevate RpoS levels, previous work indicated no effect on the Rex phenotype. Exconjugants were screened directly on plates embedded with T4*rII*, allowing simultaneous selection of integrants and identification of Rex⁻ (phenotypically Rex⁻ but genotypically *rex*$^+$) mutants based on their ability to support T4*rII* growth (Alattas MSc. Thesis, 2015)

4.1.1 Confirmation of Mutants as Phenotypically Rex⁻ and Genotypically *rex*$^+$

Strains and plasmids described in this chapter are listed in Table 3-1. *E. coli* K-12 W3110 was used to generate new T4 and T4*rII* lysates (Chapter 3). *E. coli* K-12 DH5α was used to host the pRex plasmid.

Isolates showed Rex activity attenuation of up to 1000-fold compared to the 100% *Rex*$^+$ control, as measured by T4*rII* plating efficiency (Table 4-1). The noted improvement in T4*rII* plating indicates insertional mutation of a host gene that is either directly or indirectly involved in the Rex phenotype. In all cases, abrogated or attenuated Rex activity was not due to a faulty *rex* cassette, as each isolate was subsequently lysogenized by λ (*rex*$^+$) to deliver an additional copy of the *rex* genes and then retested for Rex activity (Table 4-1). Nearly all the isolates showed similar results in both cases.

Table 4-1. Isolated integrant mutants attenuated for Rex activity.

Strain	Relative EOP of T4*rII* at wild-type level *rex*$^+$ expression[1,3]	Relative EOP of T4*rII* at dual *rex*$^+$ expression[2,3]
Controls:		
JW0427-1[3]	1.0	1.0
JW0427-1(λ)[4]	$<1.0 \times 10^{-7}$	$<1 \times 10^{-7}$
Isolates:		
JW-HA 1	2.3×10^{-5}	4.0×10^{-6}
JW-HA 2	7.0×10^{-6}	5.2×10^{-6}
JW-HA 3	1.5×10^{-5}	1.7×10^{-5}
JW-HA 4	1.0×10^{-3}	5.0×10^{-4}
JW-HA 5	1.7×10^{-5}	5.0×10^{-6}
JW-HA 6	1.4×10^{-4}	1.0×10^{-4}
JW-HA 9	5.0×10^{-6}	4.0×10^{-6}
JW-HA 11	1.6×10^{-5}	1.3×10^{-4}
JW-HA 12	1.3×10^{-5}	1.6×10^{-4}
JW-HA 19	2.0×10^{-4}	1.5×10^{-4}
JW-HA 20	8.0×10^{-6}	6.8×10^{-6}
JW-HA 21	1.6×10^{-5}	1.7×10^{-5}
JW-HA 25	1.8×10^{-5}	4.0×10^{-6}

[1] Tn-mediated insertion of the *rexA-rexB* transposable cassette at relatively random chromosomal sites into the chromosome results in insertional mutants genotypically *rexA*$^+$*rexB*$^+$ (*rex*$^+$).

[2] Transponants[1] lysogenized with λ. Hosts carry two copies of *rexA-rexB*, one from the transposon cassette and the second from the λ lysogen.

[3] *E. coli* strain JW0427-1 (Δ*clpP::kan*) (*rex*$^-$) *was* used as a negative control with a relative T4*rII* EOP of 1.0. All values are based on the averaged relative EOP from three independent assays. Isolates were previously evaluated for Rex activity during my MSc work and verified here.

[4] *E. coli* strain JW0427-1(λ) (Δ*clpP::kan*) (*rex*$^+$) used as positive control with relative T4*rII* EOP of 1.0.

All screened isolates were kanamycin (Km)-resistant (due to the host background), and, as expected, most were also tetracycline (Tc)- and ampicillin (Ap)-resistant (due to the construct backbone and transposable element) (Figure 4-1). However, a few isolates were (Ap)-sensitive, suggesting loss of the plasmid backbone and retention of only the integrated transposon. These (Ap)-sensitive isolates (Table 4-1) are particularly interesting because they likely represent true chromosomal insertions without residual plasmid, and therefore were prioritized for further analysis, while others were excluded. The presence of pRex was confirmed by plasmid extraction and agarose gel electrophoresis from the Km^R recipient cells (Figure 4-1). This representative gel shows 10 isolates, where one isolate, HA-10, did not appear to carry the plasmid, as no band was visible.

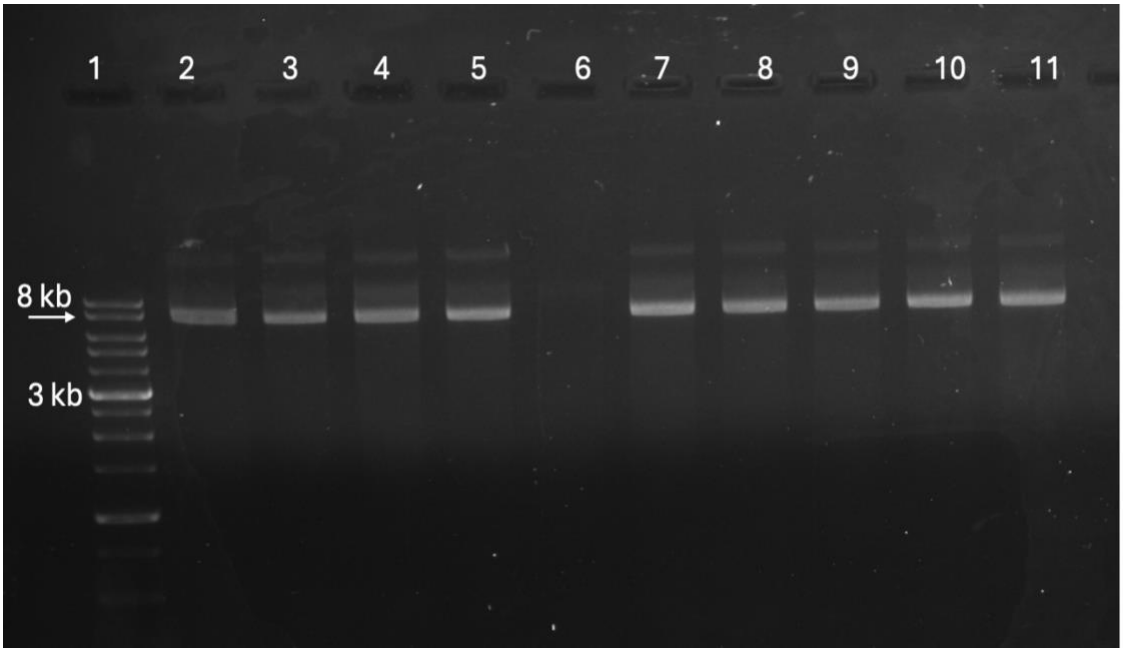


Figure 4-1. Agarose Gel Electrophoresis of Rex^- Isolate Plasmids. Lane 1: New England BioLabs 1 kb DNA ladder, Lanes 2-5, and 7 -11: expected isolated pRex plasmid band (8.2 kb). Lane 6 indicates an isolate that does not carry a plasmid, as no band appears.

4.1.2 Plasmid Curing and Rex⁻ Mutants

All isolates initially showed an attenuated Rex phenotype, allowing T4*rII* to form plaques. To confirm that this phenotype was due to chromosomal transposon insertions rather than residual plasmid, plasmid DNA was extracted from each isolate and transformed into DH5α (*λpir*), which supports pRex replication. All transformants displayed 100% Rex^+ activity in plaque assays, confirming that the *cI-rexA-rexB* cassette on pRex was intact and functional. This indicates that the loss of Rex activity in original isolates resulted from host gene disruption rather than plasmid mutation. Although pRex should not replicate in the original non-*pir* hosts, the presence of Ap^R colonies suggested that some plasmid integrants persisted, possibly through unstable integration events. Therefore, this curing and retransformation step was included to verify plasmid integrity and distinguish true chromosomal insertions from plasmid-associated effects. All Tn*10-rex* plasmids from all isolates were extracted, purified, and prepared for assessment of any mutations that occurred during the transposition mutagenesis process, following the protocols described in Chapter 3. Bacterial cells can be chemically treated with curing agents or physically by growing cells at temperatures higher than their optimal growth temperatures to eliminate plasmids from cells, or by nutritional treatments or stresses (Trevors 1986; Lauritsen et al., 2017). As all tested cured isolates demonstrated sensitivity to both T4 and T4*rII* plating compared to Rex^+ control, this suggests inactivation of the Rex phenotype has occurred due to insertional mutagenesis of a Rex-related *E. coli* host gene.

4.1.3 Inverse PCR and Identification of Rex⁻ Mutant

To identify the interrupted host genes, a set of primers was designed (Table 3-1) for colony PCR of the isolates against the terminal ends of the two IS*10* elements, aiming to locate the interrupted gene. Additionally, random primers were used under low stringency conditions to amplify regions of the host chromosome where the transposon jumped. After several rounds of PCR to amplify the knocked-out gene product, the fragments were purified, collected and sequenced. The sequencing results were compared against *E. coli* genes using the Basic Local Alignment Search Tool (BLAST,

https://blast.ncbi.nlm.nih.gov/Blast.cgi). BLAST can be used to compare query sequences against database sequences to find regions of local similarity. All sequences were determined to be fragments of pRex backbone (R6k *ori*, *Tc*, *mob*, etc). Therefore, nested PCR was applied (Ochman et al., 1990) to identify the knocked-out genes. The inverse PCR technique was developed to determine the precise position of Tn*10* insertion sites by DNA sequence analysis (Nicholas et al., 1998). Because of the similarity of the two ends of Tn*10* insertion, the insertional sequences right and left are identical except for six bases. Inverse PCR requires four critical primers to run two rounds of PCR. Using *Taq* DNA polymerase, inverse PCR can be performed according to the method described by Ochman et al. (1990) to amplify the Tn*10*-targeted according to the method described by Ochman et al. (1990) to amplify the Tn*10*-targeted fragment. The primers were synthesized and designed from the Tn*10* sequence and, in the opposite orientations to those generally employed for PCR, they allow the amplification of the upstream and/or downstream regions flanking a specified segment of DNA. They also produce hybridization probes for identifying and orienting the adjacent or overlapping clones from a DNA library. The primers were complementary to the opposite strand and, therefore, were oriented such that DNA extension proceeds outward from the core region. Primer #1 was designed specifically from the right-side insertional sequence IS*10R* of Tn*10*, allowing it to anneal to the transposable element during amplification. Primer #2 was a random primer designed to add tail-like sequences to all the amplicons outside the Tn*10* fragment, including the knocked-out gene. The product of the first-round PCR, using primers #1 and #2, provided a multitude of non-specific products, which were then used as templates for the second nested PCR round, using primers #3 and #4. Primers #3 and #4 ensured that only the amplification fragments with the desired flanking piece of DNA were amplified, thereby excluding any unwanted PCR contaminants and limiting non-specific products. The PCR reaction setup and primer design for mapping Tn*10* insertions in the host chromosome were adapted from Dr. J. Peters' lab at Cornell University, USA (Peters and Craig 2001; Bordi et al., 2008).

The PCR reaction was prepared using the designed Tn*10* primers (Table 3-1) and run for two rounds before the product was collected, purified, and analyzed on an agarose gel electrophoresis with a fragment size of approximately 950 bp (Figure 4-2).

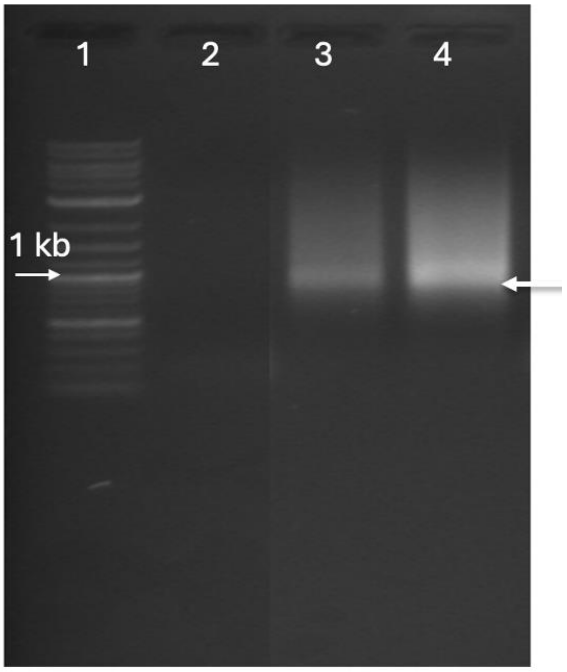


Figure 4-2. PCR Amplification of Target DNA Fragments. Lane 1: 2-log DNA ladder, Lane 2: Negative control (*Taq* polymerase control), Lane 3 and 4: Amplified PCR products (~ 950 bp).

The amplified DNA fragment in question was successfully sequenced using Primer #3. The resulting nucleotide sequence was analyzed using the BLAST (Basic Local Alignment Search Tool) algorithm against the *E. coli* genome. This analysis revealed a 94% sequence identity with the *E. coli* non-essential gene, *mglC,* that encodes a component of an ATP-binding cassette (ABC) transporter system. MglC functions as a permease involved in the transport of **m**ethyl-**g**alactoside, a sugar derivative that *E. coli* can utilize as a carbon source under certain environmental conditions (Figure 4-3; Hogg et al., 1991).

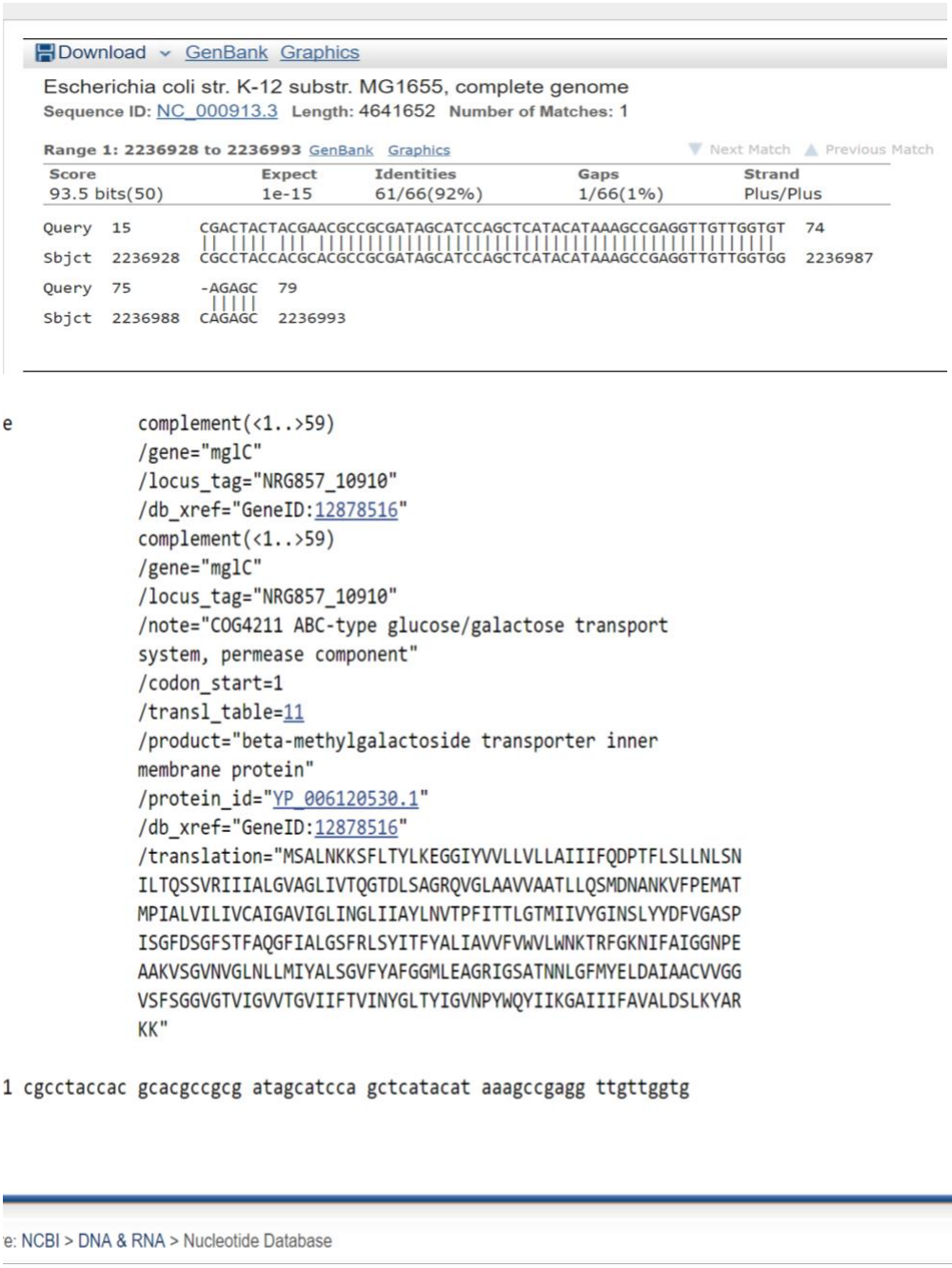


Figure 4-3. Snapshot of BLAST Results. The BLAST showed a 94% sequence identity with MglC, an *E. coli* membrane-associated protein. *Source: NCBI BLAST https://blast.ncbi.nlm.nih.gov/Blast.cgi*

4.2 Screening for Susceptible Host Proteins Influences Rex/ RII Activity

After identifying the *mglC* galactose transporter as one of the genes capable of attenuating Rex activity, along with previously identified Omps (Alattas et al., 2020), additional membrane proteins, sigma factors, stress response genes, and their regulators were assessed for their influence on Rex activity. To confirm the role of each candidate gene and rule out polar effects within operons, a genetic complementation assay was performed. For this, the wild-type allele of each disrupted gene was cloned into a pBR322-based medium-copy plasmid under its native promoter and introduced into the corresponding Keio mutant. Complementation was assessed by restoration of the Rex^+ phenotype in T4*rII* plating assays. This approach also served to verify the accuracy of the Keio mutants, as some have been reported to contain secondary mutations. In future work, additional controls could be included to confirm the specificity of complementarity.

E. coli K-12 W3110 was used to generate new T4 and T4*rII* lysates. *E. coli* single knockout mutants and their parent strain BW25113 (wt), which was also used as a positive control of the Rex phenotype, were obtained from the Keio Collection of single-gene knockouts (Coli Genetic Stock Center, USA; Baba et al., 2006). Each single knockout strain was transformed by the high-copy pHA1 (pUC19- *cI-rexA-rexB*) plasmid. *E. coli* BW25113 (wt) harbouring the pHA1 rex^+ plasmid was used as a positive control, and an empty plasmid as a negative control. Some examined mutants were lysogenized with phage λ*cI*-857 and further tested for Rex activity (Table 4-2). Bacterial strains and phages used in this assay are listed in Table 3-1.

4.2.1 Assessing the effect of glucose transporter membrane proteins on Rex activity

Upon identifying *mglC* galactose transporter (bolded in Table 4-2) as a gene influencing Rex activity, other *mgl* regulatory genes were tested to see whether they would similarly influence T4*rII* exclusion. Mutants of *mgl* and related genes from the Keio collection were transformed by the high-copy pHA1 *rex*$^+$ plasmid and were assayed for Rex activity, as shown in Table 4-2 and Figure 4-4.

Table 4-2. The effect of the membrane galactose transporter on Rex Activity.

Strain[1]	**Mutation**	**Rex Plasmid**[2]	**Relative Efficiency of Plating** [3]		
			T4(wt)	**T4*rII***	**Rex activity**
Wild type		+	0.2	$< 3.0 \times 10^{-7}$	1.0
		--	1.0	1.0	--[4]
JW2136-1	*ΔmglA*	+	7.0×10^{-2}	$< 3.0 \times 10^{-7}$	1.0
		--	0.7	0.7	--
JW2137-1	*ΔmglB*	+	0.7	$< 3.0 \times 10^{-7}$	1.0
		--	0.7	1.0	--
JW2135-1	***ΔmglC***	**+**	**0.1**	**2.0×10^{-5}**	**1.5×10^{-2}**
		--	0.7	1.0	--
JW0739-1	*ΔgalM*	+	1.0	$< 3.0 \times 10^{-7}$	1.0
		--	0.6	1.0	--
JW0740-3	*ΔgalK*	+	7.0×10^{-2}	$< 3.0 \times 10^{-7}$	1.0
		--	0.6	1.0	--
JW0741-1	*ΔgalT*	+	8.0×10^{-2}	$< 3.0 \times 10^{-7}$	1.0
		--	0.7	1.0	--
JW0742-1	*ΔgalE*	+	1.0×10^{-2}	$< 3.0 \times 10^{-7}$	1.0

		--	1.0	1.2	--
JW1224-1	*ΔgalU*	+	$< 3.0 \times 10^{-7}$	$< 3.0 \times 10^{-7}$	1.0
		--	$< 3.0 \times 10^{-7}$	$< 3.0 \times 10^{-7}$	--
JW2027-2	*ΔgalF*	+	1.0	$< 3.0 \times 10^{-7}$	1.0
		--	0.7	1.0	--
JW2910-2	*ΔgalP*	+	1.0	$< 3.0 \times 10^{-7}$	1.0
		--	0.7	1.0	--
JW2138-1	*ΔgalS*	+	0.3	$< 3.0 \times 10^{-7}$	1.0
		--	0.7	1.0	--
JW2805-1	*ΔgalR*	+	1.0	$< 3.0 \times 10^{-7}$	1.0
		--	0.7	1.0	--

1 All assayed strains are isogenic derivatives of the Keio collection wild type BW25113.

2 The Rex^+ plasmid is a pHA1 plasmid, a pUC-derived high-copy y plasmid carrying the P_M-*cI*-*rexA*-*rexB*-t_{imm} cassette.

3 relative EOPs of T4/T4*rII* were determined using BW25113 as the 100% control for T4*rII* plating and BW25113[pHA1] as the 100% control for Rex activity. Relative EOPs are determined by dividing the number of plaques for the sample by the number of plaques on the 100% control. All results represent the average from three independent plating assays. Strains (*rex*$^+$) attenuated for Rex activity showed pinpoint plaques compared to *rex*$^-$ counterparts. Bolded results are the most relevant to Rex.

4 (--) Rex activity not measured; Rex^+ plasmid or *rexA*-*rexB* cassette not present.

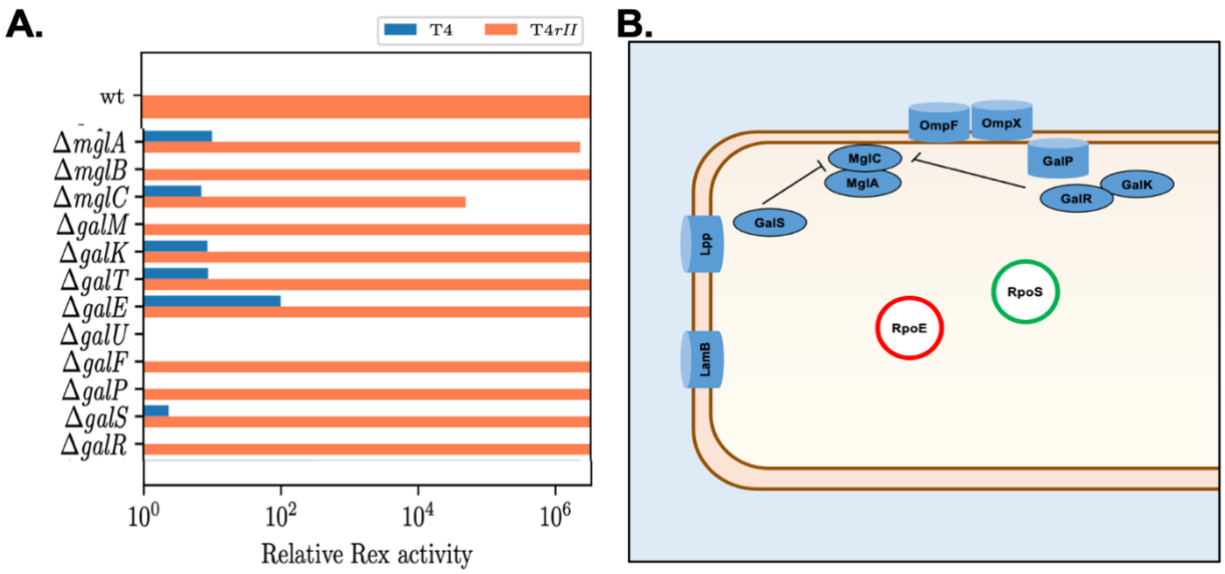


Figure 4-4. Influence of *mgl* and *gal* gene Deletions on Rex Activity. Several key membrane/cytoplasm proteins may play a role in Rex, as their deletions impact Rex activity. Deletion of *mglC* results in a 100-fold increase in T4*rII* plating, indicating a moderate reduction in Rex activity. **A.** Rex activity was assessed as the ability of pHA1-delivered *rex* genes to inhibit T4*rII* phage plating in the presence or absence of RII. Activity is calculated as the inverse of the relative EOP of the sample in *rex*$^+$ conditions (plasmid present) versus *rex*$^-$ (empty plasmid) conditions. Maximal Rex activity corresponds to complete inhibition of T4*rII* (*rII*$^-$) plating in *E. coli* BW25113 (wt) carrying the *rex*$^+$ pHA1. Absence of Rex activity is defined by full T4 (*rII*$^+$) plating in *E. coli* BW25113 (wt) in the presence of the *rex*$^+$ pHA1. **B.** While MglABC is not proven to be directly regulated by *rpoE* or *rpoS*, it is negatively regulated by *galS* and *galR*.

The wild-type parent strain carrying the *rex*$^+$ plasmid was used as a positive control for Rex and proved to be completely resistant to T4*rII* plating but exhibited near-complete sensitivity to the RII$^+$ phenotype of T4, which inhibits Rex activity. T4*rII* plating on all β-Methyl-galactoside genes deletion (Δ*mgl*) and galactose genes deletion (Δ*gal*) mutants carrying the *rex*$^+$ plasmids was similarly excluded, except for Δ*mglC,* where its mutation increased T4*rII*$^+$ plating by more than 10^2-fold in the presence of *rex* genes. Interestingly, T4 plating was affected compared to the wild type. The deletion of each of Δ*galK*, *T*, and *E* decreased T4 plating efficiency by as much as two orders of magnitude. Deletion of *galU* precluded plating of T4 and T4*rII* alike in a Rex-independent manner.

4.2.2 Assessing the effect of Sigma factors and other membrane proteins on Rex activity

Given the strong influence of outer membrane proteins on the Rex phenotype (Alattas et al., 2020), other essential membrane proteins as well as the sigma factors that govern the expression of *E. coli* membrane genes under various conditions, were examined (Table 4-3). The high-copy pHA1 *rex*$^{+}$ plasmid was used to transform all single-gene deletion mutants of interest, and the cultures were assayed for Rex activity (Figure 4-4).

Table 4-3. The impact of the membrane protein deletions on Rex activity.

Strain [1]	**Mutation**	**Rex Plasmid**[2]	**Relative Efficiency of Plating** [3]		
			T4(wt)	**T4*rII***	**Rex Activity**
Wild type		+	0.2	$< 3.0 \times 10^{-7}$	1.0
		--	1.0	1.0	--[4]
JW0729-3	***ΔtolA***	**+**	**0.3**	**0.8**	**2.7×10^{-7}**
		--	1.0	0.6	--
JW5100-1	*ΔtolB*	+	0.14	$< 3.0 \times 10^{-7}$	1.0
		--	1.0	1.0	--
JW5503-1	*ΔtolC*	+	1.0×10^{-2}	$< 3.0 \times 10^{-7}$	1.0
		--	1.0	1.0	--
JW0727-1	*ΔtolQ*	+	8.0×10^{-2}	$< 4.0 \times 10^{-7}$	1.0
		--	1.0	1.0	--
JW0728-1	*ΔtolR*	+	6.0×10^{-2}	$< 3.0 \times 10^{-7}$	1.0
		--	0.7	0.7	--
JW0731-1	*Δpal*	+	0.7	$< 3.0 \times 10^{-7}$	1.0
		--	0.8	1.0	--
JW5437-1	***ΔrpoS***	**+**	**$< 3.0 \times 10^{-7}$**	**$< 3.0 \times 10^{-7}$**	**1.0**

		--	0.7	0.7	--
UQ285	*rpoD[ts]*	+	0.3	1.0×10^{-6}	0.9
		--	0.7	0.6	--
JW3996-1	***ΔlamB***	+	**1.0×10^{-6}**	**$< 3.0 \times 10^{-7}$**	**1.0**
		--	0.7	0.8	--
JW1667-5	*Δlpp*	+	4.0×10^{-4}	3.0×10^{-3}	1.0×10^{-4}
		--	0.8	1.0	--
JW2974-1	*ΔexbB*	+	0.7	$< 3.0 \times 10^{-7}$	1.0
		--	0.8	0.8	--
JW2973-1	*ΔexbD*	+	5.0×10^{-4}	$< 3.0 \times 10^{-7}$	1.0
		--	0.8	0.8	--
JW5195-1	*ΔtonB*	+	0.8	$< 3.0 \times 10^{-7}$	1.0
		--	0.8	0.7	--
JW0146-2	*ΔfhuA*	+	2.0×10^{-2}	$< 3.0 \times 10^{-7}$	1.0
		--	0.7	0.8	--
JW5086-3	*ΔfepA*	+	1.0×10^{-6}	$< 3.0 \times 10^{-7}$	1.0
		--	0.8	0.8	--

[1] All assayed strains are isogenic derivatives of the Keio collection wild type BW25113.

[2] The Rex^+ plasmid is pHA1 plasmid - a pUC-derived high copy plasmid carrying the P_M-*cI*-*rexA*-*rexB*-t_{imm} cassette.

[3] Relative EOPs of T4/T4*rII* were determined using BW25113 as the 100% control for T4*rII* plating and BW25113[pHA1] as the 100% control for Rex activity. The relative EOPs are determined by dividing the number of plaques for the sample by the number of plaques on the 100% control. All results represent the average from three independent plating assays. Strains (*rex*$^+$) attenuated for Rex activity showed pinpoint plaques compared to *rex*$^-$ counterparts. Bolded results are the most relevant to Rex.

[4] (--) Rex activity not measured; Rex^+ plasmid or *rexA*-*rexB* cassette not present.

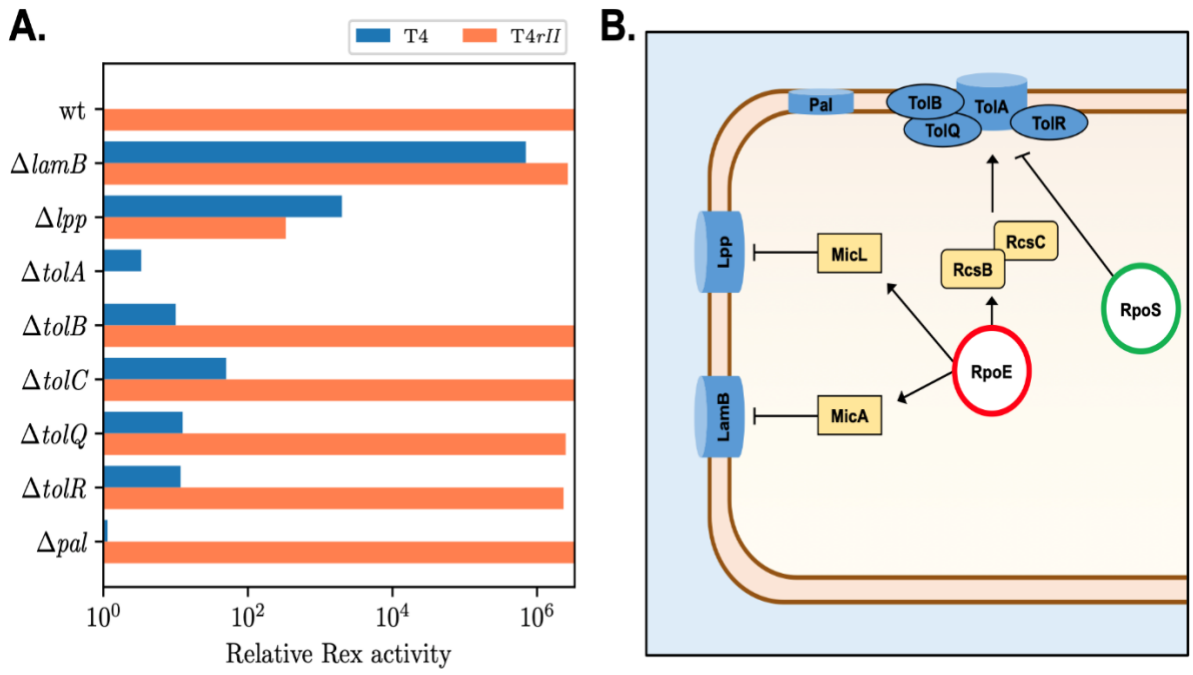


Figure 4-5. Deletions of *tolA* and Other Membrane Proteins Influence Rex Activity. Several other key membrane proteins may play a role in Rex, as their deletions impact Rex activity. In particular, Δ*tolA* completely restores T4*rII* plating, effectively abolishing Rex activity. **A.** Rex activity is defined as the ability of *rex* genes, delivered via the pHA1 plasmid, to inhibit T4*rII* plating in the presence or absence of RII. Activity is quantified as the inverse of the relative EOP of the sample in *rex*$^+$ conditions (plasmid present) versus *rex*$^-$ (empty plasmid) conditions. Maximal Rex activity corresponds to complete attenuation of T4*rII* (*rII*$^-$) plating in *E. coli* BW25113 (wt) in the presence of the *rex*$^+$ pHA1. Absence of Rex activity is indicated by full plating of T4 (*rII*$^+$) in *E. coli* BW25113 (wt) in the presence of the *rex*$^+$ pHA1. **B.** TolA is positively regulated by *rpoE* but negatively regulated by *rpoS*. Additional membrane proteins, such as Lpp and LamB are also regulated through the *rpoE* pathway.

Interestingly, full plating efficiency of T4*rII* on the *ΔtolA* (pHAp1- high copy *rex* expression) mutant transformant was observed. An indication of a complete abrogation of Rex activity. This result was confirmed upon lysogenization of the Δ*tolA* mutant by λ*rex*$^+$ (wild-type *rex*$^+$ expression level), where pinpoint T4*rII* plaques were observed compared to wild-type T4 plaques. This is counterintuitive because higher Rex expression (from pHA1) would normally be expected to enhance exclusion, not reduce it. One possible explanation is that overexpression of Rex from a multicopy plasmid in a Δ*tolA* background disrupts explicitly the balance of membrane-associated processes required for Rex function, whereas single-copy expression maintains sufficient activity to restrict T4*rII*. Additionally, this indicates the strong influence of TolA on Rex activity, which helps exclude T4*rII*; without TolA, the stoichiometry of RexA to RexB might not be maintained. Mutations in *tolQ, R,* or *C* did not significantly affect T4*rII* plating and allowed nearly complete Rex activity in a *rex*$^+$ context.

As well, the *Δpal* mutant did not show any effect on Rex, whereas the *Δlpp* mutant enhanced T4*rII* plating by 10^4-fold compared to the control in a *rex*$^+$ context. This may suggest some role for Lpp, but perhaps not Pal, in Rex. Additionally, the deletion of either *tonB* or *exbB* had no influence on T4 or T4*rII* plating. Another notable mutant was Δ*rpoS*. The *rpoS* mutant entirely abrogated T4 and T4*rII* plating alike, but only in a Rex-dependent context. No change of T4 and T4*rII* plating was observed in the absence of *rex*.

4.2.3 Assessing the Effect of Stationary Phase Regulators on Rex Activity

After the strong influence of *rpoS* in triggering Rex was confirmed, the involvement of proteins regulating sigma factor expression during *E. coli's* growth and stationary phases were assessed. All single-gene deletion mutants were transformed by the high-copy pHA1 *rex*$^+$ plasmid, and cultures were assayed for Rex activity, as shown in Table 4-4 and Figure 4-6. After assessing the Rex activity of these mutants using the high-copy Rex$^+$ plasmid, pHA1, these results were confirmed by comparing them with wild-type *rex*$^+$ (lysogeny) expression levels. Each stationary phase regulatory mutant was lysogenized by λ*cI*857 (*rex*$^+$) phage and assayed for Rex activity (Table 4-4).

Table 4-4. The stationary phase sRNAs and regulators are required for Rex activity and superinfection exclusion.

Strain [1]	Mutation	*rex*$^+$ Source[2]	Relative Efficiency of Plating [3]		
			T4(wt)	T4*rII*	Rex Activity
Wild type		pHA1	0.5	< 3.0 x 10^{-7}	1.0
		λ*cI*857	1.0	< 3.0 x 10^{-7}	1.0
		--	1.0	1.0	--[4]
JW1223-1	***ΔrssB***	**pHA1**	**0.5**	**3.0 x 10^{-3}**	**< 1.0 x 10^{-4}**
		λ*cI*857	**1.0**	**1.0**	**< 3.0 x 10^{-7}**
		--	1.0	1.0	--
JW1222-2	***ΔrssA***	**pHA1**	**3.0 x 10^{-3}**	**0.2**	**< 6.0 x 10^{-5}**
		λ*cI*857	**1.0**	**0.9**	**< 3.0 x 10^{-7}**
		--	1.0	1.0	--
JW0373-4	***ΔiraP***	pHA1	3.0 x 10^{-2}	< 3.0 x 10^{-7}	1.0
		λ*cI*857	**1.0**	**0.1**	**< 3.0 x 10^{-5}**
		--	1.0	1.0	--
JW1147-5	***ΔiraM***	pHA1	0.5	< 3.0 x 10^{-7}	1.0
		λ*cI*857	**1.0**	**0.1**	**< 3.0 x 10^{-5}**
		--	1.0	1.0	--
JW5782-2	***ΔiraD***	**pHA1**	**0.5**	**3.0 x 10^{-3}**	**< 1.0 x 10^{-4}**
		λ*cI*857	**1.0**	**1.0**	**< 3.0 x 10^{-7}**
		--	1.0	1.0	--

[1] All assayed strains are isogenic derivatives of the Keio collection wild type BW25113.

[2] The *rex*$^+$ genotype is either from pHA1 plasmid, a pUC-derived high copy plasmid carrying the P_M-*cI-rexA-rexB-*t_{imm} cassette, or λ*cI*857 (*rex*$^+$) lysogen.

[3] Relative EOPs of T4/T4*rII* were determined using BW25113 as the 100% control for T4*rII* plating and BW25113[pHA1] as the 100% control for Rex activity. Relative EOPs are determined by dividing the number of plaques for the sample by the number of plaques on the 100% control. All results represent the average from three independent plating assays. Strains (*rex*$^+$) attenuated for Rex activity showed pinpoint plaques compared to *rex*$^-$ counterparts. Bolded results are the most relevant to Rex.

[4] (--) Rex activity not measured; Rex$^+$ plasmid or *rexA-rexB* cassette not present.

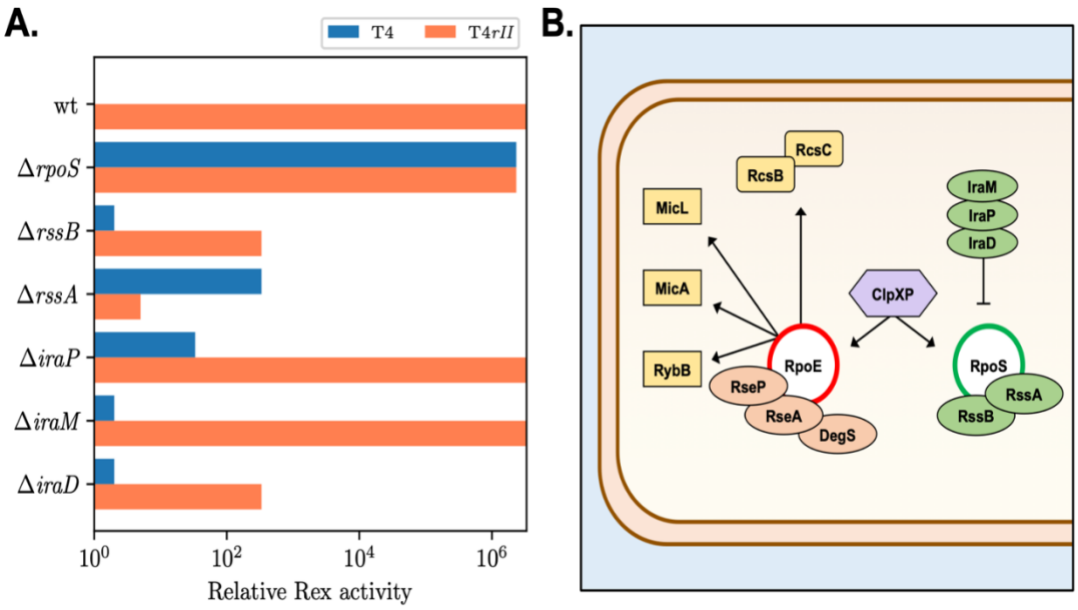


Figure 4-6. Interaction of Regulatory sRNAs and Sigma Factors with Rex Activity. The *rex* genes can inhibit T4 (*rII*$^{+}$) plating if *rpoS* is deleted. **A.** Rex activity is defined as the ability of *rex* genes, delivered via pHA1 plasmid, to inhibit T4*rII* plating in the presence or absence of RII. Activity is calculated as the inverse of the relative EOP under *rex*$^{+}$ (plasmid present) versus *rex*$^{-}$ (empty plasmid) conditions. Maximal Rex activity corresponds to complete attenuation of T4*rII* (*rII*$^{-}$) plating in *E. coli* BW25113 (wt) in the presence of the *rex*$^{+}$ pHA1. Absence of Rex activity is indicated by full plating of T4 (*rII*$^{+}$) in the presence of the *rex*$^{+}$ pHA1 in *E. coli* BW25113 (wt). **B.** The expression of *rpoS* is regulated by the anti-adaptor proteins IraM, IraP, and IraD, while the ClpXP protease complex modulates both *rpoE* and *rpoS* levels. Additionally, several small RNAs (sRNAs), including MicL, MicA, RybB, RcsB, and RcsC, are regulated through the *rpoE* pathway.

Transformants with Δ*rssA,* Δ*rssB,* or Δ*iraD* showed a notable reduction of Rex activity that ranged from 10^3 for Δ*rssA* to $>10^4$ for both Δ*rssB* and Δ*iraD,* despite high *rex*$^+$ expression from pHA1. Nonetheless, the *ΔiraM* and *ΔiraP* mutants showed minimal to no effect on Rex activity despite high *rex*$^+$ expression. Notably, nearly complete attenuation was seen in λ*cI*857 lysogens of Δ*rssA,* Δ*rssB,* and Δ*iraD* lysogens, compared to the parent strain BW25113(λ) *rex*$^+$ control. Almost total removal of Rex activity occurred when the *ΔtolA* mutant was lysogenized by λ, allowing for the reappearance of pinpoint plaques of T4*rII*. This phenomenon was also evident in the *ΔrpoS(*λ) mutant. This pattern suggests that Rex activity is more sensitive to the host background when expressed from a single-copy prophage than from a multicopy plasmid, possibly due to differences in plasmid maintenance or expression levels. The results for Δ*rssB* (expected to increase RpoS) and *ΔrpoS* (expected to decrease RpoS) are consistent with RpoS involvement in Rex regulation. In contrast, the strong effect of Δ*rssA*, as previously not linked to Rex, is unexpected and intriguing. The modest or absent effect of *iraP*, *iraM*, and *iraD* deletions under plasmid conditions, but strong effects in lysogens, may reflect differences in stress signaling or strain background. All mutants were confirmed by complementation, ruling out polar effects and supporting their direct involvement.

4.2.4 T4*rII* Infective Center Assay for Host Genes Activity with Natural *rex* Gene Dosage

To improve plaque quantification and assess morphology, T4*rII*-infected centers from the most promising deletion mutants were examined for plating efficiency (Table 4-5). This center-of-infection assay involves spotting infected cells onto a lawn of non-lysogenic *E. coli,* allowing released phage to form plaques. This process helps small plaques expand for easier observation and counting.

Table 4-5. Influence of Stress-response regulators on Rex-mediated T4*rII* exclusion

Mutation	Relative EOP of T4*rII*-infected centres[1]
–	1.0
– (λ)	$<3.0 \times 10^{-7}$
Δ*ompC* [2]	$<3.0 \times 10^{-7}$
Δ*rpoS*	0.7
Δ*tolA*	1.0
Δ*rssA*	0.9
Δ*rssB*	1.0
Δ*iraM*	0.1
Δ*iraP*	0.1
Δ*iraD*	1.0

[1]All assayed strains are *rex*$^+$ isogenic derivatives of the Keio collection wild-type BW25113, lysogenized with λ. Relative EOPs for T4/T4*rII* were determined using BW25113 as the 100% reference control for T4*rII* plating. For each assay, mutant-infected center cells were allowed to adsorb T4*rII* for 15 minutes, followed by three washes, dilution, and plating on the corresponding test strain. Data represent the average of three independent plating experiments.

[2] The Δ*ompC* mutant is a host range mutant that prevents T4 adsorption; as a result, neither phage can infect this strain.

The infective center assay proved to be a more effective method for visualizing and quantifying phage plaques, as it consistently produced larger and more countable plaques on the assay plates. This improvement in plaque clarity and resolution facilitated more accurate measurements of phage infectivity and Rex activity. Notably, the results obtained from this assay were consistent with those observed following lysogenization by λ*cI*857(*rex*$^+$), as shown in Table 4-5. This concordance reinforces our hypothesis that Rex activity is influenced by gene dosage, particularly in the context of *rex* gene expression from the prophage.

4.2.5 Complementation of Identified Host Genes Influencing the Rex Phenotype

To restore the function of each gene in the mutants that showed some or complete attenuation of Rex activity, a complementation assay was applied (Table 3-1). Restoring the normal Rex phenotype upon infection by T4*rII* would further support the involvement of these genes in the Rex phenotype.

Mutants were selected based on their most significant influence on either Rex activity or RII plating. All single-gene deletion mutants were lysogenized with λ*cI*857 (rex^+), and then cultures were assayed for Rex activity, as shown in Table 4-6.

Using the designed Forward and Reverse primers, amplification of all tested genes was obtained and successfully confirmed by agarose gel electrophoresis. The complementary plasmids were constructed as described in Figures 3-7 and 3-8. Briefly, the PCR product of each amplified gene was first inserted into the MCS of *Xba*I-linearized pUC19. The cassette of interest was then extracted from pUC19 through digestion with *BamH*I and *Sal*I and inserted into pBR322 at the same restriction sites to obtain the final complementary constructs (Figure 4-7). Each complementary construct was then transformed into the respective mutant for complementation.

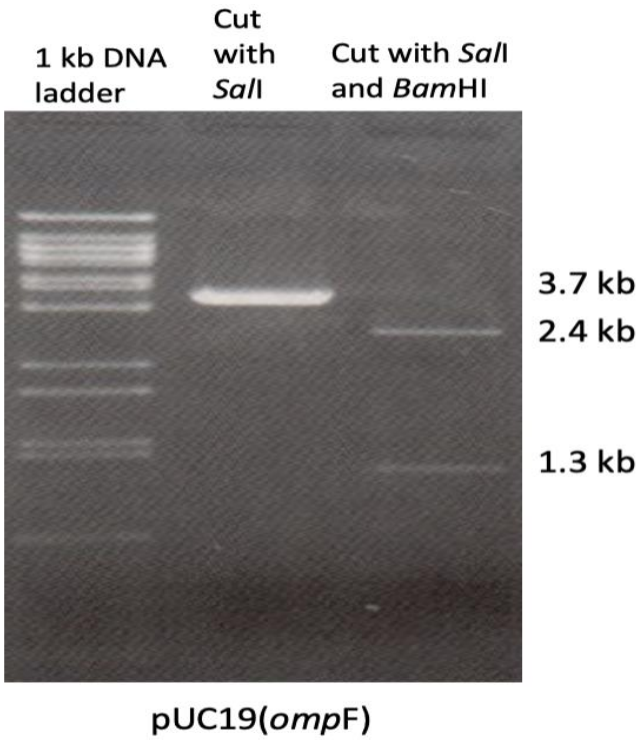


Figure 4-7. Agarose Gel Electrophoresis of the *ompF* Fragment Digested with Restriction Enzymes. Lane 1: 1 kb DNA ladder; Lane 2: *ompF* fragment digested with *Sal*I, yielding a single band of approximately 3.7 kb; Lane 3: *ompF* fragment digested with *Sal*I and *BamH*I, producing two bands of approximately 2.4 kb and 1.3 kb, consistent with expected fragment sizes based on restriction site positions.

All mutants were first lysogenized by λ*cI*857 and then tested against T4 and T4*rII* plating. All mutants (λ*cI*857) were transformed by the designated vectors and confirmed to be Tc-sensitive and Amp-resistant, indicating successful insertion of the cassette interrupting the Tc marker in pBR322. T4 (wt) and T4*rII* were then plated on the lysogenized mutants carrying their designated vectors. Rex activity was assessed against the wild-type BW25113 both with and without pBR322 as a negative control, and with λ*cI*857 lysogen as a positive control for Rex activity (Table 4-6). Complete Rex activity was restored in all mutants carrying the designated plasmids, indicating each complementing gene does indeed contribute to the Rex phenotype.

Table 4-6. Rex activity after plasmid complementation of host mutations.

Strain	Trans Complementation*	Relative EOP of T4*rII***
wild type BW25113	pBR322	1.0
	--	1.0
wild type BW25113 (λ)	pBR322	$<3.0 \times 10^{-7}$
	--	$<3.0 \times 10^{-7}$
tolA (λ)	*(tolA)*	$<3.0 \times 10^{-7}$
	--	1.0
ompX (λ)	*(ompX)*	$<3.0 \times 10^{-7}$
	--	4.5×10^{-4}
ompF (λ)	*(ompF)*	$<3.0 \times 10^{-7}$
	--	3.3×10^{-5}
ompA (λ)	*(ompA)*	$<3.0 \times 10^{-7}$
	--	5.0×10^{-4}
ompW (λ)	*(ompW)*	$<3.0 \times 10^{-7}$
	--	1.0×10^{-3}
ompR (λ)	*(ompR)*	$<3.0 \times 10^{-7}$
	--	$<3.0 \times 10^{-7}$
rpoS (λ)	*(rpoS)*	$<3.0 \times 10^{-7}$
	--	0.7
iraD (λ)	*(iraD)*	$<3.0 \times 10^{-7}$
	--	1.0
rssA (λ)	*(rssA)*	$<3.0 \times 10^{-7}$
	--	0.9
rssB (λ)	*(rssB)*	$<3.0 \times 10^{-7}$
	--	1.0
mglC (λ)	*(mglC)*	$<3.0 \times 10^{-7}$
	--	$<3.0 \times 10^{-6}$
mglA (λ)	*(mglA)*	$<3.0 \times 10^{-7}$
	--	1.0

*Plasmid pBR322 was used to deliver the gene of interest into each mutant; (--) was the control, pBR322 empty plasmid.

** Relative EOPs of T4/T4*rII* were determined using BW25113 as the 100% control for T4*rII* plating and BW25113[rex^+ λ] as the 100% control for Rex activity. Relative EOPs are determined by dividing the number of plaques for the sample by the number of plaques on the 100% control. All results represent the average from three independent plating assays. Strains (rex^+) attenuated for Rex activity showed pinpoint plaques compared to rex^- counterparts.

Some host mutations could restore T4*rII* infectivity even in the presence of *rex*$^{+}$ genes in the cell, as seen in previous experiments. In this assay, a complementation of a mutation by a functional allele of a gene in trans is utilized to restore the Rex phenotype. The wild-type BW25113 without plasmid or with pBR322 showed complete T4*rII* infectivity and no Rex activity as a result of the lack of rex^{+} genes in the cell. In contrast, the positive control BW25113 (*λ*) without plasmid or with pBR322 showed full Rex activity (< 3.0×10^{-7}) and no T4*rII* plating.

In almost all cases of mutants lysogen without the complementation plasmids, a significant to complete T4*rII* plating efficiency was observed, similar to that of the negative controls. As the complementation restores the Rex phenotype, this strongly suggests these mutations have a significant impact on Rex activity. The complete removal of Rex activity was observed when the Δ*tolA* mutants were lysogenized by λ without complementation plasmids, allowing for the reappearance of pinpoint plaques of T4*rII*. Notably, all mutant lysogens were able to restore the wild-type BW25113 (λ) phenotype and demonstrated complete T4*rII* exclusion by transforming them with the designated complementation plasmids, thus restoring the function of each deleted gene.

4.3 Developing a Rex Protein Visualization System Using GFP Fusions

A system was designed to facilitate the determination of the intracellular localization of Rex proteins through fusion with green fluorescent protein (GFP) and/or red fluorescent protein (RFP). Expression of Rex under the control of the temperature-sensitive *cI*857 was evaluated prior to and following induction by temperature shift, as well as before and after infection with bacteriophage T4 and T4*rII*.

Each of the two *rex* genes was fused to GFP using the following configurations: 1) at either the C- or N-terminal of *rex* gene, 2) with or without the presence of the other *rex* gene, and 3) with or without a linker between the fused gene and the fluorescent protein, resulting in 22 constructs (Table 3-1; Appendix C Figures C1-11). The linker used in this project is optimized for *E. coli*, p(TSGSGSGSGSGT), and the corresponding nucleotide sequence is 3'accagcggtagcggcagcggtagcggcagcggcacc'5. To note, comparative analysis revealed no significant difference in fluorescence expression, T4*rII* plating or colony morphology between constructs with and without a linker. Given the consistency of results and lack of observable impact from the linker, constructs containing the linker were excluded from further replication. Subsequent analyses were focused exclusively on the non-linker variants.

T4*rII* plating efficiency and Rex activity: the initial plan was to utilize the wild-type strain; however, T4rII plating assays revealed a Rex^- phenotype, suggesting loss of Rex activity. To address this, functional copies of *rex* genes were introduced from λ lysogens to determine whether their presence could restore Rex activity and influence transformation efficiency or the functionality of fusion proteins. Assessment began with T4 and T4*rII* plating efficiency assays at different temperatures: 25 °C, 35 °C, and 37 °C, to evaluate plaque morphology and plating efficiency under various thermal conditions (Table 4-7). Complete Rex-mediated exclusion was not observed in any construct; however, several strains exhibited partial attenuation of T4*rII* growth, suggesting residual or altered Rex activity. These findings suggest that Rex function was

not entirely abolished but may have been compromised, potentially due to altered stoichiometry or impaired functionality of RexA or RexB caused by GFP/RFP fusions. Based on these observations, constructs were subsequently analyzed in a *rex*$^{+}$ context by introducing them into λ lysogens. This approach aimed to determine whether the presence of an additional functional copy of *rex* genes could compensate for any loss of activity in the fusion constructs and restore Rex-mediated exclusion. The analysis also sought to clarify whether Rex functionality depends on the relative abundance of RexA and RexB or is significantly disrupted by the fusion design, which can be assessed by evaluating the transformation efficiency of all constructs.

For the T4*rII* plating efficiency assay, *E. coli* BW25113 [pPL451] was used as the negative control, while BW25113 transformed by pPL451 encoding wild-type *rexA-rexB* was used as the 100% *rex*$^{+}$ control. BW25113 transformed by pPL451 carrying GFP was used as the 100% fluorescent activity control (Table 4-7). All were then tested for Rex activity through T4/T4*rII* plating. Later, all were lysogenized by λ*cI*857 and retested for their Rex activity using the T4/T4*rII* plating assay (Table 4-7).

Table 4-7. The fusion site of GFP significantly affects the activity of RexA and RexB across various incubation temperatures.

construct*	*E. coli* cell s state**	**Relative efficiency of plating*** for T4(wt)**			**Relative efficiency of plating *** for T4*rII***			**Rex Activity**		
		25 °C	35 °C	37 °C	25 °C	35 °C	37 °C	25 °C	35 °C	37 °C
_	wt	1.0	1.0	1.0	1.0	1.0	1.0	--	--	--
	λ*cI*857	1.0	1.0	1.0	$< 3.0 \times 10^{-7}$	$< 3.0 \times 10^{-7}$	$< 3.0 \times 10^{-7}$	1.0	1.0	1.0
pPL451	wt	1.0	1.0	1.0	1.0	1.0	1.0	--	--	--
	λ*cI*857	1.0	1.0	1.0	$< 3.0 \times 10^{-7}$	$< 3.0 \times 10^{-7}$	$< 3.0 \times 10^{-7}$	1.0	1.0	1.0
rexA-rexB	wt	1.0	1.0	1.0	$< 3.0 \times 10^{-7}$	$< 3.0 \times 10^{-7}$	$< 3.0 \times 10^{-7}$	1.0	1.0	1.0
	λ*cI*857	1.0	1.0	1.0	$< 3.0 \times 10^{-7}$	$< 3.0 \times 10^{-7}$	$< 3.0 \times 10^{-7}$	1.0	1.0	1.0
egfp	wt	1.0	1.0	1.0	1.0	1.0	1.0	--	--	--
	λ*cI*857	1.0	1.0	1.0	$< 3.0 \times 10^{-7}$	$< 3.0 \times 10^{-7}$	$< 3.0 \times 10^{-7}$	1.0	1.0	1.0
rexA::egfp	wt	1.0	1.0	1.0	1.0	1.0	1.0	--	--	--
	λ*cI*857	1.0	1.0	1.0	2.0×10^{-6}	6.0×10^{-6}	5.0×10^{-6}	0.6	0.2	0.16

egfp::rexA	wt	1.0	1.0	1.0	1.0	1.0	1.0	--	--	--
	λ*cI*857	1.0	1.0	1.0	0.2	0.4	0.6	6.0×10^{-5}	1.3×10^{-6}	2.0×10^{-6}
rexB::egfp	wt	1.0	1.0	1.0	1.0	1.0	1.0	--	--	--
	λ*cI*857	1.0	1.0	1.0	6.0×10^{-5}	6.0×10^{-4}	1.0×10^{-5}	2.0×10^{-2}	2.0×10^{-3}	3.0×10^{-2}
egfp::rexB	wt	1.0	1.0	1.0	1.0	1.0	1.0	--	--	--
	λ*cI*857	1.0	1.0	1.0	0.4	0.2	0.2	1.2×10^{-6}	6.0×10^{-5}	6.0×10^{-5}
rexA::egfp-rexB	wt	1.0	1.0	0.9	1.0	1.0	1.0	--	--	--
	λ*cI*857	1.0	1.0	1.0	**< 5.0 x 10^{-6}**	**3.0 x 10^{-6}**	**3.0 x 10^{-6}**	0.16	0.1	0.1
egfp::rexA-rexB	wt	0.9	1.0	1.0	0.9	0.9	1.0	--	--	--
	λ*cI*857	0.8	0.9	0.8	0.8	0.5	0.8	< 3.0 x 10^{-7}	1.6×10^{-5}	< 3.0 x 10^{-7}
rexA-rexB::egfp	wt	1.0	1.0	0.9	0.9	0.9	0.9	--	--	--
	λ*cI*857	0.9	1.0	1.0	**3.0 x 10^{-5}**	**1.0 x 10^{-7}**	**1.0 x 10^{-7}**	1.0 x 10^{-2}	0.3	0.3
rexA-egfp::rexB	wt	1.0	1.0	0.9	0.9	0.9	0.9	--	--	--
	λ*cI*857	1.0	1.0	1.0	3.0×10^{-5}	6.0×10^{-5}	3.0 x 10^{-5}	1.0 x 10^{-2}	2.0×10^{-2}	1.0×10^{-2}
rexA::egfp-rexB::rfp	wt	0.8	0.9	1.0	0.8	0.8	0.9	--	--	--

	λ*cI*857	0.8	0.9	0.8	**3.0 x 10^{-6}**	**8.0 x 10^{-6}**	**8.0 x 10^{-6}**	**0.1**	**0.26**	**0.26**
egfp::rexA-rfp::rexB	wt	0.8	1.0	0.8	1.0	1.0	1.0	--	--	--
	λ*cI*857	1.0	1.0	1.0	0.8	0.6	0.6	< 3.0 x 10^{-7}	2.0 x 10^{-6}	2.0 x 10^{-6}
egfp::rexA-rexB::rfp	wt	1.0	1.0	0.8	1.0	1.0	0.8	--	--	--
	λ*cI*857	1.0	0.9	1.0	0.8	0.4	6.0 x 10^{-4}	< 3.0 x 10^{-7}	1.3 x 10^{-5}	2.0 x 10^{-3}

***** All assayed strains are isogenic derivatives of *E. coli* BW25113 from the Keio collection. All constructs were built using the pPL451 plasmid, with cassettes cloned into the MCS under the control of the CI (TS) repressor. *E. coli* BW25113 served as the host strain for all constructs.

****** Host strains included either wild-type (WT) *E. coli* BW25113 or its *λcI*857 lysogenized variant. *E. coli* BW25113 (wt), with or without pPL451 plasmid, was used as the Rex$^-$ control and as the 100% reference for T4 and T4*rII* plating efficiency. The BW25113 λ*cI*857 (*rex*$^+$) lysogen served as a positive control for Rex activity, providing an additional chromosomal copy of the *rex* genes to confer the Rex phenotype. The [pPL451 *rexA-rexB*] construct served as the 100% *rex*$^+$ control for Rex activity, while pPL451-eGFP was used as the 100% control for fluorescent protein expression.

******* The relative EOPs for T4/T4*rII* phages were determined using BW25113 as the 100% reference control for T4*rII* plating and BW25113[pPL451-*rexAB*] as the 100% reference control for Rex activity. Relative EOPs are calculated by dividing plaque-forming units (PFUs) on each test strain by PFUs on the corresponding 100% control. All relative EOP values represent the average of three independent plating assays. Rex$^+$ strains displayed markedly reduced T4*rII* EOPs, typically forming pinpoint plaques indicative of abortive infection, in contrast to the larger plaques observed on Rex$^-$ strains. At 25 °C, incubation was extended to 24–36 hours due to the slower growth of the bacteria. At 35 °C and 37 °C, plaques were counted within 16–24 hours. All reported results are the mean of three independent assays.

The *E. coli* BW25113 strains expressing different *rex::egfp* constructs were evaluated to investigate the impact of fluorescent protein fusion on Rex activity and T4*rII* plating. The negative controls (no plasmid, pPL451, and *egfp* alone in wt cells) consistently demonstrated 100% plating efficiency for T4 and T4*rII*. Consequently, there was no Rex activity across all tested temperatures, as expected. In *λcI857* lysogenic cells, the presence of *rex* genes means that *rexA-rexB*, pPL451, and *egfp* constructs exhibited 100% positive Rex function only when both *rexA* and *rexB* genes were present. The complete Rex phenotype displays 100% Rex activity when the efficiency of plating of T4*rII* is approximately 3.0×10^{-7}, at which point no plaques can be observed. As expected, pPL451 and pPL451-e*gfp* each showed no Rex activity.

At 25 °C (repressed state, no expression of Rex proteins), in both *E. coli* lysogen and non-lysogen, the GFP fusion at the N-terminus of RexA protein, whether alone or in the presence of the other *rex* gene, results in a significant reduction of Rex activity, and almost complete loss of Rex phenotype**.** This may be due to a lack of Rex activity in a repressed state, with only activity observed stemming from a leaky expression of Rex. Whereas the N-terminally-fused RexB protein, whether alone or in the presence of the other *rex* gene, results in a noticeable reduction of Rex activity, ranging from 100-fold to complete loss of Rex activity. The GFP fusion at the C-terminus of either Rex protein (*rexA::egfp* or *rexB::egfp*), whether alone or in the presence of the other *rex* gene, and only in *E. coli* lysogen, maintains modest Rex activity across constructs, showing about a 10- to 100-fold reduction in Rex activity in every instance. In wild-type strains harbouring both *rex* genes, fused either at the C- or N-terminus, T4 and T4*rII* were both able to completely abrogate Rex. Noteworthy results emerged from the double fusions of GFP and RFP at the C-terminus of both *rexA* and *rexB*, specifically the *rexA::egfp-rexB::rfp* construct, which produced the strongest Rex activity with minimal T4*rII* plating across *E. coli* lysogens. The N-terminal fusion of both Rex proteins, on the other hand, showed a complete loss of Rex activity across *E. coli* lysogen and non-lysogen cells.

At 35 °C (partial repressed state, partial expression of Rex proteins), in both *E. coli* lysogen and non-lysogen, the GFP fusion at the N-terminus of RexA protein, whether alone or in the presence of the other *rex* gene, results in a significant reduction of Rex activity, and almost complete loss of Rex phenotype**.** GFP fusion at the N-terminus of the RexB protein, whether alone or in the presence of the other rex gene, also results in a significant reduction of Rex activity. Interestingly, in the case of the *rexA-egfp::rexB* construct in lysogenized cells, only a modest 100-fold reduction was observed. The GFP fusion at the C-terminus of either Rex protein (*rexA::egfp or rexB::egfp*), whether in the presence or absence of the other *rex* gene, retained strong Rex activity across constructs, but only in lysogens. A reduction in Rex activity of approximately 10- to 100-fold was observed in every such instance. To note, T4 and T4*rII* alike, were both able to completely abrogate Rex activity in all non-lysogenic cells, harbouring both Rex proteins, fused either at the C- or N- terminus. Notably, the double fusions of GFP and RFP at the C-terminus of both RexA and RexB, particularly the *rexA::egfp-rexB::rfp* construct, exhibited the strongest Rex activity with minimal T4*rII* plating across *E. coli* lysogens. The N-terminal fusion of both Rex proteins, on the other hand, showed a complete loss of Rex activity in both *E. coli* lysogen and non-lysogen cells, similar to what was observed at 25 °C.

At 37 °C (derepressed state), very similar results to those at 35 °C were observed. In both *E. coli* lysogens and non-lysogens, GFP fusion at the N-terminus of either Rex protein, whether alone or in the presence of the other *rex* gene, leads to significant reductions in Rex activity, except in the case of the *rexA-egfp::rexB* construct in the lysogen, which mostly retained activity with only a 100-fold reduction. The GFP fusion at the C-terminus of either Rex protein (*rexA::egfp or rexB::egfp*), whether in the presence or absence of the other *rex* gene, retains strong Rex activity across constructs only in the *E. coli* lysogen. Exhibiting a reduction in Rex activity of approximately 10- to 100-fold in every instance. Again, in non-lysogenic cells harbouring both Rex proteins and fused at either terminal, T4 and T4*rII*

were able to abrogate Rex completely. Also, double fusions of GFP and RFP at the C-terminus of both RexA and RexB, particularly the *rexA::egfp-rexB::rfp* construct, exhibited the strongest Rex activity with minimal T4*rII* plating across *E. coli* lysogens. The N-terminal fusion of both Rex proteins, on the other hand, resulted in a complete loss of Rex activity in both *E. coli* lysogen and non-lysogen cells, similar to the effect observed at different temperatures. Notably, the *egfp::rexA-rexB::rfp* construct exhibited modest Rex activity at higher temperatures but showed a 1000-fold reduction in Rex and a 10^4-fold increase in T4*rII* plating in the lysogen. Overall, these observations suggest that the presence of a fluorescent protein may attenuate Rex activity, reducing but not completely abolishing the Rex phenotype. The data further suggest that while fluorescently tagged Rex proteins lose their ability to fully mediate Rex function, they retain the capacity to interfere with or competitively inhibit the activity of untagged Rex proteins.

Transformation efficiency: The relative transformation efficiency was calculated to assess the effect of the fluorescent tag on Rex activity, particularly in cases where both Rex proteins were fluorescently tagged. The transformation efficiency of all GFP/RFP fusion constructs was calculated at multiple temperatures: 23 °C (room temperature, inactive CI repressor), 30 °C (inactive CI), 35 °C and 37 °C (activated CI) (Table 4-8).

Table 4-8. Assessing the Relative Transformation Efficiency of GFP-*rex* Combination Constructs at Various Temperatures.

Construct*	***E. coli* cellular state****	**Relative efficiency of transformation*** **			
		23 °C	**30** °C	**35** °C	**37** °C
--	wt	5 x 10^{-2}	0.7	1.0	1.0
	λ*cI857*	6 x 10^{-2}	0.8	1.0	n/a****
[rexA-rexB]	wt	5 x 10^{-4}	1 x 10^{-2}	1 x 10^{-2}	1 x 10^{-2}
	λ*cI857*	7 x 10^{-4}	1 x 10^{-2}	1 x 10^{-2}	5 x 10^{-4}
[*egfp*]	wt	5 x 10^{-4}	1 x 10^{-2}	1 x 10^{-2}	1 x 10^{-2}
	λ*cI857*	6 x 10^{-4}	1 x 10^{-2}	1 x 10^{-2}	n/a
rexA::egfp	wt	5 x 10^{-4}	6 x 10^{-3}	6 x 10^{-3}	5 x 10^{-6}
	λ*cI857*	6 x 10^{-4}	8 x 10^{-3}	7 x 10^{-3}	n/a
egfp::rexA	wt	4 x 10^{-4}	3 x 10^{-3}	5 x 10^{-3}	7 x 10^{-7}
	λ*cI857*	4 x 10^{-4}	5 x 10^{-3}	6 x 10^{-3}	n/a
rexB::egfp	wt	4 x 10^{-4}	1 x 10^{-2}	9 x 10^{-3}	5 x 10^{-6}
	λ*cI857*	5 x 10^{-4}	1 x 10^{-2}	1 x 10^{-2}	n/a
egfp::rexB	wt	5 x 10^{-4}	8 x 10^{-3}	7 x 10^{-3}	5 x 10^{-8}
	λ*cI857*	4 x 10^{-4}	8 x 10^{-3}	8 x 10^{-3}	n/a
rexA::egfp-rexB	wt	3 x 10^{-4}	5 x 10^{-3}	5 x 10^{-3}	6 x 10^{-5}
	λ*cI857*	5 x 10^{-4}	5 x 10^{-3}	6 x 10^{-3}	5 x 10^{-6}
egfp::rexA-rexB	wt	5 x 10^{-6}	**1 x 10^{-6}**	**6 x 10^{-5}**	3 x 10^{-6}
	λ*cI857*	6 x 10^{-5}	**5 x 10^{-7}**	**3 x 10^{-5}**	3 x 10^{-7}
rexA-rexB::egfp	wt	5 x 10^{-5}	7 x 10^{-3}	8 x 10^{-3}	5 x 10^{-5}

	λcI857	2 x 10^{-5}	8 x 10^{-3}	1 x 10^{-2}	6 x 10^{-6}
rexA-egfp::rexB	wt	7 x 10^{-5}	5 x 10^{-3}	8 x 10^{-3}	3 x 10^{-6}
	λcI857	3 x 10^{-5}	7 x 10^{-3}	8 x 10^{-3}	5 x 10^{-7}
rexA::egfp-rexB::rfp	wt	2 x 10^{-6}	8 x 10^{-3}	7 x 10^{-3}	8 x 10^{-5}
	λcI857	4 x 10^{-5}	8 x 10^{-3}	9 x 10^{-3}	7 x 10^{-6}
egfp::rexA-rfp::rexB	wt	3 x 10^{-7}	3 x 10^{-3}	8 x 10^{-2}	5 x 10^{-6}
	λcI857	6 x 10^{-7}	4 x 10^{-3}	**5 x 10^{-5}**	8 x 10^{-8}
egfp::rexA-rexB::rfp	wt	8 x 10^{-6}	4 x 10^{-3}	4 x 10^{-3}	3 x 10^{-6}
	λcI857	6 x 10^{-6}	6 x 10^{-3}	5 x 10^{-3}	5 x 10^{-8}

* All constructs were derived from the pPL451 plasmid, with cassettes cloned into the MCS under the control of the CI (TS) repressor. (--) indicates the pPL451 plasmid (empty), as a negative control. *E. coli* BW25113 served as the host strain for all constructs.

** *E. coli* BW25113 was used either in its wild-type (wt) form or lysogenized with λ*cI*857(TS). For transformation efficiency assays, *E. coli* BW25113 (wt) or (λ*cI*857) carrying the empty pPL451 vector served as the negative control. [pPL451 *rexA-rexB*] was used as the 100% *rex*$^{+}$ control for Rex activity and transformation efficiency, while pPL451-eGFP served as the 100% control for fluorescent activity.

*** The relative efficiency of transformation was calculated as: the transformation efficiency of the test plasmid/ transformation efficiency of pPL451 control at 35 °C. For each transformation, 100 µL was plated on both LB and LB + Amp plates. Transformants were incubated overnight at room temperature (23 °C), 30 °C, 35 °C, and 37 °C. Some plates at 23 °C were left for over 36 hours to allow colonies to reach a countable size. All values represent the average of three independent transformation assays.

**** The "n/a" indicates that either the cells were fully lysed at the tested temperature, 37 °C, or that no data were available for the corresponding condition.

Initially, the plan was to use the wild-type strain as a host to test all fusion constructs and evaluate the impact of the fusions on Rex and its activity. However, results from the T4*rII* plating efficiency assay indicated a Rex^- phenotype, suggesting a loss of Rex activity, as mentioned earlier in the T4*rII* plating efficiency and Rex activity section and explained in the discussion. Therefore, Rex was reintroduced into the system to assess whether its presence in λ lysogens influences transformation efficiency or restores Rex activity in fusion constructs.

At 23 °C, the transformation efficiency was generally low across most constructs, regardless of host cell state (lysogens or non-lysogens), similar to pPL451 controls (with or without an eGFP tag). This observation suggests that cooler temperatures create suboptimal conditions for plasmid uptake and possibly affect transformation efficiency. All strains with only one *rex* gene (i.e. either *rexA* or *rexB,* in the absence of the other), regardless of the type or site of GFP fusion, exhibited moderate to similar efficiency to the controls. However, in the presence of both genes and dual tags with GFP and RFP, the transformation efficiency is notably lower than that of the controls. The majority exhibited a 1000-fold reduction in transformation efficiency and slow colony formation.

At 30 °C, transformation efficiency improved by approximately 100 to 1000-fold for nearly all transformants compared to 23 °C. This temperature appeared to support optimal cellular conditions for plasmid uptake, and several strains reached peak efficiency, similar to those transformed by solo *rex* gene fusion constructs. One interesting finding from the pPL451 (*egfp::rexA-rexB*) construct is that, although all constructs showed enhanced transformation efficiency, this particular construct exhibited a 10^4-fold reduction compared to the 100% controls.

At 35 °C, transformation efficiency remained relatively stable but showed some slight variability among certain transformants. Some maintained high efficiency comparable to the controls, while others, such as the *egfp::rexA-rfp::rexB* construct, began to show a decline, particularly among *E. coli*

lysogens. The *egfp::rexA-rexB* construct showed the lowest transformation efficiency in both lysogens and non-lysogens.

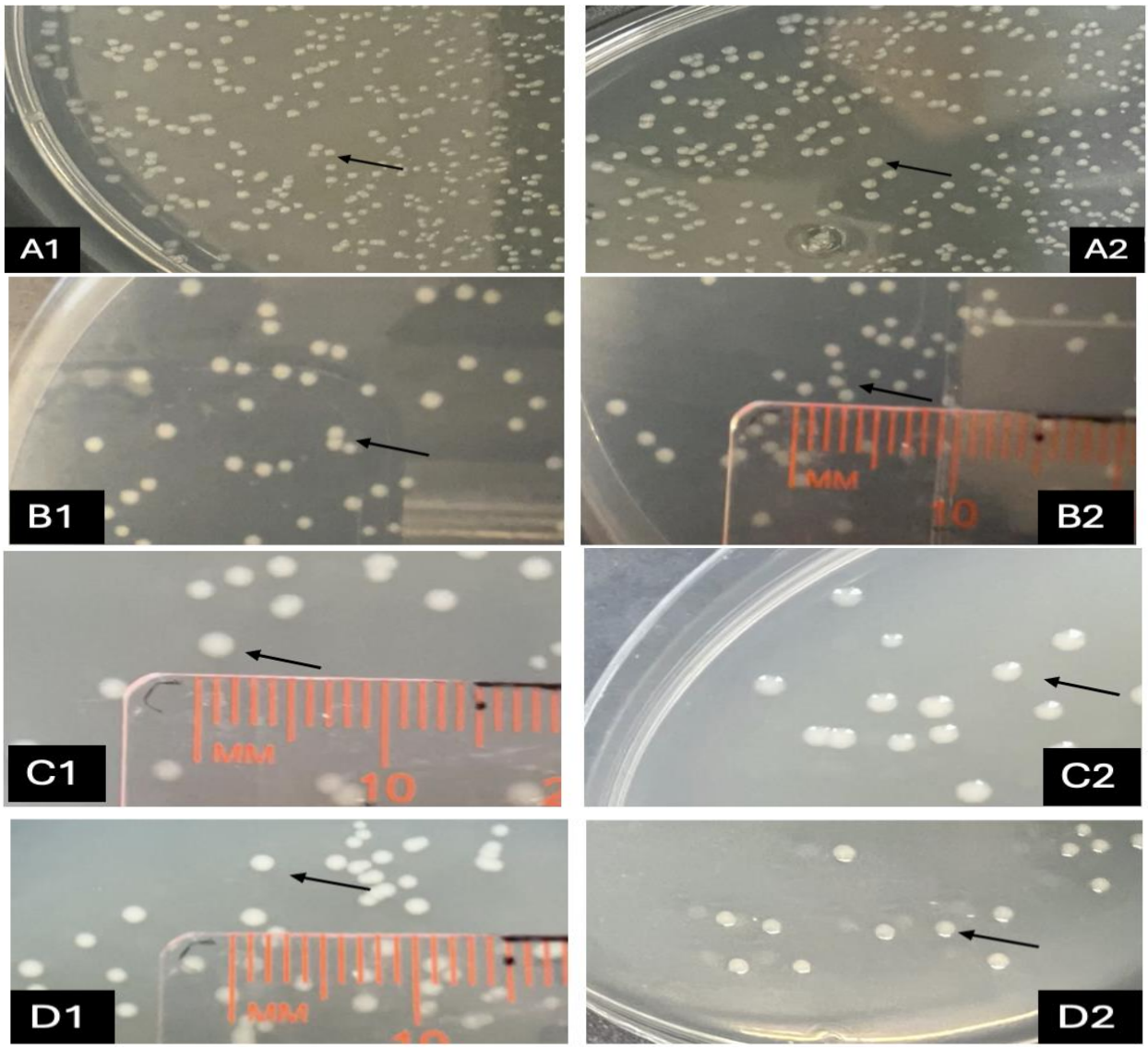
At 37 °C, the transformation efficiency decreased significantly with a 10^4-fold reduction compared to the 100% controls for both wild-type and lysogenized cells. The effect was most striking when cells were in the lysogenic form: all transformed lysogens were able to grow at lower temperatures (i.e., the repressed state, where Rex proteins are not expressed) but were barely able to do so at 37 °C (i.e., the unrepressed state, where Rex proteins are expected to be expressed) compared to 100% controls.

While some λ*cI*857 lysogens were able to grow on LB supplemented with ampicillin, which selects for the pPL451 plasmid, they were unable to grow on LB without antibiotics at 37 °C. This observation was noted with all strains that had only one *rex* gene, in the absence of the other (i.e., either *rexA* or *rexB*), regardless of the type or site of GFP fusion or which Rex protein was tagged (see discussion for suggested explanation). In the presence of both genes, where one is fused with GFP, the transformation efficiency is significantly lower than that of the controls. The transformation efficiency is reduced by approximately 100 to 10^4 times compared to controls.

Colony morphology: Colony morphology and growth characteristics were evaluated for *E. coli* strains harbouring plasmids encoding GFP-fused RexA or RexB proteins in the absence or presence of the corresponding partner protein (RexA or RexB). Transformed colonies were observed after 24 hours of incubation. Colonies of *E. coli* BW25113 [pPL451], the 100% *rex*$^+$ control, and the pPL451-*egfp* control all exhibited the same characteristics at the same temperatures. The colonies exhibited a wild-type morphology, characterized by regular, round, shiny, and smooth surfaces (Figure 4-8). The majority of non-lysogenic transformants exhibited a morphology similar to that of the controls at 23 °C. Still, they always tended to be smaller than the controls, even after incubation at the same temperature. The site of GFP fusion — either N-terminal or C-terminal — substantially influenced both

colony size and texture. The site of GFP fusion influences the size of the colonies expressing either RexA or RexB in the absence of the other protein (RexA or RexB).

At 30 °C (repressed state, no expression of Rex proteins), colonies of *E. coli* BW25113 [pPL451] lysogens, the 100% *rex*$^{+}$ control, and the pPL451-eGFP control all exhibited wild-type morphology: regular in shape, round, shiny, with smooth surfaces (Figures 4-8 A). All transformants exhibited no difference in morphology compared to the controls at 30 °C, although they did exhibit some differences in size. Interestingly, C-terminal fusion colonies were generally larger and flatter, especially on LB plates, compared to N-terminal fusion colonies, which were smaller and raised; however, the difference in size is not significant among all transformants at 30 °C (Figures 4-8 D-E). The differences between the C-terminal and the N-terminal fusions are clear but not significant when comparing RexA fusions with RexB: the RexA fusion is slightly smaller in size than the RexB fusion at 30 °C (Figures 4-8 B-C).


A1
A2
B1
MM
10
B2
C1
MM
10
C2
D1
MM
D2

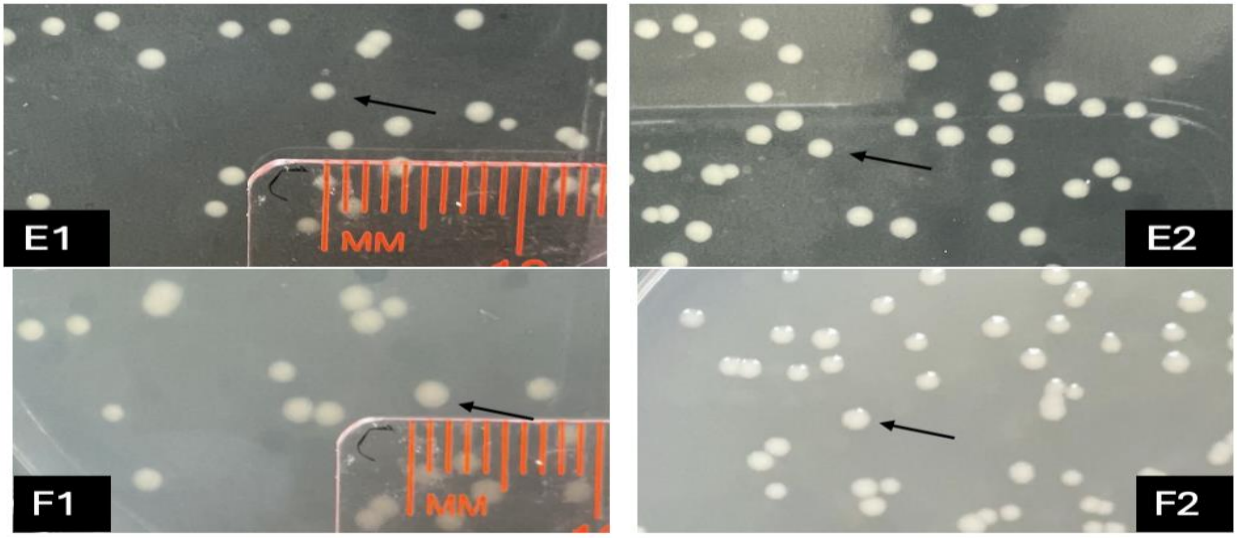
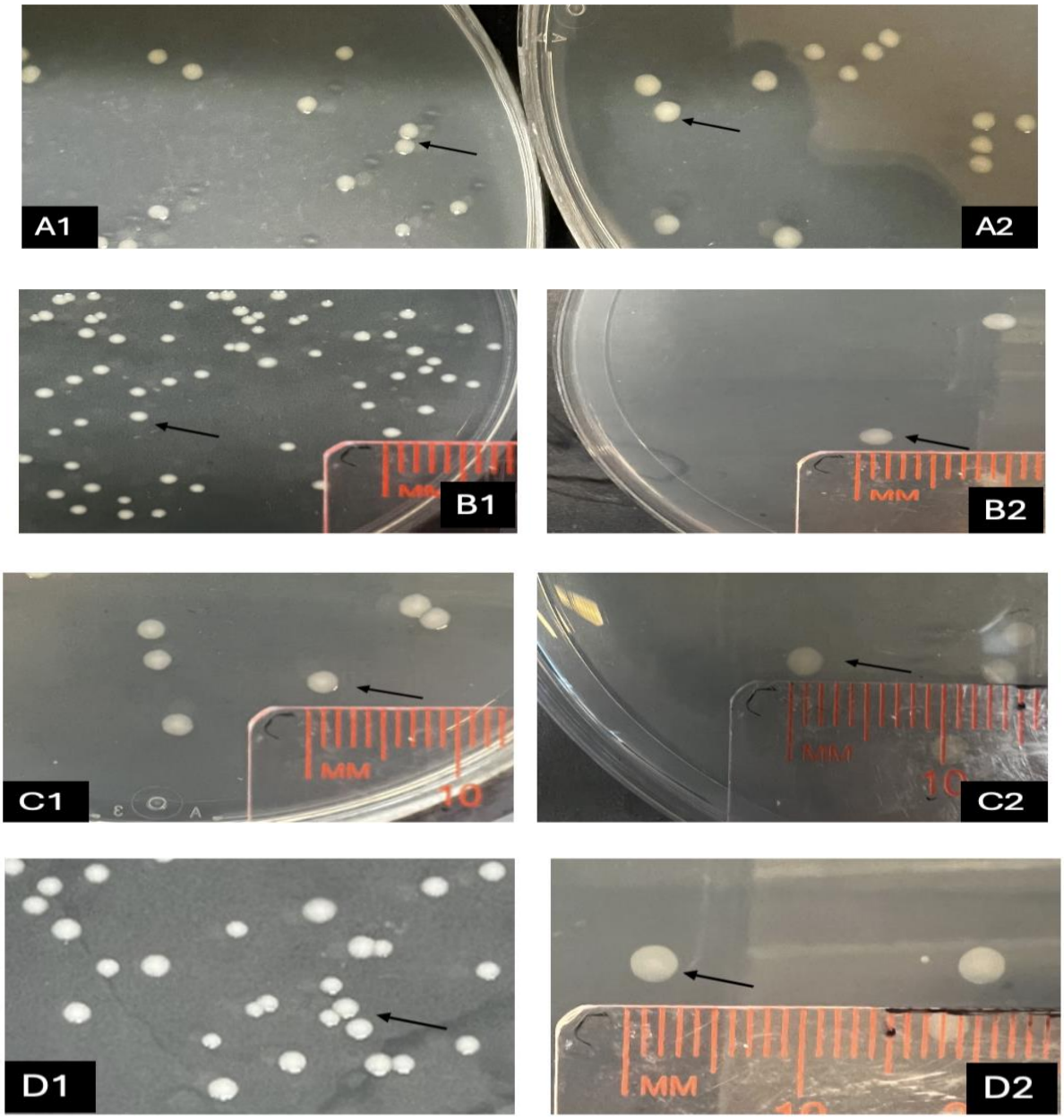


Figure 4-8. Colony Morphology of *E. coli* BW25113 [pPL451-*rex*] Lysogens at 30 °C. A1. Colonies harbouring [pPL451-*rex*$^{+}$] exhibit wild-type morphology, regular, small, and shiny; **A2.** Colonies harbouring pPL451(empty vector) exhibit wild-type morphology, regular, small, and shiny. **B1.** Colonies with [pPL451 *egfp::rexA*] construct also display wild-type morphology, with individual colonies measuring ~ 1 mm; **B2.** Colonies with [pPL451 *rexA::egfp*] construct exhibit wild-type morphology, with individual colonies measuring ~ 1 mm. **C1.** Colonies with [pPL451 *egfp::rexB*] construct show wild-type morphology with colony sizes of ~ 2 mm; **C2.** Colonies with [pPL451 *rexB::egfp*] construct exhibit wild-type morphology with colony sizes of ~ 2 mm. **D1.** Colonies harbouring pPL451(*egfp::rexA-rexB*) show wild-type morphology and with individual colonies measuring ~ 1 mm; **D2.** Colonies harbouring [pPL451 *rexA::egfp-rexB*] construct exhibit wild-type morphology, with individual colonies measuring ~ 1 mm. **E1.** Colonies with [pPL451 *rexA-egfp::rexB*] construct also exhibit wild-type morphology, with individual colonies measuring ~ 1 mm; **E2.** Colonies harbouring [pPL451 *rexA-rexB::egfp*] construct exhibit wild-type morphology, with individual colonies measuring ~ 1 mm. **F1.** Colonies harbouring [pPL451 *rexA*::*egfp-rexB::rfp*] construct exhibit wild-type morphology, with colony sizes of ~ 2 mm; **F2.** Colonies harbouring [pPL451 *egfp::rexA-rfp::rexB*] construct exhibit wild-type morphology, with colony sizes of ~ 1 mm. An arrow in each image indicates representative colonies.

At 37 °C (derepressed state, expression of Rex proteins), colonies of *E. coli* BW25113 [pPL451] lysogens, the 100% *rex*$^{+}$ control, and the pPL451-*egfp* control all exhibited different morphology: larger in shape, round, matte, and with flat surfaces (Figure 4-9 A). All transformants exhibited no difference in morphology compared to the controls at 37 °C. Notably, C-terminal fusion colonies were generally larger and flatter, especially on LB plates, compared to N-terminal fusion colonies, which were smaller and raised; however, the difference in size was noticeable among all transformants at 37 °C (Figure 4-9 B2-C2). The *egfp::rexA* colony is very similar to the control colony in size (around 1 mm) but exhibits a mucoid appearance (Figure 4-9 B1). The C-terminal fusion resulted in larger colonies (approximately 2 mm) compared to the control, but they remained sticky (Figure 4-9 B2). The N-terminal fusion of GFP to RexB in the absence of RexA produced larger colonies, approximately 2 mm, and flatter, with less shine compared to controls (Figure 4-9 C1). The colony of cells encoding the RexB plasmid, where eGFP is fused to the C-terminus of RexB, is larger than the N-terminal fusion (about 2-3 mm) while maintaining a similar texture and appearance (Figure 4-9 C2). The C-terminal fusion of both GFP and RFP to RexA and RexB, respectively, resulted in a colony size of approximately 4 mm (Figure 4-9 F2), which is significantly larger than the control. In contrast, the N-terminal fusion of both GFP and RFP to RexA and RexB yielded a colony size of about 3 mm (Figure 4-9 F1), larger than the control but smaller than that of the C-terminal fusion.


A1
A2
B1
B2
C1
C2
D1
D2

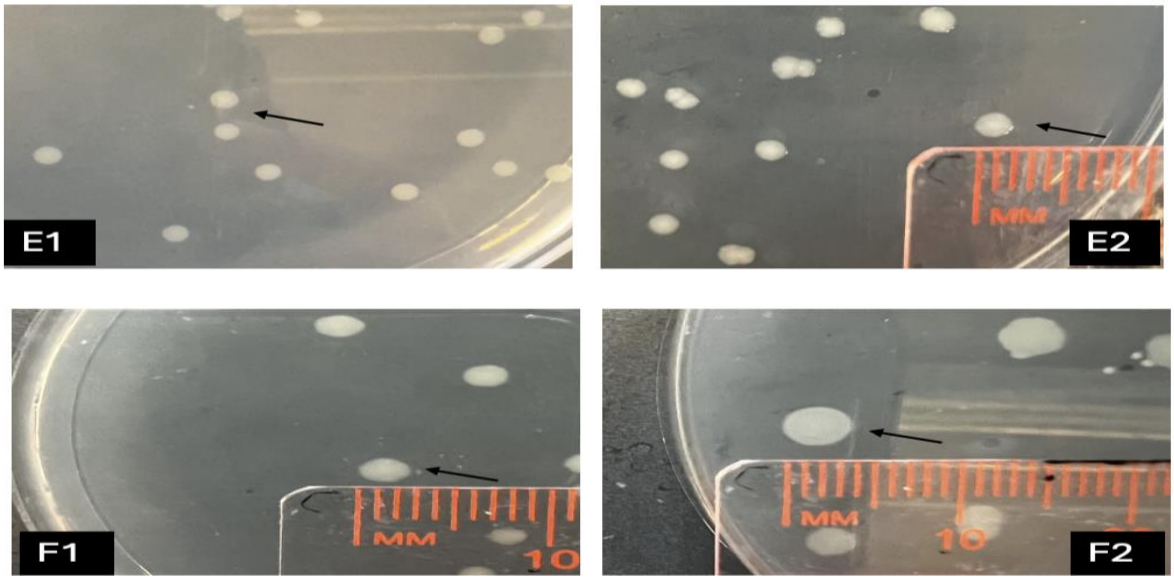


Figure 4-9. Colony Morphology of *E. coli* BW25113 [pPL451-*rex*] lysogens at 37 °C. A1. Colonies harbouring pPL451(wt) construct exhibit wild-type morphology: regular, small, and shiny; **A2**. Colonies harbouring the [pPL451 -*rex*$^{+}$] construct exhibit wild-type morphology but are slightly larger than those with the empty vector. **B1.** Colonies with [pPL451 *egfp::rexA*] construct exhibit small (~ 1 mm) and matte in texture; **B2.** Colonies with [pPL451 *rexA::egfp*] construct exhibit larger (~ 2 mm) and also matte in texture. **C1.** Colonies harbouring [pPL451 *egfp::rexB*] construct are large (~ 2 mm) and matte in texture; **C2.** Colonies harbouring [pPL451 *rexB::egfp*] construct are also large (~ 2 mm) and matte in appearance. **D1.** Colonies with [pPL451 *egfp::rexA-rexB*] construct are large and matte, measuring ~ 2 mm in size; **D2.** Colonies with [pPL451 *rexA::egfp-rexB*] construct exhibit large and matte appearance, measuring ~ 3 mm in size. **E1.** Colonies harbouring [pPL451 *rexA-egfp::rexB*] construct are small (~ 1 mm) and matte; **E2.** Colonies with [pPL451 *rexA-rexB::egfp*] construct are larger and matte, measuring ~ 2 mm in size. **F1.** Colonies harbouring [pPL451 *egfp::rexA-rfp::rexB*] construct exhibit large (~ 3 mm) and matte; **F2.** Colonies harbouring [pPL451 *rexA*::*egfp-rexB::rfp*] construct exhibit very large and matte colony morphology, measuring ~ 4 mm. Representative colonies are indicated by arrows in each image.

After observing colony morphology across all constructs and controls at the tested temperatures, a quantitative analysis was conducted at 37 °C, the condition under which the greatest diversity in colony size and texture was observed (Figure 4-10). Each of the 11 experimental constructs and 3 control plasmids (pPL451 empty vector, -*egfp*, and *rexA*-*rexB*) was assessed by observing 200 colonies grown under identical environmental conditions, media, and incubation time. The only variable was the type of harboured constructs. Colony diameters were measured in millimetres using digital callipers and validated with image analysis software. Only well-formed, circular, and isolated colonies with diameters between 0.5 mm and 5 mm were included to ensure measurement accuracy and biological relevance. Colonies were considered consistent if their size fell within ±10% of the mean colony size for that construct, a threshold selected to capture natural biological variation while identifying constructs that introduce morphological instability. This approach aligns with established practices in phenotypic reproducibility assessments in microbiology (Macleod et al., 2021; MDAR Working Group 2020).

Outliers were identified using the 1.5 x interquartile range (IQR) rule and excluded only if visually confirmed to be irregular, merged, or texturally distinct from the control phenotype. Colonies that differed in appearance, texture, or size from the control group were excluded to maintain consistency in phenotype classification. The percentage of consistent colonies per construct was calculated using the formula:

Percentage consistent = (consistent colonies / total colonies tested) x 100

The results demonstrated a high degree of uniformity, with consistency values ranging from 87% to 98%. Control constructs exhibited the highest consistency (196/200 colonies for both pPL451 empty vector and pPL451-*egfp*, while the [pPL451 *rexA*-*rexB*] constructs were approximately 95% consistent

(190/200). At the same time, most constructs containing GFP fusions showed greater variability (94%-96%), slightly lower but still high consistency. Notably, the N-terminal fusion of GFP and RFP to both RexA and RexB constructs showed the lowest consistency at 87% among the tested constructs, suggesting that this configuration introduces variability in colony development. The N-terminal fusion produced colonies that were larger in size, with an average diameter of ~3 mm; however, some outliers reached 5 mm or were smaller than 2 mm. Despite similar surface texture, these outliers were excluded from the analysis due to their deviation from the dominant colony phenotype of this construct, *e.g., egfp::rexA-rfp::rexB*. Importantly, re-streaking confirmed that the dominant phenotype was stable, indicating that the observed variation probably reflects initial growth differences rather than heritable mutations. These inconsistencies may stem from disrupted membrane localization or impaired function of either Rex protein due to the N-terminal fusions, or from imbalanced expression levels, resulting in the observed heterogeneity in colony size and growth dynamics. The average consistency across all samples was 94.3%, with a standard deviation of ± 2.9% and a margin of error of ±2% at a 95% confidence level (Biology Notes Online, 2024; Macleod et al., 2021). These findings indicate generally low inter-sample variability between most constructs, resulting in a stable and reproducible colony morphology under the tested conditions. Only the dual N-terminal fusion construct showed substantial inconsistencies in colony morphology. This quantitative framework provides a robust basis for evaluating phenotypic stability across genetically modified *E. coli* strains.

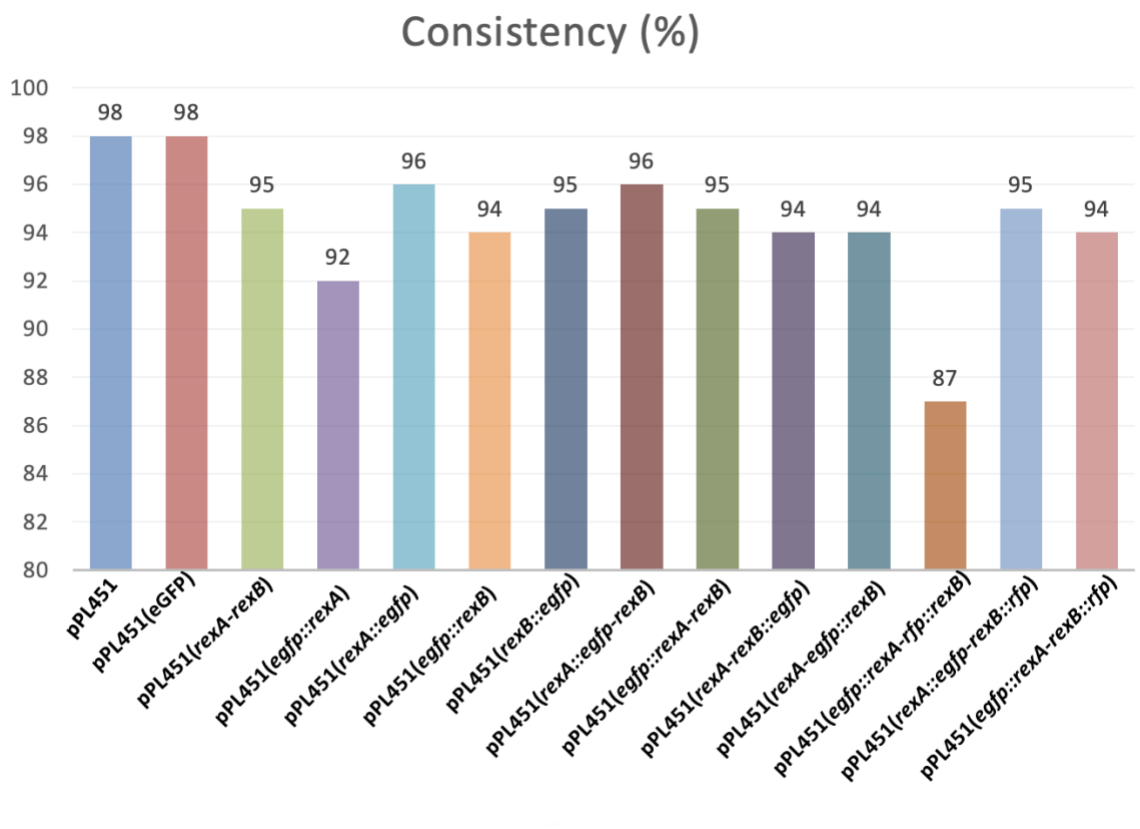
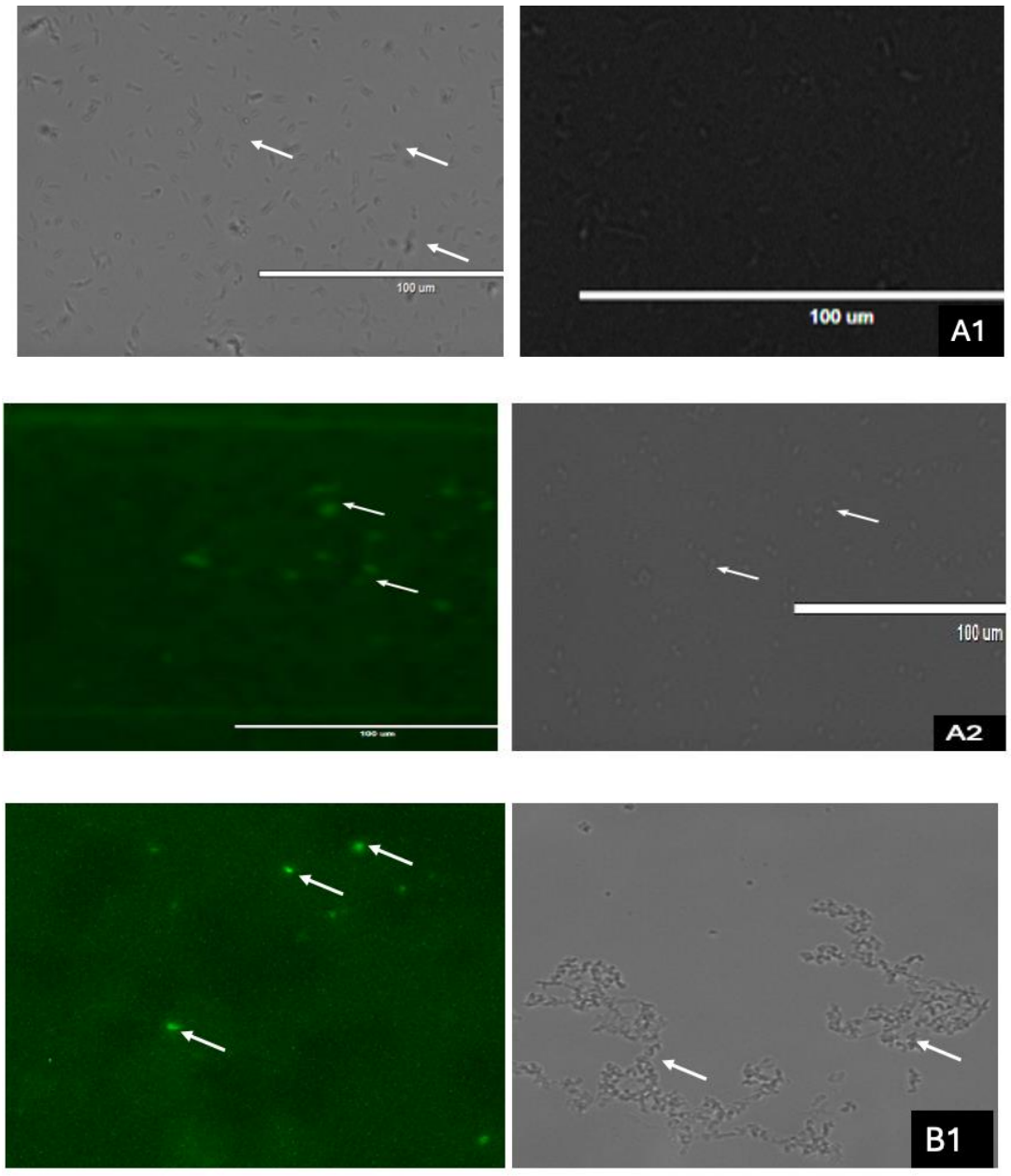
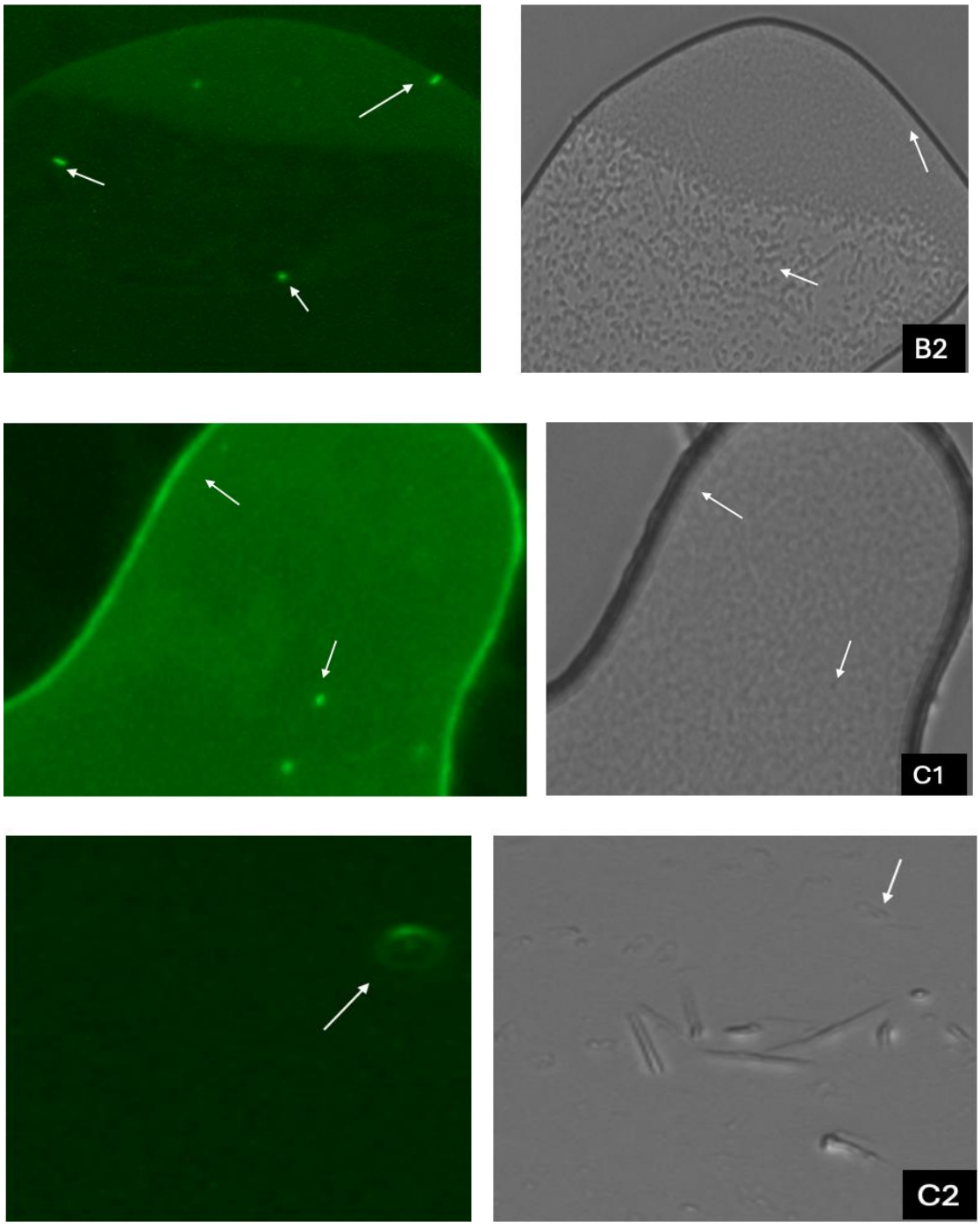


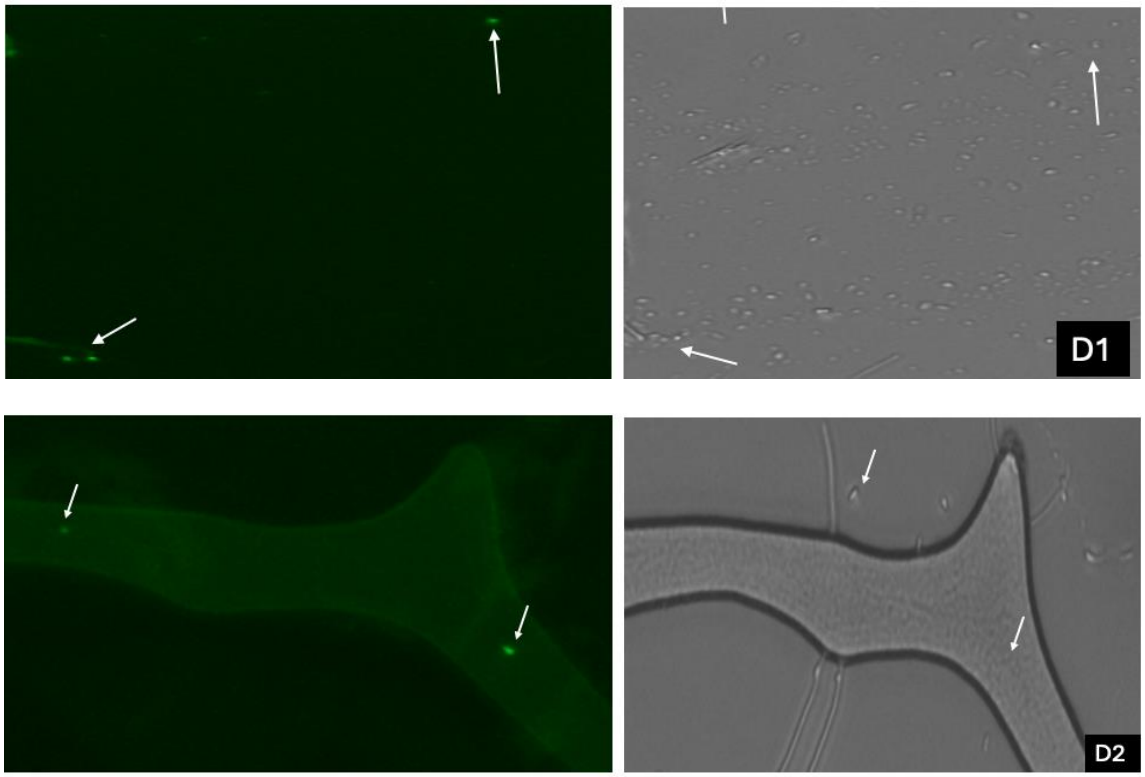
Figure 4-10. Colony Morphology Consistency of *E. coli* BW25113 [pPL451-*rex*] lysogens at 37 °C. The bar chart displays the percentage of colonies exhibiting consistent morphology for each construct and control, based on 200 colonies per sample. Constructs vary by the orientation of GFP/RFP fusion (N-terminal or C-terminal) and the type of Rex protein expressed (either RexA or RexB, or both).

Rex under the microscope: To investigate whether Rex proteins retain functionality when fused to fluorescent tags, a series of *rex*::e*gfp* constructs were examined for their ability to express the Rex phenotype upon infection with T4*rII*. Observations of reduced transformation efficiency, changes in colony morphology, and temperature-dependent Rex activity suggest that the fusion may affect Rex expression and its subsequent function in a construct-dependent way. To further characterize these constructs, they were examined under the microscope to gain insight into their behaviour before and after temperature induction. The primary aim of the fluorescent protein fusion is to develop a system capable of eventually localizing Rex proteins within the host cell and to enable future assessment of Rex activity under varying conditions. This includes monitoring expression before and after temperature induction, as well as before and after infection with T4 and T4*rII*. All strains were grown overnight at 25 °C, then either induced at 37 °C for 60-90 min or maintained uninduced at 30 °C until testing. The wild-type strain served as a negative control for GFP imaging (Figure 4-11 A1), while the pPL451-*egfp* plasmid was utilized as a 100% control for GFP expression (Figure 4-11 A2). To enhance imaging quality and reduce background noise, all samples were fixed with 4% paraformaldehyde (PFA) in phosphate-buffered saline (PBS). Microscopy was performed using a 60x objective lens, which enabled visualization of the fluorescent signal but not individual protein molecules. As this setup does not permit accurate quantification of expression levels or the number of fluorescent cells, the analysis focused on the presence or absence of detectable fluorescence and a qualitative estimation of fluorescence intensity. To approximate the relative expression levels of GFP across constructs, grayscale background images were compared with corresponding GFP fluorescence images for each Rex fusion construct. This approach allowed for a semi-quantitative assessment of GFP expression, providing insight into the relative fluorescence output of each tagged Rex protein. Imaging was conducted using the EVOS FL Auto fluorescence imaging system (ThermoFisher Scientific, Canada),

which supports simultaneous detection in multiple fluorescent channels, including RFP and GFP, and is suitable for co-expression and dual-tagging experiments.




B2
C1
C2


D1
D2

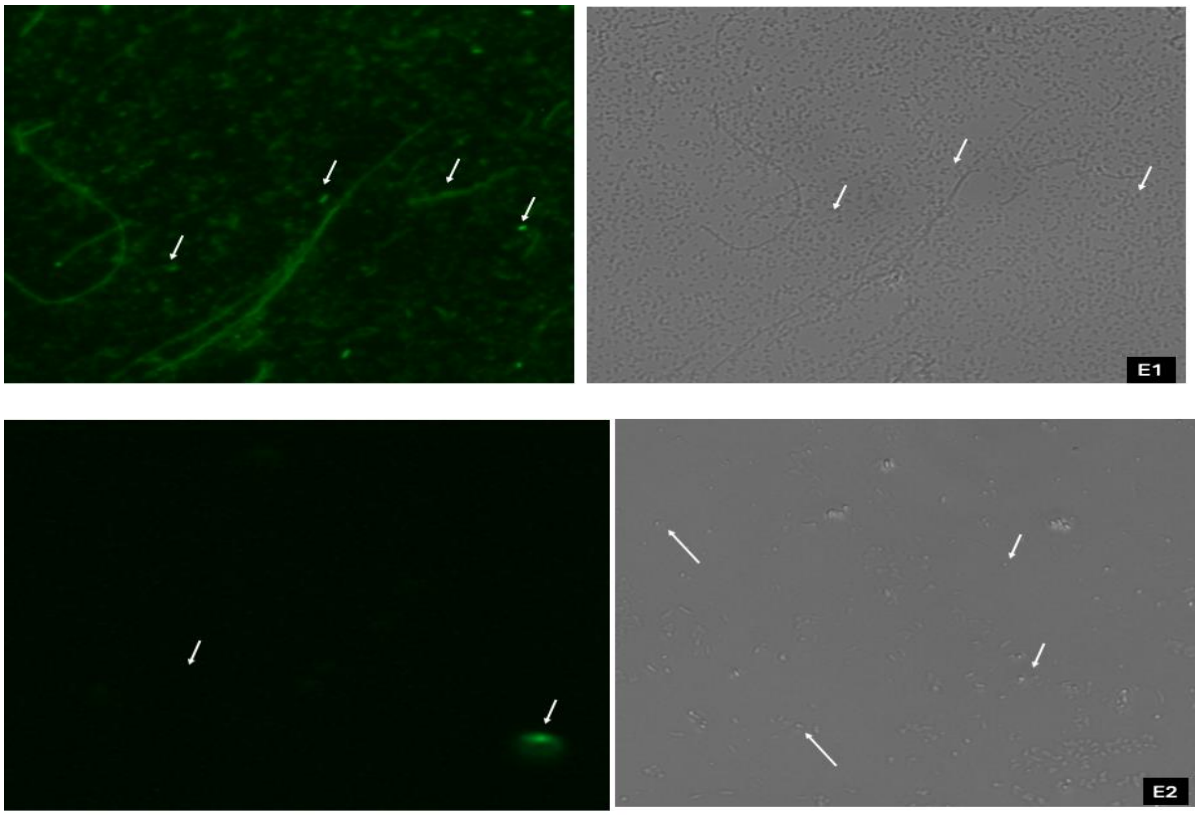


Figure 4-11. Fluorescence Microscopy of *E. coli* BW25113 lysogen harbouring [pPL451 *rex::egfp*] plasmids (single expression). A1. BW25113 (pPL451) shows no GFP expression/lack of GFP tag; the grayscale background shows cells with no fluorescence. **A2.** BW25113 [pPL451 egfp] exhibits strong GFP fluorescence upon induction, confirming successful expression of the GFP tag. **B1.** BW25113 [pPL451 *rexA::egfp*], where GFP fusion at the C-terminal of RexA shows a detectable signal of GFP**. B2.** BW25113 [pPL451 *egfp::rexA*], where an N-terminal GFP tag to RexA reveals a few spots with GFP expression. **C1.** BW25113 [pPL451(*rexB::egfp*)], where C-terminal fusion to RexB shows some GFP signal. **C2.** BW25113 [pPL451(*egfp::rexB*)], where an N-terminal fusion to RexB exhibits a very faint GFP signal. **D1.** BW25113 [pPL451 *rexA::egfp-rexB*], where the GFP signal is moderately observed but is not significant when the tag is fused to the C-terminal of RexA in the presence of RexB. **D2.** BW25113 [pPL451*egfp::rexA-rexB*], where an N-terminal fusion to RexA in the presence of RexB shows a limited GFP signal. **E1.** BW25113 [pPL451 *rexA-rexB::egfp*], where the GFP expression signal was widespread when the tag was attached to the C-terminal of RexB in the presence of RexA. **E2.** BW25113 [pPL451 *rexA-egfp::rexB*], where Limited GFP expression occurs when tagged to RexB at the N-terminal in the presence of RexA. All cells were grown at 30 °C and then induced at 37 °C, after which they were treated with 4% PFA and PBS for improved imaging. Images taken using EVOS FL Auto imaging Microscope using a 60x objective lens. Arrows point to key regions of GFP/RFP fluorescence, highlighting areas of successful expression.

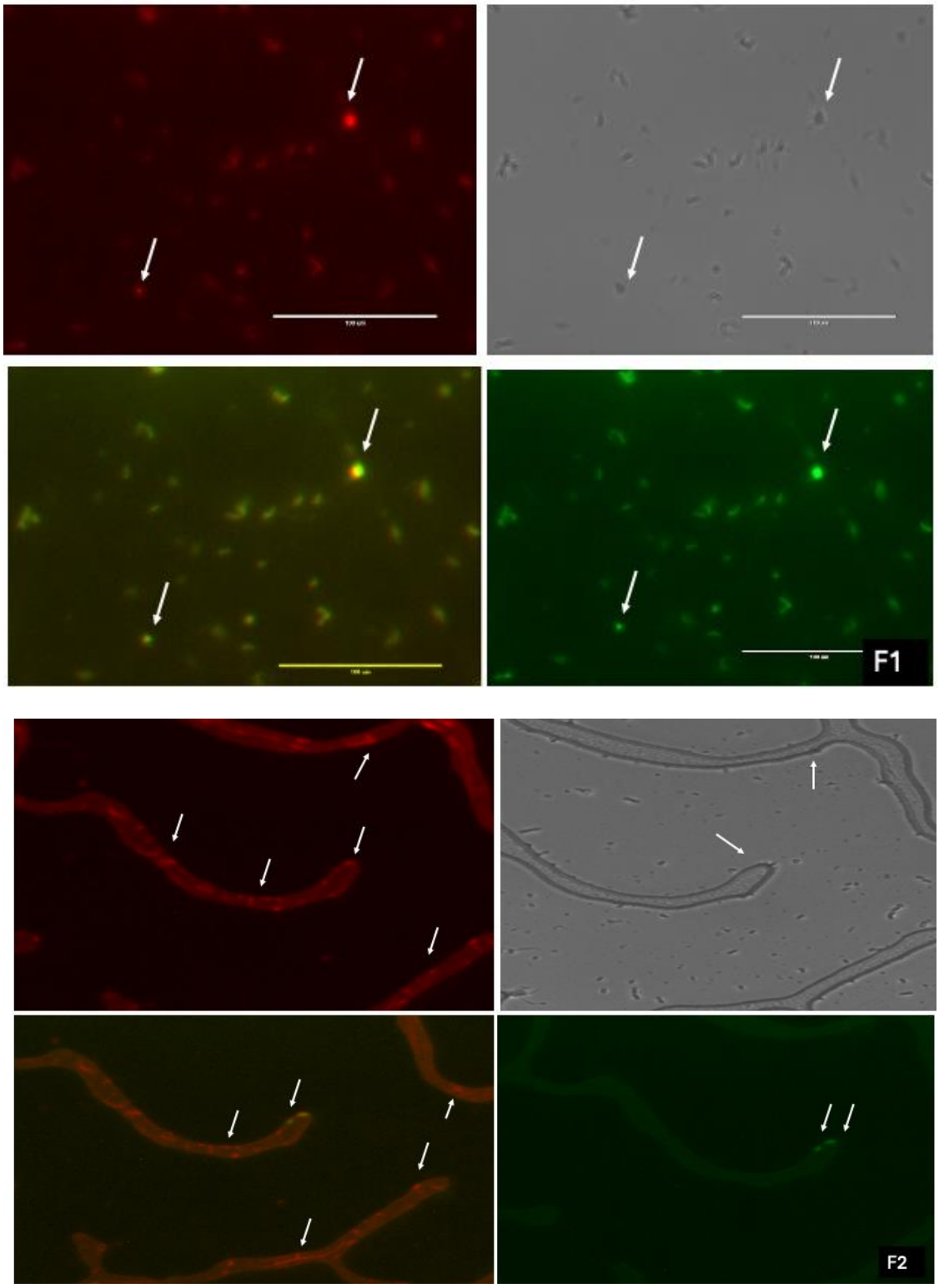
The *rexA::egfp* construct image (Figure 4-11 B1) reveals widespread GFP fluorescence across the image, suggesting a successful GFP protein fusion and uptake of the vector. The N-terminal fusion imaging has shown very little to no GFP expression in either RexA or RexB (Figures 4-11 B2 and C2). Imaging of the *egfp::rexA* construct revealed clusters of cells with low or undetectable GFP fluorescence, despite successful selection and induction, suggesting that the lack of signal is unlikely due to plasmid uptake. Instead, these observations suggest that N-terminal fusion may impair proper folding, localization, or function of RexA, thereby affecting GFP fluorescence.

Given that constructs with N-terminal RexA and RexB fusions still interfere with untagged Rex activity, the fluorescent proteins appear to lose full Rex functionality while retaining the ability to disrupt pr block the activity of native Rex proteins. The interference, combined with altered localization, likely contributes to the observed variability in fluorescence. Similar scenarios were observed concerning the presence of both *rexA* and *rexB* genes, where one is tagged with GFP while the other is not.

The C-terminal fusion showed better protein expression and was more prominent. In the case of the *rexA-rexB::egfp* construct (Figure 4-11 E1), several distinct possible cellular outlines and potential fluorescent signals are more discernible, and the tagged protein expression is apparent. In comparison, the N-terminal fusion (*rexA-egfp::rexB*) exhibited very faint, and in some cases, no GFP expression per image, as no distinct GFP-positive structures were evident (Figure 4-11 E2).

Our observations clearly indicate that the expression of the tagged protein varies between RexA and RexB, as well as between N-terminal and C-terminal fusions. From the visualization of the GFP/RFP-expressing constructs, the C-terminal fusion of GFP to RexA or RexB showed significantly more noticeable protein expression compared to the N-terminal fusion (Figures 4-11 B-E). However, this difference should not be interpreted as a direct correlation with Rex activity. Instead, the data suggest that fluorescence may be influenced by protein localization or structural constraints imposed by the

fusion, rather than by survival outcomes in T4*rII* plating assays. Constructs with N-terminal fusions still interfere with untagged Rex, suggesting that while these fusions lose full Rex functionality, they retain the ability to disrupt Rex activity, which may also affect fluorescence patterns.


F1
F2

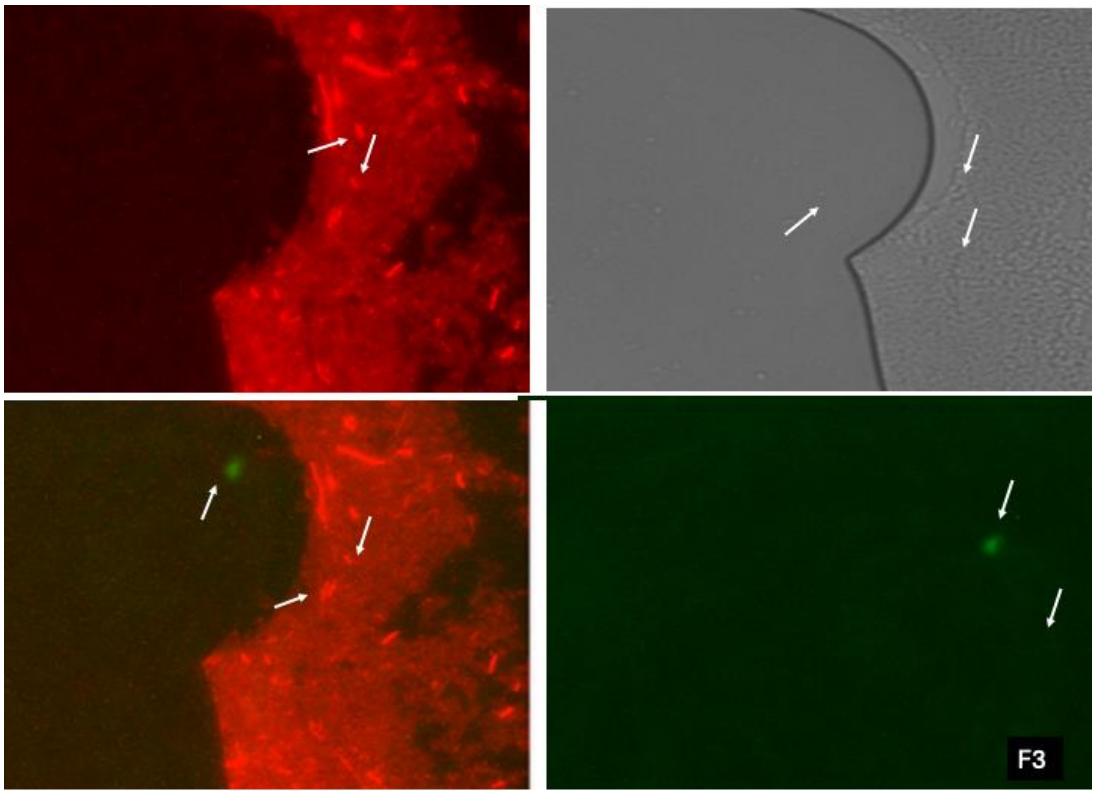


Figure 4-12. Fluorescence Microscopy of *E. coli* BW25113 lysogens harbouring [pPL451 *rex::egfp*] plasmids (Dual expression). F1. *E. coli* BW25113 [pPL451 *rexA::egfp-rexB::rfp*], where the C-terminal fusion of both RexA and RexB with GFP and RFP demonstrates the co-expression of both proteins in the same context cells. Strong green and red fluorescence signals indicate successful expression, with yellow regions in the merged images indicating overlapping fluorescence signals from GFP and RFP, consistent with co-expression. **F2.** BW25113 [pPL451 *egfp::rexA- rfp::rexB*], where an N-terminal fusion of both RexA and RexB with GFP and RFP. Fluorescence signals vary between channels, and overlay images reveal limited co-expression, suggesting differential expression or stability of the tagged proteins. **F3.** BW25113 [pPL451 *egfp::rexA-rexB::rfp*], where the fusion of GFP at the N-terminal of RexA and RFP at the C-terminal of RexB. GFP signal is weak, while RFP is more prominent, resulting in limited overlap and suggesting reduced expression or stability of the GFP-tagged construct. All cells were grown at 30 °C and then induced at 37 °C, after which they were treated with 4% PFA and PBS for improved imaging. Images taken using EVOS FL Auto imaging Microscope with a 60x objective lens. Red for RPF expression, green for GFP expression, and yellow in merged images for co-expression/ overlapping fluorescence. Arrows point to key regions of GFP/RFP fluorescence, highlighting areas of successful expression.

Interesting results were also observed where GFP and RFP proteins were used to tag RexA and RexB simultaneously. C-terminal fusion of GFP and RFP to RexA and RexB, respectively, demonstrated significant Rex activity and very low infectivity upon infection with T4*rII*. Here, the C-terminal double tag has allowed evident and recognizable expression of both proteins in most cells (Figure 4-12 F1). Conversely, the N-terminal fusions of both proteins have displayed very low success rates, as evidenced by exhibiting faint and weak double protein expression, as seen in the image (Figure 4-12 F2).

In most e*gfp::rexA-rfp::rexB* constructs, only RFP was expressed in most cells, with minimal or no expression of GFP (Figure 4-12 F2). In cases of simultaneous C- and N-terminal fusions, such as in the e*gfp::rexA-rexB::rfp* construct, the RFP-expressing cells are significantly higher than those of GFP-expressing cells (Figure 4-12 F3). This may relate to the site of fusion or enhanced protein expression resulting from the fusion of RFP at the C-terminus versus GFP at the N-terminus of Rex proteins. All observations and explanations are detailed in the discussion chapter.

Building on the qualitative fluorescence microscopy observations, a semi-quantitative analysis was performed to estimate the proportion of fluorescent cells expressing GFP and/or RFP across all Rex fusion constructs in both wild-type and λ lysogen *E. coli* BW25113 strains. This step was vital for providing a more objective comparison of expression efficiency between constructs and for validating the visual trends observed under the microscope.

For each construct, the total number of cells was counted from brightfield images, while GFP- and RFP-positive cells were tallied from their respective fluorescence channels. Co-expression was evaluated by identifying cells displaying overlapping green and red fluorescence in merged images. To ensure consistency and comparability, the analysis was standardized by counting 100 cells per image across all samples. This provided uniform sampling and reduced variability caused by differences in

cell density or field of view. GFP-positive cells, RFP-positive cells, and co-expressing cells were counted, and the corresponding fluorescence rates were calculated using the following equation:

$$\text{Fluoresent cell rate (\%)} = \left(\frac{\text{number of fluoresent cells}}{\text{total number of cells}}\right) \text{x100}$$

This formula was applied separately for GFP+, RFP+, and GFP+ RFP+ (co-expressing) cells (Table 4-9).

No detectable GFP or RFP fluorescence was observed in any of the tested constructs when expressed in wild-type non-lysogenic cells, including single and dual fusions (e.g., *rexA::egfp, egfp::rexA, rexB::egfp, rexA-rexB::egfp, rexA-egfp::rexB, egfp::rexA-rexB::rfp*). Both negative control *E. coli* BW25113 [pPL451] and positive control BW25113 [pPL451 *egfp*] behaved as expected, confirming the lack of signal was specific to the Rex fusion constructs rather than a technical issue. Cells were grown at 30 °C and induced at 37 °C for 30-60 min before fluorescence analysis.

These findings suggest that fluorescent tagging, particularly in the absence of a λ lysogen context, severely compromises Rex protein function and/or localization, resulting in undetectable fluorescence under the tested conditions.

Table 4-9. Summary of fluorescent cell counts and expression rates in λ lysogen *E. coli* BW25113 harbouring *rex::egfp* constructs.

Construct*	Total Cells	GFP+ Cells	GFP+ (%)**	RFP + Cells	RFP + (%)**	GFP+ RFP+ Cells	Co-expression (%)**
--	100	N/D	N/D	N/D	N/D	N/D	N/D ***
egfp	100	83	83	N/D	N/D	N/D	83
rexA-rexB	100	N/D	N/D	N/D	N/D	N/D	N/D
rexA::egfp	100	50	50	N/D	N/D	N/D	50
egfp::rexA	100	20	20	N/D	N/D	N/D	20
rexB::egfp	100	75	75	N/D	N/D	N/D	75
egfp::rexB	100	40	40	N/D	N/D	N/D	40
rexA::egfp-rexB	100	43	43	N/D	N/D	N/D	43
egfp::rexA-rexB	100	25	25	N/D	N/D	N/D	25
rexA-rexB::egfp	100	90	90	N/D	N/D	N/D	90
rexA-egfp::rexB	100	30	30	N/D	N/D	N/D	30
rexA::egfp-rexB::rfp	**100**	**100**	**100**	**100**	**100**	**100**	**100**
egfp::rexA-rfp::rexB	100	20	20	50	50	10	20
egfp::rexA-rexB::rfp	100	20	20	70	70	10	20

*Constructs were expressed in λ lysogen *E. coli* BW25113. *E. coli* BW25113 [pPL451] served as a negative control, while the BW25113 [pPL451 *egfp*] was used as a positive control for GFP expression. Cells were grown at 30 °C and induced at 37 °C for 30-60 min before fluorescence analysis.

**Expression rate refers to the percentage of cells exhibiting green (GFP), red (RFP), or both signals.

*** N/D indicates no detectable expression or that the data are not applicable for the given construct.

This analysis revealed apparent differences in expression efficiency depending on the fusion orientation and genetic background. In the wild-type context, none of the constructs, including both positive and negative controls, exhibited detectable fluorescence. As a result, subsequent experiments were conducted under λ lysogen conditions (Table 4-9). Notably, lysogen strains expressing C-terminally tagged constructs exhibited higher levels of expression and co-expression compared to other configurations.

Remarkably, the *rexA::egfp-rexB::rfp* construct showed the highest expression and co-expression rates, consistent with the strong, widespread fluorescence observed microscopically (Figure 4-12 F1). In contrast, N-terminal fusions (e.g., *egfp::rexA-rfp::rexB*) showed reduced fluorescence, consistent with many cells lacking detectable signal (Figure 4-12 F2). Mixed fusion constructs, such as *egfp::rexA-rexB::rfp*, displayed a clear imbalance in expression, with the RFP signal dominating over GFP (Figure 4-12 F3). The quantification step not only supports the microscopy findings but may also provide a reproducible framework for comparing expression dynamics across constructs.

Chapter 5

Discussion

5.1 Identification of the Interrupted Genes Responsible for the Rex⁻ Phenotype

Existing insights into how the ionic environment influences Rex activity led to the discovery of potential key roles of outer membrane proteins in Rex phenotype during my Master's thesis research, serving as the rationale for the research presented in this thesis. Building upon this key finding, a hypothesis was suggested that many other *E. coli* host genes, regulators, or factors play a role in influencing or sustaining Rex activation during infection. To identify other potential host factors, a set of phenotypically Rex$^-$ but genotypically *rex*$^+$ mutants was generated using a one-step mutagenesis approach. Here, the analysis of these mutants and, based on that work, the elucidation of novel host genes that may influence the Rex phenotype is presented.

Briefly, the R6K origin of replication (*ori* R6K γ) system is a widely used tool in bacterial genetics for generating random gene insertions and mutations. Replication requires the π protein, which is encoded by the *pir* gene. In *pir*-negative hosts, a plasmid with an R6K *ori* acts as a suicide vector, since the plasmid and any genes encoded on it cannot persist. It is therefore handy for delivering transposons that integrate into the genome, disrupting genes and facilitating mutagenesis. In 1994, a study by de Lorenzo and Timmis successfully used R6K *ori*-based suicide plasmids to deliver mini-Tn*5* and mini-Tn*10* transposons into Gram-negative bacteria. The authors demonstrated that the system enabled efficient random mutagenesis, creating stable mutants with selectable phenotypes, thereby validating its utility

for genetic studies in diverse bacterial hosts (de Lorenzo and Timmis 1990, 1994). More recently, Anderson (2006) developed the BioBrick part BBa-J61001 as a modular transposon delivery system, which includes the R6K origin of replication and Tn*5* transposon elements, designed for random genomic insertion. While effective for gene delivery, its random insertion can disrupt the function of the target genes or regulatory elements (Anderson, J. 2006; Aachen 2019; Hutchison et al., 2019). In my work, Rex$^-$ mutants were generated using a one-step mutagenesis plasmid system, "pRex" (pHA02), which utilizes this principle. This plasmid carries λ *rexA-rexB* genes under the control of λ P_R promoter, and *cI*[ts] regulator, along with a tetracycline (Tc) insertional antibiotic marker flanked by two Tn*10* insertion sequences. Upon introduction into *E. coli*, the Tn*10* transposon randomly inserts into the genome, disrupting genes while simultaneously conferring the *rexA-rexB* genotype. Candidates that were genotypically *rex*$^+$, but phenotypically Rex$^-$ or attenuated for Rex activity, indicated the disruption of genes involved in Rex function. Thirteen such mutants were isolated during Alattas' MSc thesis (2015). These isolates were confirmed to be genotypically *rex*$^+$, while also exhibiting strong attenuation or complete loss of Rex activity.

To determine whether the observed Rex$^-$ phenotype in the Rex$^-$ mutant candidates resulted directly from the Tn*10-rex* cassette delivered via the one-step insertional mutagenesis system or as a result of an unexpected mutation occurring during or after the mutagenesis process, further analysis was conducted. To investigate this, all isolates were cured of their pRex plasmids and assessed for their sensitivity to T4 and T4*rII* phage. Several cured isolates remained sensitive to T4*rII*, indicating a loss of Rex activity despite being genotypically *rex*$^+$. When these isolates were transformed by pHA1 (pUC19-based plasmid carrying a functional *rex* operon*;* Figure 3-1), Rex activity was not fully restored. This suggested that the Rex$^-$ phenotype was not due to a defective *rex* cassette, but rather due to insertional disruption of host genes involved in the Rex pathway. The fact that several isolates

remained Rex⁻ even after reintroduction of additional functional copies of the *rex* operon supports the hypothesis that insertional disruption of host genes, rather than defects in the *rex* cassette itself, was responsible for the loss in phenotype. To confirm the genetic basis of the Rex⁻ phenotype, targeted sequencing of insertion sites was performed to identify disrupted genes and validate their role in Rex activity.

5.1.1 Inverse PCR and Identification of Rex⁻ Mutant:

To identify which host genes were disrupted in the 13 Rex⁻ isolates (Table 4-1), PCR using primers targeting the ends of the Tn*10* transposon was performed under low-stringency conditions to amplify adjacent genomic regions. However, sequencing and BLAST analysis revealed that all amplified fragments matched the pRex plasmid backbone, including the R6K *ori* origin, tetracycline resistance Tc, and *mob* genes, rather than host DNA. This suggests that the entire plasmid had integrated into the genome, not just the transposon. As a result, standard PCR-based mapping was ineffective due to the presence of overlapping sequences from multiple plasmid regions. This outcome, while not the intended outcome of transposon mutagenesis, is a well-documented phenomenon, particularly in systems involving conjugative plasmids. Conjugative plasmids, by their nature, carry mob genes and often recombination-prone elements that can facilitate unintended integration events. For instance, studies have shown that IS elements or recombination-prone sequences can mediate full plasmid integration, particularly when transposase activity is unregulated or when plasmid architecture facilitates recombination (Kvitko et al., 2012; Riley et al., 2023). Similar outcomes have been reported in systems using Tn*5* and r6K *ori*-based vectors, such as the iGEM part BBa-J61001, where unintended integration of plasmid backbone sequences led to gene disruption (Anderson, J. 2006; Hutchison et al., 2019). Although antibiotic resistance markers can help distinguish between simple insertions and full plasmid integration, these markers alone are not always conclusive, as both situations may share the same resistance profile. Therefore, confirming insertion events remains crucial, since full plasmid integration

can hide the detection of true gene knockouts and complicate downstream functional analysis (Zucca et al., 2013).

Instead, an inverse PCR was used to amplify the interrupted genes. Amplified fragments from inverse PCR were sequenced, and one amplicon from the isolate HA-11 was identified as the *E. coli* non-essential gene *mglC*. The gene *mglC,* a known hydrophobic ABC transporter permease that functions in **m**ethyl-**g**alactoside transport (Hogg et al*.,* 1991; Death et al.,1993; Death and Ferenci 1994). MglC is likely situated on the internal side of the inner membrane (Harayama et al., 1983), which is notable given that RexB is also inner membrane-associated (Parma et al., 1992). This spatial proximity raises the possibility of a physical or functional interaction between MglC and RexB. Given that RexA might operate in the cytoplasm and interact with RexB, the membrane orientation of MglC could potentially facilitate or modulate Rex system activity. Interestingly, previous studies indicate that *mgl*A and *mgl*B mutants primarily affect transport and chemotaxis (Ordal and Adler 1974). In contrast, *mgl*C disruption strongly impairs transport without significantly altering chemotaxis (Ordal and Adler 1974), suggesting a distinct role for MglC within the operon. The lack of a similar effect from *mgl*A or *mgl*B mutations in this context may imply that MglC has an additional, previously unrecognized function beyond sugar transport —possibly related to membrane organization or interaction with other inner membrane proteins such as RexB. While these observations are intriguing, the current evidence does not suffice to confirm a direct mechanistic role for MglC in Rex-mediated exclusion.

5.2 Screening for Susceptible Host Proteins Involved in Rex/ RII Activity

The *E. coli* envelope is a complex structure of various molecules that play critical functions in the cell's life. About 30% of the *E. coli* proteome consists of membrane proteins (Kalwarczyk et al., 2012; Antoine Gautier 2014); in fact, over half of the *E. coli* cell mass is protein (Schönheit et al., 2016), and its concentration ranges from 200 to 320 mg/ml (Cayley et al., 1991; Elowitz et al., 1999). This shows the critical role and involvement of the protein composition in a cell's integrity and function. In *E. coli*, it is estimated that approximately 1000 of the approximately 4200 proteins are membrane proteins, with roughly 600 confirmed as residing in the membrane (Daley et al., 2005; Martin and Sawyer 2019; Sueki et al., 2020). As of 2023, a significant number of newly identified proteins were membrane proteins; however, they are not well characterized in terms of their functions and structures (Toyofuku et al, 2023).

Small proteins, sigma factors, and their associated regulators also constitute a significant percentage of *E. coli* proteins. Seven sigma factors and their regulators are crucial for modulating gene expression and protein activity, especially under stress conditions. Membrane proteins play a crucial role in this regulatory network (Urtecho et al., 2023; Qiu et al., 2024).

In earlier work, several outer membrane proteins were identified as potential mediators of Rex activity (Alattas, MSc Thesis, 2015). The pronounced impact of their absence on Rex function suggests that the outer membrane plays a critical role in either the cellular localization of Rex components or in the triggering of Rex-mediated exclusion. This observation implies that structural or signalling elements associated with the outer membrane may be integral to the activation or regulation of the Rex system. However, the precise mechanism by which these proteins influence Rex activity remains to be elucidated (Figure 5-1).

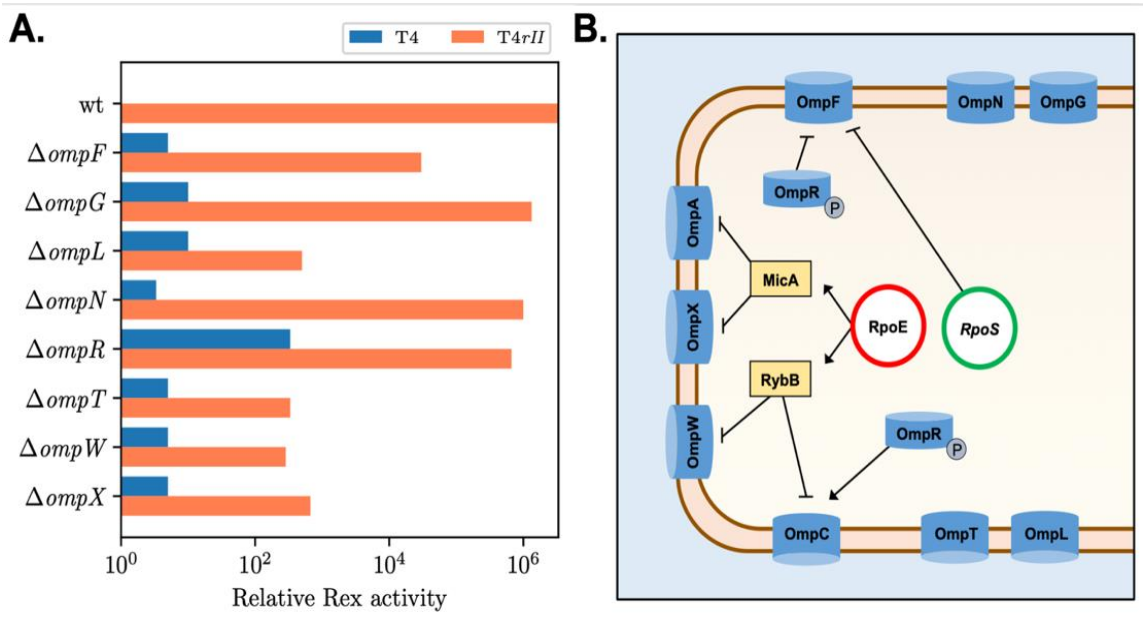


Figure 5-1. Role of Outer Membrane Proteins in Modulating Rex Activity. Deletion of specific Omps appears to attenuate Rex activity, suggesting a potential role in its mechanism. In particular, Δ*ompF*, Δ*ompL*, Δ*ompT*, Δ*ompW*, and Δ*ompX* exhibited reduced Rex-mediated inhibition of T4*rII* plating. **A.** Rex activity is defined as the ability of pHA1-delivered *rex* genes to reduce plating in the presence or absence of RII. Activity is quantified as the inverse of the relative EOP of the sample in *rex*$^+$ conditions (plasmid present) compared to *rex*$^-$ conditions (empty plasmid). Maximal Rex activity corresponds to complete attenuation of T4*rII* (*rII*$^-$) plating in the presence of the *rex*$^+$ pHA1 in *E. coli* BW25113 (wt). In contrast, the absence of Rex activity is indicated by full plating of T4 (*rII*$^+$) in the presence of the *rex*$^+$ pHA1 in *E. coli* BW25113 (wt). **B.** Omps are known to mediate ion transport across the outer membrane and are regulated by the alternative sigma factors RpoE and RpoS.

To build upon the earlier findings involving the *omp* knockouts, the analysis was extended to examine the influence of additional membrane-associated and related proteins on the Rex-mediated exclusion. This was achieved using the Keio collection, which allows systematic investigation of single-gene knockouts (Baba et al., 2006). Each mutant strain was either transformed by the high-copy pHA1 *rex*$^+$ plasmid or was lysogenized by λ*cI*857[Ts] to assess Rex activity under native expression levels. These were then assayed for T4*rII* plating efficiency and Rex activity. The high-copy plasmid pHA1 encodes

the *rexA-rexB* genes under the control of the p_M promoter, which is regulated by *cI* repressor, and exhibits overexpression of these genes. Previous studies have shown that this does not disrupt the exclusion phenotype, provided the stoichiometric balance between *rexA* and *rexB* is maintained (Slavcev and Hayes 2003; Snyder and McWilliams 1989). By increasing *rex* gene dosage, it was expected that only knockouts of host genes directly involved in Rex function would significantly impair exclusion.

To validate these findings under physiological conditions, λ*cI*857 lysogens were used, allowing for temperature-inducible expression of *rex* genes. The λ*cI*857 repressor is active at 30 °C, where it binds to p_R and p_L to prevent transcription, including that of the *rex* genes. In contrast, at 42 °C, CI is inactivated, permitting expression (Restrepo-Pineda et al., 2021). As such, λ*cI*857 lysogens can grow at 30 °C, where viability at 42 °C is used as a genetic confirmation of lysogeny. At 42 °C, CI depression facilitates phage growth in λ*cI*857 lysogens, resulting in cell lysis and host cell death. This system enabled the evaluation of Rex activity at both overexpressed and native expression levels.

Over 50 knockout strains were individually tested under low and high rex^+ gene dosage conditions. However, a subset of strains was eliminated from this analysis due to poor growth characteristics, transformation inefficiency, or instability under selective conditions. These limitations likely reflect essential gene disruption, metabolic burdens, or plasmid-host incompatibilities, which can compromise the reproducibility and interpretability of phenotypic assays under stress-inducing conditions such as elevated temperature or high *rex* expression. The wild-type strain BW25113 (wt) harbouring the rex^+ plasmid pHA1 served as a positive control, exhibiting complete resistance to T4*rII* plating and near-complete sensitivity to T4 RII^+ plating. On the other hand, the wt strain lacking the rex^+ plasmid showed almost complete sensitivity to both T4 wt and T4*rII* mutant. The more than 10^6-fold difference in plating efficiency between T4 (rII^+) and T4(rII^-) underscores the strength of the Rex phenotype and

the critical role of T4's *rIIA* and *rIIB* genes in modulating this interaction. For each mutant harbouring the *rex*$^{+}$ plasmid, Rex activity was quantified relative to these controls.

Rex activity was defined as the ability of pHA1-delivered *rex* genes to reduce plating in the presence or absence of RII. Activity was derived by taking the inverse of the relative EOP of the sample in *rex*$^{+}$ conditions (plasmid) compared to *rex*$^{-}$ conditions (no plasmid). Maximal Rex activity was defined by the complete attenuation of T4*rII* (*rII*$^{-}$) plating in the presence of the *rex*$^{+}$ pHA1 in *E. coli* BW25113 (wt). The absence of Rex activity is full plating of T4 (*rII*$^{-}$) in the presence of the *rex*$^{+}$ pHA1 in *E. coli* BW25113 (wt), where the $< 3.0 \times 10^{-7}$ represents the cutoff of sensitivity.

Initial attempts to assess Rex activity using a standard T4/T4*rII* overlay assay were hindered by the formation of small plaques in several examined host mutants. These mutants, which appeared to attenuate Rex activity, made plaque visualization and quantification unreliable. To address this limitation, an infective center assay was employed, where infected cells were diluted and plated on host cells before lysis, creating infected centers that generated larger, more distinct phage bursts from individual infection events. The selected mutants and isogenic parent strains were λ*cI*857 lysogens previously characterized in earlier experiments (Tables 4-2, 4-3, and 4-4).

T4*rII*-infected centers were examined for plating efficiency at an MOI of 3, ensuring, based on Poisson distribution, that a single phage particle infected most cells. This approach significantly improved plaque visibility and counting accuracy across all tested mutants (Table 4-5). The formation of small plaques in specific mutants may reflect partial activation of the Rex system, reduced phage replication efficiency, or host physiological changes that limit phage burst size. In particular, RexA and RexB are known to disrupt membrane potential and cellular energetics upon activation, which can lead to abortive infection and reduced phage yield (Benzer 1955; Ennis and Cohen 1968). Mutations that modulate this

response, either by weakening Rex function or altering host susceptibility, can result in smaller, less distinct plaques, complicating standard overlay-based quantification.

5.2.1 Assessing Rex Activity in Mutants of Glucose Transporter Membrane Proteins Suspected to be Involved in T4*rII* Exclusion

As a starting point, the Δ*mglC* was investigated, previously identified as a candidate influencing Rex phenotype through the one-step mutagenesis approach detailed in Chapters 4.1 and 5.1. Transformation of a Δ*mglC* mutant with the high-copy *rex*$^+$ plasmid pHA1 exhibited more than 10^2-fold reduction in Rex activity compared to the wild-type control, supporting the initial observation (Alattas et al., 2020). MglC is part of a complex operon expressing Mgl-Gal proteins (Boos et al.,1971; Death et al., 1993; Death and Ferenci 1994). While this result suggests a role for *mglC* in modulating Rex function, the underlying mechanism remains unresolved, and the possibility of indirect effects, such as altered membrane composition or transport dynamics, must be considered. Further analysis revealed that the deletion of *mglA*, a co-transcribed gene in the same operon, also reduced T4 (*rII*$^+$) plating by more than 10-fold in a *rex*$^+$ context. Given that the plating assays can vary by up to 10-fold due to experimental error, this reduction may not be considered biologically significant. Nonetheless, the result raises the possibility that *mglA* may influence RII activity, either independently or synergistically with Rex. Similarly, deletions of *galK*, *galT*, and *galE*, genes involved in galactose metabolism, also demonstrated a decrease in T4 plating efficiency by as much as two orders of magnitude. These findings suggest that the *mgl-gal* operon may contribute to optimal RII$^+$ function, potentially by supporting host physiological conditions favourable to phage replication. However, these effects remain correlative. Additional investigations could include targeted complementation of mglA and mglC knockouts, co-immunoprecipitation or crosslinking assays to test for physical interactions with Rex components, and metabolic profiling to assess whether altered energy or sugar transport impacts Rex or RII activity.

It is not strictly necessary for these proteins to interact directly with Rex to influence exclusion; they may act indirectly by modulating membrane potential, transport systems, or metabolic fluxes critical for Rex activation. These experiments would clarify whether the observed effects reflect direct mechanistic roles or broader physiological dependencies.

Notably, deletion of *galU* precluded plating of T4 and T4*rII* alike in a Rex-independent manner. This finding aligns with earlier findings by Dharmalingam et al. (1982), who similarly reported that T4 cannot replicate in *galU* mutants, although the underlying mechanism was unknown. Notably, T4*rII* plating on all Δ*mgl* and Δ*gal* mutants carrying the rex^+ plasmids was similarly excluded, suggesting that while these operons may influence RII activity of T4, they are not essential for Rex-mediated exclusion.

5.2.2 Assessing Rex Activity of Other Membrane Proteins that May Influence Rex Activity

The investigation was extended to include other essential periplasmic and internal membrane proteins. Notably, knockouts of *tolA*, *lamB*, and to a marginal degree, *lpp*, *tolR*, and *tolQ*, enhanced T4 (rII^+) plating specifically under rex^+ conditions. This phenotype was not observed in rex^- backgrounds, suggesting a functional connection between these genes and the RII system. Although Rolfe and Campbell (1977) previously noted that T4*rII* could plate on λrex^+ lysogens harbouring a *tolA, tolB,* or *tolP* null mutation, these findings have not been widely reproduced. In this study, the full plating efficiency of T4*rII* was observed in the Δ*tolA* mutant but not in Δ*tolB*, even though both mutants were sourced from the Keio collection and confirmed by PCR. The discrepancy may reflect differences in the nature of the mutations (e.g., polar effects, secondary mutations, or strain background), or functional redundancy within the Tol-Pal system that compensates for *tolB* loss but not *tolA*. This result was confirmed using λrex^+ lysogeny (wild-type rex^+ expression level), where T4*rII* formed pinpoint plaques compared to wild-type T4.

The deletion of *tolA* imparted the abrogation of Rex activity, restoring nearly complete T4*rII* plating efficiency. In contrast, knockouts of *tolQ*, *R*, and *B* showed no significant effect, suggesting a more specific role for TolA in modulating Rex and/or RII activity. While the observation is compelling, it does not establish a direct mechanistic link. The Tol proteins are known to maintain cell membrane stability and integrity, as well as participate in outer membrane porin assembly and the synthesis of lipopolysaccharide (Lazzaroni et al., 1999; Lloubès et al., 2001). Tol forms a complex with the membrane-bound Pal lipoprotein (Tol-Pal complex) (Cascales et al., 2002). However, knocking out *pal* surprisingly did not affect Rex activity.

Alongside Omps, Tol proteins are involved in the import and export of micro- and macromolecules. TolA has three domains that span the periplasm and extend to the outer membrane, bridging interactions between outer- and inner-membrane proteins (Levengood-Freyermuth et al., 1993; Derouiche et al., 1996). The TolQRA operon, which includes *tolA*, is primarily transcribed under the control of the housekeeping sigma factor σ^D. The Rcs phosphorelay system can also affect its expression, as the RcsC sensor protein positively regulates TolQRA expression (Clavel et al., 1996). Additionally, the Rcs system indirectly promotes the translation of the general stress sigma factor σ^S via the small RNA RprA, thereby promoting the general stress response (Majdalani and Gottesman 2005; Bouillet et al., 2024). This regulatory pathway allows Rcs signaling to integrate envelope stress signals with global stress adaptation mediated by σ^S.

TolA also indirectly regulates OmpF by increasing *ompF* expression through downregulation of *ompC* expression; as such, *ompF* expression is downregulated in *tolA* mutants (Lazzaroni et al., 1986; Derouiche et al., 1996). Deletion of *tolA* also reduces LamB levels, resulting in the onset of cell stress responses (Derouiche et al., 1996). These pleiotropic effects complicate interpretations, as the observed Rex attenuation may result from broader envelope instability rather than direct interaction. Mutations in *tolA* exhibit altered cell morphology, making bacterial cells highly leaky and sensitive to external

stresses, including infections; however, they also render them resistant to colicins (Meury and Devilliers 1999; Lloubès et al., 2001; Lazzaroni et al., 2002). Colicin entry into *E. coli* requires the TolQRA inner membrane complex and the periplasmic protein TolB, as well as outer membrane proteins such as OmpA, and pore-forming proteins OmpF and OmpC (Journet et al., 2001; Isnard et al., 1994; Zakharov et al., 2004). TolB plays a critical role in colicin uptake by interacting with colicin N-terminal domains and bridging the outer membrane lipoprotein Pal with TolA in the inner membrane (Isnard et al., 1994; Szczepaniak et al., 2020). Deletion of *tolB* abolishes colicin sensitivity, confirming its essential role in this process (Journet et al., 2001). Outer membrane porins such as OmpF and OmpC also contribute to colicin translocation by forming part of the translocon that threads colicin domains across the outer membrane (Francis et al., 2021; Zakharov et al., 2004). These findings highlight a strong mechanistic analogy between colicin import and Rex-mediated exclusion, as both systems involve enveloping-spanning complexes and membrane potential-driven processes, although the Rex mechanism remains less well understood (Parma et al., 1992; Beppu et al., 1975). Notably, the deletion of any of these demonstrated at least some increase in T4*rII* plating compared to the *rex*$^+$ control. There appears to be a strong analogy between the colicin and Rex systems.

While the Pal lipoprotein is crucial in maintaining cell wall organization and intramembrane connections, the Δ*pal* mutant surprisingly did not exhibit any effect on Rex. Pal typically functions as part of the Tol-Pal complex, where the absence of Tol affects Pal's ability to maintain cell wall organization and intramembrane connections (Cascales et al., 2002). On the other hand, Lpp appears to have some influence on Rex. The *Δlpp* mutant showed a 10^4-fold increase in T4*rII* plating and a similar decrease in T4 plating, compared to the *rex*$^+$ control in the *rex*$^+$ context. This suggests that Lpp might play a role in maintaining conditions necessary for Rex-mediated exclusion. Lpp, a major pro-lipoprotein, is the most abundant outer membrane lipoprotein in *E. coli* and anchors the outer membrane to the peptidoglycan layer, contributing to envelope stability (Bernadac et al., 1998). Loss of Lpp

disrupts this structural link, leading to periplasmic leakage and vesicle formation, resulting in phenotypes similar to those of *tol-pal* mutants. Such envelope perturbations could alter the proton motive force or membrane potential, both of which are critical for Re functions (Parma et al., 1992). Transcription of *lpp*, like other membrane proteins, is under the regulation of σ^E, emphasizing its role in stress responses. Additionally, Lpp interacts with the Tol-Pal system, which is involved in energy transduction across the envelope; its absence may impair Rex's ability to sense or respond to phage infection signals. Therefore, the observed plating phenotype likely reflects a compromised Rex exclusion mechanism due to altered envelope integrity and energy coupling. Although Qi et al. (2015) reported rapid degradation of *lpp* transcripts during T4 infection, no effect was observed on T4 or T4*rII* plating in the absence of *rex* genes. In contrast, in a *rex*$^+$ context, both T4 and T4*rII* phages plated at moderate efficiency, suggesting a possible role for Lpp in sustaining Rex activity rather than initiating it. While Lpp does not regulate Tol-Pal expression, *tolA* mutations decrease *lpp* expression (Cascales et al., 2000), implying a regulatory link. Lpp may serve as a structural intermediary between TolA and Omps, although direct interaction between TolA and OmpA remains unconfirmed. TolA indirectly interacts with a TolB-Pal-Lpp-OmpA complex, as well as the rest of the Omps (Lloubès et al., 2001).

While knockout of *lamB* did not improve the plating efficiency of T4*rII* in a *rex*$^+$ context, it significantly reduced the plating efficiency of T4 (*rII*$^+$) by approximately 10^6-fold. This suggests that RII's ability to circumvent Rex is impaired in the absence of *lamB*. LamB is primarily responsible for maltose uptake but also serves as a receptor for λ adsorption (Randall Hazelbauer and Schwartz 1973).

It is a highly abundant protein and exhibits dynamic spatial localization throughout the outer membrane (Gibbs et al., 2004). Like OmpA, its expression is regulated by σ^E and by the small RNA MicA, along with other *mal* operon genes; *lamB* can also be upregulated by σ^S. Mutations in *lamB* are highly detrimental to the cell, causing severe defects in the inner membrane, disrupting the proton motive force, and unfolding Omps (Death et al., 1993). These physiological changes could indirectly impair

T4 growth, independent of Rex, by altering energy-dependent processes or receptor availability. Therefore, the observed phenotype may not solely reflect Rex activity but could also suggest a broader envelope stress effect.

To verify Rex-specific involvement, comparison with *rex*$^{-}$ lysogen or plasmid-based Rex expression would be required. Alternatively, this phenotype could represent a "hyper-Rex" effect, where envelope perturbations amplify Rex-mediated exclusion. Interestingly, Δ*lamB* showed near-complete abrogation of both T4 (*rII*$^{+}$) and T4*rII* plating in *rex*$^{+}$ conditions, but regular plating in *rex*$^{-}$ backgrounds. This supports a model in which mutations that destabilize the membrane, particularly those that impair the proton motive force, place cells in a heightened Rex-sensitive state, referred to here as a" superRex" phenotype. In this state, cells exhibit Rex-mediated exclusion even in the absence of canonical RII triggers, suggesting that membrane stress alone may be sufficient to activate RexB toxicity. This suggests that LamB may interact with RII and/or Rex, although direct interactions remain unconfirmed.

5.2.3 Assessing the Effect of Sigma Factors and Their Regulatory Elements Mutations on Rex Activity

Given that σ^S regulates many Rex-involved membrane proteins, the role of sigma factors and their associated regulatory elements was next investigated. Knockout of *rpoS* completely abrogated T4 (*rII*$^{+}$) and T4*rII* plating alike in a *rex*$^{+}$ context, indicating that σ^S is essential for both Rex activity and RII-mediated bypass. Additionally, knockouts of the stationary phase σ^S regulators that modulate σ^S (*rpoS*) expression, specifically Δ*rssA*, Δ*rssB*, and Δ*iraD,* partially restored T4*rII* plating, with increases of approximately 10^6-fold for Δ*rssA*, $>10^4$ for both Δ*rssB* and Δ*iraD*. These regulators typically promote RpoS degradation or limit its accumulation, so their deletion likely increases σ^S levels, thereby enhancing stress response pathways that counteract Rex-mediated exclusion. However, minimal to no effect on Rex activity was observed in the Δ*iraM* and Δ*iraP* mutants under high *rex*$^{+}$ expression,

suggesting that not all RpoS modulators influence this phenotype equally. Each of these σ^S regulator mutants was also lysogenized with λ*cI*857 (*rex*$^+$) and assayed for Rex activity (Table 4-4). As expected under native *rex* gene expression, attenuation of Rex activity was more pronounced in Δ*rssA,* Δ*rssB,* and Δ*iraD* lysogens compared to the parent strain BW25113(λ) *rex*$^+$ control, suggesting a gene dosage-dependent effect. The strong dependence on σ^S raises the possibility that Rex activity is integrated with global stress signaling, and that a 'super-Rex' state — where elevated σ^S comparisons with *rex*-lysogens or plasmid-based Rex expression are necessary, as the observed phenotypes could also reflect broader envelope or energy-related defects rather than Rex alone.

σ^S (RpoS) is a global stress response regulator essential for cell survival during the stationary phase, controlling the expression of over 10% of all *E. coli* genes (Weber et al., 2005). Entry into the stationary phase upon exposure to extrinsic or intrinsic stress initiates σ^E activation, which downregulates growth-phase genes and upregulates stress response genes (Chen et al., 2004). During the growth phase, RpoS protein levels are maintained at low levels primarily through proteolysis by the ClpXP protease, which targets RpoS after it is delivered by the adaptor protein RssB (Schweder et al., 1996; Battesti et al., 2015). Under stress conditions, anti-adaptor proteins IraD, IraM, and IraP stabilize the *rpoS* transcript by interacting with RssB, preventing RpoS degradation and allowing its accumulation (Bouillet et al., 2024). Importantly, ClpXP is a protease that breaks down proteins, not RNA, and its role in RpoS regulation is post-translational, not at the mRNA level. σ^E activation during envelope stress occurs through proteolytic cascades involving DegS and RseP, which degrade the anti-sigma factor RseA, freeing σ^E to initiate transcription of stress response genes (Alba and Gross 2004). As a result, stimulating the σ^E response alters Omp stability, leading to changes in cell morphology. In a Δ*rpoS* context, the absence of *rpoS* transcripts may free ClpXP to enhance *rpoE* expression, thereby activating the σ^E pathway. This shift alters the stability of outer membrane proteins and cell morphology.

The *ompF* expression is primarily regulated by the EnvZ/OmpR two-component system in response to osmolarity. It is negatively regulated post-transcriptionally by the small RNA MicF, which inhibits *ompF* translation (Pratt and Silhavy 1996; Patten et al., 2004). Notably, the expression of *ompF* is elevated in *rpoS* mutants with no significant change in OmpC levels, indicating that σ^S indirectly represses *ompF* during the stationary phase, likely through global stress response pathways rather than direct MicF regulation (Pratt and Silhavy 1996; Patten et al., 2004). In this study, *rpoS* mutants exhibited complete exclusion of both T4 and T4*rII* in the presence of *rex*, which might be explained by the overexpression of σ^E-controlled TolA, LamB, and OmpF and their direct influence/interaction with Rex. Wild-type levels of plating by both T4 and T4*rII* alike were observed in the absence of *rex*. A similar hyper-Rex phenotype was also evident in *ompA* mutants, which may suggest the involvement of *rpoS* in "triggering" Rex.

Given the strong influence of *omp* genes, *tolA*, and *rpoS* on Rex activity, it is plausible that the σ^E pathway may also be intimately connected to Rex regulation. σ^E is an essential factor that governs transcriptional activation of many downstream genes, including the periplasmic proteins and degradation factors. It has been implicated in a cell lysis pathway involving small RNAs MicA and RybB, which reduce the levels of Omps, leading to the eventual disintegration of the outer membrane (Murata et al., 2012). A similar pattern is observed when *E. coli* cells enter the stationary phase, where elevated σ^E activity leads to decreased expression of *ompA, ompC,* and *ompW* (Kabir et al., 2005). Interestingly, *E. coli* sigma factors σ^E and σ^S share homology with T4 gp-55, the T4 late sigma factor responsible for degrading the periplasmic peptidoglycan layer approximately 5 minutes post-infection (Kassavetis and Geiduschek 1984; Arisaka 2005). This timing closely aligns with the onset of Rex (7–10 min), which suggests that σ^E may serve as a key regulatory node in the Rex exclusion mechanism.

5.2.4 Complementation of Deletion Mutants Restores the Rex Phenotype

To validate the involvement of specific host genes in Rex activity, genetic complementation assays were performed on selected mutants from the Keio collection of single-gene knockouts that previously exhibited partial or complete attenuation of Rex function. The complementation test is a classical genetic approach to map gene function, identify gene interactions, and understand genetic pathways. Genetic complementation can be achieved by introducing the wild-type gene of interest in a plasmid, which is the defective gene of a mutant, into the same mutant, allowing for testing of the restoration of function or phenotype (Benzer 1955; Jacob and Monod 1961; Gravel 1982; Yook 2005).

Each mutant was first lysogenized with λ*cI857* (*rex*$^{+}$) and then transformed by a plasmid carrying the corresponding wild-type gene. Successful transformation was confirmed by tetracycline sensitivity and ampicillin resistance, indicating proper insertion of the complementing cassette into the pBR322 backbone. In nearly all mutant lysogens lacking the complementing plasmid, T4*rII* plating was restored to levels comparable to the negative controls, indicating a loss of Rex activity. However, transformation with the appropriate complementing plasmid fully restored the Rex phenotype in each case, demonstrating that the deleted genes are indeed required for Rex function. This complementation not only reinstated T4*rII* exclusion but also restored wild-type T4 plating efficiency, further supporting the functional recovery of the host from the cellular effects imparted by the chromosomal gene deletion.

Notably, Δ*tolA* mutants showed a complete loss of Rex activity when lysogenized by λ*cI*857, allowing T4*rII* to form pinpoint plaques. In contrast, Δ*rpoS* mutants lysogenized by λ*cI*857 showed no plating for either T4 or T4*rII*, but this defect was strictly Rex-dependent, as both phages plated normally in a *rex*$^{-}$ background. Upon complementation with plasmids expressing the respective wild-type genes, both mutants regained full Rex function, confirming the essential role of TolA and RpoS in the exclusion mechanism. The *ΔrpoS* mutant was especially notable: with *rex*$^{+}$ genes present, the absence of *rpoS* entirely prevented T4 and T4*rII* plating, indicating that RpoS is essential not only for Rex activity but

also for maintaining the host's permissiveness to phage infection. This suggests a broader function for σ^S-regulated pathways, potentially involving membrane integrity, energy balance, or stress response regulation, which could all impact phage-host interactions and Rex activation.

These findings collectively reinforce the conclusion that genes such as *tolA*, *ompA*, *ompF*, *ompW*, *ompX*, *ompT*, *lpp*, *mglC*, and *rpoS* strongly influence the Rex exclusion phenotype. Their roles appear to span structural, regulatory, and stress-response functions, many of which converge on envelope integrity and sigma factor-mediated transcriptional control. These genes play critical roles in maintaining cellular osmotic balance and are part of the stationary phase and/or membrane distress regulons.

Figure 5-2 summarizes the Rex activity profiles of these key *E. coli* host factors, comparing T4 and T4*rII* phage infectivity across mutant and control strains.

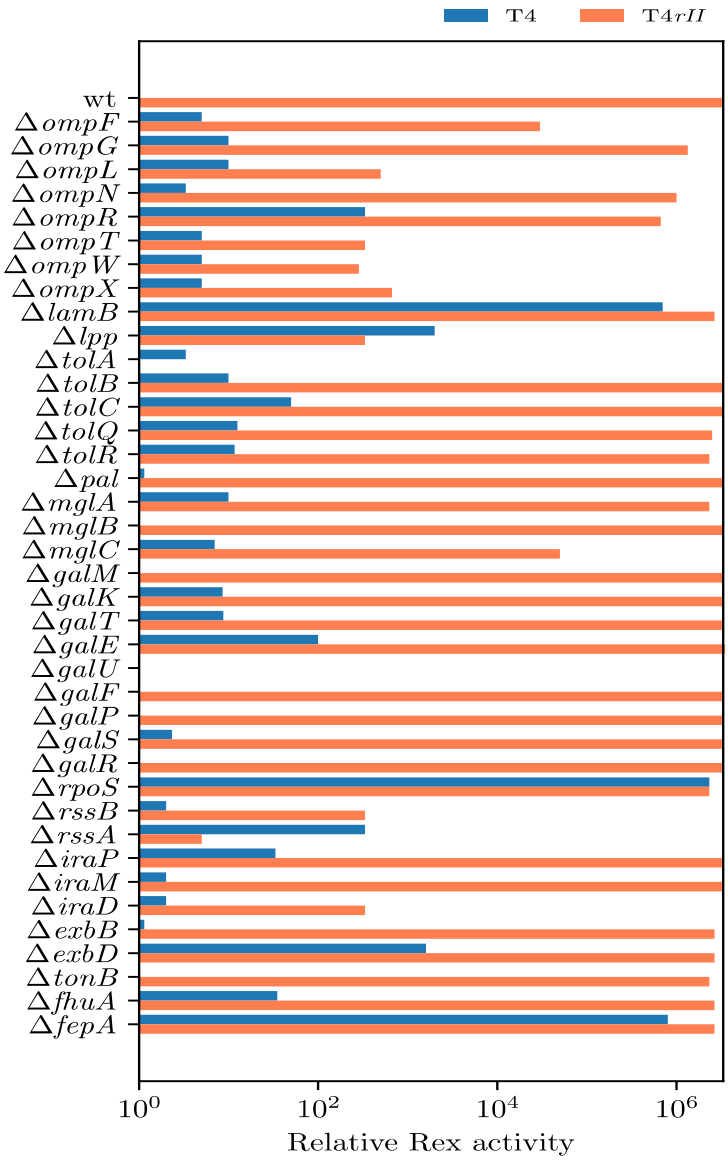


Figure 5-2. Rex Activity Assay. Rex activity refers to the ability of *rex* genes, delivered via the pHA1 plasmid (pUC19-based construct), to reduce phage plating in the presence or absence of RII function. Activity is quantified as the inverse of the relative EOP of the sample under *rex*$^+$ conditions (with plasmid) compared to *rex*$^-$ conditions (empty plasmid). Maximal Rex activity is defined as complete attenuation of T4*rII* (*rII*$^-$) phage plating in *E. coli* BW25113 (wt) in the presence of the *rex*$^+$ pHA1. Conversely, the absence of Rex activity is indicated by full plating of T4 (*rII*$^+$) in the presence of the *rex*$^+$ pHA1 in *E. coli* BW25113 (wt).

5.3 Development of a Visualization System of Rex Proteins Using Fluorescent Tagging

The development of a fluorescent protein translational fusion system for Rex proteins would be beneficial for visualizing their cellular localization under different physiological conditions. The system was based on the pPL451 plasmid (Figure 3-3), a functional plasmid designed for the multicopy, temperature-inducible expression of genes via the λ P_R promoter, which is regulated by the temperature-sensitive CI857 repressor. Fluorescent reporters (GFP or RFP) were fused to *rexA, rexB*, or both, at either the N- or C-terminus, with or without the corresponding unfused gene (Table 3-1). Constructs included configurations such as *rexA::egfp–rexB*, *rexB::egfp*, and dual fusions like *rexA::egfp–rexB::rfp*. This design allowed us to assess the impact of fusion orientation and co-expression on Rex activity.

<u>*Regulatory behaviour of the system:*</u> the expression of the Rex fusion constructs is strictly temperature-dependent due to CI857 encoded on both the plasmid and the λ prophage. At low temperatures (23- 30 °C), CI857 remains active, repressing P_R and reducing *rex* expression from the plasmid, while the prophage remains in a lysogenic state. At intermediate temperatures (35- 37 °C), CI857 begins to lose activity, resulting in partial derepression of P_R and allowing strong *rex* fusion expression from the plasmid, while the prophage remains largely silent. This results in an asymmetric state where plasmid expression is high, but the prophage stays silent. At 42 °C, CI857 is entirely inactive, resulting in full derepression of P_R and potentially triggering prophage induction. The most insightful regulatory behaviour occurs at 35–37 °C, where the balance between CI activity and promoter accessibility reveals the system's dynamic regulation (Hoffmann et al., 1999; Valdez-Cruz et al., 2010; Ptashne 1986).

Experimental design and controls: Functionality was tested in *E. coli* BW25113 (wt) and its *λcI*857 lysogen by T4/T4*rII* plating at 23 °C, 30 °C, 35 °C**,** and 37 °C, combined with fluorescence microscopy. The benefit of the "off state" conferred by the pPL451 conditional expression plasmid also allows us to examine the Rex proteins at various times after infection by either T4*rII* or T4 (wt). To evaluate the system and analyze Rex's function, several analytical methods were employed. T4*rII* plating was critical for quantitatively assessing Rex activity, while transformation efficiency and colony morphology ensured that the constructs were viable. Additionally, fluorescence microscopy provided visual evidence of protein expression and localization within the cell.

Controls confirmed that GFP alone did not affect Rex activity: *λcI*857 lysogens carrying pPL451(*egfp*) retained complete exclusion, while wild-type cells did not. However, all fluorescently tagged constructs exhibited reduced Rex activity compared to the 100% rex^+ control, with T4*rII* plating observed in every case. This suggests that fusion disrupts Rex protein stability or stoichiometry, both of which are crucial for exclusion.

Impact of fusion orientation on Rex function: Indeed, certain N-terminal tags can hinder translation initiation or ribosome scanning, thereby reducing protein expression efficiency (Sørensen and Mortensen 2005). N-terminal fusions and modifications can also significantly impair protein stability and folding, leading to misfolded or aggregated proteins that are toxic to the host cell or cause metabolic stress, manifesting as slower-growing and smaller colonies (Sørensen and Mortensen 2005). While C-terminal fusions are generally more tolerated, they can still interfere with protein folding and stability (D'Accolti et al., 2023). Additionally, promoter strength and plasmid copy number significantly influence how tag position affects protein expression levels (Shao et al., 2021).

These considerations are critical for Rex proteins, where structural integrity and stoichiometric balance between RexA and RexB are essential for function. GFP (eGFP) is widely used for tagging due to its stability and robust fluorescence, but it exhibits weak dimerization under physiological conditions.

When fused to RexA, it may artificially stabilize interactions with RexB even at a 1:1 stoichiometry, potentially triggering inappropriate activation of the Rex system. In contrast, RFP variants, such as dsRed, are prone to tetramerization, which can dramatically alter the stoichiometry of the complexes. A RexB::dsRed fusion could therefore disrupt the finely tuned RexA:RexB ratio required for proper exclusion activity, as proposed by Parma et al. (1992). Such oligomerization effects may also influence membrane insertion and channel formation by RexB, further destabilizing the system. Moreover, the bulky nature of fluorescent proteins can sterically hinder critical interaction domains, particularly at the N-terminus of RexA, which is implicated in sensing and initiating activation, and at the N-terminal membrane-anchoring region of RexB. These disruptions, combined with tag-induced oligomerization, highlight the importance of carefully selecting the tag type, fusion orientation, and expression context when studying protein complexes like Rex, where stoichiometry and structural integrity are closely linked to function. Overall, these results highlight the phenotypic consistency of colony morphology across most constructs, emphasizing the importance of fusion orientation and expression context in synthetic biology applications.

Initial tests in a *rex*$^{-}$ background (wild-type host) showed that none of the tagged constructs conferred the Rex phenotype, as T4*rII* efficiently plated across all constructs. This raised two possibilities: 1) the fusion partially or completely abolished RexA and RexB function, or 2) the fusion disrupted stoichiometry or stability rather than eliminating function entirely. To distinguish between these scenarios, the constructs were introduced into a *rex*$^{+}$ context (*λcI*857 lysogen), which provides an additional copy of functional *rex* genes. If the tagged proteins retained partial functionality, they might complement or interfere with the native Rex system. This approach was critical for determining whether the loss of activity was absolute or due to altered stoichiometry. The Rex system requires precise interaction between RexA and RexB at defined ratios. Overexpression of RexA relative to RexB is

lethal, while RexB overexpression abrogates exclusion and allows superinfecting phage plating. These principles guided the interpretation of fusion effects. Two complementary strategies were used to assess the functions of RexA and RexB. First, the Rex activity assay by applying the T4*rII* plating efficiency to determine whether tagged RexB could still participate in exclusion when overexpressed and paired with native RexA. Second, the transformation efficiency readings in the *rex*$^+$ context, where RexA functionality and activity can be assessed, are likely influenced by the overexpression of RexA relative to RexB, which would probably trigger the Rex phenotype and lead to cell death. Constructs overexpressing functional RexA were expected to yield very low transformation efficiency in the *rex*$^+$ background.

In general, the fusion of GFP/RFP tags significantly affected the Rex phenotype by attenuating Rex activity either entirely or to some extent, compared to the 100% Rex activity control. Unfortunately, none of the designed fluorescently tagged constructs, especially those encoding both *rex* genes, demonstrated a complete Rex phenotype when plated against T4*rII*. N-terminal tagging of RexA was most disruptive, causing a nearly complete loss of activity (~a 10^4-fold reduction), particularly at 25 °C. This likely reflects the essential role of RexA's N-terminus in sensing and initiating activation via interaction with RexB. In contrast, C-terminal tagging of RexA preserved partial function (~a 10-fold reduction), suggesting that this region stabilizes the RexA-RexB complex but tolerates modification. RexB fusions were less sensitive overall, consistent with its structural flexibility and membrane anchoring role; C-terminal tagging was better tolerated than N-terminal tagging, aligning with previous findings (Parma et al., 1992).

Dual C-terminal fusions (*rexA::egfp-rexB::rfp*) produced the most Rex activity with minimal T4*rII* plating across all temperatures, especially at 37 °C, where CI857 derepression maximizes plasmid expression without full prophage induction (Ptashne 1986). This configuration preserves RexA's N-

terminus and RexB's N-terminal membrane anchor intact, maintaining essential interactions. In lysogenic strains, this temperature places the prophage near the threshold of induction, a state previously associated with a Rex$^-$ phenotype and elevated RexB expression (Parma et al., 1992). Under these conditions, even subtle disruptions in RexA-RexB stoichiometry, such as those caused by fusion orientation or tag-induced oligomerization, may significantly impact Rex system activity and downstream phenotypes. That could explain the behaviour of some fused constructs at this temperature, including the overexpression of RexB and the abrogation of Rex activity, which results in the Rex$^-$ phenotype. For instance, *the egfp::rexA-rexB* construct showed no Rex activity in *rex*$^-$ cells; partial activity was observed in *rex*$^+$ cells, suggesting that N-terminal tagging inactivated RexA, while overexpressed RexB disrupted stoichiometry and abrogated exclusion. On the other hand, the *rexA::egfp-rexB* construct showed better Rex activity in *rex*$^+$ cells, suggesting that C-terminal tagging of RexA allows limited function of Rex when paired with native Rex proteins, and as a result, better functional stoichiometry. RexB fusions exhibited some activity and inhibited T4*rII* plating, possibly due to partial RexB function or a stochiometric imbalance that triggered Rex-mediated cell death. Nevertheless, all tagging reduced activity to some degree, likely due to steric hindrance or altered oligomerization.

These observations align with the known structural role: RexA's N-terminus mediates sensing and initial interaction with RexB, while its C-terminus stabilizes the complex and interacts with CI. RexB, a multi-pass membrane protein, anchors via its N-terminus and utilizes its C-terminal cytoplasmic loop to interact with RexA, enabling membrane depolarization and cell death (Parma et al., 1992; Thomason, L. C. et al., 2021). Disruption of these domains by tagging likely impairs activation or stability of the complex. This may explain the nearly complete inhibition of the Rex phenotype when GFP was fused

to the N-terminal of RexA in almost all cases. These critical data would help us understand the effect of fluorescent proteins at different fusion sites for RexA and RexB.

Transformation efficiency across constructs and temperatures: The transformation efficiency varied significantly across constructs and temperatures. At room temperature (23 °C), colonies required ~ 36 h to become countable, and the lowest efficiencies were observed for constructs with direct fusions to Rex proteins, particularly dual fusions (e.g., *egfp::rexA-rfp::rexB*). This may suggest that fusion to either protein immediately impacts transformation efficiency. Reductions were more pronounced in wild-type hosts than in *λcI*857 lysogens, likely due to the physiological and molecular changes associated with lysogeny. The λ prophage represses lytic genes and reduces nuclease activity (e.g., RecBCD), enhancing plasmid stability and transformation efficiency (Lee H. et al., 2022; Catalão and Pimentel 2018; Oppenheim et al., 2005).

At 30 °C and 35 °C, transformation efficiencies were generally similar to those at 23 °C, except for *egfp::rexA-rexB* construct, which exhibited an approximately 10,000-fold reduction in both wild-type and lysogenic cells. This severe drop likely reflects the inactivation of RexA due to N-terminal tagging, combined with the overexpression of RexB, creating a stoichiometric imbalance that destabilizes the Rex system. Another scenario is that the N-terminal fusion of RexA causes the overexpression of RexA relative to RexB; as a result, RexB could be knocked out, which would trigger Rex and lead to cell death. The surviving cells would be very few and could be Rex^{-} colonies. This interpretation aligns with T4*rII* plating results, where these constructs showed almost complete abrogation of Rex activity, and Rex^{-} would form plaques regardless of the rex^{+} genotype. Overexpression of RexB alone, or in excess relative to RexA, is known to disrupt membrane homeostasis and can be toxic, as RexB is a multi-pass inner membrane protein with ion channel-like properties (Parm et al., 1992: Shao and Black 1996; Snyder and McWilliam 1989). Such overproduction can overload the Sec/YidC insertion

machinery, activate envelope stress response, and reduce cell viability, leading to very low transformation efficiency (Miroux and Walker 1996; Wagner et al., 2008).

At 37 °C, the transformation efficiency decreased significantly (up to 10,000-fold) for both wild-type and lysogen cells. Several factors likely contribute. First, the inactivation of CI857 at this temperature derepresses the λP_R promoter, leading to the strong overexpression of Rex fusions immediately after transformation. Second, in lysogens, prophage induction may occur, resulting in cell lysis (Jechlinger et al., 1999). Third, the overexpression of RexA relative to RexB can trigger the Rex system, resulting in membrane depolarization and ATP depletion, which is lethal to the cell and causes cell death (Parma et al., 1992; Thomason L. C. et al., 2021). These findings illustrate that low transformation efficiency is not solely a cloning artifact, but rather reflects the physiological burden of expressing toxic or membrane-associated proteins. This is well-documented for inner membrane proteins in *E. coli*, where high-level expression often causes growth arrest or cell death unless expression is tightly controlled (Miroux and Walker 1996; Wagner et al., 2008).

In the context of Rex, the effect is amplified by the system's sensitivity to stoichiometry: imbalances between RexA and RexB can either abrogate exclusion or trigger cell death, both of which reduce colony recovery and low transformation efficiency.

Unexpectedly, some *λcI*857 lysogens harbouring Ap^R constructs grew on ampicillin-containing media but failed to grow on non-selective LB at 37 °C. This suggests that antibiotic pressure retained plasmids expressing toxic proteins (e.g., solo RexA or RexB), whereas non-selective conditions favoured plasmid loss or revealed toxicity. RexA and RexB behave analogously to a toxin-antitoxin-like system: when expressed independently, either protein can exert a toxic effect on the host cell (Parma et al., 1992; García-Ruiz et al., 2000; Jurėnas et al., 2022). RexA may form incomplete signaling complexes, while RexB, functioning as a membrane ion channel, can disrupt the membrane potential and lead ion

leakage, as well as ATP depletion, membrane depolarization and cell death (Parma et al., 1992; Shao and Black 1996; Slavcev and Hayes 2004; Snyder and McWilliams, 1989; Jurėnas et al., 2022).

Colony morphology and fusion orientation: Colony morphology varied with the construct and incubation temperatures. Colonies of *E. coli* BW25113 [pPL451], 100% *rex*$^+$ control, and [pPL451-*egfp*] displayed uniform wild-type morphology: round, shiny appearance and smooth surfaces. At 30 °C, colonies from all strains closely resembled their respective controls in shape and size, regardless of the fusion site or type of protein expressed (Figure 4-8). At 37 °C, where the λ*cI* repressor is largely derepressed and expression from the p_L promoter is active, including RexA and RexB, residual repressor activity (~1%) persists (Ptashne 1986), meaning that expression is not fully maximal. Furthermore, high gene dosage from plasmid-based constructs further boosts expression levels, which may overstate the effect of Rex protein overexpression and lead to differences, especially in lysogenic strains. Control colonies remained small, regular, and smooth, traits that were highly consistent (96%-98%) and served as reliable benchmarks for morphological stability. Wild-type (non-lysogenic) colonies grown at 37 °C exhibited no significant morphological deviations from the controls. Lysogenic colonies incubated at 37 °C appeared larger, flatter, wider, and duller than controls, except for some lysogens, which were small and resembled the wild-type colonies at 23 °C, possibly reflecting heterogeneous expression or differential tolerance to Rex protein toxicity (Figure 4-9).

Fusion orientation strongly correlated with morphology. Colonies expressing dual C-terminal fusion (e.g., *rexA::egfp-rexB::rfp*) were larger, flatter, and more uniform (with 95% consistency), suggesting that this orientation is less disruptive to protein function. Colonies expressing *egfp::rexA* were small (~ 1 mm), with a consistency of about 93%, but appeared shinier and stickier, suggesting altered extracellular interactions or due to eGFP's weak dimerization stabilizing inappropriate RexA-RexB interactions (Figure 4-9 B1, Parma et al., 1992). eGFP is known to weakly dimerize, and when fused

to RexA, it may artificially stabilize interaction with RexB, even at a 1:1 stoichiometry, potentially triggering inappropriate activation of the Rex system (Parma et al., 1992). As a result, influences colony morphology. In contrast, *rexA::egfp* colonies were larger and flatter (~ 2 mm) with consistency similar to that of the controls (96%) (Figure 4-9 B2), suggesting that C-terminal tagging affects interaction domains differently, potentially hindering complex formation but reducing toxicity.

The N-terminal fusion of GFP to RexB, in the absence of RexA, produced colonies (~ 2 mm), which are flatter with a matte appearance, lacking the shininess that is present in the control morphology (Figure 4-9 C1). This suggests impaired surface structuring or altered cellular envelope composition. The colony formed of cells carrying the *rexB::egfp* construct (C-terminal fusion) is larger than that with the N-terminal fusion, measuring approximately 2-3 mm. Despite this, it maintains a similar flat and dull surface texture and appearance, which indicates that the C-terminal fusion of GFP promotes growth while preserving the altered colony appearance (Figure 4-9 C2). The smaller size of the control colonies may suggest that the expression of functional RexA and RexB, particularly with C-terminal fusions, could enhance growth due to their involvement in phage exclusion or cell viability pathways.

Across 200 colonies per construct, 10 of the 11 experimental groups showed relatively high internal consistency (92-96%), despite differences in average colony size (ranging from 1 mm to 4 mm). The most striking observation was the dual N-terminal fusion of both RexA and RexB, which exhibited the lowest phenotypic consistency at 87%, as confirmed by both quantitative analysis and visual inspection. Although this dual fusion conferred some stability, it also introduced morphological heterogeneity, possibly due to potential variability in protein expression, folding, localization, or interaction caused by the N-terminal tags. RexB, as a membrane-bound ion channel, relies on proper membrane insertion and interaction with RexA for activation (Parma et al., 1992). N-terminal fusion may interfere with signal peptides or membrane-targeting sequences, leading to mislocalization or dysfunctional channel activity. Similarly, RexA, which is likely a cytoplasmic sensor, may be hindered in its ability to activate

RexB when a bulky fluorescent tag obstructs its N-terminus. Fusions at the N-terminus have been noted to more frequently disrupt signal peptides, translational initiation, or protein folding and stability than C-terminal fusions, which generally tolerate fusion tags better. This can affect protein solubility and bacterial health (D'Accolti et al., 2023).

Visualization of Rex fusion constructs by fluorescence microscopy: Building on phenotypic assays, fluorescence microscopy was employed to confirm the expression of GFP- and RFP-tagged Rex proteins and evaluate how fusion orientation influences expression and stability.

Cells carrying *rex::egfp/rfp* constructs were grown at 25 °C and induced at 37 °C for 60-90 minutes (Ptashne 1986; Valdez-Cruz et al., 2010). The wild-type strain carrying the pPL451 plasmid served as a negative control for GFP imaging, showing no fluorescence (Figure 4-11 A1). In contrast, the pPL451-*egfp* plasmid was used as a 100% control for GFP imaging and showed sufficient fluorescence to discern individual cells to some extent, confirming plasmid functionality (Figure 4-11 A2). Images were acquired using a 60× oil immersion objective, including transmitted light with no GFP emission, GFP emission, and RFP emission. Although it provides high-resolution imaging and excellent light-gathering capacity, it has limitations. It does not provide sufficient magnification to resolve the precise subcellular localization of fluorescently tagged proteins, especially in small bacteria like *E. coli*. For more comprehensive visualization, both at the cellular level and across a broader field of view, a total magnification of 400x or higher is often recommended (Swift and Colarusso 2022). This enables better contextual imaging of fluorescence distribution while maintaining sufficient resolution for qualitative analysis.

The C-terminal GFP fusion to RexA or RexB displayed noticeably higher fluorescence than the N-terminal fusions, consistent with T4*rII* plating data showing better Rex activity for C-terminal

constructs (Figure 4-11). For example, *rexA::egfp* produced bright GFP-positive aggregates (Figures 4-11 B1 and C1), whereas *egfp::rexA* and *egfp::rexB* showed weak or undetectable fluorescence (Figures 4-11 B2 and C2). Constructs with C-terminal GFP fusion in co-expression contexts (e.g., *rexA-rexB::egfp*) also exhibited noticeable fluorescence (Figures 4-11 D1 and E1), while N-terminal fusion lacked defined GFP-positive structures (Figures 4-11 D2 and E2). These findings suggest that C-terminal tagging might preserve expression and folding better than N-terminal tagging.

Dual-tagging experiments (e.g., *rexA::egfp-rexB::rfp*) revealed noticeable co-expression of GFP and RFP in most cells, with many puncta appearing yellow/orange, indicating co-localization (Figure 4-12 F1). This pattern aligns with high Rex activity observed in plating assays. Differences in fluorescence intensity suggest variable expression of folding efficiency between RexA and rexB. RFP signal often appeared more uniform, supporting the idea that RexB tolerates tagging better than RexA. In contrast, N-terminally tagged constructs (e.g., *egfp::rexA–rfp::rexB*) exhibited minimal or no detectable GFP and dominant RFP fluorescence, with only a few cells showing dual fluorescence (Figure 4-12 F2), suggesting impaired RexA expression or stability. Mixed fusions (e.g., *egfp::rexA–rexB::rfp*) showed similar bias toward RFP expression (Figure 4-12 F3). These observations reinforce that N-terminal tagging of RexA significantly impairs expression and function, while C-terminal tagging supports better co-expression and likely preserves stoichiometry.

Semi-quantitative fluorescence analysis suggested that fusion orientation has a strong influence on expression dynamics. C-terminal fusion, particularly *rexA::egfp-rexB::rfp*, demonstrated the highest expression and co-expression rates, whereas N-terminal fusions exhibited markedly reduced fluorescence. Mixed constructs showed imbalanced expression, dominated by RFP, underscoring the sensitivity of Rex proteins to tag position.

Mechanistically, these results highlight that RexA's N-terminus is critical for activation and interaction with RexB, making it highly sensitive to tagging. RexB tolerates tagging better, especially at the C-terminus, likely due to its structural flexibility. Tag-induced oligomerization further complicates stoichiometry: eGFP weakly dimerize, and dsRed (RFP) forms tetramers, potentially stabilizing inappropriate interactions or disrupting the RexA:RexB ratio (Parma et al., 1992). These findings underscore the importance of rational construct design in synthetic biology, where both expression efficiency and functional integrity are crucial.

Fluorescence imaging and semi-quantitative analysis exhibited that C-terminal tagging is the most compatible strategy for Rex proteins, enabling robust expression and partial preservation of function. N-terminal tagging, particularly of RexA, should be avoided unless functional disruption is intended. Dual C-terminal tagging might offer the best balance between visualization and activity, providing a practical approach for future localization studies.

5.4 A Proposed Model for Rex and RII Suppression of Rex

Based on the data derived in this work and combined with previous findings from Alattas MSc thesis (2015), A link between membrane proteins, sigma factors, and their regulators to the activation, manifestation, and exclusion mechanism is proposed (Figure 5-3). Additional puzzle pieces are uncovered herein to complement the initially proposed model in Alattas (2015). Overall, it is proposed that, in the absence of RII proteins, Rex-mediated abrogation of T4 replication is driven by the interplay between σ^S- and σ^E-governed regulons.

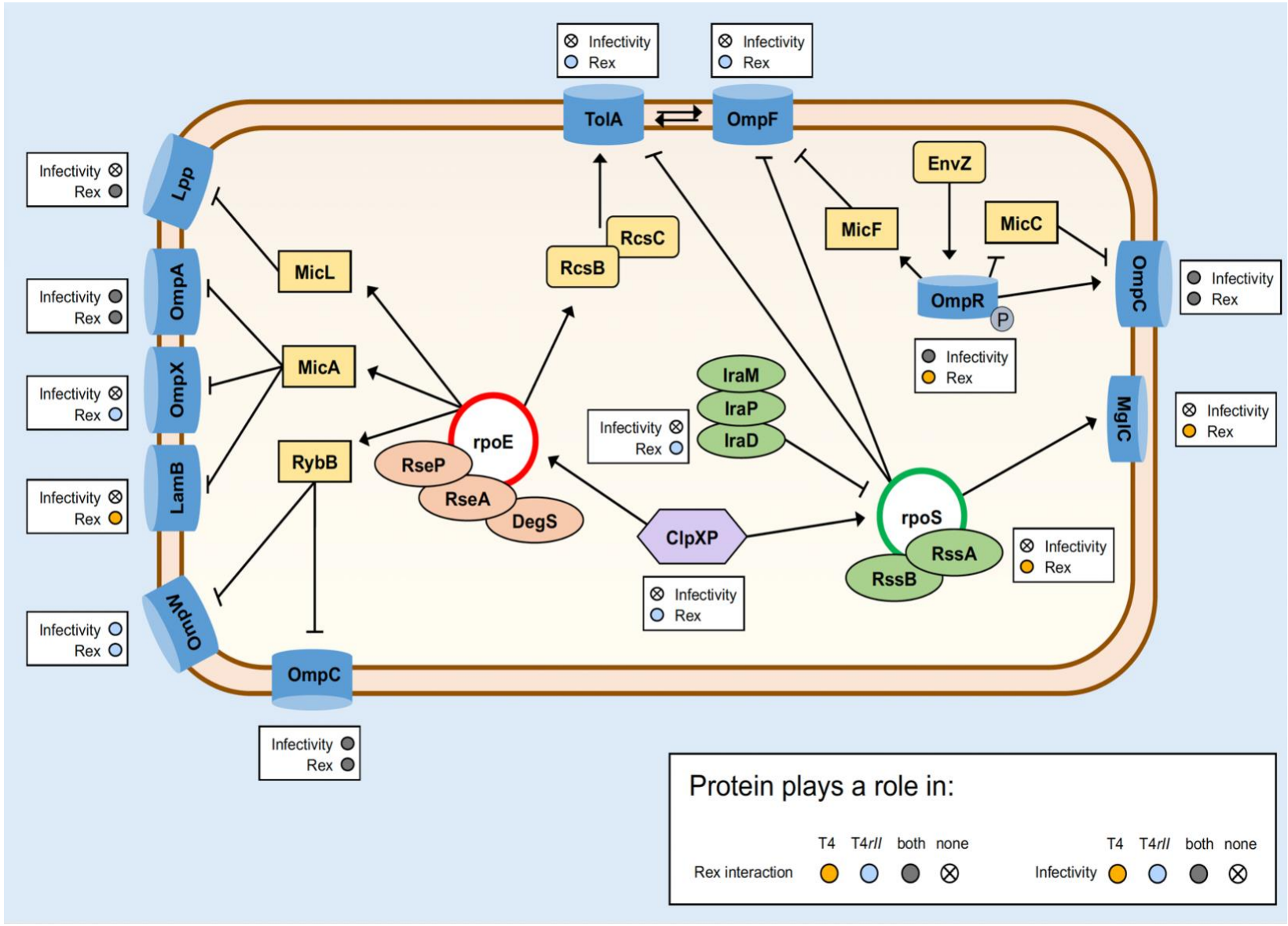

Infectivity
Rex
TolA
OmpF
Lpp
OmpA
OmpX
LamB
OmpW
OmpC
MicL
MicA
RybB
RcsB
RcsC
rpoE
RseP
RseA
DegS
IraM
IraP
IraD
ClpXP
rpoS
RssA
RssB
EnvZ
MicF
MicC
OmpR
P
MgIC
Protein plays a role in:
Rex interaction
Infectivity
T4
T4rII
both
none

Figure 5-3. Model of T4 and T4*rII* Infection in a *rex*$^+$ *E. coli* Cell (The Rex Mechanism). Upon infection, the host activates stress response pathways involving *rpoE*/*rpoS*, depending on the presence or absence of RII gene product. Rex system activation is hypothesized to be triggered via TolA, leading to a physiological shift toward a stationary-like phase as a defense mechanism. OM: outer membrane, IM: inner membrane; blue cylinders indicate membrane proteins; green ovals indicate regulatory proteins of *rpoS* expression; red ovals indicate regulatory proteins of *rpoE* expression; yellow boxes indicate either small RNAs or regulatory proteins involved in the expression of membrane proteins. Small circles next to a protein indicate a) their role in T4 infectivity (yellow), T4*rII* (blue), both (grey), or neither (X); b) postulated interaction with RexA and/or RexB: only in the presence of RII (T4) (yellow), only in the absence of RII (T4*rII*) (blue), regardless of RII presence (with either phage) (grey). Pointed arrowheads indicate stimulation or upregulation, while bars indicate inhibition or downregulation.

T4 infection activates host stress responses: Upon infection, T4 first adsorbs to OmpC on the outer membrane and injects its DNA into the host cell, causing disturbances in periplasmic and cytoplasmic osmolarity (Arisaka 2005) and activating membrane sensors such as OmpX and TolA. A σ^E-mediated stress response is triggered in response to envelope stress (Dam et al., 2018). Membrane and osmotic stress also trigger σ^S activation and the induction of stationary-phase genes (Hengge-Aronis et al., 1991, 1993). ClpXP typically degrades RpoS via RssB during growth, but under stress, anti-adaptors IraD, IraM, and IraP block this interaction, stabilizing RpoS (Schweder et al., 1996; Battesti et al., 2015; Gottesman 2019). During T4 infection, Rex may mimic stress conditions that elevate anti-adaptors IraD, IraM, and IraP, thereby outcompeting ClpXP and stabilizing active σ^S levels. Free ClpXP would then be available to elevate σ^E levels. Generally, in the absence of Rex, T4 infection would lead to cell lysis within 15 minutes (Bryan et al., 2016). Not surprisingly, phage infection is a significant stress trigger; overall, the initiation of T4 infection is expected to activate stress response pathways, leading to high expression levels of both σ^E and σ^S in the absence of Rex. This regulatory shift likely contributes to the stationary-phase-like state observed during Rex activation.

As OmpA expression is directly linked to σ^E activation, depleted levels of OmpA in the cell may "prime" *rex*$^+$ cells for exclusion. The potent inhibition of T4 and T4*rII* plating in Δ*ompA* mutants is heavily Rex-dependent, as it was not seen in the *rex*$^-$ mutant. This suggests that OmpA may be a target for inactivation by Rex protein(s) and that RII proteins may competitively inhibit this inactivation. Alternatively, RII suppression of Rex relies upon its interaction with OmpA. Either way, the incomplete abrogation of T4 plating in a Δ*ompA* context suggests that *ompA* is not the only host gene involved.

Rex onset increases *tol* and *rpoE* expression but reduces *rpoS* expression: In a Rex$^+$ environment, the onset of Rex is postulated to start with membrane-bound RexB binding with multiple RexA proteins (Parma et al*.,* 1992). This enables RexB-mediated efflux of cations, resulting in further membrane destabilization and depolarization. Activated stress response pathways should replenish the depleted pools of outer membrane proteins (including OmpX, OmpW, OmpF, or Lpp) in response to T4 infection. Moreover, membrane instability also stimulates *tol* expression to maintain cell integrity. TolA would further stimulate σ^E activity, leading to increased expression of *tol-pal*, *lamB*, *lpp,* and *ompA,* thereby restoring membrane integrity. From this study, only the *tolA* mutant could completely abrogate Rex activity on its own. Thus, TolA must serve as one of the key controllers that maintain Rex activation and exclusion, due to its transmembrane position, which facilitates interaction with both RexA and RexB This hypothesis suggests that direct TolA interaction with Rex proteins would activate the formation of the RexB-RexA active complex.

Based on their shared membrane-bound location, RexB could interact with RssB instead of σ^S, freeing σ^S from the RssAB-ClpXP complex. This would again free ClpXP to elevate σ^E levels and expression of the membrane stress regulon. Cytoplasmic RexA could also bind IraD, preventing its upregulation of σ^S. The activation of Rex is, therefore, believed to be associated with high σ^E levels, but growth-phase levels of σ^S.

Rex manifestation is a stationary-like phase: After Rex-mediated efflux of cytoplasmic cations (K^+ efflux), the cell must compensate by stimulating phosphatases and *ompF* to restore cell osmolarity. Given the observed modulation of Rex activity by both OmpA and OmpW, their regulator σ^E is expected to direct the harsh physiological cellular conditions associated with Rex via *micA* and/or *rybB* expression (Parma et al., 1992). Stress-induced upregulation of *ompF* would lead to heightened *ompA* expression and subsequent decreased *ompC* expression, which reduces T4 adsorption and superinfection. This could explain what has been previously observed upon activation of Rex: cells enter into a temporary growth arrest state, where they become resistant and protected against T4 superinfection (Slavcev and Hayes 2003). Lpp must play an essential role in Rex exclusion, as previously noted, since disruption in Lpp expression significantly reduces Rex activity in T4*rII* (Figure 4-5). This module postulates that the membrane-bound RexAB complex is maintained through Lpp, a structural membrane protein, whose own expression is regulated by σ^E.

This stationary-like phase resembles σ^E-dependent cell lysis during the early stationary phase, where only about 10% of the cell population survives. Prolonged Rex activity eventually starves the cells of necessary nutrients and can eventually lead to cell lysis. This cell lysis could also be explained by the most recent knowledge about the function of RexA, as a molecular switch that transitions from the lysogenic to the lytic cycle through interaction with CI to induce the lytic cycle (Thomason et al., 2021). RexA appears to be crucial in this story; it detects abnormal DNA, such as T4*rII*, and activates RexB, which induces membrane stress through the efflux of ions. At the same time, it binds to the CI repressor to activate lytic promoters while σ^E triggers the stress response due to envelope depolarization caused by RexB. The activation of Rex would promote σ^E cell lysis, and vice versa, whereby σ^E activation might support Rex in maintaining its activity; all of this is initiated and sustained by RexA. From previous (Slavcev and Hayes 2002) and this study results, Rex protects its host against T4 cell lysis for days, after which the harsh ionic environment could stop Rex, allowing T4 replication to resume and

kill the host cell. Any interruption of the Rex system will also disrupt the delicately maintained balance between σ^E and σ^S, also leading to σ^E-mediated death. This model postulates that as long as the balance between σ^E and σ^S is kept, some surviving Rex cells would eventually escape T4*rII* infection.

RII attenuates Rex exclusion: RII localizes to the inner membrane of the host and is expressed early during T4 infection, approximately 10 minutes following superinfection (Takacs and Rosenbusch 1975; Mosig et al., 1984), where RexB is also localized (Parma et al., 1992). While the precise timing and mechanism of RII localization remain unclear, its early expression suggests a role in counteracting Rex activation or the interaction of RssB and RssA with σ^S, thereby preventing the binding of anti-adaptors to RpoS and σ^S degradation. This study found that both T4 and T4*rII* fail to plate on *rex*$^+$ Δ*rpoS* mutants (Table 4-3, Figure 4-5), suggesting that RpoS-dependent pathways influence the Rex phenotype; somehow, RII interactions with σ^S might be necessary for T4 infection. In the absence of RII, the combination of RexA and RexB activity may stabilize σ^S levels, thereby leading to the exclusion phenotype. Conversely, if RII is present, it could bind σ^S to activate it similarly to IraD, leading to elevated σ^S pathways. As such, σ^S-RII interactions would be required to interrupt the onset of the Rex-mediated protective phase. Similarly, LamB, a σ^E-controlled porin localized in the outer membrane, was also implicated in Rex function in this study's results. RII may require both proteins to inactivate Rex successfully. LamB is under the control of σ^E, thus representing a vital link between RII, σ^E, σ^S, and Rex.

In conclusion, bacterial cells are highly capable of quickly perceiving and adapting to environmental changes and stresses, enabling them to survive. The Rex exclusion mechanism is a powerful example of such a protective mechanism against superinfecting T4 mutants. These observations support a model in which Rex activation and T4 counter-defence involve complex interactions with host stress regulons, but the exact molecular connections remain to be elucidated.

It is now believed that new pieces of the longstanding Rex puzzle have been assembled: namely, that Rex exclusion is driven by the balance of activated σ^E to σ^S pathways. Impairment of key players in either pathway attenuates Rex's ability to exclude T4*rII* plating. A number of these players are membrane proteins, which is not that surprising given the plethora of structurally observable characteristics associated with the onset of the Rex phenotype. Disruptions in cell membrane permeability have been previously shown to render cells more sensitive to superinfecting T4. Understanding the individual functions of these factors and clarifying their exact interactions may help to solve the Rex puzzle. Comprehending Rex can ultimately provide key clues and strategies for developing eukaryotic exclusion systems and control mechanisms.

Chapter 6

Conclusion and Future Directions

6.1 Conclusion

Despite Rex's historic role in advancing our understanding of modern molecular genetics, the mechanism governing the bacteriophage λT4*rII* exclusion (Rex) phenotype has remained unresolved for about 70 years. The Rex phenotype is recognized as a sophisticated and multifactorial antiviral defense strategy in *E. coli* lysogens that selectively targets and prevents the replication of T4*rII* mutant phages. The identification of host genes that influence Rex activity has long been pursued to better understand the exclusionary mechanism. In this work, *E. coli* mutations were identified through both a "top-down" mutagenic approach and a "bottom-up" screening of candidate genes for the influence of Rex activity. A single-step insertional mutagenesis system was constructed to generate and screen *E. coli* that are genotypically *rex*$^{+}$ and yet phenotypically compromised for exclusion activity. Applying this one-step genetic selection and screening system, one gene of interest, *mglC,* was identified. The gene encodes a 336-amino-acid hydrophobic protein that, when deleted, was observed to attenuate Rex activity by more than a hundredfold. Further investigations revealed that, beyond classical membrane proteins, a broader regulatory network is involved in modulating Rex-mediated exclusion. This includes structural and transport proteins such as TolA and MglC, along with regulatory elements associated with the general stress response, most notably the alternative sigma factor RpoS (σ^{S}). Other interesting candidates were examined and found to exhibit varying degrees of influence on Rex activity. Tol proteins, sigma factors, and their regulators may be implicated in triggering some of the physiological manifestations of Rex or may serve as sites of competition and interaction with RII. For the first time,

the significant impact of TolA, RssA, RssB, and IraD on Rex was demonstrated, with the deletion of their genes resulting in the complete abrogation of Rex activity.

To complement this genetic work, fluorescent tagging experiments were conducted using GFP and RFP fusions at both the N- and C-termini of RexA and RexB. These studies revealed that fusion orientation and co-expression may significantly impact Rex activity, with N-terminal fusions generally disrupting the function and stability of Rex proteins. In contrast, C-terminal fusions may retain partial activity. This suggests that the proper folding, localization, and complex formation of the Rex proteins are crucial for exclusion function. The free N-terminal of RexA and the C-terminal of RexB might be necessary for maintaining the stoichiometry and stability of Rex activity and exclusion. It is therefore concluded that fusing the C-terminal of both RexA and RexB proteins could represent the optimal strategy for implementing terminal tagging in future studies.

Collectively, these findings substantially refine the understanding of the Rex exclusion mechanism, illustrating it as an integrated, multilayered system influenced by gene expression dynamics, membrane composition, stress signalling pathways, and RNA-based regulation. The Rex system is exemplified as a form of programmed cellular responses that balances self-destruction with population-level protection and prophage maintenance. Its study offers valuable insights into bacteriophage-host coevolution, innate bacterial immunity, and the molecular principles behind superinfection exclusion and controlled cell death in prokaryotic organisms.

6.2 Future Directions

Many proteins identified as essential influencers of the Rex phenotype — including the Rex proteins themselves and RII proteins — are well characterized; however, several key areas remain insufficiently understood. This could be due to several factors that hinder progress in their studies. The structural complexity of these proteins poses significant challenges, particularly because many are embedded within the lipid bilayer, complicating their isolation and analysis using conventional biochemical and structural methods. Furthermore, these proteins fulfill a vast multitude of functions that may be involved in a wide range of cellular processes, including, but not limited to, maintaining cell structure, nutrient transport, signalling, phage defence, and more. All these factors contribute to the complexity of understanding their role in the cell and characterizing them. Some of these portions possess a hydrophobic nature, making it more difficult to extract, purify, and stabilize them without causing aggregation or loss of functionality during the process. Additionally, some proteins operate as part of multi-component complexes; to study one, it is necessary to examine the others to grasp the overall function or process.

While researchers continue to develop innovative techniques and approaches to better understand the bacterial and phage proteins, several new hypotheses and lines of inquiry have emerged from the results compiled in the preceding chapters. These questions can form the basis for new research directions, which will further advance the understanding of a powerful exclusion system and its potential application as an advanced nature-derived biotechnological tool.

1. Functional fluorescence tagging and localization

Since the discovery of the λ T4*rII* exclusion phenotype, researchers have invested considerable effort in analyzing this powerful exclusion mechanism and identifying the leading players behind this phenomenon. However, the topology of Rex proteins within the cell remains unclear, particularly for RexA. While its properties suggest a cytoplasmic localization, RexB is situated in the inner membrane. Determining the precise localization of RexA is critical for understanding its interactions with RexB and other host proteins. Further studies should explore the role of the free N-terminus of RexA and the C-terminus of RexB in complex formation and activation. Fluorescent protein tagging remains a valuable approach for visualizing these proteins in vivo. However, findings from this study indicate that fusion orientation can significantly influence Rex function, with C-terminal fusion preserving activity more effectively than N-terminal fusions. The analysis of Rex-GFP constructs revealed that fusion site selection could inhibit the activity of the Rex proteins and impact their ability to inhibit T4*rII* plating. Nevertheless, C-terminal fusions were found to maintain Rex stability and functionality, making them suitable for live-cell imaging and visualizing the Rex protein interactions and locations before and after infection with T4 and T4*rII*.

To enhance visualization and detect low-abundance proteins, future work could incorporate GFP-specific antibodies in immunofluorescence assays. This would amplify the signal and improve detection sensitivity, especially in cases where direct fluorescence is weak or inconsistent. Additionally, quantification studies using flow cytometry or plate readers could further assess expression levels under varying conditions, correlating protein abundance with cellular outcomes, such as stress or cell death. Also, testing alternative fluorescent tags, such as mNeonGreen and mCherry, could enhance signal strength or compatibility with Rex proteins without compromising their stability and function. Another effective technique that may help subcellularly localize Rex proteins is the use of membrane markers

in combination with biochemical fractionation, which can distinguish membrane-associated from cytoplasmic pools (Xie, S. et al., 2020). Membrane markers are specific proteins or molecules that are known to reside in particular membrane locations, serving as a reference point to localize the protein of interest. This technique is commonly used in immunofluorescence microscopy or Western blotting following fractionation. Biochemical fractionation entails breaking open cells and separating organelles based on size, density, or other properties by using either differential centrifugation or density gradient centrifugation. Subsequently, each separated fraction would be analyzed for the presence of the protein of interest by using either Western blotting, enzyme assays, or mass spectrometry. By co-analyzing with known markers for specific compartments, like membrane-bound proteins like TolA (Germon et al., 2001), it would be possible to pinpoint where Rex proteins are enriched, offering insights into their functional roles, especially in processes like membrane depolarization or stress responses.

Additionally, immunohistochemistry using antibodies against the fluorescent tags (e.g., anti-GFP or anti-RFP) can provide more definitive localization data and allow evaluating synthesis/stability of proteins, especially when fluorescence signals are weak or ambiguous (Del Valle 2022). This technique would enable the amplification of the signal and the more precise detection of tagged proteins within the cell. It also addresses a current limitation in the study, where fluorescence was visualized but not confirmed by antibody staining. Furthermore, employing higher total magnification (e.g., 400x or higher) during imaging would improve spatial resolution and enable more accurate assessment of protein distribution across the cell population and within individual cells (Swift and Colarusso 2022).

2. Isolation and identification of Rex- and RII-mediated protein-protein interactors (see Appendix D for plasmid figures and protocol)

The identification of protein interactions between RexA and RexB, RexA/B and RII, as well as other host proteins, provides invaluable information on the molecular basis of the exclusion mechanism. Building on the success of the approaches developed in this thesis, from the insertional mutagenesis strategy to the overexpression of *rexA-rexB* in single-gene mutants, which effectively identified key genes that may be involved in Rex-mediated activity, future work should focus on dissecting these molecular interactions in greater detail. The Tandem Affinity Purification (TAP tagging) system is one of the best techniques to isolate and purify functional gene product(s)/protein(s) complexes from bacterial cells since the tag addition, to some extent, does not affect the tagged protein function, membrane protein folding, or interfere with the molecular interaction processes and analysis (Viala and Bouveret, 2017). The TAP tag consists of two IgG binding domains of *Staphylococcus aureus* protein A (ProtA) and a calmodulin binding peptide (CBP), separated by a TEV protease cleavage site (Figure Appendix D-1). ProtA binds tightly to an IgG matrix, and TEV protease is required to elute material under standard conditions. Both the N- and C-termini of the TAP tag can be used to fuse the target protein with high affinity and recover it upon purification. Proteins that co-purify with the tagged protein can be identified by mass spectrometry (Appendix D-2 and 3).

Applying TAP tagging to Rex and RII proteins, as well as other membrane-associated components, could provide critical insights into their interaction networks. The system involves the fusion of a TAP tag to the protein of interest, such as RexA, RexB, or RII protein, for instance. The tagged protein can then be introduced to act as a bait to “fish” for its partner protein(s) in the host cell. Tap-tagging Rex vectors have been constructed (Figures Appendix D-1 and D-2) and verified against T4 and T4*rII* plating. C-terminal fusion of the Tap tag cassette did not interfere with Rex activity, and the constructs

showed complete exclusion of T4*rII* on plates, similar to a *rex*$^{+}$ control. The TAP sequence was fused to the C-terminus of *rexA* and *rexB* in single and co-expression *rex* contexts, where only one *rex* gene carried the tag at a time. Thus, both proteins can be expressed, but only one serves as the "bait" at any given time. The expression of each and any fusion protein should be maintained at its wild-type level to avoid any interaction with any stressors or non-associated partners (Swaffield et al., 1996; Puig et al., 2001).

However, certain limitations must be addressed. RexB is predicted to be a membrane-bound protein and likely requires specialized fractional processing; its isolated soluble form may not form the natural interactions otherwise seen in the wild-type environment. To compensate for these potential limitations, TAP should also be applied to T4*rII*- and T4-infected cells, "triggered" for Rex, potentially permitting the capture of altered protein interactions resulting from Rex activation as well as the capture of any potential Rex-RII interactions. To further enhance the detection of native or transient interactions, a cross-linking strategy should be employed in tandem. This technique covalently stabilizes protein complexes in vivo before cell lysis, helping preserve weak or membrane-associated interactions that might otherwise be lost during purification (Tang and Bruce 2009).

Furthermore, the TAP tagging protocol was initially designed for studying yeast proteins; therefore, it requires significant optimization for application to bacterial and phage proteins. These include differences in protein expression machinery, codon usage, and the presence of membrane-bound or periplasmic proteins, which are more common in bacterial systems. Additionally, the harsh conditions often required to lyse bacterial cells can disrupt delicate protein-protein interactions, and the presence of bacterial proteases may degrade tagged proteins. Therefore, adopting TAP tagging for bacterial and phage proteins involves careful consideration of tag placement, expression conditions, and purification protocols to preserve native interactions and protein integrity (Loughran and Walls 2016).

3. Examine the parallels or analogues between Rex and components of other bacterial and mammalian viral exclusion systems

The Rex exclusion system in *E. coli,* characterized initially in bacteriophage λ, shares conceptual and functional parallels with several other bacterial and even mammalian viral defence systems. One notable example is the BREX (Bacteriophage Exclusion) system, which is a fascinating example of a similar exclusion system to Rex. BREX confers non-CRISPR-based phage resistance, where DNA modification and restriction-like mechanisms impede phage replication. Unlike CRISPR or restriction-modification systems, BREX can identify bacterial DNA by adding methyl groups to distinguish it from phage DNA. This process is powered by the encoded enzyme BrxX, which utilizes S-adenosylmethionine (SAM) as a cofactor (Li et al., 2024; Went et al., 2024). This system parallels Rex in its ability to discriminate between self and non-self genetic elements. Rex can specifically distinguish λ DNA from T4 DNA and exclusively target the superinfecting phage, thereby preventing replication of the invading phage. These systems, though mechanistically distinct, reflect and exemplify a sophisticated level of host defense strategies that operate across diverse bacterial species (Li et al., 2024; Went et al., 2024).

The Rex-like exclusion systems, PREX, are currently under investigation for their potential applications to enhance phage therapy and industrial microbiology. These systems could inform phage design for therapeutic purposes and to prevent phage contamination in fermentation processes through engineered bacterial resistance (Usman et al., 2023). RexA and RexB are believed to act as colicins and anti-colicins due to their similar responses to external stress, i.e. the manifestation of membrane depolarization leading to cell death. Specifically, RexB causes membrane depolarization in *E. coli,* potentially leading to host cell death to prevent infection by superinfecting phage; colicin E1 and K (the bacteriocin-toxic proteins) are produced by cells to kill closely related strains (de Zamaroczy and Chauleau 2011; Wong et al., 2021). The mechanism of action of both RexB and colicin E1 and K is

highly similar: membrane dysfunction, loss of ATP, and ion leakage. Both strategies highlight how phage defence and bacterial warfare can converge on similar molecular tactics.

Future applications of such exclusion systems could lead to novel anti-viral strategies, including both therapeutic and prophylactic approaches. For example, Rex could be used as a biosensor to detect phages or induce membrane stress, assisting the body in eliminating the phage without causing infection. The system can be programmed for cell death or phage resistance using engineered synthetic Rex systems in industrial strains.

Furthermore, to ensure biosafety, kill-switches or anti-toxin modules could be integrated to prevent unintended activation of the system in the absence of specific triggers. For example, synthetic kill-switches have been engineered to induce cell death in response to specific environmental cues or the absence of a tightly regulated inducer, ensuring contaminant control and biosafety. Similar to the use of a toxin-antitoxin module, where the antitoxin is only produced under controlled conditions, removal of the inducer results in toxin buildup and cell death. (Zhang et al., 2025).

Additionally, quorum sensing (QS) can be used to restrict activation to high-density cultures or specific growth phases, ensuring that the system is only triggered under appropriate physiological conditions (Naga and Shaaban 2023). In QS-based systems, bacteria produce and detect signaling molecules called autoinducers. When a threshold concentration is reached, signalling a high cell density, QS-regulated promoters can activate the expression of the desired system. This ensures the system is only active when the bacterial population is sufficiently large, reducing the risk of premature or leaky expression (Naga et al., 2024).

More research is needed on phage and bacterial defence strategies, which will be essential for translating these exclusion mechanisms in prokaryotic and eukaryotic systems into practical applications for infection prevention and treatment.

4. Evolutionary context of RexA and RexB in Anti-Phage defense systems

The Rex system, initially described in bacteriophage λ, represents one of the earliest known abortive infection (Abi) systems, functioning as a defense mechanism against superinfecting phages such as T4*rII*. Recent structural and functional studies have provided new insights into RexA and RexB, revealing that RexA is a non-specific DNA-binding protein capable of influencing the bistable switch, while RexB is a membrane-anchored ion channel that mediates membrane depolarization upon activation (Adams et al., 2024; NCBI CDD, 2023).

Modern comparative analyses suggest that Rex-like systems are not unique to λ but are present in other temperate phages, indicating a broader evolutionary distribution (Adams et al., 2024). RexA homologs occur in multiple temperate phages, and these homologs dimerize and bind DNA. For instance, homology to the recombination regulator RdgC, which undergoes a DNA-dependent conformational change (Adams et al., 2024). RexB belongs to a conserved family of inner-membrane ion channels associated with Abi systems, which are widespread among bacteria and prophages (NCBI CDD, 2023). More broadly, several studies now show that prophages are hotspots for anti-phage systems, regulatory encoding Abi-like, membrane-disrupting, or replication-blocking defenses with built-in self-immunity to avoid harming the resident prophage. This will place Rex squarely in an extensive, mobile defensive repertoire maintained by temperate phages (Owen et al., 2021; Rousset et al., 2022). However, the co-occurrence of RexA and RexB as a functional pair appears to be a hallmark of lambdoid phages, suggesting that their evolution may have been driven by selective pressures to protect lysogens from competing phages. Future genomic surveys are necessary to determine whether RexA and RexB always co-occur and to what extent they are encoded in bacterial chromosomes versus prophage genomes. For instance, a genome-miming analysis of *rexA/rexB* synteny across Enterobacteriaceae and related lambdoid should quantify co-occurrence (is RexA always paired with RexB?) and genomic context

(strictly prophage vs. host-encoded islands), leveraging the PF15968/PF15969 domain definitions as HMM seeds (NCBI CDD: RexB superfamily and RexA family annotations; Wang et al., 2023).

The “superRex” phenotypes observed in some mutants in this study may reflect an evolutionary trajectory in which Rex originally evolved to block a broader range of phages, including T4 and others, before the emergence of phage-encoded countermeasures such as RII. This dynamic exemplifies the Red Queen hypothesis, where bacteria and phages engage in a continuous arms race, each evolving new strategies to overcome the other’s defenses (Hampton et al., 2020; Brockhurst et al., 2014). Similar evolutionary conflicts have been documented for CRISPR-Cas systems, BREX, and other anti-phage mechanisms, reinforcing the notion that Rex is part of a larger network of bacterial immunity systems shaped by intense selective pressure. Critically, many prophage-encoded defenses carry self-immunity circuits to prevent auto-toxicity upon induction, a logic highly relevant to Rex regulation in λ lysogens and mirrored in other systems (e.g., Tha, BstA). These systems can trigger host cell death upon phage infection while incorporating a built-in self-immunity mechanism to prevent accidental activation during lysogeny (Owen et al., 2021; Rousset et al., 2022; Rostøl et al., 2024).

The dual role of Rex, as a prophage-encoded defense system that also safeguards the lysogen, adds an intriguing twist to this evolutionary narrative. Unlike many bacterial defense systems that primarily serve the host, Rex benefits both the prophage and the host by preventing superinfection and maintaining lysogeny. This cooperative advantage may explain the persistence of Rex-like systems in temperate phages. Future research should explore whether similar prophage-encoded systems exist in other bacterial lineages and whether Rex-like proteins have been co-opted into host genomes as part of integrated defense strategies.

Letters of Copyright Permission

Copyright permissions were obtained for the reuse of the published papers

OXFORD UNIVERSITY PRESS LICENSE
TERMS AND CONDITIONS

Nov 20, 2024

This Agreement between Hibah Yaseen Alattas ("You") and Oxford University Press ("Oxford University Press") consists of your license details and the terms and conditions provided by Oxford University Press and Copyright Clearance Center.

License Number	5913331245832
License date	Nov 20, 2024
Licensed content publisher	Oxford University Press
Licensed content publication	Genetics
Licensed content title	Identification of *Escherichia coli* Host Genes That Influence the Bacteriophage Lambda (λ) T4*rII* Exclusion (Rex) Phenotype
Licensed content author	Alattas, Hibah; Wong, Shirley
Licensed content date	Dec 1, 2020
Type of Use	Thesis/Dissertation
Institution name	
Title of your work	Advancing understanding of the bacteiophage lambda T4rII exclusion phenotype-PhD Thesis
Publisher of your work	University of Waterloo- School of pharmacy
Expected publication date	Apr 2025

Permissions cost	0.00 CAD
Value added tax	0.00 CAD
Total	0.00 CAD
Title of new work	Advancing understanding of the bacteiophage lambda T4rII exclusion phenotype-PhD Thesis
Institution name	University of Waterloo- School of pharmacy
Expected presentation date	Apr 2025
The Requesting Person / Organization to Appear on the License	Hibah Yaseen Alattas
Requestor Location	Ms. Hibah Alattas 4029-1A Victoria St S waterloo, ON n2g 1c5 Canada
Publisher Tax ID	GB125506730
Billing Type	Invoice
Billing Address	Ms. Hibah Alattas 4029-1A victoria St s waterloo, ON n2g 0c5 Canada
Total	0.00 CAD
Terms and Conditions	

SPRINGER NATURE LICENSE
TERMS AND CONDITIONS

Jun 16, 2025

This Agreement between Hibah Alattas ("You") and Springer Nature ("Springer Nature") consists of your license details and the terms and conditions provided by Springer Nature and Copyright Clearance Center.

License Number	6050801452980
License date	Jun 16, 2025
Licensed Content Publisher	Springer Nature
Licensed Content Publication	Current Genetics
Licensed Content Title	A snapshot of the λ T4rII exclusion (Rex) phenotype in Escherichia coli
Licensed Content Author	Shirley Wong et al
Licensed Content Date	Apr 20, 2021
Type of Use	Thesis/Dissertation
Requestor type	academic/university or research institute
Format	print and electronic
Portion	full article/chapter
Will you be translating?	no
Circulation/distribution	100 - 199

Author of this Springer Nature content	yes
Title of new work	Advancing understanding of the bacteiophage lambda T4rII exclusion phenotype-PhD Thesis
Institution name	University of Waterloo- School of pharmacy
Expected presentation date	Aug 2025
The Requesting Person / Organization to Appear on the License	Hibah Alattas
Requestor Location	Ms. Hibah Alattas 4029-1A Victoria st S Waterloo, ON N2G 1c5 Canada
Billing Type	Invoice
Billing Address	Ms. Hibah Alattas 4029-1A Victoria st S Waterloo, ON N2G 1c5 Canada
Total	0.00 CAD

Terms and Conditions

Springer Nature Customer Service Centre GmbH Terms and Conditions

The following terms and conditions ("Terms and Conditions") together with the terms specified in your [RightsLink] constitute the License ("License") between you as Licensee and Springer Nature Customer Service Centre GmbH as Licensor. By clicking 'accept' and completing the transaction for your use of the material ("Licensed Material"), you confirm your acceptance of and obligation to be bound by these Terms and Conditions.

1. Grant and Scope of License

SPRINGER NATURE LICENSE
TERMS AND CONDITIONS

Jun 16, 2025

This Agreement between Hibah Alattas ("You") and Springer Nature ("Springer Nature") consists of your license details and the terms and conditions provided by Springer Nature and Copyright Clearance Center.

License Number	6050850640062
License date	Jun 16, 2025
Licensed Content Publisher	Springer Nature
Licensed Content Publication	Molecular Genetics and Genomics
Licensed Content Title	Stationary phase-like properties of the bacteriophage λ Rex exclusion phenotype
Licensed Content Author	R. A. Slavcev et al
Licensed Content Date	Mar 5, 2003
Type of Use	Thesis/Dissertation
Requestor type	academic/university or research institute
Format	print and electronic
Portion	figures/tables/illustrations
Number of figures/tables/illustrations	1
Will you be translating?	no

Circulation/distribution	100 - 199
Author of this Springer Nature content	no
Title of new work	Advancing understanding of the bacteiophage lambda T4rII exclusion phenotype-PhD Thesis
Institution name	University of Waterloo- School of pharmacy
Expected presentation date	Aug 2025
Portions	Changes in cell morphology mediated by multicopy Rex plasmid. Fig. 4a p.44
The Requesting Person / Organization to Appear on the License	Hibah Alattas
Requestor Location	Ms. Hibah Alattas 4029-1A Victoria st S Waterloo, ON N2G 1c5 Canada
Billing Type	Invoice
Billing Address	Ms. Hibah Alattas 4029-1A Victoria st S Waterloo, ON N2G 1c5 Canada
Total	0.00 CAD
Terms and Conditions	

Springer Nature Customer Service Centre GmbH Terms and Conditions

References

1. Abedon, S. T., Hyman, P., Thomas, C. (2003). Experimental Examination of Bacteriophage Latent-period Evolution as a Response to Bacterial Availability. Appl. Environ. Microbiology, 69:7499-7506.
2. Adams, M.C., Schiltz. C.J., Sun. J., Hosford, C.J., Johnson, V.M, Pan, H., Borbat, P.P., Freed, J.H., Thomason, L.C., Court, C., Court, D.L., Chappie, J.S. (2024). The crystal structure of bacteriophage λ RexA provides novel insights into the DNA-binding properties of Rex-like phage exclusion proteins. *Nucleic Acids Research*, *52*(8), 4659–4675. https://doi.org/10.1093/nar/gkae212
3. Adams, J., Helling, R.B., Vargas, C.N. (1987). Evolution of *Escherichia coli* during growth in a constant environment. Genetics 116: 349–358.
4. Ades, S. E., Grigorova, I. L., Gross, C. A. (2003). Regulation of the alternative sigma factor sigma (E) during initiation, adaptation, and shutoff of the extracytoplasmic heat shock response in *Escherichia coli*. Journal of Bacteriology, 185(8), 2512–2519.
5. Agostini, F., Zagalak, J., Attig, J. (2021). Intergenic RNA Mainly Derives from Nascent Transcripts of Known Genes. Genome Biol 22, 136. https://doi.org/10.1186/s13059-021-02350-x
6. Aizenman, E., Engelberg-Kulka, H., Glaser, G. (1996). An *Escherichia coli* Chromosomal "Addiction Module" Regulated by Guanosine [penta] Tetraphosphate: A Model for Programmed Bacterial Cell Death. *PNAS*, 93(12), 6059–6063
7. Alattas, H. (2015). Isolation and Characterization of Host Mutations that Suppress the Bacteriophage Lambda (λ) Rex Phenotype (Master's thesis). Retrieved from UWSpace: https://uwspace.uwaterloo.ca/items/f1026f83-727e-49f9-b8b4-9a6f0cf37d42
8. Alattas, H., Wong, S., Slavcev, R. A. (2020). Identification of *Escherichia coli* Host Genes That Influence the Bacteriophage Lambda (λ) T4*rII* Exclusion (Rex) Phenotype. *Genetics*, *216*(4), 1087–1102. https://doi.org/10.1534/genetics.120.303643
9. Alba, B. M., Gross, C. A. (2004). Regulation of the *Escherichia coli* Sigma-Dependent Envelope Stress Response. Molecular microbiology, 52(3), 613–619. https://doi.org/10.1111/j.1365-2958.2003.03982.x

10. Altmann, T., Gennery, A. R. (2016). DNA Ligase IV Syndrome: A Review. Orphanet J Rare Dis 11, 137.
11. Ames, C.F., Ames, B.N. (1965). The multiplication of T4rll phage in *E. coli* K-12 (λ) in the presence of polyamines. Biochem. Biophys. Res. Commun. 18,639647.
12. Andersen C, Hughes C, Koronakis V. (2000). Chunnel vision. Export and efflux through bacterial channel-tunnels. EMBO Rep.1:313–8.
13. Anderson, J. (2006). Part:BBa_J61001 [R6K Origin of Replication and Tn5 Transposon System]. Registry of Standard Biological Parts, iGEM. Retrieved from https://parts.igem.org/Part:BBa_J61001
14. Apirakaramwong, A., Fukuchi, J., Kashiwagi, K., Kakinuma, Y., Ito, E., Ishihama, A., Igarashi, K. (1998). Enhancement of Cell Death Due to Decrease in Mg^{2+} Uptake by OmpC (cation-selective porin) Deficiency in Ribosome Modulation Factor-deficient Mutant. Biochem. Biophys. Res. Commun. 251, 482–487.
15. Arisaka, F. (2005). Assembly and Infection Process of Bacteriophage T4. Chaos, 15(4).
16. Asmar, A. T., Collet, J-F. (2018). Lpp, the Braun Lipoprotein, turns 50—Major Achievements and Remaining Issues, FEMS Microbiology Letters, Volume 365, Issue 18, fny199, https://doi.org/10.1093/femsle/fny199
17. Baba, T., Ara, T., Hasegawa, M., Takai, Y., Okumura, Y., Baba, M., Mori, H. (2006). Construction of *Escherichia coli* K-12 In-frame, Single-Gene Knockout Mutants: The Keio Collection. Molecular Systems Biology, 2, 2006.0008.
18. Baek, K, Svenningsen S, Eisen H, Sneppen K, Brown S. (2003). Single-cell Analysis of λ Immunity Regulation. Journal of Molecular Biology, 334: 363–372.
19. Batchelor, E., Walthers, D., Kenney, LJ, Goulian, M. (2005). The *Escherichia coli* CpxA-CpxR Envelope Stress Response System Regulates Expression of the Porins OmpF and OmpC. J Bacteriol187:.https://doi.org/10.1128/jb.187.16.5723-5731.2005
20. Battesti, A., Majdalani, N., Gottesman, S. (2011). The RpoS-Mediated General Stress Response in *Escherichia coli*. Annu Rev Microbiol. 65:189–213.
21. Battesti, A., Hoskins, J. R., Tong, S., Milanesio, P., Mann, J. M., Kravats, A., Tsegaye, Y. M., Bougdour, A., Wickner, S., Gottesman, S. (2013). "Anti-adaptors Provide Multiple Modes for Regulation of the RssB Adaptor Protein." Genes & Development, 27(24), 2722-2735.

22. Battesti, A., Majdalani, N., Gottesman, S. (2015). Stress Sigma Factor RpoS Degradation and Translation are Sensitive to the State of Central Metabolism. Proc. Natl. Acad. Sci. U.S.A. 112, 5159–5164
23. Belfort, M. (1978). Anomalous Behaviour of Bacteriophage Lambda Polypeptides in Polyacrylamide Gels: Resolution, Identification, and Control of the Lambda Rex Gene Product. J. Virology, 28, 270-278.
24. Belousov, M. V., Kosolapova, A. O., Fayoud, H., Sulatsky, M. I., Sulatskaya, A. I., Romanenko, M. N., Bobylev, A. G., Antonets, K. S., Nizhnikov, A. A. (2023). OmpC and OmpF Outer Membrane Proteins of *Escherichia coli* and *Salmonella enterica* Form Bona Fide Amyloids. International journal of molecular sciences, 24(21), 15522. https://doi.org/10.3390/ijms242115522
25. Benner-Luger, D., Boos, W. (1988). The *mglB* Sequence of *Salmonella typhimurium* LT2; Promoter Analysis by Gene Fusions and Evidence for a Divergently Oriented Gene Coding for the *mgl* Repressor. Mol. Gen. Genet. 214:579-587.
26. Benz, R. (1988). Structure and Function of Porins from Gram-negative Bacteria. Annu. Rev. Microbiology, 42:359–393.
27. Benzer, S. (1955). Fine Structure of a Genetic Region in Bacteriophage. Proceedings of the National Academy of Sciences of the United States of America, 41(6), 344–354.
28. Benzer, S. (1959). On the Topology of the Genetic Fine Structure. Proceedings of the National Academy of Sciences 45(11): 1607.
29. Benzer, S. (1962). The Fine Structure of the Gene. Scientific American 206(1): 70-84.
30. Beppu, T., Yamamoto, H., Arima, K. (1975). Inhibtory Effect of Colicin E2 on Transport Systems of *Escherichia coli* in the Presence of the *rex* Gene of Lambda Prophage. Antimicrobial agents and chemotherapy, 8(6), 617–626. https://doi.org/10.1128/AAC.8.6.617
31. Bernadac, A., Gavioli, M., Lazzaroni, J. C., Raina, S., Lloubès, R. (1998). Escherichia coli *tol-pal* Mutants Form Outer Membrane Vesicles. *Journal of bacteriology*, *180*(18), 4872–4878. https://doi.org/10.1128/JB.180.18.4872-4878.1998
32. Billen, D., Levan, A., Hsu, I., Kellogg, D. S., Benzer, B. (1961). On The Topography of The Genetic Fine Structure. In *Proc. Soc. Exp. Biol. & Med* (Vol. 47, Issue 2).
33. Biology Notes Online. (2024, March 27). Colony morphology of bacteria and examples. https://biologynotesonline.com/colony-morphology-of-bacteria-and-examples/ Biology Notes

Online. (2024, March 27). Colony morphology of bacteria and examples. https://biologynotesonline.com/colony-morphology-of-bacteria-and-examples/

34. Bolivar, F., Rodriguez, R. L., Betlach, M. C., Boyer, H. W. (1977). Construction and characterization of new cloning vehicles. I. Ampicillin-resistant derivatives of the plasmid pMB9. *Gene*, *2*(2), 75–93. https://doi.org/10.1016/0378-1119(77)90074-9
35. Boos, W., Lucht, J.M. (1996). *Escherichia coli* and *Salmonella:* Cellular and Molecular Biology, 2nd ed., ASM Press, Washington, pp. 1175–1209.
36. Boos, W., Sarvas, M. (1970). Close Linkage Between a Galactose-Binding Protein and Beta-Methylgalactoside Peramease in *E. coli*. Eur. J. Biochem. 13,526-533
37. Bordi, C., Butcher, BG., Shi, Q., Hachmann, AB., Peters, JE., Helmann, JD. (2008). In vitro Mutagenesis of Bacillus Subtilis by Using a Modified Tn7 Transposon with an Outward-Facing Inducible Promoter. Appl. Environ. Microbiol. 74:3419 –3425
38. Bouillet, S., Hamdallah, I., Majdalani, N., Tripathi, A., Gottesman, S. (2024). "A Negative Feedback Loop is Critical for Recovery of RpoS after Stress in *Escherichia coli*." *PLOS Genetics*, 20(3): e1011059https://doi.org/10.1371/journal.pgen.1011059
39. Bouveret, E., R. Derouiche, A. Rigal, R. Lloube`s, C. Lazdunski, H. Be´ne´detti. (1995). Peptidoglycan-Associated Lipoprotein-TolB Interaction. J. Biol. Chem. 270:11071–11077.
40. Breaker, RR. (2011). Prospects for Riboswitch Discovery and Analysis. Mol Cell. 43:867-79.
41. Brock, M.L. (1965). The Effects of Polyamines on the Replication of T4*rll* Mutants in *Escherichia coli K*-12(λ). Virology, 26,221-227.
42. Brockhurst, M. A., Chapman, T., King, K. C., Mank, J. E., Paterson, S. Hurst, G. D. (2014). Running with the Red Queen: The Role of Biotic Conflicts in Evolution. Proceedings. Biological sciences, 281(1797), 20141382. https://doi.org/10.1098/rspb.2014.1382
43. Bryan, D., El-Shibiny, A., Hobbs, Z., Porter, J., Kutter, E. M. (2016). Bacteriophage T4 Infection of Stationary Phase *E. coli*: Life after Log from a Phage Perspective. *Frontiers in Microbiology*, *7*, 1391. https://doi.org/10.3389/fmicb.2016.01391
44. Buller, C.S., Astrachan, L. (1968). Replication of T4*rll* Bacteriophage in *Escherichia coli* K-12(A). J. Viral. 2, 298-307.
45. Burch, L.H., Zhang, L., Chao, F.G., Xu, H., Drake, J.W. (2011). The Bacteriophage T4 Rapid-Lysis Genes and Their Mutational Proclivities. J Bacteriol 193:.
46. Carlson, K., Miller, E. S., Karam, J. D. (1994). Molecular Biology of Bacteriophage T4. American Society for Microbiology: Washington, DC.

47. Cascales, E., Bernadac, A., Gavioli, M., Lazzaroni, J-C., Lloubes, R. (2002). Pal Lipoprotein of *Escherichia coli* Plays a Major Role in Outer Membrane Integrity. J Bacteriol. February 1;184(3):754–9. https://doi.org/10.1128/JB.184.3.754-759.2002
48. Cascales, E., Gavioli, M., Sturgis, J. N., Lloubes, R. (2000). Proton Motive Force Drives the Interaction of the Inner Membrane TolA and Outer Membrane Pal Proteins in *Escherichia coli. Molecular Microbiology*, *38*(4), 904–915. https://doi.org/10.1046/j.1365-2958.2000.02190.x
49. Casjens, S. R., Hendrix, R. W. (2015). Bacteriophage lambda: An Early Pioneer and Still Relevant. Virology, 479-480, 310–330.
50. Catalão, M. J., Pimentel, M. (2018). Mycobacteriophage Lysis Enzymes: Targeting the Mycobacterial Cell Envelope. Viruses, 10(8), 428.
51. Cayley, S., Lewis, B. A., Guttman, H.J., Record, M.T. (1991). Characterization of the Cytoplasm of *Escherichia coli* K-12 as A Function of External Osmolarity. Implications for Protein-DNA Interactions in Vivo. J Mol Biol. 222:281–300. doi: 10.1016/0022-2836(91)90212-o.
52. Chatterjee, Sujoy, Eli Rothenberg. (2012). Interaction of Bacteriophage l with Its *E. coli* Receptor, LamB. Viruses 4, no. 11: 3162-3178.
53. Chen, S., Zhang, A., Blyn, L. B., Storz, G. MicC, (2004). A Second Small-RNA Regulator of Omp Protein Expression in *Escherichia coli.* J. Bacteriology, 186:6689–6697.
54. Clavel, T., Lazzaroni, J. C., Vianney, A., Portalier, R. (1996). Expression Of the TolQRA Genes of *Escherichia Coli* K-12 Is Controlled by The RcsC Sensor Protein Involved in Capsule Synthesis. Molecular microbiology, 19(1), 19–25. https://doi.org/10.1046/j.1365-2958.1996.343880.x
55. Clavel, T., Germon, P., Vianney, A., Portalier, R., Lazzaroni, J. C. (1998). TolB protein of *E. coli* K-12 Interacts with the Outer Membrane Peptidoglycan-Associated Proteins Pal, Lpp and OmpA. Mol. Microbiol. 29:359–367.
56. Colowick, M.S., Colowick, S.P. (1983). Membrane ATPase Activation on Infection of *E. coli* K(λ) Cells with Phage *rII* Mutants. Trans. N.Y. Acad. Sci. 41:35–40. https://doi.org/10.1111/j.2164-0947.1983.tb02781.x
57. Court, D.L., Oppenheim, A.B., Adhya, S.L. (2007). A New Look at Bacteriophage λ Genetic Networks. J Bacteriology, 189(2), 298–304. https://doi.org/10.1128/jb.01215-06

58. Cowan, S. W., Schirmer, T., Rummel, G., Steiert, M., Ghosh, R., Pauptit, R. a, Rosenbusch, J. P. (1992). Crystal Structures Explain the Functional Properties of Two *E. coli* Porins. Nature, 358(6389), 727–733.
59. Csiszovszki, Z., Krishna, S., Orosz, L., Adhya, S., Semsey, S. (2011). Structure and Function of the D-galactose Network in Enterobacteria. MBio. doi: 10.1128/mBio.00053-11.
60. D'Urso, G., Guyomar, C., Chat, S., Giudice, E. Gillet, R. (2023). Insights into the Ribosomal Trans-translation Rescue System: Lessons from Recent Structural Studies. The FEBS journal, 290(6), 1461–1472. https://doi.org/10.1111/febs.16349
61. Daegelen, P.,Brody, E. (1990). The *rIIA* Gene of Bacteriophage T4. II. Regulation of its Messenger RNA Synthesis. *Genetics*, *125*(2), 249–260. https://doi.org/10.1093/genetics/125.2.249
62. Dalebroux, Z.D., Swanson, M.S. (2012). ppGpp: Magic Beyond RNA Polymerase. Nat. Rev. Microbiol. 10:203–212.
63. Daley, D.O., Rapp, M., Granseth, E., Melén, K., Drew, D., von-Heijne, G. (2005). "Global Topology Analysis of the *Escherichia coli* Inner Membrane Proteome". Science (Report). 308 (5726): 1321–3.
64. Dam, S., Pagès, J.-M., Masi, M. (2018). Stress Responses, Outer Membrane Permeability Control, and Antimicrobial Resistance in Enterobacteriaceae. *Microbiology*, *164*(3), 260–267. https://doi.org/10.1099/mic.0.000613
65. Daniels, D.L., Schroeder, J.L., Szybalski, W, Sanger, F., Coulson, A.R., Hong, G.F., Hill, D.F., Peterser, G.B., Blattner, F.R. (1983). Phage Lambda's Accessory Genes, In Court, D., Oppenheim, A.B., Lambda II. Cold Spring Harbor Laboratory, Cold Spring Harbor, NY, pp. 251-277.
66. Darcan, C., Özkanca, R. (2008). OmpC-OmpF Porin Proteins Expressions of *Escherichia coli* in Nutrient Broth and the Role of EnvZ, OmpR, H-NS, AcP and RpoS on this Expression.
67. Dassa, E., Bouige, P. (2001). The ABC of ABCs: A Phylogenetic and Functional Classification of ABC Systems in Living Organisms. Res Microbiol. 152:211–229.
68. de Lorenzo, V., Herrero, M., Jakubzik, U., Timmis, K. N. (1990). Mini-Tn5 Transposon Derivatives for Insertion Mutagenesis, Promoter Probing, and Chromosomal Insertion of Cloned DNA in Gram-Negative Eubacteria. *Journal of bacteriology*, *172*(11), 6568–6572. https://doi.org/10.1128/jb.172.11.6568-6572.1990.

69. de Lorenzo, V., Timmis, K. N. (1994). Analysis and Construction of Stable Phenotypes in Gram-Negative Bacteria with Tn*5*- and Tn*10*-derived Mini-transposons. *Methods in enzymology*, *235*, 386–405. https://doi.org/10.1016/0076-6879(94)35157-0
70. Del Valle, L. (Ed.). (2022). Immunohistochemistry and Immunocytochemistry: Methods and protocols. In Methods in Molecular Biology (Vol. 2422). Springer. https://doi.org/10.1007/978-1-0716-1948-3
71. de Zamaroczy, M., Chauleau, M. (2011). Colicin killing: Foiled cell defense and hijacked cell functions. In D. Drider & S. Rebuffat (Eds.), Prokaryotic Antimicrobial Peptides: From Genes to Applications (pp. 255–276). Springer. https://doi.org/10.1007/978-1-4419-7692-5_14
72. Death, A., Ferenci, T. (1993). The Importance of the Binding- Protein-Dependent Mgl System to the Transport of Glucose in *Escherichia coli* Growing on Low Sugar Concentrations. Res Microbiol 144: 529–537.
73. Death, A., Ferenci, T. (1994). Between Feast and Famine: Endogenous Inducer Synthesis in the Adaptation of *Escherichia coli* to Growth with Limiting Carbohydrates. J Bacteriol 176: 5101–5107.
74. Dela Vega, L., Delcour, H. (1996). Polyamines Decrease *Escherichia coli* Outer Membrane Permeability. Journal of Bacteriology, 178(13), 3715–21.
75. Derouiche, R., Gavioli, M., Bénédetti, H., Prilipov, A., Lazdunski,C., Lloubès, R. (1996). TolA Central Domain Interacts with *Escherichia coli* Porins. EMBO J. 15 6408–6815.
76. Dharmalingam, K., Revel, H. R., Goldberg, E. B. (1982). Physical Mapping and Cloning of Bacteriophage T4 Anti-restriction Endonuclease Gene. J. Bacteriol. 149:694–699.
77. DiRienzo, J.M., Nakamura K., Inouye M. (1978). The Outer Membrane Proteins of Gram-negative Bacteria: Biosynthesis, Assembly, and Functions. Annu. Rev. Biochem. 47:481–532.
78. Doermann, A.H. (1948). Lysis and Lysis Inhibition with *Escherichia coli* Bacteriophage. J. Bacterial, 55, 257-275.
79. Dupont, M., James, C.E., Chevalier, J., Pagès, J.M. (2007). An Early Response to Environmental Stress Involves Regulation of OmpX and OmpF, Two Enterobacterial Outer Membrane Pore-Forming Proteins. Antimicrob Agents Chemother. 51(9):3190-8. doi: 10.1128/AAC.01481-06. Epub 2007 Jul 2 PMID: 17606680; PMCID: PMC2043185.
80. D'Accolti, M., Bellotti, D., Dzień, E., Leonetti, C., Leveraro, S., Albanese, V., Marzola, E., Guerrini, R., Caselli, E., Rowińska-Żyrek, M., Remelli, M. (2023). Impact of C and N-terminal

Protection on the Stability, Metal Chelation and Antimicrobial Properties of Calcitermin. Scientific Reports, 13, 18228.

81. Echols, H., Green, L. (1971). Establishment and Maintenance of Repression by Bacteriophage Lambda: the Role of the *cI, cII and cIII* Proteins. Proc. Natl. Acad. Sci. U.S.A. 68, 2190-2194.
82. Edgell, D.R., Gibb, E.A., Belfort, M. (2010). Mobile DNA Elements in T4 and Related Phages. Virol J 7, 290.
83. Ehrenstein, G., Lipmann, F., Maxwell, E. S., Sager, R., Weinstein, I. B., Ashkenazi, Apgar, Y., Holley, R. W., Merrill, Rendi, S. H., Ochoa, S., Benzer, S., Weisblum, D, B., Notani, G., Schwartz, J. H., Zinder, N. (1963a). Biophysical Characteristics of the RNA-Containing Bacterial Virus R17*. In *J. Biol. Chem* (Vol. 49).
84. Ehrenstein, G., Lipmann, F., Maxwell, E. S., Sager, R., Weinstein, I. B., Ashkenazi, Apgar, Y., Holley, R. W., Merrill, Rendi, S. H., Ochoa, S., Benzer, S., Weisblum, D, B., Notani, G., Schwartz, J. H., Zinder, N. (1963b). Biophysical Characteristics of the RNA-Containing Bacterial Virus R17*. In *J. Biol. Chem* (Vol. 49).
85. Eick-Helmerich, K., Braun, V. (1989). Import of Biopolymers into *Escherichia coli*: The Nucleotide Sequences of the *exbB* and *exbD* Genes are Homologous to Those of the tolQ and tolR Genes, Respectively. J. Bacteriol. 171, 5117-5126.
86. Eisenhauer, H.A., Shames, S., Pawelek, P.D., Coulton, J.W. (2005). Siderophore Transport Through *Escherichia coli* Outer Membrane Receptor FhuA with Disulphide-tethered Cork and Barrel Domains. J Biol Chem. 280:30574–80.
87. Eitinger, T., Rodionov, D.A., Grote, M., Schneider, E. (2011). Canonical and ECF-type ATP-Binding Cassette Importers in Prokaryotes: Diversity in Modular Organization and Cellular Functions. FEMS Microbiol Rev 35:3–67.
88. Elowitz, M.B., Surette, M.G., Wolf, P.E., Stock, J.B., Leibler, S. (1999). Protein Mobility in the Cytoplasm of *Escherichia coli*. J Bacteriol. 181(1):197-203. doi: 10.1128/JB.181.1.197-203.1999. PMID: 9864330; PMCID: PMC103549.
89. Engelberg-Kulka, H., Reches, M., Narasimhan, S., Schoulaker-Schwarz, R., Klemes, Y., Aizenman, E., Glaser, G. (1998). *rexB* of Bacteriophage Lambda is An Anti-cell Death Gene. Proc Natl Acad Sci USA.95:15481–15486.
90. Engelberg-Kulka, H., Glaser, G. (1999). Addiction modules and programmed cell death and anti-death in bacterial cultures. Annu. Rev. Microbiol. 53: 43–70.

91. Engelberg-Kulka, H., Kumar, S. (2015). Yet Another Way that Phage λ Manipulates Its *Escherichia coli* Host: *rexB* is Involved in the Lysogenic-Lytic Switch.
92. Ennis, H. L., Cohen, P. S. (1968). Control of phage and host ribonucleic acid synthesis in phage T4 infected *Escherichia coli. Virology*, *36*(2), 193–200. https://doi.org/10.1016/0042-6822(68)90136-0
93. Feklístov, A., Sharon, B. D., Darst, S. A., Gross, C. A. (2014). Bacterial Sigma Factors: A Historical, Structural, and Genomic Perspective. Annu. Rev. Microbiol. 68 357–376. 10.1146/annurev-micro-092412-155737.
94. Ferguson, A.D., Braun, V., Fiedler, H.P., Coulton, J.W., Diederichs, K., Welte, W. (2000). Crystal Structure of the Antibiotic Albomycin in Complex with the Outer Membrane Transporter FhuA. Protein Sci. 9:956–63.
95. Ferguson, A. D., Hofmann, E., Coulton, J. W., Diederichs, K., Welte, W. (1998). An Internal Affinity-tag for Purification and Crystallization of the Siderophore Receptor FhuA, Integral Outer Membrane Protein from *Escherichia coli* K-12 Science 282, 2215–2220.
96. Fix, D. (1993). The *rex* Genes of Lambda Prophage Modify Ultraviolet Light and N-methyl-N Nitrosourea-Induced Responses to DNA Damage in *Escherichia coli. Mutation Res.* 303,143-150.
97. Flynn, J.M., Levchenko, I., Sauer, R.T., Baker, T.A. (2004). Modulating Substrate Choice: The SspB Adaptor Delivers a Regulator of the Extracytoplasmic-Stress Response to the AAA+ Protease ClpXP for Degradation. Genes Dev.18(18):2292–2301.
98. Fralick, J., L. Burns-Keliher. (1994). Additive effect of *tolC* and *rfA* Mutations on the Hydrophobic Barrier of the Outer Membrane of Escherichia coli K-12. J. Bacteriol. 176:6404–6406.
99. Francis, M. R., Webby, M. N., Housden, N. G., Kaminska, R., Elliston, E., Chinthammit, B., Lukoyanova, N., Kleanthous, C. (2021). Porin Threading Drives Receptor Disengagement and Establishes Active Colicin Transport Through *Escherichia coli* OmpF. The EMBO Journal, 40(21), e108610. https://doi.org/10.15252/embj.2021108610
100. Fung, T.J., MacLister, L.I., Rothfield. (1978). Role of Murein Lipoprotein in Morphogenesis of the Bacterial Division Septum: Phenotype Similarity of *ikyd* and *ipo* Mutants J. Bacteriol, 133, pp. 1467-1471.

101. Gaddum, J. H., Silver, A., B Swan, A. A., Exptl Physiol, Q. J., Woolley, D. W., Shaw, E., Biol Chem, J., Benzer, B. (1947). FINE STRUCTURE OF A GENETIC REGION IN BACTERIOPHAGE. In *Abstr. XIX Intern. Physiol. Congr* (Vol. 68, Issue 2).

102. Garen, A. (1961). Physiological Effects of *rll* Mutations in Bacteriophage T4. Virology 14,151-163.

103. Gautier A. (2014). Structure Determination of α-helical Membrane Proteins by Solution-State NMR: Emphasis on Retinal Proteins. *Biochimica et biophysica acta*, *1837*(5), 578–588. https://doi.org/10.1016/j.bbabio.2013.06.009

104. Georg, J., Hess, W.R. (2011). Cis-antisense RNA: Another Level of Gene Regulation in Bacteria. Microbiol Mol Biol Rev. 75:286-300.

105. Gerace, E., Moazed, D. (2015). Affinity Purification of Protein Complexes Using TAP Tags. Methods Enzymol. 559:37–52.

106. Ghai, Ishan. (2023). A Barrier to Entry: Examining the Bacterial Outer Membrane and Antibiotic Resistance. Applied Sciences 13, no. 7: 4238.

107. Gogol, E.B., Rhodius, V.A., Papenfort, K., Vogel, J., Gross, C.A. (2011). Small RNAs Endow a Transcriptional Activator with Essential Repressor Functions for Single-Tier Control of a Global Stress Regulon *Proceedings of the National Academy of Sciences of the United States of America*, *108*(31), 12875–12880. https://doi.org/10.1073/pnas.1109379108

108. Gottesman S. (2019). Trouble is Coming: Signaling Pathways that Regulate General Stress Responses in Bacteria. The Journal of biological chemistry, 294(31), 11685–11700. https://doi.org/10.1074/jbc.REV119.005593

109. Gottesman, S., Roche, E., Zhou, Y., Sauer, R. T. (1998). The ClpXP and ClpAP Proteases Degrade Proteins with Carboxy-terminal Peptide Tails Added by the SsrA-tagging System. *Genes & development*, *12*(9), 1338–1347. https://doi.org/10.1101/gad.12.9.1338

110. Gravel, R. (1982). Genetic Heterogeneity and Complementation Analysis: General Principles and Studies in Propionic Acidemia. Academic Press:53-61. doi:10.1016/B978-0-12-751860-2.50011-5

111. Groth, A. C., Calos, M. P. (2004). Phage Integrases: Biology and Applications. Journal of molecular biology, 335(3), 667–678.

112. Guillier M, Gottesman S, Storz G. (2006). Modulating the outer membrane with small RNAs. Genes Dev. 20:2338–2348.

113. Guild, N., Gayle, M., Sweeney, R., Hollingsworth, T., Modeer, T., Gold, L. (1988). Transcriptional Activation of Bacteriophage T4 Middle Promoters by the MotA Protein. Journal of molecular biology, 199(2), 241–258. https://doi.org/10.1016/0022-2836(88)90311-7

114. Gussin, G.N., Peterson, V. (1972). Isolation and Properties of *rex*-Mutants of Bacteriophage Lambda. J. Virol, 10, 760-765.

115. Hampton, H. G., Watson, B. N. J. Fineran, P. C. (2020). The Arms Race Between Bacteria and their Phage Foes. Nature, 577(7790), 327–336. https://doi.org/10.1038/s41586-019-1894-8

116. Handler, S., Kirkpatrick, C.L. (2024). New Layers of Regulation of the General Stress Response Sigma Factor RpoS. Front. Microbiol. 15:1363955. doi: 10.3389/fmicb.2024.1363955

117. Harayarna, S., Bolfinger, I., Lino, T., Hazelbauer, C. (1983). Characterization of the *mgl* Operon of *Escherichia coli* by Transposon Mutagenesis and Molecular Cloning. J Bacteriol 153,408-41 5.

118. Hayes, S., Bull1, H. J., Tulloch, J. (1997). The Rex Phenotype of Altruistic Cell Death Following Infection of a λ Lysogen by T4*rII* Mutants Is Suppressed by Plasmids Expressing OOP RNA. In *Gene* (Vol. 189).

119. Hayes, S., Szybalski, W. (1973). Control of Short Leftward Transcripts from the Immunity and *ori* Regions in Induced Coliphage Lambda (Vol. 126).

120. Hayes, S., Slavcev, R. (2005). Polarity within pM and pE Promoted Phage Lambda *cI-rexA-rexB* Transcription and its Suppression, 49, 37–49.

121. Hazan, R., Engelberg-Kulka, H. (2004). *Escherichia coli mazEF*-Mediated Cell Death as a Defense Mechanism that Inhibits the Spread of Phage P1. Mol Genet Genomics 272, 227–234

122. Heffernan, E. J., Wu, L., Louie, J., Okamoto, S., Fierer, J., Guiney, D. G. (1994). Specificity of the Complement Resistance and Cell Association Phenotypes Encoded by the Outer Membrane Protein Genes *rck* from *Salmonella typhimurium* and *ail* from *Yersinia enterocolitica*. Infection and Immunity, 62(11), 5183–5186.

123. Heinemannt, S. F., Spiegelman, W. G. (1970). Control of Transcription of the Repressor Gene in Bacteriophage Lambda. In Proceedings of the National Academy of Sciences (Vol. 67, Issue 3).

124. Held, K.G., Postle, K. (2002). ExbB and ExbD do not Function Independently in TonB-dependent Energy Transduction. J Bacteriol184: 5170–5173.

125. Hengge-Aronis, R. (2002). Signal Transduction and Regulatory Mechanisms Involved in Control of the σ^S (RpoS) Subunit of RNA Polymerase. Microbiol Mol Biol Rev 66: 373–395.
126. Hengge-Aronis, R., Klein, W., Lange, R., Rimmele, M., Boos, W. (1991). Trehalose Synthesis Genes are Controlled by the Putative Sigma Factor Encoded by *rpoS* and are Involved in Stationary-Phase Thermotolerance in *Escherichia coli. Journal of Bacteriology*, *173*(24), 7918–7924. https://doi.org/10.1128/jb.173.24.7918-7924.1991
127. Hengge-Aronis, R., Lange, R., Henneberg, N., Fischer, D. (1993). Osmotic Regulation of *rpoS*-dependent Genes in *Escherichia coli*. *Journal of Bacteriology*, *175*(1), 259–265. https://doi.org/10.1128/jb.175.1.259-265.1993
128. Hershey, A.D. (1946). Mutation of Bacteriophage with Respect to the Type of Plaque. Genetics 31,620 640.
129. Higgins, C. F. (2001). ABC transporters: Physiology, Structure and Mechanism—An Overview. Res. Microbiol. 3:205–210.
130. Hoess, R. H., Foeller, C., Bidwell, K., Landy, A. (1980). Site-specific Recombination Functions of Bacteriophage Lambda: DNA Sequence of Regulatory Regions and Overlapping Structural Genes for Int and Xis. Proceedings of the National Academy of Sciences of the United States of America, 77(5), 2482–2486.
131. Hoffman, C. S., Wright, A. (1985). Fusions of Secreted Proteins to Alkaline Phosphatase: An Approach for Studying Protein Secretion (hybrid proteins/protein transport/signal sequence). In *Genetics* (Vol. 82).
132. Hoffmann, F., Arís, A., Carbonell, X., Rohde, M., Corchero, J. L., Rinas, U., & Villaverde, A. (1999). Heat-inactivation of plasmid-encoded CI857 repressor induces gene expression from Ind^- lambda prophage in recombinant *Escherichia coli*. FEMS Microbiology Letters, 177(2), 327–334. https://doi.org/10.1111/j.1574-6968.1999.tb13750.x
133. Hogg, R. W., Voelker, C., Von Carlowitz, I. (1991). Nucleotide Sequence and Analysis of the *mgl* Operon of *Escherichia coli* K12. Mol. Gen. Genet. 229, 453 459. https://doi.org/10.1007/BF00267469
134. Hong, H., Patel, D. R., Tamm, L. K., Van Den Berg, B. (2006). The Outer Membrane Protein OmpW Forms an Eight-Stranded Barrel with a Hydrophobic Channel. Journal of Biological Chemistry, 281(11), 7568–7577.
135. Horváth, P., Hunziker A., Tuboly C., Krishna S., Semsey S. (2010). Genetic Flexibility of Regulatory Networks. Proc. Natl. Acad. Sci. U. S. A. 107:12998–13003.

136. Hryckowian, A. J., Battesti, A., Lemke, J. J., Meyer, Z. C., Welch, R. A. (2014). "IraL Is an RssB Anti-adaptor That Stabilizes RpoS during Logarithmic Phase Growth in *Escherichia coli* and Shigella." mBio

137. Hsu, C.L., Chong, S.Y., Lin, C.Y. (2021). Histone Dynamics During DNA Replication Stress. J Biomed Sci 28, 48

138. Hua, S.S., Markovitz, A. (1975). Regulation of Galactose Operon at the *gal* Operator-Promoter Region in *Escherichia coli* K-12. J Bacteriol.122:510–517.

139. Huang, W.M. (1975). Membrane-associated Proteins of T4-infected Escherichia coli. Virology, 66, 508-521.

140. Hutchison, C. A., Smith, H. O., Pfannkoch, C., Venter, J. C. (2019). Polar Effects of Transposon Insertion into a Minimal Bacterial Genome. Journal of Bacteriology, 201(15), e00185-19. https://doi.org/10.1128/JB.00185-19

141. iGEM Team Aachen. (2019). Characterization of oriR6K (BBa_J61001) for Conjugative Plasmid Delivery. iGEM 2019 Project Wiki. Retrieved from https://2019.igem.org/Team:Aachen/part

142. Isnard, M., Rigal, A., Lazzaroni, J. C., Lazdunski, C., Lloubes, R. (1994). Maturation and Localization of the TolB Protein Required for Colicin Import. Journal of bacteriology, 176(20), 6392–6396. https://doi.org/10.1128/jb.176.20.6392-6396.1994

143. Jacob, F., Monod, J. (1961). Genetic Regulatory Mechanisms in The Synthesis of Proteins. *Journal of molecular biology*, *3*, 318–356. https://doi.org/10.1016/s0022-2836(61)80072-7

144. Jacquemin-Sablon, A., Lanni, Y.T. (1973). Lambda-repressed Mutants of Bacteriophage T5. I. Isolation and Genetical Characterization. Virology, 6,230-237.

145. Jechlinger, W., Szostak, M. P., Witte, A., Lubitz, W. (1999). Altered Temperature Induction Sensitivity of the Lambda *pR/cI857* System for Controlled Gene *E* Expression in *Escherichia coli.* FEMS microbiology letters, 173(2), 347–352.

146. Johnson, J. R., Hall, D. H. (1973). Isolation and Characterization of Mutants of Bacteriophage T4 Resistant to Folate Analogs. Virology, 53(2), 413–426. https://doi.org/10.1016/0042-6822(73)90221-3

147. Josslin, R. (1971). Physiological Studies on the *t* Gene Defect in T4-Infected *Escherichia coli*. Virology, 44, 101-107.

148. Journet, L., Bouveret, E., Rigal, A., Lloubes, R., Lazdunski, C., Bénédetti, H. (2001). Import of Colicins Across the Outer Membrane of *Escherichia Coli* Involves Multiple Protein Interactions in the Periplasm. Molecular microbiology, 42(2), 331–344. https://doi.org/10.1046/j.1365-2958.2001.02592.x

149. Jurėnas, D., Fraikin, N., Goormaghtigh, F., Van Melderen, L. (2022). Biology and Evolution of Bacterial Toxin-Antitoxin Systems. Nature Reviews. Microbiology, 20(6), 335–350. https://doi.org/10.1038/s41579-021-00661-1

150. Kabir, M. S., Yamashita, D., Koyama, S., Oshima, T., Kurokawa, K., Maeda, M., Yamada, M. (2005). Cell Lysis Directed by Sigma E in Early Stationary Phase and Effect of Induction of the *rpoE* Gene on Global Gene Expression in *Escherichia coli*. Microbiology, 151(8), 2721–2735.

151. Kai, T., Ueno, H., Otsuka, V., Morimoto, W., Vonesaki, T. (1999). Gene 61.3 of Bacteriophage T4 is the Spackle Gene. Virology, 260,254-259.

152. Kalwarczyk, T., Tabaka, M., Holyst, R. (2012). Biologistics--diffusion Coefficients for the Complete Proteome of *Escherichia coli*. Bioinformatics. Nov 15;28(22):2971-8. doi: 10.1093/bioinformatics/bts537. PMID: 22942021; PMCID: PMC3496334.

153. Karzai, A. W., Roche, E. D., Sauer, R. T. (2000). The SsrA-SmpB System for Protein Tagging, Directed Degradation and Ribosome Rescue. *Nature structural biology*, *7*(6), 449–455. https://doi.org/10.1038/75843

154. Killmann, H., Videnov, G., Jung, G., Schwarz, H., Braun, V. (1995). Identification of Receptor Binding Sites by Competitive Peptide Mapping: Phages TI, TS, and 480, and Colicin M Bind to the Gating Loop of FhuA. J Bacterid /77:694-698.

155. Kleanthous, C. (2010). Swimming Against the Tide: Progress and Challenges in Our Understanding of Colicin Translocation. Nat Rev Microbiol. 8:843–848.

156. Koebnik, R., Locher, K. P., Van Gelder, P. (2000). Structure and Function of Bacterial Outer Membrane Proteins: Barrels in a Nutshell. Mol Microbiol. 37(2):239–53.

157. Kolodkin-Gal, I., Engelberg-Kulka, H. (2006). Induction of *Escherichia coli* chromosomal *mazEF* by stressful conditions causes an irreversible loss of viability. *Journal of bacteriology*, *188*(9), 3420–3423. https://doi.org/10.1128/JB.188.9.3420-3423.2006

158. Kortmann, J., Narberhaus, F. (2012). Bacterial RNA Thermometers: Molecular Zippers and Switches. Nat Rev Microbiol. 10:255-65.

159. Kosaka, T., Murata, M. Yamada, M. (2017). Survival Strategy of *Escherichia coli* in Stationary Phase: Involvement of σ^E-Dependent Programmed Cell Death. InTech. doi: 10.5772/67672. https://www.intechopen.com/chapters/54396

160. Krinke, L., Mahoney, M., Wulff, DL. (1991). The Role of the OOP Antisense RNA in Coliphage λ Development. Mol. Microbiology, 5: 1265–1272.

161. Kutter, E., Gachechiladze, K., Poglazov, A. (1995). Evolution of T4-related Phages. Virus Genes 11, 285–297.

162. Kvitko, B. H., Bruckbauer, S., Prucha, J., McMillan, I., Breland, E. J., Lehman, S., Mladinich, K., Choi, K.-H., Karkhoff-Schweizer, R., Schweizer, H. P. (2012). A Simple Method for Construction of *pir*$^+$ Enterobacterial Hosts for Maintenance of R6K Replicon Plasmids. BMC Research Notes, 5(157). https://doi.org/10.1186/1756-0500-5-157

163. Lan, C., Igo, M.M. (1998). Differential Expression of the OmpF and OmpC Porin Proteins in *Escherichia coli* K-12 Depends upon the Level of Active OmpR. J Bacteriol180:.https://doi.org/10.1128/jb.180.1.171-174.1998

164. Landsmann, J., Kroger, M., Hobom, G. (1982). The *rex* Region of Bacteriophage Lambda: Two Genes Under Three-Way Control. Gene, 20, 11-24.

165. Lauritsen, I., Porse, A., Sommer, M.O.A. (2017). A Versatile One-Step CRISPR-Cas9-Based Approach to Plasmid-Curing. Microb Cell Fact 16, 135.

166. Lazzaroni, J. C., Dubuisson, J. F., Vianney, A. (2002). The Tol Proteins of *Escherichia coli* and Their Involvement in the Translocation of Group A Colicins. Biochimie 84, 391–397.

167. Lazzaroni, J. C., Fognini-Lefebvre, N., Portalier, R. (1986). Effects of IkyB Mutations on the Expression of *ompF, ompC* and *lamB* Porin Structural Genes in *E. coli* K-12. FEMS Microbiol. Lett. 33:235–239.

168. Lazzaroni, J.C., Germon, P., Ray, M.C., Vianney, A. (1999). The Tol proteins of *Escherichia coli* and Their Involvement in the Uptake of Biomolecules and Outer Membrane Stability, FEMS Microbiol. Lett. 177 191e197.

169. Lazzaroni, J. C., Vianney, A., Popot, J. L., Benedetti, H., Samatey, F., Lazdunski, C., Portalier, R., Geli, V. (1995). Transmembrane Alpha-helix Interactions are Required for the Functional Assembly of the *E. coli* Tol Complex. J. Mol. Biol. 246:1–7.

170. Lederberg, E.M., Lederberg, J. (1953). Genetic Studies of Lysogenicity in *Escherichia coli.* Genetics. 38(1):51-64. doi: 10.1093/genetics/38.1.51. PMID: 17247421; PMCID: PMC1209586.

171. Lee, H. J., Kim, H. J., Lee, S. J. (2022). Control of λ Lysogenic *Escherichia coli* Cells by Synthetic λ Phage Carrying *cI* Antisense. ACS synthetic biology, 11(11), 3829–3835.
172. Lee, S., Lewis, D. E. A., Adhya, S. (2018). The Developmental Switch in Bacteriophage λ: A Critical Role of the Cro Protein. Journal of molecular biology, 430(1), 58–68.
173. Lengeler, J., Hermann, KO., Unsold, HJ., Boos, W. (1971). The Regulation of the Methylgalactoside Transport System and of the Galactose-Binding Protein of *Escherichia coli* K-12. Eur J Biochem 19: 457-470
174. Levengood-Freyermuth, S.K., Click, E.M., Webster, R.E. (1993). Role of the Carboxyl-Terminal Domain of TolA in Protein Import and Integrity of the Outer Membrane. J Bacteriol. 175:222–228.
175. Li, B., Kwasniewski, M., Kirchner, J., Brockrath, R. (1992). RexAB Proteins of Bacteriophage a Enhance the Effect of Photolyase-Dimer Complexes on lacZ Gene Expression in *Escherichia coli*. Mol. Gen. Genet. 231, 480-484.
176. Li, M., Moyle, H., Susskind, M.M. (1994). Target of the Transcriptional Activation Function of Phage λ *cl* Protein. *Science* 263, 75-77.
177. Li, Q., Li, Z., Fei, X. (2022). The role of TolA, TolB, and TolR in Cell Morphology, OMVs Production, and Virulence of *Salmonella Choleraesuis*. AMB Expr 12, 5.
178. Li, S., Xu, T., Meng, X., Yan, Y., Zhou, Y., Duan, L., Tang, Y., Zhu, L., Sun, L. (2024). Ocr-mediated Suppression of BrxX Unveils a Phage Counter-defence Mechanism. *Nucleic acids research*, *52*(14), 8580–8594. https://doi.org/10.1093/nar/gkae608
179. Li, Y. (2011). The Tandem Affinity Purification Technology: An Overview. Biotechnology Letters, 33(7), 1487–1499. https://doi.org/10.1007/s10529-011-0592-x[1](https://link.springer.com/article/10.1007/s10529-011-0592-x)
180. Lill, Y., Jordan, L.D., Smallwood, C.R., Newton, S.M., Lill, M.A., Klebba, P.E. (2016). Confined Mobility of TonB and FepA in *Escherichia coli* Membranes. PLoS ONE 11(12): e0160862.
181. Lima, S., Guo, M.S., Chaba, R., Gross, C.A., Sauer, R.T. (2013). Dual Molecular Signals Mediate the Bacterial Response to Outer-Membrane Stress. Science. 340:837–841.
182. Liu, M. Y., Romeo, T., Gong, M., Brun-Zinkernagel, A. M. (1993). Identification and Molecular Characterization of *csrA*, a Pleiotropic Gene from *Escherichia coli* that Affects Glycogen Biosynthesis, Gluconeogenesis, Cell Size, and Surface Properties. J Bacteriol 175, 4744–4755.

183. Lloubes, R., Cascales, E., Walburger, A., Bouveret, E., Lazdunski, C., Bernadac, A. (2001). The Tol-Pal Proteins of the *Escherichia coli* Cell Envelope: An Energized System Required for Outer Membrane Integrity? Res. Microbiol. 152, 523–529. 10.1016/S0923-2508(01)01226-8.

184. Loughran, S. T., Walls, D. (2016). Tagging Recombinant Proteins to Enhance Solubility and Aid Purification. In Protein Chromatography (pp. 131–156). Springer. https://doi.org/10.1007/978-1-4939-6412-3_8

185. Macleod, M., Collings, A. M., Graf, C., Kiermer, V., Mellor, D., Swaminathan, S., Sweet, D., & Vinson, V. (2021). The MDAR (Materials Design Analysis Reporting) Framework for transparent reporting in the life sciences. *Proceedings of the National Academy of Sciences of the United States of America*, *118*(17), e2103238118. https://doi.org/10.1073/pnas.2103238118

186. Mattson, T., Van Houwe, G., Epstein, R. H. (1978). Isolation and Characterization of Conditional Lethal Mutations in the *mot* Gene of Bacteriophage T4. Journal of Molecular Biology, 126(3), 551–570. https://www.sciencedirect.com/science/article/abs/pii/002228367890058X

187. MDAR (Materials Design Analysis Reporting) Framework for transparent reporting in the life sciences, *Proc. Natl. Acad. Sci. U.S.A.* 118 (17) e2103238118, https://doi.org/10.1073/pnas.2103238118 (2021).

188. Maclean, D.J., Sargent, J.A., Tommerup, I.C., Ingram, D.S. (1974). Hypersensitivity as a Primary Event in Resistance to Fungal Parasites. Nature, 249, 186-187.

189. Majdalani, N., & Gottesman, S. (2005). The Rcs Phosphorelay: A Complex Signal Transduction System. Annual review of microbiology, 59, 379–405. https://doi.org/10.1146/annurev.micro.59.050405.101230

190. Martin, J., Sawyer, A. (2019). Elucidating the Structure of Membrane Proteins. BioTechniques, 66(4), 167–170. https://doi.org/10.2144/btn-2019-0030.

191. Mathelié-Guinlet, M., Asmar, A.T., Collet, J.F. (2020). Lipoprotein Lpp Regulates the Mechanical Properties of the *E. coli* Cell Envelope. Nat Commun. 14;11(1):1789. doi: 10.1038/s41467-020-15489-1. PMID: 32286264; PMCID: PMC7156740.

192. Matz, K., Schmandt, M., Gussin, G. (1982). The *rex* Gene of Bacteriophage λ is Really Two Genes. Genetics, 102, 319-327.

193. May, J.M, Sherman, D.J, Simpson, B.W., Ruiz, N., Kahne, D. (2015). Lipopolysaccharide Transport to the Cell Surface: Periplasmic Transport and Assembly into the Outer Membrane. Philos Trans R Soc Lond B Biol Sci370:20150027.

194. McCarthy, J.E.G. (1988). Expression of the *unc* Genes in *Escherichia coli*. J Bioenerg Biomembr 20, 19–39.

195. MDAR Working Group. (2020). MDAR Framework: A minimum reporting standard for life sciences. Retrieved from https://www.pnas.org/doi/abs/10.1073/pnas.2103238118?url_ver=Z39.88-2003&rfr_id=ori%3Arid%3Acrossref.org&rfr_dat=cr_pub++0pubmed

196. Mecsas, J., Rouviere, P. E., Erickson, J. W., Donohue, T. J., Gross, C. (1993). The Activity of Sigma E, an *Escherichia coli* Heat-inducible Sigma-factor, is Modulated by Expression of Outer Membrane Proteins. Genes & Development 7(12B), 2618–2628.

197. Meury J., Devilliers, G. (1999). Impairment of Cell Division in *tolA* Mutants of *Escherichia coli* at Low and High Medium Osmolarities. Biol. Cell 91: 67–75. https://doi.org/10.1111/j.1768-322X.1999.tb01085.x

198. Meyer, B.J., Maurer, R. and Ptashne, M. (1980). Gene Regulation at the Right Operator (OR) of Bacteriophage Lambda. 0R1, 0R2, and 0R3: Their Roles in Mediating the Effects of Repressor and *cro*. J. *Mol. Biology,* 139, 163-194.

199. Miller, E. S., Kutter, E., Mosig, G., Arisaka, F., Kunisawa, T., Rüger, W. (2003). Bacteriophage T4 Genome. Microbiology and Molecular Biology Reviews, 67(1), 86-156.

200. Mimura, C.S., Holbrook, S.R., Ames, G.F-L. (1991). Structural Model of the Nucleotide-Binding Conserved Component of Periplasmic Permeases. Proc Natl Acad Sci USA 88 : 84-88

201. Miroux, B., Walker, J. E. (1996). Over-production of Proteins in *Escherichia coli*: Mutant Hosts that Allow Synthesis of Some Membrane Proteins and Globular Proteins at High Levels. Journal of molecular biology, 260(3), 289–298. https://doi.org/10.1006/jmbi.1996.0399

202. Misra, R., Reeves, P. R. (1987). Role of *micF* in the *toic*-mediated Regulation of OmpF, a Major Outer Membrane Protein of *Escherichia coli* K-12. J. Bacteriol. 169:4722-4730.

203. Missiakas, D., Mayer, M.P., Lemaire, M., Georgopoulos, C., Raina, S. (1997). Modulation of the *Escherichia coli* σ^E (RpoE) Heat-shock Transcription-factor Activity by the RseA, RseB and RseC Proteins. Mol. Microbiol. 24, 355–371

204. Mitchell, A. M., Wang, W., Silhavy, T. J. (2016). “Novel RpoS-Dependent Mechanisms Strengthen the Envelope Permeability Barrier during Stationary Phase.” Journal of Bacteriology

205. Miyakoshi, M, Chao, Y, Vogel, J. (2015). Cross-talk Between ABC Transporter mRNAs Via a Target mRNA-derived Sponge of the GcvB Small RNA. EMBO J. e201490546.

206. Mosig, G., Shaw, M., Garcia, G. M. (1984). On the Role of DNA Replication, Endonuclease VII, and RII Proteins in Processing of Recombinational Intermediates in Phage T4. *Cold Spring Harbor Symposia on Quantitative Biology*, *49*, 371–382. https://doi.org/10.1101/SQB.1984.049.01.044

207. Muffler, A., Fischer, D., Altuvia, S., Storz, G., Hengge-Aronis, R. (1996). The response regulator RssB controls stability of the σ^S subunit of RNA polymerase in *Escherichia coli*. EMBO J 15:1333–1339.

208. Murata, M., Noor, R., Nagamitsu, H., Tanaka, S., Yamada, M. (2012). Novel Pathway Directed by Sigma E to Cause Cell Lysis in *Escherichia coli*. Genes to Cells, 17(3), 234–247.

209. Müller, C., Crowe-McAuliffe, C. Wilson, D. N. (2021). Ribosome Rescue Pathways in Bacteria. Frontiers in microbiology, 12, 652980. https://doi.org/10.3389/fmicb.2021.652980

210. Naga, N. G., Shaaban, M. I. (2023). Quorum Sensing and Quorum Sensing Inhibitors of Natural Origin. In Drug Discovery and Design Using Natural Products (pp. 395–416). Springer. https://doi.org/10.1007/978-3-031-35205-8_13

211. Naga, N. G., Shaaban, M. I., El-Metwally, M. M. (2024). An Insight on the Powerful of Bacterial Quorum Sensing Inhibition. European Journal of Clinical Microbiology & Infectious Diseases, 43, 2071–2081. https://doi.org/10.1007/s10096-024-04920-w[1](https://link.springer.com/article/10.1007/s10096-024-04920-w)

212. Nagamitsu, H., Murata, M., Kosaka, T., Kawaguchi, J., Mori, H. Yamada, M. (2013). Crucial Roles of MicA and RybB as Vital Factors for σ-dependent Cell Lysis in *Escherichia coli* Long-term Stationary Phase. Journal of molecular microbiology and biotechnology, 23(3), 227–232. https://doi.org/10.1159/000350370

213. NCBI CDD: RexB Superfamily (PF15968/cl24515) and RexA (PF15969) Family Annotations (2023). https://www.ncbi.nlm.nih.gov/Structure/cdd/cl24515

214. Nichols, BP., Shafiq, O., Meiners, V. (1998). Sequence Analysis of Tn10 Insertion Sites in a Collection of *Escherichia coli* Strains Used for Genetic Mapping and Strain Construction. J Bacteriol,180(23):6408–11.

215. Nie, D., Hu, Y., Chen, Z. (2020). Outer Membrane Protein A (OmpA) as a Potential Therapeutic Target for Acinetobacter Baumannii Infection. J Biomed Sci 27, 26.

216. Nikaido, H. (2003). Molecular Basis of Bacterial Outer Membrane Permeability Revisited. Microbiol Mol Biol; 67(4): 593-656. doi: 10.1128/MMBR.67.4.593-656.2003. PMID: 14665678; PMCID: PMC309051.

217. Noinaj, N., Guillier, M., Barnard, T.J., Buchanan, S.K. (2010). TonB-dependent Transporters: Regulation, Structure, and Function. Annu Rev Microbiol. 64:43±60.

218. Noor, R. (2015). Mechanism to Control the Cell Lysis and the Cell Survival Strategy in Stationary Phase Under Heat Stress. SpringerPlus 4, 599.

219. Notley-McRobb, L., Ferenci, T. (1999). Adaptive mgl-regulatory Mutations and Genetic Diversity Evolving in Glucose-limited *Escherichia coli* Populations. Environ Microbiol. 1: 33–43.

220. Notley-McRobb, L., Ferenci, T. (1999). The Generation of Multiple Coexisting *mal*-regulatory Mutations Through Polygenic Evolution in Glucose-limited Populations of *Escherichia coli*. Environ Microbiol. 1: 45–52.

221. Ochman, H., Medhora, M. M., Garza, D., Hartl, D. L. (1990). Amplification of Flanking Sequences by Inverse PCR, p. 219–227. In M. A. Innis, D. H. Gelfand, J. J. Sninsky, and T. J. White. (ed.), PCR protocols: a Guide to Methods and Applications. Academic Press, San Diego, Calif.

222. Ordal, G. W., Adler, J. (1974). Properties Of Mutants in Galactose Taxis and Transport. *Journal of bacteriology*, *117*(2), 517–526. https://doi.org/10.1128/jb.117.2.517-526.1974

223. Oppenheim, A. B., Kobiler, O., Stavans, J., Court, D. L., Adhya, S. (2005). Switches in Bacteriophage Lambda Development. Annual Review of Genetics, 39, 409–429. DOI: 10.1146/annurev.genet.39.073003.113656

224. Otto, K., Hermansson, M. (2004). Inactivation of *ompX* Causes Increased Interactions of Type 1 Fimbriated *Escherichia coli* with Abiotic Surfaces. Journal of Bacteriology, 186(1), 226–234.

225. Owen, S. V., Wenner, N., Dulberger, C. L., Rodwell, E. V., Bowers-Barnard, A., Quinones-Olvera, N., Rigden, D. J., Rubin, E. J., Garner, E. C., Baym, M. Hinton, J. C. D. (2021). Prophages Encode Phage-defense Systems with Cognate Self-immunity. Cell host & microbe, 29(11), 1620–1633.e8. https://doi.org/10.1016/j.chom.2021.09.002

226. Ozawa, Y., Mizushima, S. (1983). Regulation of Outer Membrane Porin Protein Synthesis in *Escherichia coli* K-12: *ompF* Regulates the Expression of *ompC*. *Journal of Bacteriology*, *154*(2), 669–675. https://doi.org/10.1038/s41579-019-0199-0

227. Ozols, J. (1990). Amino Acid Analysis. In: Deutscher MP, editor. Methods in enzymology. New York: Academic Press; pp. 587–601.

228. Paddison, P., Abedon, S. T., Dressman, H. K., Gailbreath, K., Tracy, J., Mosser, E., Neitzel, J., Guttman, B., Kutter, E. (1998a). The Roles of the Bacteriophage T4 *r* Genes in Lysis Inhibition and Fine-Structure Genetics: A New Perspective. *Genetics*, *148*(4), 1539–1550. https://doi.org/10.1093/genetics/148.4.1539

229. Paddison, P., Abedon, S. T., Dressman, H. K., Gailbreath, K., Tracy, J., Mosser, E., Neitzel, J., Guttman, B., Kutter, E. (1998b). The Roles of the Bacteriophage T4 *r* Genes in Lysis Inhibition and Fine-Structure Genetics: A New Perspective. https://academic.oup.com/genetics/article/148/4/1539/6034650

230. Parma, D.H., Snyder, M., Sobolevski, S., Nawrox, M., Brody, E., Gold, L. (1992). The Rex System of Bacteriophage λ: Tolerance and Altruistic Cell Death. Genes Development, 6,497-510.

231. Pande, S., Makela, A., Dove, S.L., Nickels, S.L., Hochschild, A., Hinton, D.M. (2002). The Bacteriophage T4 Transcription Activator MotA Interacts with the Far-C-Terminal Region of the σ70 Subunit of *Escherichia coli* RNA Polymerase. J Bacteriol 184:.

232. Pao, C.C., Speyer, J.F. (1975). Mutants of T7 Bacteriophage Inhibited by Lambda Prophage. Proc. Natl. Aca. Sci. U.S.A. 72, 3642-3646.

233. Patten, C. L., Kirchhof, M. G., Schertzberg, M. R., Morton, R. A., Schellhorn, H. E. (2004). Microarray Analysis of RpoS-mediated Gene Expression in *Escherichia coli* K-12. Mol. Genet. Genomics272, 580–591.

234. Peters, J. E., Craig, N. L. (2001). Tn7 Recognizes Target Structures Associated with DNA Replication Using the DNA-binding Protein TnsE. Genes & Dev 15, 737-747.

235. Pilsl, H., Smajs, D., Braun, V. (1999). Characterization of Colicin S4 and its Receptor, OmpW, a Minor Protein of the *Escherichia coli* Outer Membrane. J. Bacteriol. 181, 3578–3581.

236. Pratt, L.A., Silhavy, T.J. (1996). The Response Regulator SprE Controls the Stability of RpoS. Proc Natl Acad Sci USA. 93:2488–2492

237. Ptashne, M. (1986). "A Genetic Switch. Gene Control and Phage lambda".

238. Ptashne M. (1986). Gene Regulation by Proteins Acting Nearby and At a Distance. Nature, 322(6081), 697–701. https://doi.org/10.1038/322697a0

239. Ptashne, M. (2004). Genetic Switch: Phage Lambda Revisited, 2nd ed. Cold Spring Harbor Laboratory Press, Cold Spring Harbor, NY.

240. Ptashne, M. (2006). Lambda's Switch: Lessons From a Module Swap. Curr. Biol.16:R459–R462.

241. Puig, O., Caspary, F., Rigaut, G., Rutz, B., Bouveret, E., Bragado-Nilsson, E. (2001). The Tandem Affinity Purification (TAP) Method: A General Procedure of Protein Complex Purification. Methods 24, 218–229. 10.1006/meth.2001.1183

242. Qi, D., Alawneh, A. M., Yonesaki, T., Otsuka, Y. (2015). Rapid Degradation of Host mRNAs by Stimulation of RNase E Activity by Srd of Bacteriophage T4. Genetics 201: 977–987. https://doi.org/10.1534/genetics.115.180364

243. Qiu, S., Wan, X., Liang, Y., Lamoureux, C.R., Akbari, A., Palsson, B.O. (2024). Inferred Regulons are Consistent with Regulator Binding Sequences in *E. coli*. PLoS Comput Biol 20(1): e1011824.

244. Queen, C., Rosenberg, M. (1981). A Promoter of pBR322 Activated by cAMP Receptor Protein. Nucleic Acids Res.9, 3365–3377.

245. Ramanculov, E., Young, R. (2001). An Ancient Player Unmasked: T4 *rI* Encodes a t-Specific Antiholin. Mol. Microbiol. 41:575–783.887.

246. Ramanculov, E., Young, R. (2001). Functional Analysis of the Phage T4 Holin in a Context. Mol. Genet. Genomics 265:345–353.888.

247. Ramanculov, E., Young, R. (2001). Genetic Analysis of the T4 Holin: Timing and Topology. Gene 265:25–36.

248. Randall Hazelbauer, L., Schwartz, M. (1973). Isolation of the Bacteriophage Lambda Receptor from *Escherichia coli*. *Journal of Bacteriology*, *116*(3), 1436–1446.

249. Rangarajan, A.A. (2022). Regulation of Gene Expression in Eukaryotes. In: Kar, D., Sarkar, S. (eds) Genetics Fundamentals Notes. Springer, Singapore.

250. Ranquet, C., Gottesman, S. (2007). Translational Regulation of the *Escherichia coli* Stress Factor RpoS: A Role for SsrA and Lon. J Bacteriol. Jul;189(13):4872-9. doi: 10.1128/JB.01838-06. Epub 2007 Apr 20. PMID: 17449615; PMCID: PMC1913435.

251. Rasmussen, A.A., Eriksen, M., Gilany, K., Udesen, C., Franch, T., Petersen, C., Valentin-Hansen, P. (2005), Regulation of *ompA* mRNA Stability: The Role of a Small Regulatory RNA in Growth Phase-dependent Control. Mol. Microbiology, 58:1421–1429

252. Restrepo-Pineda, S., O Pérez, N., Valdez-Cruz, N. A., Trujillo-Roldán, M. A. (2021). Thermoinducible Expression System for Producing Recombinant Proteins in *Escherichia coli*: Advances and Insights. *FEMS microbiology reviews*, *45*(6), fuab023. https://doi.org/10.1093/femsre/fuab023

253. Rhodius, V.A., Suh, W.C., Nonaka, G., West, J., Gross, C.A. (2006). Conserved and Variable Functions of the σ^E Stress Response in Related Genomes. PLoS Biol. 4, e2 10.1371/journal.pbio.0040002

254. Ried, G., Henning, U. (1987). A Unique Amino Acid Substitution in the Outer Membrane Protein OmpA Causes Conjugation Deficiency in *Escherichia coli* K-12. FEBS Letters, 223(2), 387–390.

255. Riley, L. A., Payne, I. C., Tumen-Velasquez, M., Guss, A. M. (2023). Simple and rapid site-specific integration of multiple heterologous DNAs into the *Escherichia coli* chromosome. Journal of Bacteriology, 205(2), e00338-22. https://doi.org/10.1128/jb.00338-22

256. Riley, M., Abe, T., Arnaud, M.B., Berlyn, M.K,, Blattner, F.R., Chaudhuri, R.R., Glasner, J.D., Horiuchi, T., Keseler, I.M,, Kosuge, T., Mori, H., Perna, N.T., Plunkett, G 3rd., Rudd, K.E., Serres, M.H., Thomas, G.H., Thomson, N.R., Wishart, D., Wanner, B.L. (2005). *Escherichia coli* K-12: a Cooperatively Developed Annotation Snapshot. Nucleic Acids Res; 34(1):1-9. doi: 10.1093/nar/gkj405. PMID: 16397293; PMCID: PMC1325200.

257. Rizzolo, K., Yu, A. Y. H., Ologbenla, A., Kim, S. R., Zhu, H., Ishimori, K., Thibault, G., Leung, E., Zhang, Y. W., Teng, M., Haniszewski, M., Miah, N., Phanse, S., Minic, Z., Lee, S., Caballero, J. D., Babu, M., Tsai, F. T. F., Saio, T., Houry, W. A. (2021). Functional Cooperativity Between the Trigger Factor Chaperone and The ClpXP Proteolytic Complex. Nature communications, 12(1), 281. https://doi.org/10.1038/s41467-020-20553-x.

258. Rodriguez-Aliaga, P., Ramirez, L., Kim, F., Bustamante, C., Martin, A. (2023). Substrate-translocating loops regulate mechanochemical coupling and power production in AAA+ protease ClpXP. *Nature Structural & Molecular Biology*. Retrieved from https://www.nature.com/articles/nsmb.3298.pdf

259. Rolfe, B. G., Campbell, J. H. (1977). Genetic and Physiological Control of Host Cell Lysis by Bacteriophage Lambda. *Journal of Virology*, *23*(3), 626–636.

http://www.pubmedcentral.nih.gov/articlerender.fcgi?artid=515874&tool=pmcentrez&rendertype=abstract

260. Rostøl, J. T., Quiles-Puchalt, N., Iturbe-Sanz, P., Lasa, Í. Penadés, J. R. (2024). Bacteriophages Avoid Autoimmunity from Cognate Immune Systems as an Intrinsic Part of their Life Cycles. Nature microbiology, 9(5), 1312–1324. https://doi.org/10.1038/s41564-024-01661-6

261. Rossi, R., Montecucco, A., Ciarrocchi, G., Biamonti, G. (1997). Functional Characterization of the T4 DNA Ligase: A New Insight into the Mechanism of Action. *Nucleic acids research*, *25*(11), 2106–2113. https://doi.org/10.1093/nar/25.11.2106

262. Rotman, B., Guzman R. (1982). Identification of the *rnglA* Gene Product in the Beta Methylgalactoside Transport System of *Escherichia coli* Using Plasmid DNA Deletions Generated in Vitro. J Biol Chem 257: 9030-9034

263. Ruiz, N., Kahne, D., Silhavy, T.J. (2009). Transport of Lipopolysaccharide Across the Cell Envelope: The Long Road of Discovery. Nat. Rev. Microbiol. 7:677–683.

264. Rousset, F., Depardieu, F., Miele, S., Dowding, J., Laval, A. L., Lieberman, E., Garry, D., Rocha, E. P. C., Bernheim, A. Bikard, D. (2022). Phages and their Satellites Encode Hotspots of Antiviral Systems. Cell host & microbe, 30(5), 740–753.e5. https://doi.org/10.1016/j.chom.2022.02.018

265. Ruiz, N., Peterson, C. N., Silhavy, T. J. (2001). RpoS-dependent Transcriptional Control of *sprE*: Regulatory Feedback Loop. J. Bacteriol. 183, 5974–5981

266. Ruiz-Orera, J., Hernandez-Rodriguez, J., Chiva, C., Sabidó, E., Kondova, I., Bontrop, R., Marqués-Bonet, T., Albà, M.M. (2015). Origins of de novo Genes in Human and Chimpanzee. PLoS Genet. 11: e1005721.

267. Saberi, F., Kamali, M., Najafi, A. (2016). Natural Antisense RNAs as mRNA Regulatory Elements in Bacteria: A Review on Function and Applications. Cell Mol Biol Lett 21, 6. https://doi.org/10.1186/s11658-016-0007-z

268. San Millan, J. L., Boyd, D., Dalbey, R., Wickner, W., Beckwith, J. (1989). Use of phoA Fusions to Study the Topology of the *Escherichia coli* Inner Membrane Protein Leader Peptidase. J. Bacteriol. 171, 5536–5541.

269. Sauerbier, W., Puck, S. M., Brautigam, A. R., Hirsch-Kauffmann2, M. (1969). Control of Gene Function in Bacteriophage T4 I. Ribonucleic Acid and Deoxyribonucleic Acid Metabolism in T4*rII*-Infected Lambda-Lysogenic Hosts. In *JOURNAL OF VIROLOGY* (Vol. 4, Issue 5).

270. Saurin, W., Hofnung, M., Dassa, E., (1999). Getting in or out: Early Segregation Between Importers and Exporters in the Evolution of ATP-binding Cassette (ABC) Transporters, J. Mol. Evol. 48 ;22–41.

271. Sawitzke, J. A, Thomason, L. C., Costantino, N., Bubunenko, M., Datta, S., Court, D. L. (2007). Recombineering: In vivo Genetic Engineering in *E. coli*, S. enterica, and Beyond. *Methods in Enzymology*, *421*(06), 171–199. https://doi.org/10.1016/S0076-6879(06)21015-2

272. Schnaitman, C. A., McDonald, G. A. (1984). Regulation of Outer Membrane Protein Synthesis in *Escherichia coli* K-12: Deletion of *ompC* Affects Expression of the OmpF Protein. Journal of Bacteriology, 159(2), 555–563. https://doi.org/10.1128/jb.159.2.555-563.1984

273. Schweder, T., Lee, K. H., Lomovskaya, O., Matin, A. (1996). Regulation of *Escherichia coli* Starvation Sigma Factor (sigma s) by ClpXP Protease. *Journal of Bacteriology*, *178*(2), 470–476. https://doi.org/10.1128/jb.178.2.470-476.

274. Schoulaker-Schwarz, R., Dekel-Gorodetsky, L., Engelberg-Kulka, H. (1991). Proc Natl Acad Sci USA88:4996–5000.

275. Schoulaker-Schwarz, R., Aloni, Y., Friedberg, D. (1991). An Additional Function for Bacteriophage Lambda Rex: The *rexB* Product Prevents Degradation of the Lambda O Protein. Proceedings of the National Academy of Sciences, 88(11), 4996-5000.

276. Schwartz, M., Roa, M., Débarbouillé, M. (1981). Mutations That Affect *lamB* Gene Expression at a Posttranscriptional Level. Proceedings of the National Academy of Sciences of the United States of America, 78(5), 2937–2941. http://www.jstor.org/stable/10735

277. Schönheit, P., Buckel, W., Martin, W.F. (2016). On the Origin of Heterotrophy. Trends Microbiol. (1):12-25. doi: 10.1016/j.tim.2015.10.003. p.14.

278. Sekiguchi, M. (1966). Studies on the Physiological Defect in *rll* Mutants of Bacteriophage T4. J. Mol. Biology, 16, 503-522.

279. Shao, B., Rammohan, J., Anderson, D. A., Alperovich, N., Ross, D., Voigt, C. A. (2021). Single-cell Measurement of Plasmid Copy Number and Promoter Activity. *Nature Communications*, *12*(1). https://doi.org/10.1038/s41467-021-21734-y

280. Shinedling, S., Parma, D., Gold, L. (1987). Wild-type Bacteriophage T4 is Restricted by the Lambda *rex* Genes. *J. Virol.*, *61*(12), 3790–3794. http://jvi.asm.org/cgi/content/long/61/12/3790.

281. Slavcev, R., Funnell, B. E. (2005). Identification and Characterization of a Novel Allele of Escherichia coli *dnaB* Helicase That Compromises the Stability of Plasmid P1, 187(4), 1227–1237.

282. Slavcev, R., Hayes, S. (2003). Blocking the T4 Lysis Inhibition Phenotype. Gene, 321, 163–171.

283. Slavcev, R., Bull, H. J., Hayes, S. (2003). Bacteriophage λ Repressor Allelic Modulation of the Rex Exclusion Phenotype, 229(1975), 225–229.

284. Slavcev, R., Hayes, S. (2002). Rex-Centric Mutualism. J Bacteriology, 184, 857858.

285. Slavcev, R., Hayes, S. (2003). Stationary phase-like Properties of the Bacteriophage Lambda Rex Exclusion Phenotype. Molecular genetics and genomics: MGG, 269(1), 40–8.

286. Slavcev, R., Hayes, S. (2004). Over-expression of *rexA* Nullifies T4*rII* Exclusion in Escherichia coli K(λ) Lysogens. *Canadian Journal of Microbiology*, *50*(2), 133–136. https://doi.org/10.1139/w03-115.

287. Smith, S. C., Joshi, K. K., Zika, J. J., Trinh, K., Kamajaya, A., Chien, P., Ryan, K. R. (2014). "Cell Cycle-dependent Adaptor Complex for ClpXP-mediated Proteolysis Directly Integrates Phosphorylation and Second Messenger Signals." PNAS, 111(36), 13335-13340.

288. Snyder, L., McWilliams, K. (1989). The *Rex* Genes of Bacteriophage Lambda Can Inhibit Cell Function without Phage Superinfection. Gene, 81, 17-24.

289. Sommer, R. J. (2020). Phenotypic Plasticity: From Theory and Genetics to Current and Future Challenges. *Genetics*, *215*(1), 1–13. https://doi.org/10.1534/genetics.120.303163

290. Sørensen, H. P., Mortensen, K. K. (2005). Soluble Expression of Recombinant Proteins in the Cytoplasm of *Escherichia coli*. Microbial Cell Factories, 4(1), 1. https://doi.org/10.1186/1475-2859-4-1

291. Srividhya, K. V., Krishnaswamy, S. (2004). A Simulation Model of *Escherichia coli* Osmoregulatory Switch Using E-CELL System. BMC Microbiology, 4, 44.

292. Sueki AStein, F., Savitski, M.M., Selkrig, J., Typas, A. (2020). Systematic Localization of *Escherichia coli* Membrane Proteins. mSystems5:10.1128/msystems.00808-19. https://doi.org/10.1128/msystems.00808-19

293. Sugawaras, E., Nikaido, H. (1992). Pore-forming Activity of OmpA Protein of *Escherichia coli.* J Biol Chem. 267:2507–2511.

294. Suh, S.J., Silo-Suh, L., Woods, D.E., Hassett, D.J., West, S.E., Ohman, D.E. (1999). Effect of *rpoS* Mutation on the Stress Response and Expression of Virulence Factors in Pseudomonas Aeruginosa. J Bacteriol 181:3890–3897.

295. Sun, D., Wang, B., Zhu, L., Chen, M., Zhan, L. (2013). Block and Boost DNA Transfer: Opposite Roles of OmpA in Natural and Artificial Transformation of *Escherichia coli.* PLoS One 8: e59019.

296. Suzuki, T., Ueguchi, C., Mizuno, T. (1996). "H-NS Regulates OmpF Expression Through *micF* Antisense RNA in *Escherichia coli."* Journal of Bacteriology, 178(12), 3650-3653.

297. Swaffield, J. C., Melcher, K., Johnston, S. A. (1996). Correction: A highly Conserved ATPase Protein as a Mediator Between Acidic Activation Domains and the TATA-binding Protein. Nature, 379(6566), 658

298. Swift, L. H., Colarusso, P. (2022). Fluorescence microscopy: A field guide for biologists. In Methods in Molecular Biology (Vol. 2440). Springer. https://doi.org/10.1007/978-1-0716-2051-9_1

299. Szczepaniak, J., Press, C., Kleanthous, C. (2020). The Multifarious Roles of Tol-Pal in Gram-Negative Bacteria. FEMS microbiology reviews, 44(4), 490–506. https://doi.org/10.1093/femsre/fuaa018

300. Takacs, B.J., Rosenbusch, J.P. (1975). Modification of *Escherichia coli* Membranes in the Pre-Replicative Phase of T4 Infection. Specificity of Association and Quantification of Bound Phage Proteins. J. BioI. Chern. 250, 2339-2350.

301. Tang, X., Bruce, J. E. (2009). Chemical Cross-linking for Protein–Protein Interaction Studies. In Mass Spectrometry of Proteins and Peptides (pp. 283–293). Humana Press. https://doi.org/10.1007/978-1-59745-493-3_17

302. Thomason, L. C., Court, D. L. (2022). Study of Ren, RexA, and RexB Functions Provides Insight into the Complex Interaction Between Bacteriophage λ and Its Host, *Escherichia coli*. *PHAGE (New Rochelle, N.Y.)*, *3*(3), 153–164. https://doi.org/10.1089/phage.2022.0020

303. Thomason, L. C., Schiltz, C. J., Court, C., Hosford, C. J., Adams, M. C., Chappie, J. S., Court, D. L. (2021). Bacteriophage λ RexA and RexB Functions Assist the Transition from Lysogeny to Lytic Growth. *Molecular Microbiology*, *116*(4), 1044–1063. https://doi.org/10.1111/mmi.14792.

304. Tomoyuki, K., Masayuki, M., Mamoru, Y. (2017). Survival Strategy of *Escherichia coli* in Stationary Phase: Involvement of σ^E-Dependent Programmed Cell Death, *Escherichia col*i -

Recent Advances on Physiology, Pathogenesis and Biotechnological Applications, Dr. Amidou Samie (Ed.), InTech, DOI: 10.5772/67672.

305. Toothman, P., Herskowitz, I. (1980b). Rex-dependent Exclusion of Lambdoid Phages II. Determinants of Sensitivity to Exclusion. Virology, 102, 147-160.
306. Toyofuku, M., Schild, S., Kaparakis-Liaskos, M., Eberl, L. (2023). Composition and functions of bacterial membrane vesicles. *Nature Reviews Microbiology*. https://doi.org/10.1038/s41579-023-00875-5
307. Trevors, J.T. (1986). Plasmid Curing in Bacteria, FEMS Microbiology Reviews, Volume 1, Issue 3-4., Pages 149–157.
308. Udekwu, K. I., Darfeuille, F., Vogel, J., Reimegård, J., Holmqvist, E., Wagner, E. G. H. (2005). "Hfq-dependent Regulation of OmpA Synthesis is Mediated by an Antisense RNA." Genes & Development, 19(19), 2355-2366.
309. Urtecho, G., Insigne, K. D., Tripp, A. D., Brinck, M. S., Lubock, N. B., Acree, C., Kim, H., C. T., Kosuri, S. (2023). Genome-wide Functional Characterization of *Escherichia coli* Promoters and Sequence Elements Encoding Their Regulation. eLife 12:RP92558 https://doi.org/10.7554/eLife.92558.1
310. Usman, S. S., Uba, A. I., Christina, E. (2023). Bacteriophage Genome Engineering for Phage Therapy to Combat Bacterial Antimicrobial Resistance as an Alternative to Antibiotics. *Molecular biology reports*, *50*(8), 7055–7067. https://doi.org/10.1007/s11033-023-08557-4
311. Valentin-Hansen, P., Johansen, J., Rasmussen, A. a. (2007). Small RNAs Controlling Outer Membrane Porins. Current Opinion in Microbiology, 10(2), 152–155.
312. Valdez-Cruz, N., Caspeta, L., Pérez, N. O., Ramírez, O. T., & Trujillo-Roldán, M. A. (2010). Production of recombinant proteins in *E. coli* by the heat inducible expression system based on the phage lambda *pL* and/or *pR* promoters. Microbial Cell Factories, 9, 18. https://doi.org/10.1186/1475-2859-9-18
313. Van Duyne, G. D., Landy, A. (2024). Bacteriophage Lambda Site-specific Recombination. In *Molecular Microbiology* (Vol. 121, Issue 5, pp. 895–911). John Wiley and Sons Inc. https://doi.org/10.1111/mmi.15241
314. Viala, J. P. M., Bouveret, E. (2017). Protein-Protein Interaction: Tandem Affinity Purification in Bacteria. *Methods in molecular biology (Clifton, N.J.)*, *1615*, 221–232. https://doi.org/10.1007/978-1-4939-7033-9_18

315. Vinson, H. M., Gautam, A., Olet, S., Gibbs, P. S., Barigye, R. (2010). Molecular Analysis of Porin Gene Transcription in Heterogenotypic Multidrug-Resistant *Escherichia coli* Isolates from Scouring Calves. *The Journal of antimicrobial chemotherapy*, *65*(9), 1926–1935. https://doi.org/10.1093/jac/dkq246

316. Vogt, J., Schulz, G. E. (1999). The Structure of the Outer Membrane Protein OmpX from *Escherichia coli* Reveals Possible Mechanisms of Virulence. Structure, 7(10), 1301–1309.

317. Von Heijne, G. (1986). The Distribution of Positively Charged Residues in Bacterial Inner Membrane Proteins Correlates with the Transmembrane Topology. EMBO J. 5, 30213027.

318. Vytvytska, O., Jakobsen, J. S., Balcunaite, G., Andersen, J. S., Baccarini, M., von Gabain, A. (1998). "Host Factor I, Hfq, Binds to *Escherichia coli ompA* mRNA in a Growth Rate-dependent Fashion and Regulates its Stability." PNAS, 95(24), 14118-14123.

319. Wang, A., Lin, K. (2001). Effects of N-Acetylglucosamine and α-Methylglucoside on Bacteriophage T4 Adsorption to *Escherichia coli* B23, 1(December), 54–63.

320. Wang, J., Chitsaz, F., Derbyshire, M. K., Gonzales, N. R., Gwadz, M., Lu, S., Marchler, G. H., Song, J. S., Thanki, N., Yamashita, R. A., Yang, M., Zhang, D., Zheng, C., Lanczycki, C. J. Marchler-Bauer, A. (2023). The Conserved Domain Database in 2023. Nucleic acids research, 51(D1), D384–D388. https://doi.org/10.1093/nar/gkac1096

321. Wang, Y. (2002). The function of OmpA in *Escherichia coli*. Biochemical and Biophysical Research Communications, 292(2), 396–401.

322. Washizaki A., Yonesaki, T., Otsuka, Y. (2016) Characterization of the Interactions Between *Escherichia coli* Receptors, LPS and OmpC, and Bacteriophage T4 Long Tail Fibers. Microbiologyopen 5: 1003–1015.

323. Weber, H., Polen, T., Heuveling, J., Wendisch, V. F., Hengge, R. (2005). Genome-wide Analysis of the General Stress Response Network in *Escherichia coli*: σ^S-dependent Genes, Promoters, and Sigma Factor Selectivity. J. Bacteriol. 187, 1591–1603

324. Wagner, S., Klepsch, M. M., Schlegel, S., Appel, A., Draheim, R., Tarry, M., Högbom, M., van Wijk, K. J., Slotboom, D. J., Persson, J. O., de Gier, J. W. (2008). Tuning *Escherichia coli* for Membrane Protein Overexpression. Proceedings of the National Academy of Sciences of the United States of America, 105(38), 14371–14376. https://doi.org/10.1073/pnas.0804090105

325. Weickert, M.J., Hogg, R.W., Adhya, S. (1991). Locations and Orientations on the *Escherichia coli* Physical Map of the *mgl* Operon and *galS*, a New Locus for Galactose U-induction. J Bacteriol 173: 7412–7413.

326. Weickert, M.J., Adhya, S. (1992a). A Family of Bacterial Regulators Homologous to Gal and Lac Repressors. J. Biol. Chem. 267: 15869–15874.

327. Weickert, M.J., Adhya, S. (1992b). Isorepressor of the *gal* Regulon in *Escherichia coli*. J Mol Biol 226: 69–83.

328. Weickert, M.J., Adhya, S. (1993). The Galactose Regulon of *Escherichia coli*. Mol Microbiol 10: 245–251.

329. Went, S. C., Picton, D. M., Morgan, R. D., Nelson, A., Brady, A., Mariano, G., Dryden, D. T. F., Smith, D. L., Wenner, N., Hinton, J. C. D., Blower, T. R. (2024). Structure and Rational Engineering of The PglX Methyltransferase and Specificity Factor for BREX Phage Defence. Nature Communications, 15, Article 51629. https://doi.org/10.1038/s41467-024-51629-7[1](https://www.nature.com/articles/s41467-024-51629-7.pdf)

330. Wessel, D., Flügge, U.I. (1984). A Method for Quantitative Recovery of Protein in Dilute Solution in the Presence of Detergents and Lipids. Anal. Biochem.138:141–143.

331. Wexler, H. (2002). Outer-membrane Pore-forming Proteins in Gram-negative Anaerobic Bacteria. Clin. Infect. Dis. 35: S65–S71.

332. Wong, S., Alattas, H., Slavcev, R. (2021). A Snapshot of the λ T4*rII* Exclusion (Rex) Phenotype in *Escherichia coli*. *Curr Genet* **67**, 739–745. https://doi.org/10.1007/s00294-021-01183-2.

333. Wu, X. Bin, Tian, L. H., Zou, H. J., Wang, C. Y., Yu, Z. Q., Tang, C. H., Pan, J. Y. (2013). Outer Membrane Protein OmpW of *Escherichia coli* is Required for Resistance to Phagocytosis. Research in Microbiology, 164(8), 848–855.

334. Xie, S., Du, Y., Zhang, Y., Wang, Z., Zhang, D., He, L., Qiu, L., Jiang, J., Tan, W. (2020). Aptamer-based Optical Manipulation of Protein Subcellular Localization in Cells. Nature Communications, 11, Article 1347. https://doi.org/10.1038/s41467-020-15113-2

335. Yem, D.W., Wu, H.C. (1978). Physiological Characterization of an *Escherichia coli* Mutant Altered in the Structure of Murein Lipoprotein. J Bacteriol 133:1419–1426.

336. Yook, K. (2005). Complementation. In: WormBook: The Online Review of C. elegans Biology. Pasadena (CA): WormBook; 2005-2018.

337. Young, R. (1992). Bacteriophage Lysis: Mechanisms and Regulation. Microbial. Rev. 56, 430-481.

338. Yu, F., Mizushima, S. (1982). Roles of Lipopolysaccharide and Outer Membrane Protein *ompC* of *Escherichia coli* K-12 in the Receptor Function for Bacteriophage T4. Journal of Bacteriology, 151(2), 718–722.

339. Zakharov, S. D., Eroukova, V. Y., Rokitskaya, T. I., Zhalnina, M. V., Sharma, O., Loll, P. J., Zgurskaya, H. I., Antonenko, Y. N., Cramer, W. A. (2004). Colicin Occlusion of OmpF and TolC Channels: Outer Membrane Translocons for Colicin Import. Biophysical journal, 87(6), 3901–3911. https://doi.org/10.1529/biophysj.104.046151

340. Zeman, M., Cimprich, K. (2014). Causes and Consequences of Replication Stress. Nat Cell Biol 16, 2–9. https://doi.org/10.1038/ncb2897

341. Zhang Y, Stöppelkamp I, Fernandez-Pernas P, Allram M, Charman M, Magalhaes AP, Piedavent-Salomon M, Sommer G, Sung YC, Meyer K, Grams N, Halko E, Dongre S, Meierhofer D, Malszycki M, Ilik IA, Aktas T, Kraushar ML, Vastenhouw N, Weitzman MD, Grebien F, Niskanen H, Hnisz D. (2025). Probing Condensate Microenvironments with a Micropeptide Killswitch. Nature 643, 1107–1116. https://doi.org/10.1038/s41586-025-09141-5

342. Zhou, Y., Gottesman, S. (1998). Regulation of proteolysis of the stationary-phase sigma factor RpoS. Journal of bacteriology, 180(5), 1154–1158.

343. Zivanovic, Y., Confalonieri, F., Ponchon, L., Lurz, R., Chami, M., Flayhan, A., Renouard, M., Huet, ADecottignies. P., Davidson, A. R., Breyton, C., Boulanger, P. (2014). Insights into Bacteriophage T5 Structure from Analysis of Its Morphogenesis Genes and Protein Components. J Virol88:.https://doi.org/10.1128/jvi.02262-13.

344. Zucca, S., Pasotti, L., Politi, N., Cusella De Angelis, M. G., Magni, P. (2013). A Standard Vector for The Chromosomal Integration and Characterization of Biobrick™ Parts in *Escherichia Coli*. Journal of Biological Engineering, 7(12). https://jbioleng.biomedcentral.com/articles/10.1186/1754-1611-7-12

Appendix A

Solutions and Buffers

Unless otherwise stated, all media and buffers were prepared following the recipes in this chapter. All *E. coli* strains were cultured in Luria–Bertani (LB) liquid medium, while plaque assays were made on top agar. Phage lysates were isolated and preserved in Tris-NaCl (TN) buffer.

Table 0-1. Solutions and Buffers

Solutions and Buffers	Purpose	Recipe and Preparation
Growth Media		
Luria Bertani (LB) Broth (BD Difco, Mississauga, Canada)	A rich nutrient media for optimum growth of bacterial cultures	10 g of tryptone, 5 g of yeast abstract, and 5 g of NaCl were added to 1L of ddH_2O. Antibiotic was added (as needed) after LB Broth was autoclaved and allowed to cool for 1 h. Broth with antibiotic was stored at 4 ºC, or otherwise stored at RT.
Luria Bertani (LB) Agar (BD Difco, Mississauga, Canada)	A rich semi-solid media for optimum growth of bacterial cells on semi-solid media (plates)	10 g of tryptone, 5 g of yeast abstract, 5 g of NaCl, and 12.5 g of Bacto agar were added to 1L of ddH_2O. Antibiotic was added (as needed) after LB Agar was autoclaved and allowed to cool for 1 h. Media was poured into sterile mono-plates (Fischer Brand, Ottawa, Canada) at a volume of approximately 35 mL per plate. The media

		was allowed to solidify at RT for approximately 2 h stored at 4 ºC.
Luria Bertani (LB) Top Agar (BD Difco, Mississauga, Canada)	A rich media to suspend bacterial cultures and phages and give a good dispersion of cells as a plate overlay	10 g of tryptone, 5 g of yeast abstract, 5 g of NaCl, and 7 g of Bacto agar were added to 1L of ddH_2O. 50 mL aliquots were prepared, autoclaved and stored in a 55 ºC water bath.
Super Optimum Broth with Catabolic repression (SOC) (BD Difco, Mississauga, Canada)	A rich media to recover cells after electroporation	10 g of tryptone, 5 g of yeast abstract, and 5 g of NaCl were added to 1L of ddH_2O in addition to 1M $MgCl_2$ and 1M glucose. SOC media was then autoclaved and stored at RT.
2X Yeast Extract Tryptone (2xYT)	A rich media for bacterial growth	16 g of yeast extract, 10 g of tryptone, and 10 g of NaCl were added to 1L of ddH_2O. 2xYT was then autoclaved and stored at RT.

Antibiotic stocks

Ampicillin stock (Ap) (Sigma Aldrich, Oakville, Canada)	Ap was used to select for cells transformed by plasmids: pUC19, pBSL180, pBSL199, pPL451, pBS1947, pHA1, and pHA2	Small aliquots of stock ampicillin were prepared at a final concentration of 50 µg/mL. Ampicillin stock powder was dissolved into sterile ddH_2O and filter sterilized. Ampicillin stock was stored at -20 ºC and thawed solution was added to media to a final concentration of 100 µg/mL.

Kanamycin stock (Km) (Sigma Aldrich, Oakville, Canada)	Km was employed as a second antibiotic to screen for Δ*clpP* and Δ*omp* and Keio collection mutant strains.	Small aliquots of kanamycin stock solution were prepared at a final concentration of 25 µg/mL by dissolving kanamycin stock powder into sterile ddH_2O and filter satirizing. The stock was stored at -20 ºC and thawed solution was added as necessary to media at a final concentration of 50 µg/mL.
Tetracycline stock (Tc) (Sigma Aldrich, Oakville Canada)	Tetracycline was employed as a second antibiotic marker to screen for pHA2 plasmid, *in tandem* with kanamycin antibiotic to screen for Rex^- mutants.	Small aliquots of tetracycline stock solution were prepared at a final concentration of 20 µg/mL by dissolving tetracycline stock powder into 1:1 50% of sterile ddH_2O and 50% of 95% ethanol. Tetracycline stock was stored in foil wrap to protect from light degradation at -20 ºC, and thawed solution was added to media as necessary at a final concentration of 20 µg/mL. *Note:* all unused stock, plates, or broth containing tetracycline was protected from light degradation while stored.

Buffers

Tris NaCl (TN) Buffer (Fisher Bioreagents, Ottawa, Canada)	Used to make serial phage dilutions and to store phage	0.1 M NaCl and 0.02 M of Tris-HCl were added to 1 L of ddH_2O and adjusted to a pH of 7.8. The solution was autoclaved and cooled to RT for storage.
50X Tris-Acetate-EDTA (TAE) Buffer (Fisher Bioreagents, Ottawa, Canada)	To separate DNA fragments (bands) based on their sizes when running samples	50X TAE buffer consists of 242 g Tris Base (MW = 121.1 g/mol), 57.1 mL glacial acetic acid, and 100 mL of 0.5 M EDTA per 1 L.

	through gel electrophoresis	50X TAE solution was diluted in ddH_2O to a final concentration of 0.5X and stored at RT.
Protein A binding buffer	Protein purification	5 mL of 1M Tris-HCl pH 8, 15 mL of 5M NaCl, 5 mL of 10% NP-40 and 475 mL of ddH_2O (500 mL final volume) was mixed and stored at 4 ºC.
TEV cleavage buffer	Protease cleavage	1 mL of 1M Tris-HCl pH 8, 3 mL of 5M NaCl, 1 mL of 10% NP-40, 100 µL of 0.5M EDTA, 100 µL of 1M DTT and 95 mL of ddH_2O was mixed and stored at 4 ºC.
Calmodulin binding buffer	Protein purification	5 mL of 1M Tris-HCl pH 8, 15 mL of 5M NaCl, 5 mL of 10% NP-40, 500 µL of 1M magnesium acetate, 500 µL of 1M imidazole, 1 mL of 1M $CaCl_2$, 348.5 µL of 14.3M β-mercaptoethanol and 473 mL of ddH_2O was mixed and stored at 4 ºC.
Calmodulin elution buffer	Protein elution	1 mL of 1M Tris-HCl pH 8, 3 mL of 5M NaCl, 1 mL of 10% NP-40, 100 µL of 1M magnesium acetate, 100 µL of 1M imidazole, 200 µL of 1M EGTA, 69.7 µL of 14.3M β-mercaptoethanol and 94.5 mL of ddH_2O was mixed and stored at 4 ºC
TCA Washing Buffer	Protein precipitation wash	70 mL of acetone, 20 mL of ethanol, 5 mL of Tris (pH 8), and 5 mL of ddH_2O was mixed and stored at 4 ºC.
PBS buffer	buffer solution to wash and remove any debris from bacterial cultures before GFP	To make 1X PBS: 137 mM NaCl, 2.7 mM KCI, 10 mM Na_2HPO_4, 1.8 mM KH_2PO_4, and pH 7.4. mixed and stored at 4 ºC in the dark.

	fluorescence exam and imaging	

Screening Reagents

Isopropyl β-D-1-thiogalactopyranoside (IPTG) solution (Fisher Bioreagents, Ottawa, Canada	For the induction of *lac*Z gene expression in the pUC19 vector required for white/blue colony screening, and the induction of the transposable element to be inserted into host chromosomal DNA.	2.38 g of IPTG powder was dissolved in 100 mL ddH_2O to a final concentration of 100 mM IPTG. Products were filter sterilized and then stored at -20 ºC.
5-bromo-4-chloro-3-indolyl-beta-D-galacto-pyranoside (X-Gal) solution (Omega Bio-Tek, Norcross, USA	To use in combination with IPTG for white/blue colony screening denoting disruption of the *lacZ*α genetic element and $LacZ^-$ phenotype in M15 Δ*lacZ* cells (see Table 1 for genetic description). After *lacZ* induction by the gratuities inducer, IPTG, X-Gal particles are	20 mg of X-Gal powder was dissolved in 20 mL of dimethylsulfoxide (DMSO, Fisher Bioreagents, Ottawa, Canada). Unused X-Gal plates/stock were protected from light degradation at -20 ºC.

	hydrolyzed by $LacZ^{+}$ cells inducing blue colour in non-recombinant colonies.	

Gels

0.8% DNA agarose gel	To separate DNA fragments and make them visible under UV light.	4 µL of Ethidium Bromide (EtBr) solution (Bio-Rad, Mississauga, Canada) was added to molten agarose gel just before pouring the melted agarose into the gel cast. The gel solidified at RT before use.
SDS-PAGE gel (Bio-Rad, Hercules, USA)	To separate extracted proteins and identify their presence on an immunoblot	4-5% stacking and 8-10% resolving gels were prepared using the Bio-Rad MINI Protean TGX Stain-Free Gel Kit (Hercules, USA). Equal volumes of Buffer A and Buffer B were mixed. 5 mL of TEMED and 50 µL of APS were added for the stacking gel 4 mL of TEMED and 100 µL of APS were added for the resolving gel. The resolving gel solution was added first to the gel cast and then the stacking gel on top with the inserted comb and allowed to solidify at RT before use.

Appendix B

Supplementary DNA data

The sequences of *rexA*, *rexB*, and *cI* of Enterobacteria phage lambda, NC_001416.1

>RexB (35825-36259 complement)

ATGCGGAACAGAATCATGCCTGGTGTTTACATAGTAATAATTCCTTACGTTATCGTAAGCATTTGCTATC
TCCTTTTCCGCCACTACATTCCTGGTGTTTCTTTTTCAGCTCATAGAGATGGTCTTGGGGCGACATTGTC
ATCATATGCAGGAACCATGATTGCAATCCTGATTGCTGCCTTGACGTTTCTAATCGGAAGCAGAACGCGC
CGACTGGCCAAGATTAGAGAGTATGGGTATATGACATCGGTAGTTATTGTCTATGCCCTTAGTTTTGTTG
AGCTTGGAGCTTTGTTTTTCTGCGGGTTATTGCTTCTTTCCAGCATAAGCGGCTACATGATACCCACTAT
CGCCATCGGCATTGCCTCTGCATCGTTCATTCATATATGCATCCTTGTTTTCCAACTATATAATTTGACC
AGAGAACAAGAATAA

>RexA (36275-37114 complement)

ATGAAGAATGGTTTTTATGCGACTTACCGCAGCAAAAATAAAGGGAAAGATAAGCGCTCAATAAACCTGT
CTGTTTTCCTTAATTCTCTGCTGGCTGATAATCATCACCTGCAGGTTGGCTCCAATTATTTGTATATTCA
TAAAATCGATGGAAAAACTTTTCTCTTTACCAAAACAAATGACAAGAGTCTGGTTCAGAAGATAAATCGC
TCTAAAGCTTCAGTTGAAGATATTAAGAACAGCCTCGCAGATGACGAATCATTGGGATTCCCATCTTTTT
TGTTTGTTGAAGGCGACACCATTGGTTTTGCCAGAACTGTTTTCGGGCCGACCACATCCGATCTGACAGA
TTTTTTAATCGGGAAAGGAATGTCATTAAGCAGTGGAGAGCGCGTTCAGATAGAGCCACTGATGAGGGGA
ACCACCAAAGACGATGTTATGCATATGCATTTCATCGGCCGAACAACGGTGAAGGTAGAAGCCAAGCTAC
CTGTATTTGGCGATATATTAAAGGTCTTAGGGGCAACAGATATTGAAGGGGAGCTTTTTGACTCATTGGA
TATAGTCATTAAGCCAAAATTTAAAAGGGATATAAAAAAGGTTGCCAAGGATATTATTTTTAACCCGTCA
CCTCAATTTTCAGACATTAGCCTGCGGGCAAAAGATGAGGCCGGAGATATTTTAACAGAACATTATCTAT
CAGAAAAAGGCCATCTCTCAGCGCCTCTGAACAAGGTCACCAATGCTGAGATAGCTGAAGAGATGGCATA
TTGCTACGCAAGAATGAAAAGTGATATACTGGAATGTTTTAAAAGGCAGGTGGGCAAAGTTAAGGATTAA

>CI (37227-37940 complement)

ATGAGCACAAAAAAGAAACCATTAACACAAGAGCAGCTTGAGGACGCACGTCGCCTTAAAGCAATTTATG
AAAAAAAGAAAAATGAACTTGGCTTATCCCAGGAATCTGTCGCAGACAAGATGGGGATGGGGCAGTCAGG
CGTTGGTGCTTTATTTAATGGCATCAATGCATTAAATGCTTATAACGCCGCATTGCTTGCAAAAATTCTC
AAAGTTAGCGTTGAAGAATTTAGCCCTTCAATCGCCAGAGAAATCTACGAGATGTATGAAGCGGTTAGTA
TGCAGCCGTCACTTAGAAGTGAGTATGAGTACCCTGTTTTTTCTCATGTTCAGGCAGGGATGTTCTCACC
TGAGCTTAGAACCTTTACCAAAGGTGATGCGGAGAGATGGGTAAGCACAACCAAAAAAGCCAGTGATTCT
GCATTCTGGCTTGAGGTTGAAGGTAATTCCATGACCGCACCAACAGGCTCCAAGCCAAGCTTTCCTGACG
GAATGTTAATTCTCGTTGACCCTGAGCAGGCTGTTGAGCCAGGTGATTTCTGCATAGCCAGACTTGGGGG
TGATGAGTTTACCTTCAAGAAACTGATCAGGGATAGCGGTCAGGTGTTTTTACAACCACTAAACCCACAG
TACCCAATGATCCCATGCAATGAGAGTTGTTCCGTTGTGGGGAAAGTTATCGCTAGTCAGTGGCCTGAAG
AGACGTTTGGCTGA

Appendix C

Plasmid Maps of GFP-Rex Constructs

This section illustrates the N-terminal fusion constructs used to study RexA and RexB expression and visualization in *E. coli* BW25113 (wild type) and λ lysogens. The collection includes RexA, RexB, RexA-RexB (fusion at RexA), and RexA-RexB (fusion at RexB).

Each construct was generated with and without a flexible linker to assess the impact of spatial separation on protein folding and function. The linker sequence used is provided in Table 3-1. All constructs were expressed under identical conditions and analyzed via fluorescence microscopy.

Plasmid constructs were designed using SnapGene software.

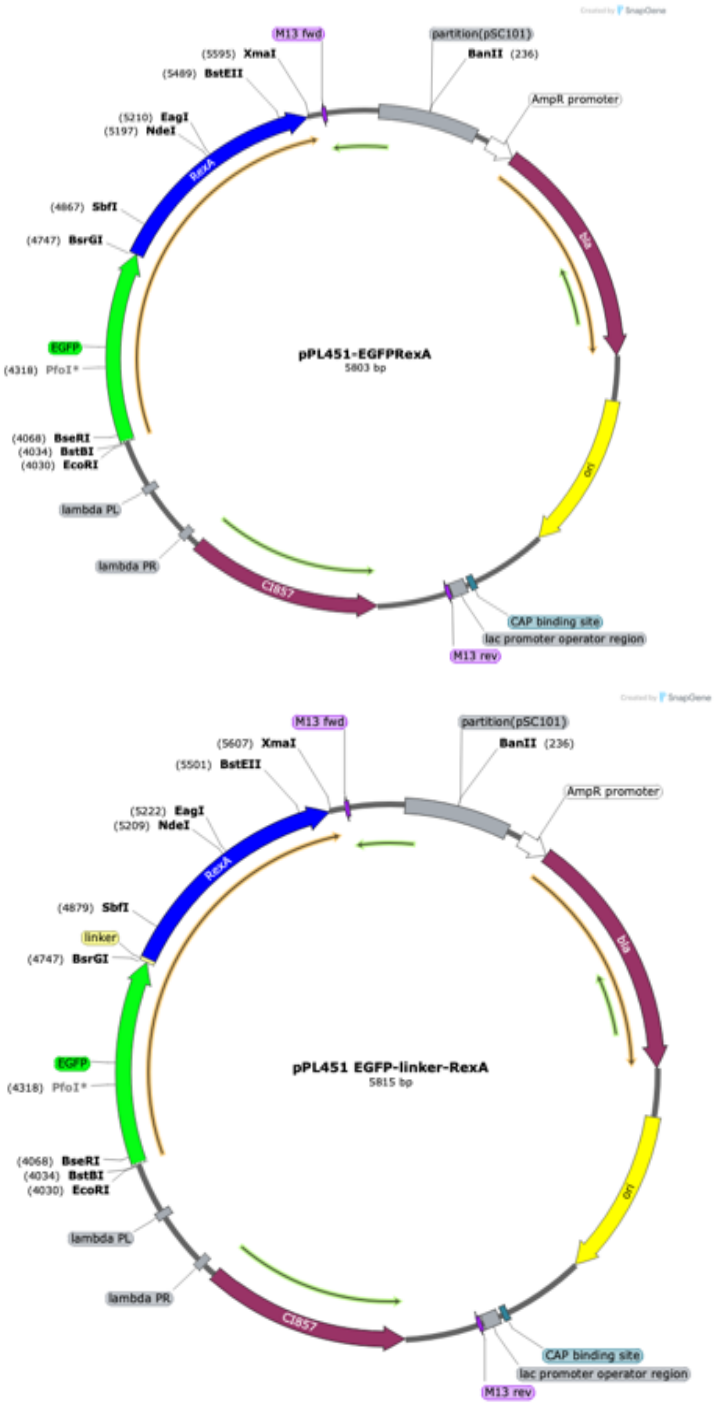


Figure C-1. Plasmid Maps of eGFP::RexA Constructs with and without Linker. Plasmid maps showing the design of eGFP::RexA constructs used for N-terminal tagging of RexA with eGFP. Two versions were generated: one with a direct fusion of eGFP to the N-terminus of RexA, and one with a flexible linker inserted between eGFP and RexA to improve folding and reduce steric hindrance. Both constructs were cloned into pPL451 backbone for expression in *E. coli* cells.

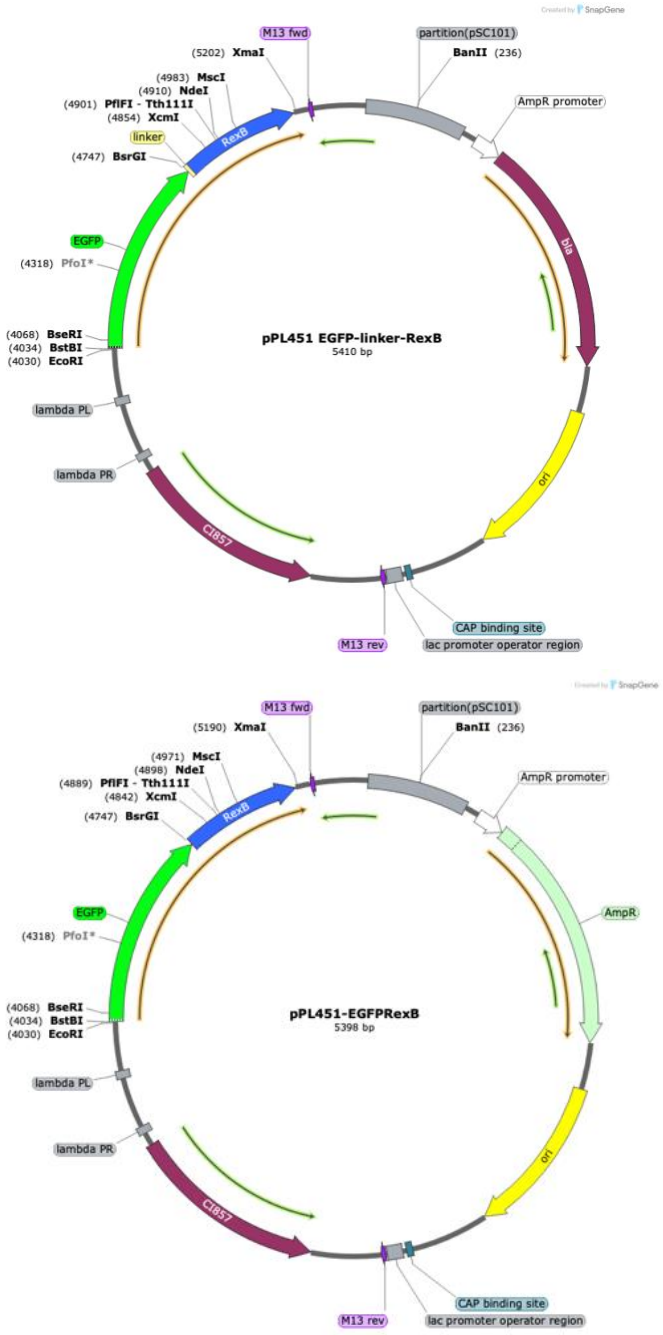
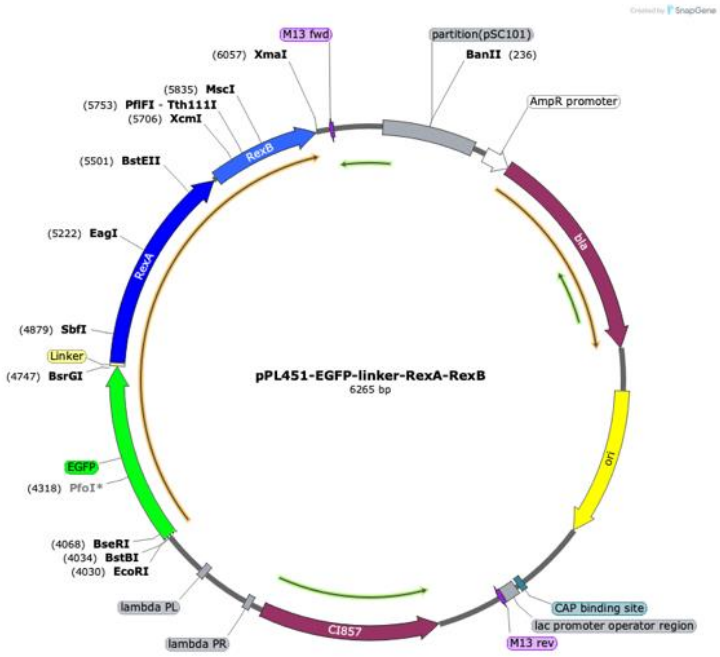


Figure 0-2. Plasmid Maps of eGFP::RexB Constructs with and without Linker. Plasmid maps showing the design of eGFP::RexB constructs used for N-terminal tagging of RexB with eGFP. Two versions were generated: one with a direct fusion of eGFP to the N-terminus of RexB, and one with a flexible linker inserted between eGFP and RexB to improve folding and reduce steric hindrance. Both constructs were cloned into pPL451 backbone for expression in *E. coli* cells.



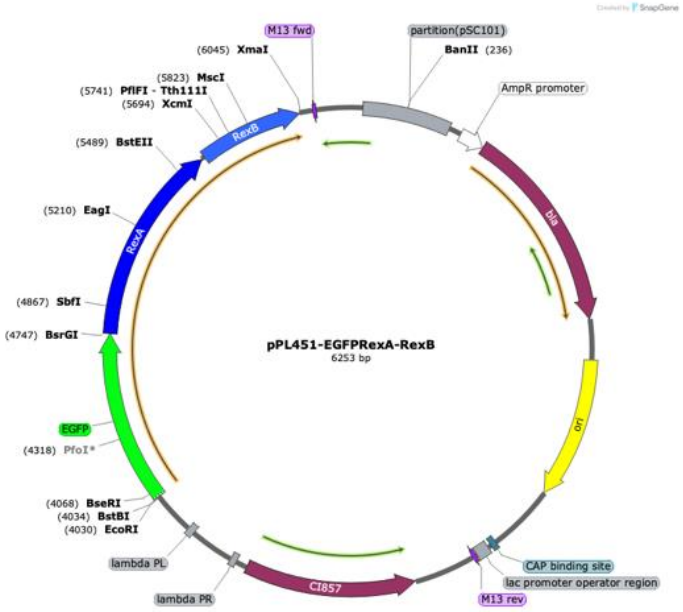


Figure 0-3. Plasmid Maps of eGFP::RexA-RexB Constructs with and without Linker. Plasmid maps showing the design of eGFP::RexA-RexB constructs used for N-terminal tagging of RexA with eGFP. Two versions were generated: one with a direct fusion of eGFP to the N-terminus of RexA in the presence of RexB, and one with a flexible linker inserted between eGFP and RexA to improve folding and reduce steric hindrance. Both constructs were cloned into pPL451 backbone for expression in *E. coli* cells.

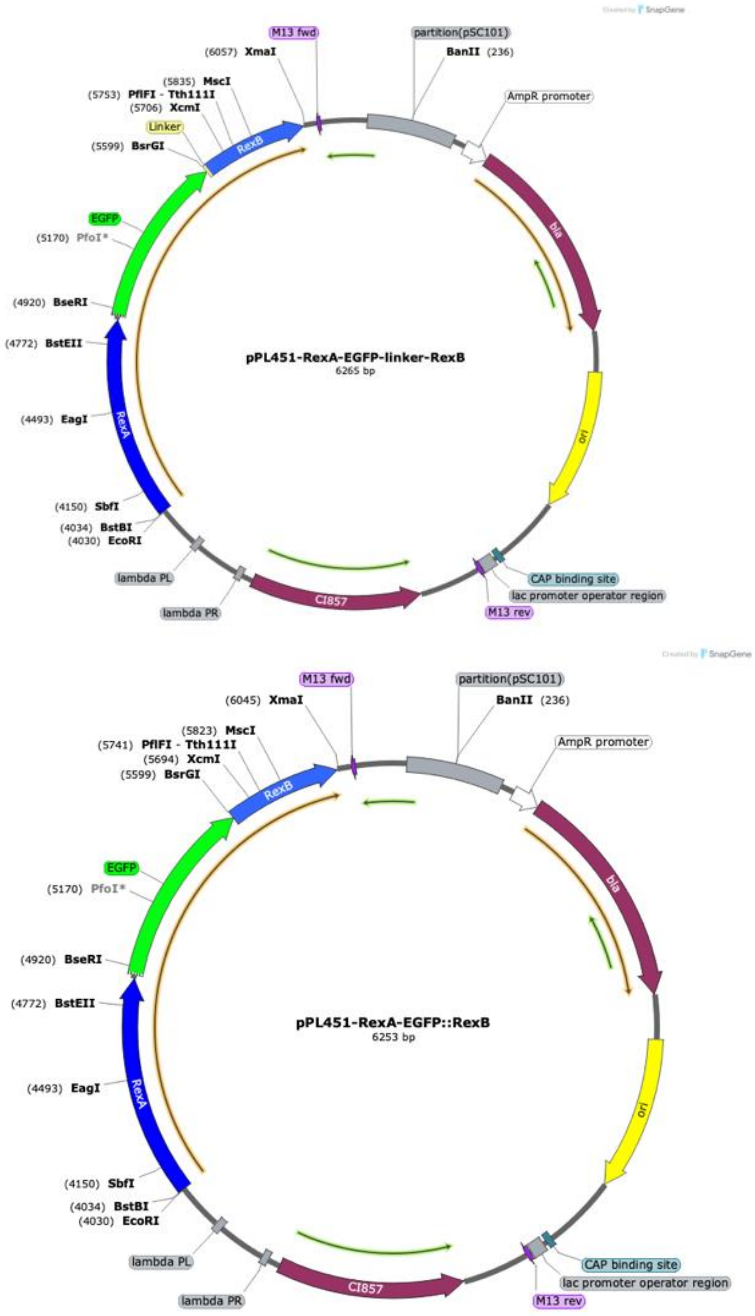


Figure 0-4. Plasmid Maps of RexA-eGFP::RexB Constructs with and without Linker. Plasmid maps showing the design of RexA-eGFP::RexB constructs used for N-terminal tagging of RexB with eGFP in the presence of RexA. Two versions were generated: one with a direct fusion of eGFP to the N-terminus of RexB in the presence of RexA, and one with a flexible linker inserted between eGFP and RexB to improve folding and reduce steric hindrance. Both constructs were cloned into the pPL451 backbone for expression in *E. coli* cells.

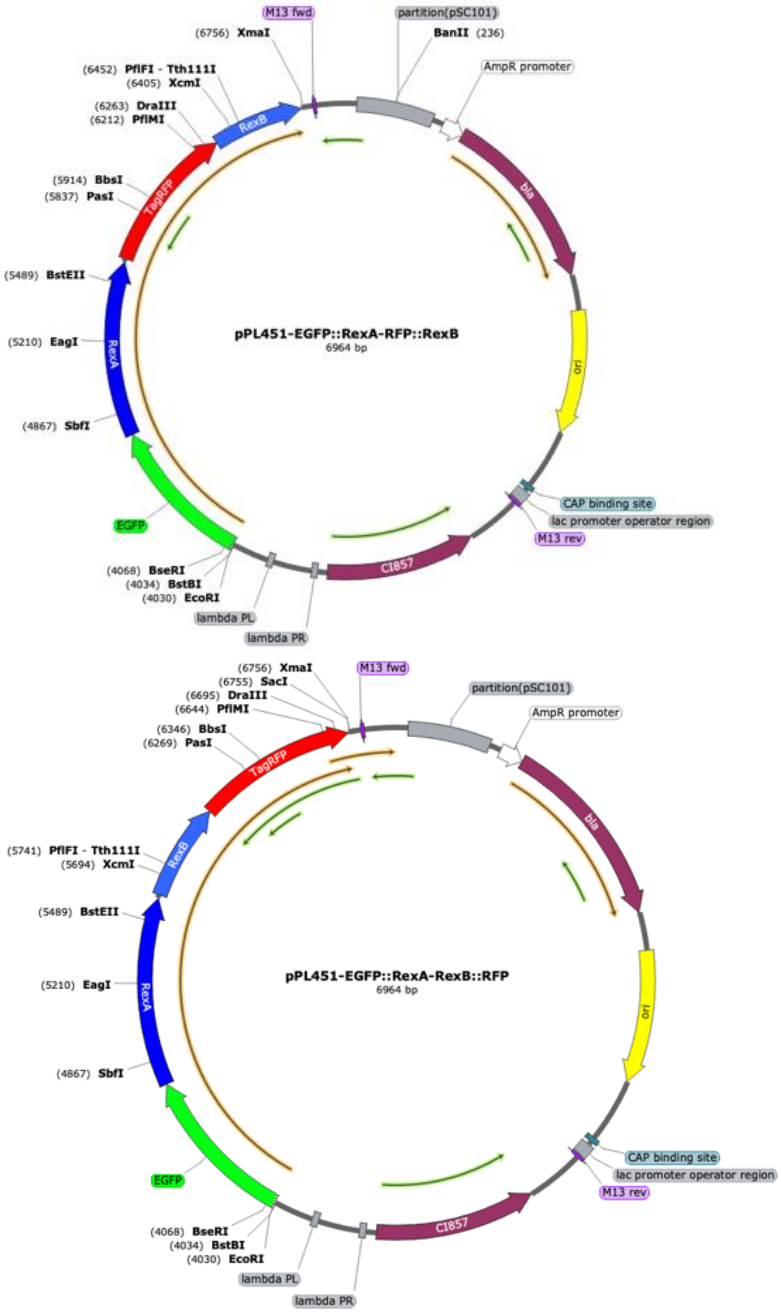


Figure 0-5. Plasmid Maps of Dual-Tagged Rex Constructs: eGFP::RexA-RFP::RexB and eGFP::RexA-RexB::RFP. Plasmid maps showing the design of eGFP::RexA-RFP::RexB constructs used for N-terminal tagging of RexA and RexB with eGFP and RFP, respectively. The second construct, eGFP::RexA-RexB::RFP, was generated by fusing eGFP to the N-terminal of RexA and RFP to the C-terminal of RexB. Both constructs were cloned into pPL451 backbone for expression in *E. coli* cells. The dual-tag configuration enables the simultaneous visualization of both proteins, allowing for the assessment of their interactions.

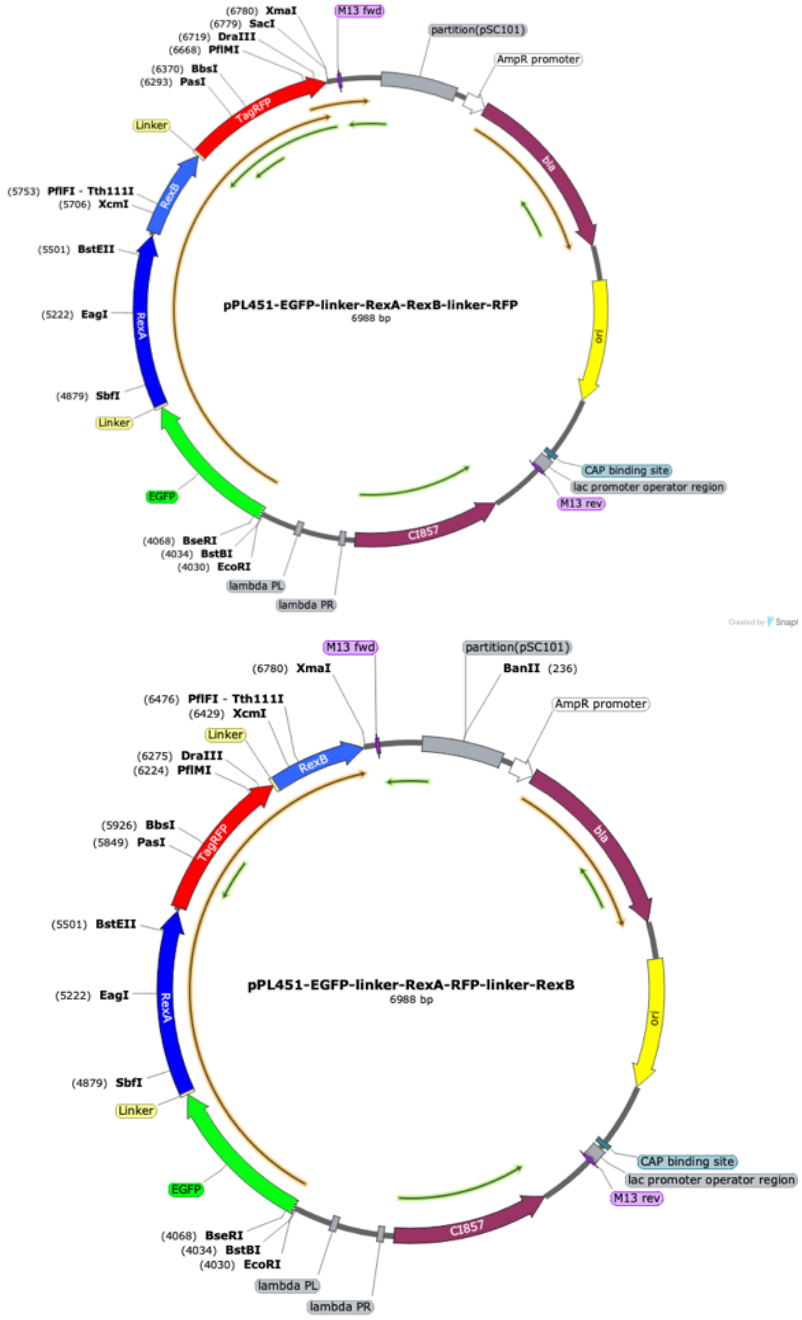


Figure 0-6. Plasmid Maps of Dual-Tagged Rex Constructs: eGFP::RexA-RFP::RexB and eGFP::RexA-RexB::RFP with linker. Plasmid maps showing the design of eGFP::RexA-RFP::RexB constructs used for N-terminal tagging of RexA and RexB with eGFP and RFP, respectively. The second construct, eGFP::RexA-RexB::RFP, was generated by fusing eGFP to the N-terminal of RexA and RFP to the C-terminal of RexB. The linker sequence was inserted between the Rex protein and the tag. Both constructs were cloned into pPL451 backbone for expression in *E. coli* cells. The dual-tag configuration enables the simultaneous visualization of both proteins and allows for the assessment of their interactions.

This section illustrates the C-terminal fusion constructs used to study RexA and RexB expression and visualization in *E. coli* BW25113 (wild type) and λ lysogens. The collection includes RexA, RexB, RexA-RexB (fusion at RexA), and RexA-RexB (fusion at RexB).

Each construct was generated with and without a flexible linker to assess the impact of spatial separation on protein folding and function. The linker sequence used is provided in Table 3-1. All constructs were expressed under identical conditions and analyzed via fluorescence microscopy.

Plasmid constructs were designed using SnapGene software.

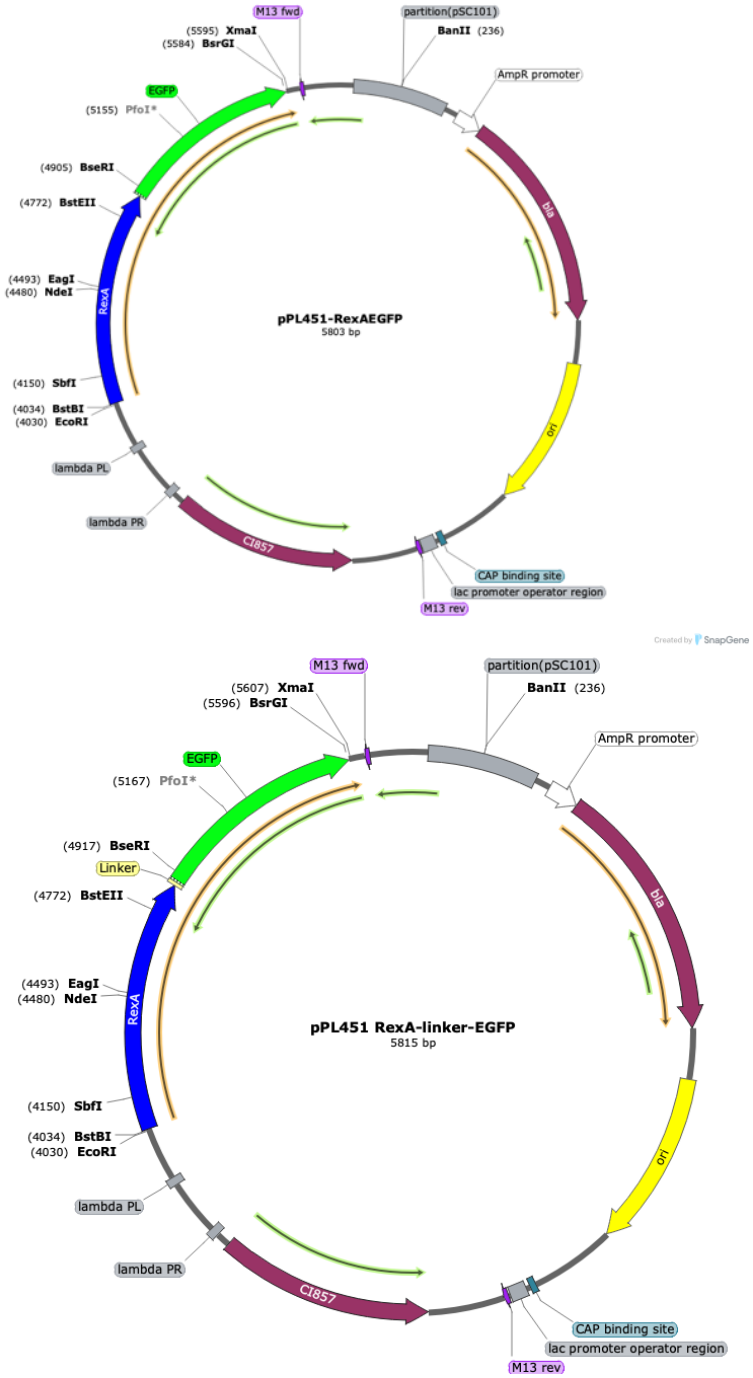


Figure 0-7. Plasmid Maps of RexA::eGFP Constructs with and without Linker. Plasmid maps showing the design of RexA::eGFP constructs used for C-terminal tagging of RexA with eGFP. Two versions were generated: one with a direct fusion of eGFP to the C-terminus of RexA, and one with a flexible linker inserted between eGFP and RexA to improve folding and reduce steric hindrance. Both constructs were cloned into the pPL451 backbone for expression in *E. coli* cells.

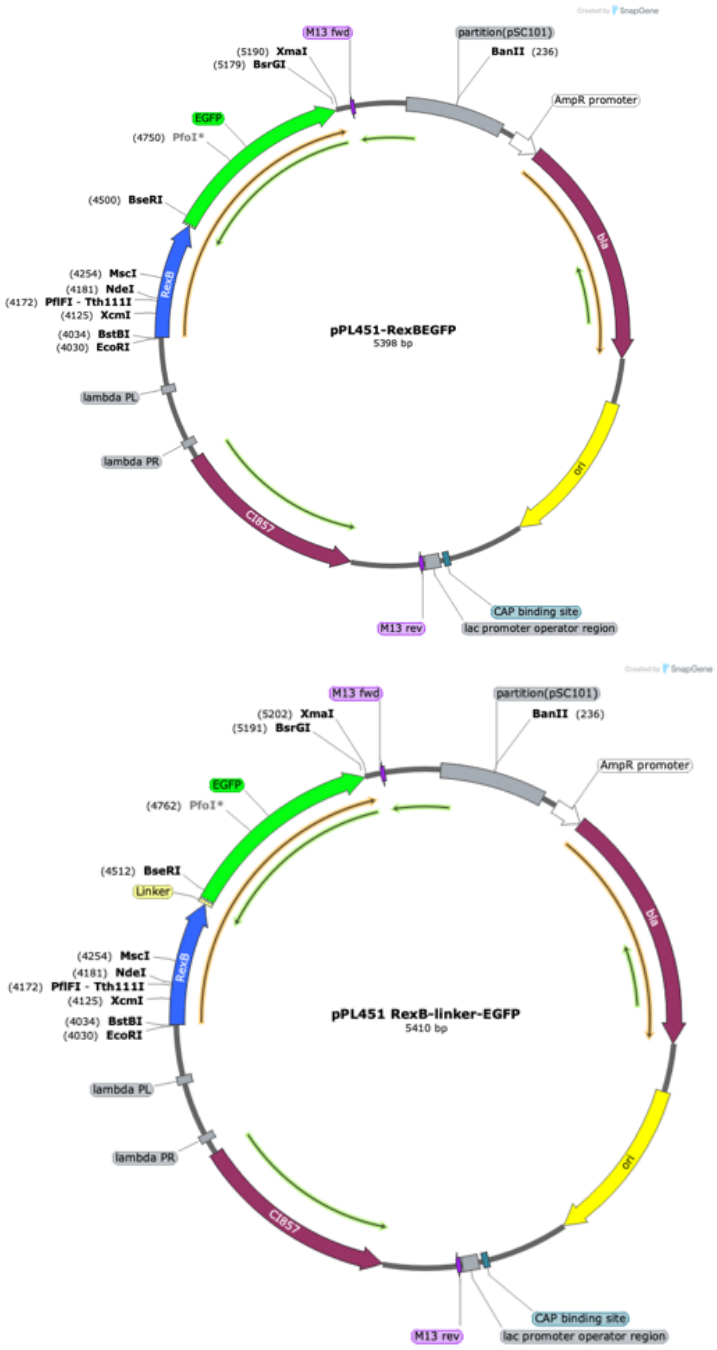


Figure C-8. Plasmid Maps of RexB::eGFP Constructs with and without Linker. Plasmid maps showing the design of RexB::eGFP constructs used for C-terminal tagging of RexB with eGFP. Two versions were generated: one with a direct fusion of eGFP to the C-terminus of RexB, and one with a flexible linker inserted between eGFP and RexB to improve folding and reduce steric hindrance. Both constructs were cloned into the pPL451 backbone for expression in *E. coli* cells.

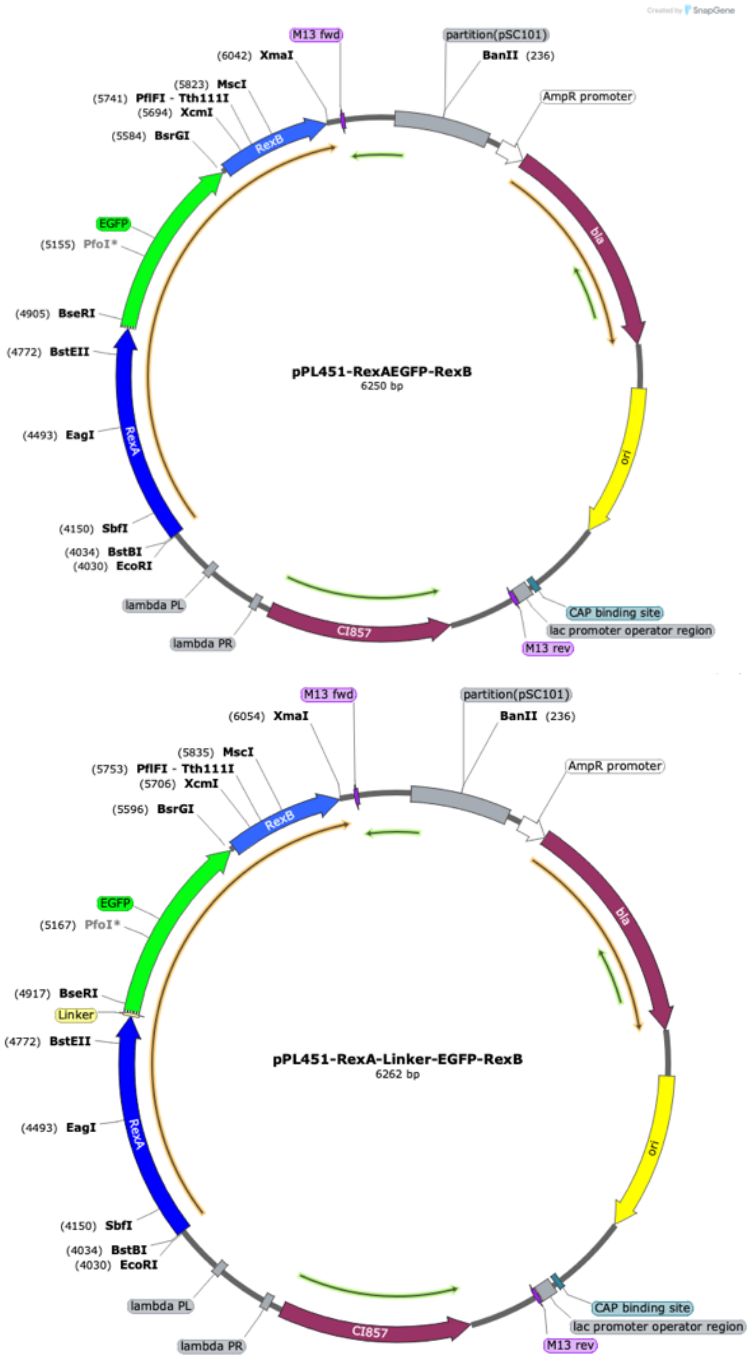


Figure 0-9. Plasmid Maps of RexA::eGFP-RexB Constructs with and without Linker. Plasmid maps showing the design of RexA::eGFP-RexB constructs used for C-terminal tagging of RexA with eGFP. Two versions were generated: one with a direct fusion of eGFP to the C-terminus of RexA in the presence of RexB, and one with a flexible linker inserted between eGFP and RexA to improve folding and reduce steric hindrance. Both constructs were cloned into the pPL451 backbone for expression in *E. coli* cells.

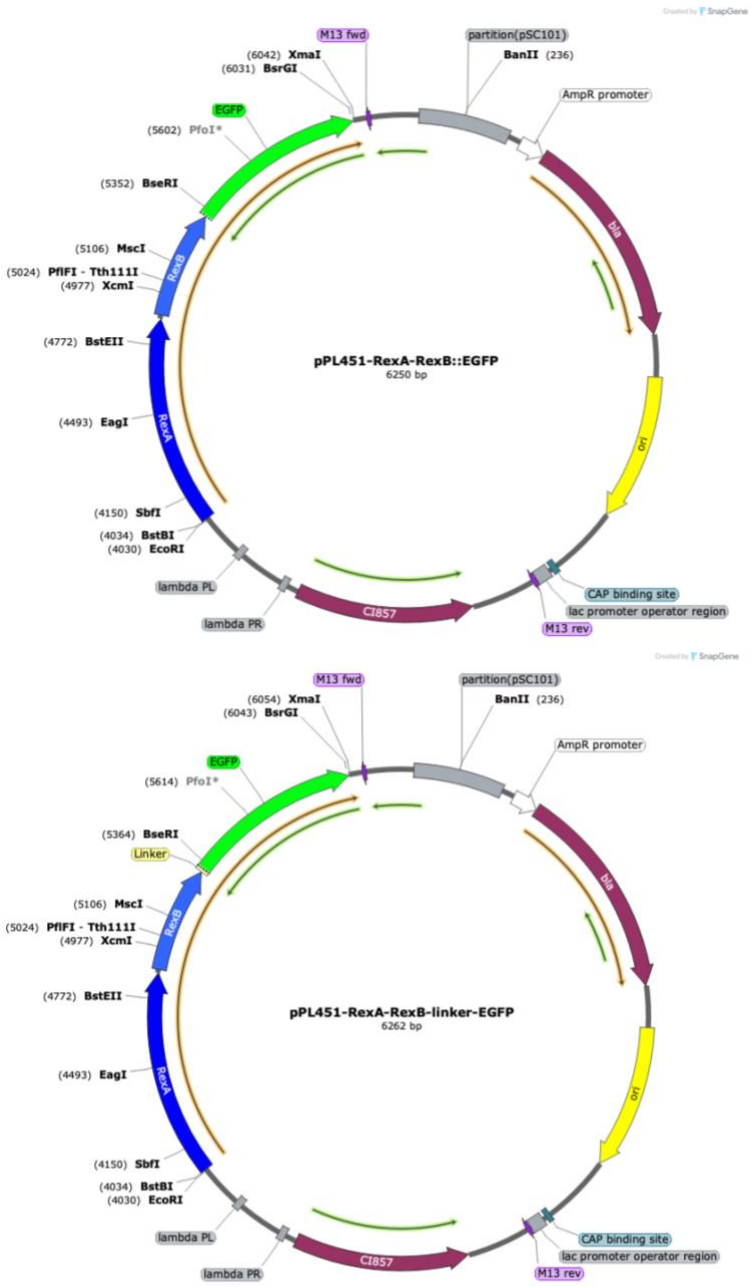


Figure 0-10. Plasmid Maps of RexA-RexB::eGFP Constructs with and without Linker. Plasmid maps showing the design of RexA-RexB::eGFP constructs used for C-terminal tagging of RexB with eGFP. Two versions were generated: one with a direct fusion of eGFP to the C-terminus of RexB in the presence of RexA, and one with a flexible linker inserted between eGFP and RexB to improve folding and reduce steric hindrance. Both constructs were cloned into the pPL451 backbone for expression in *E. coli* cells.

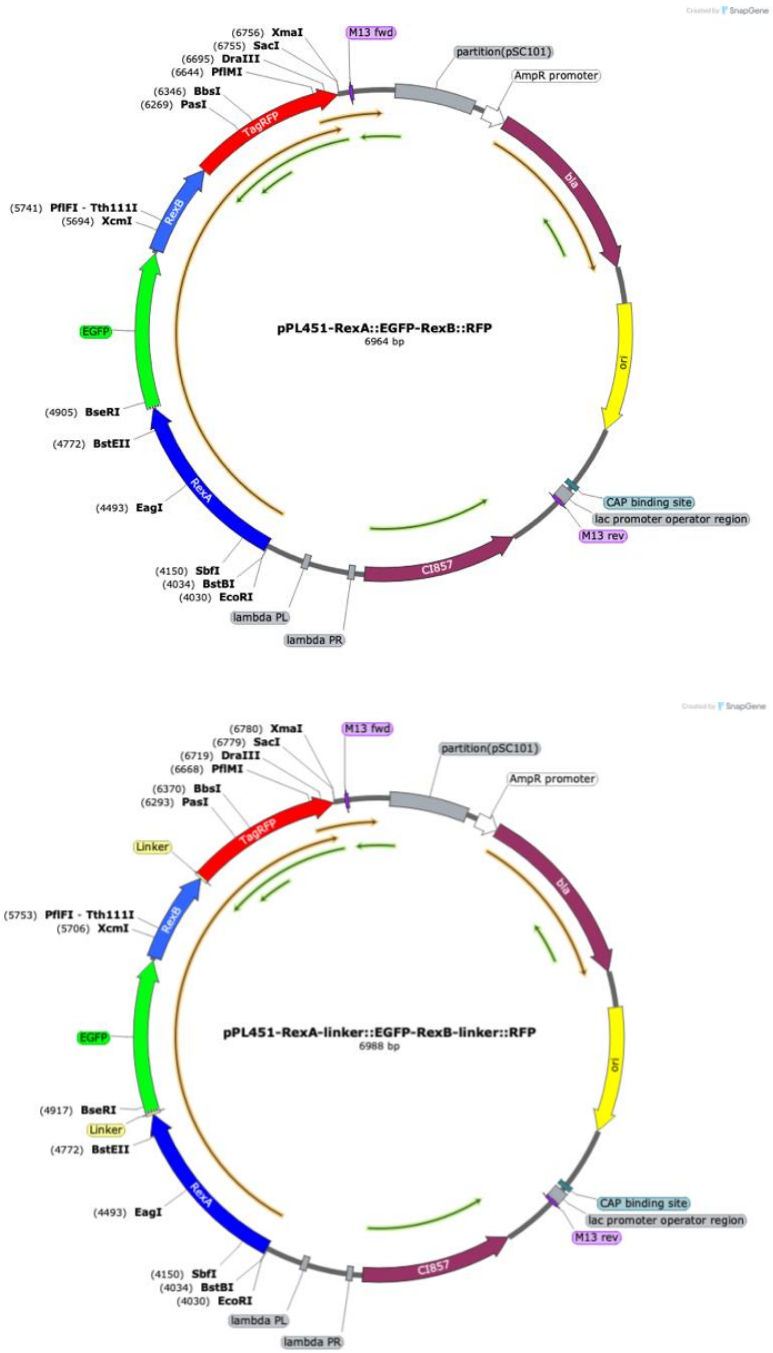
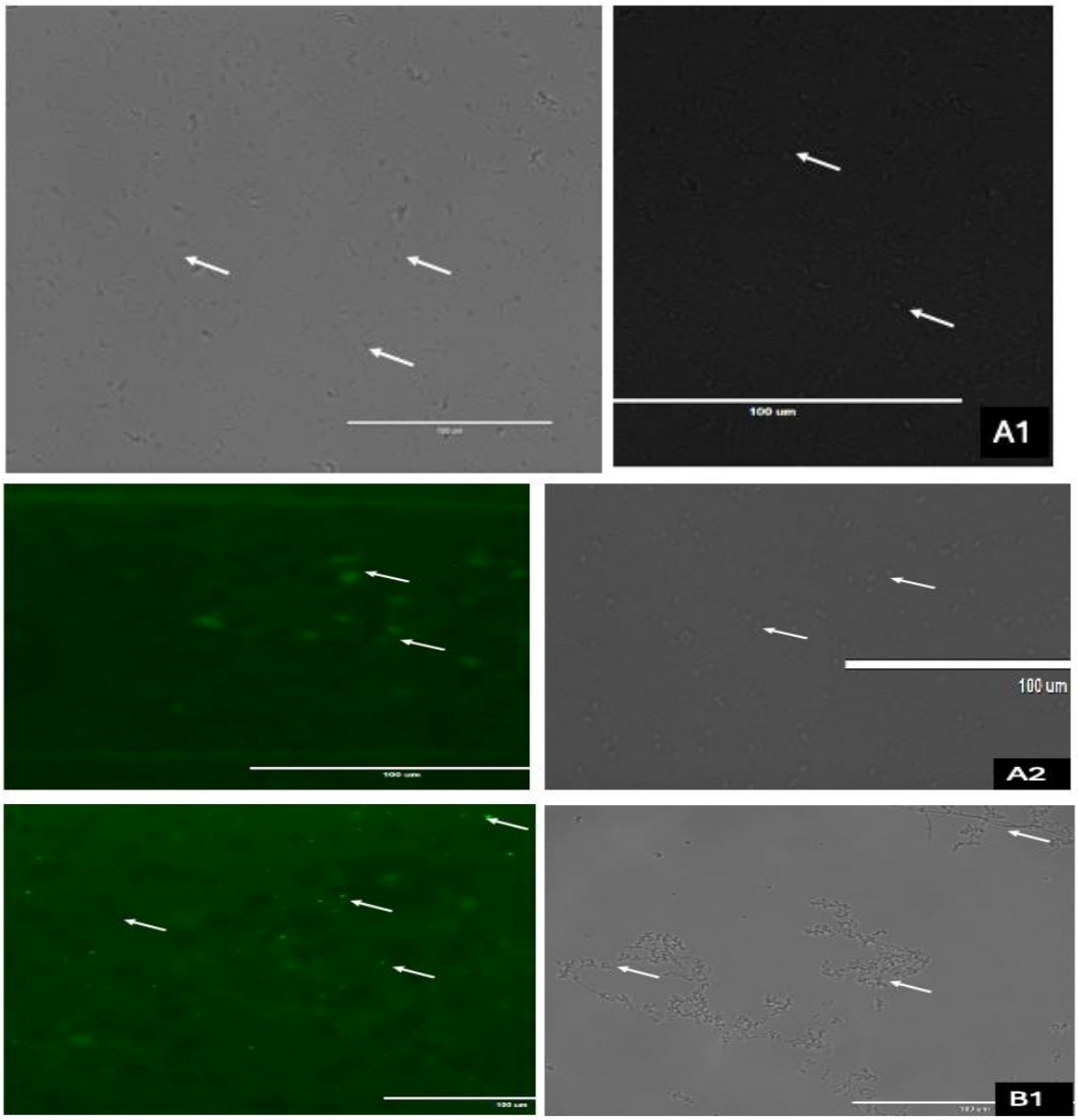
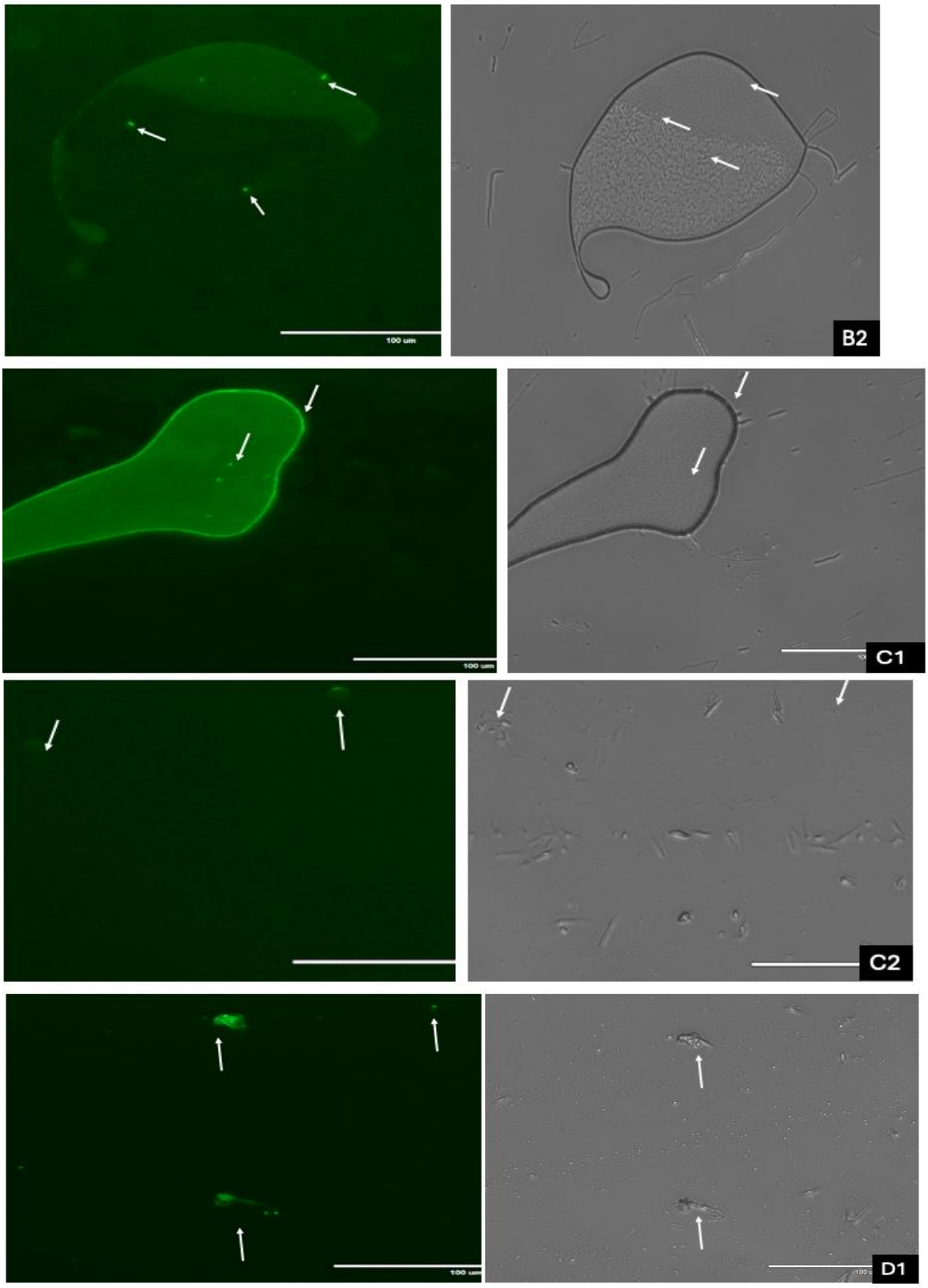
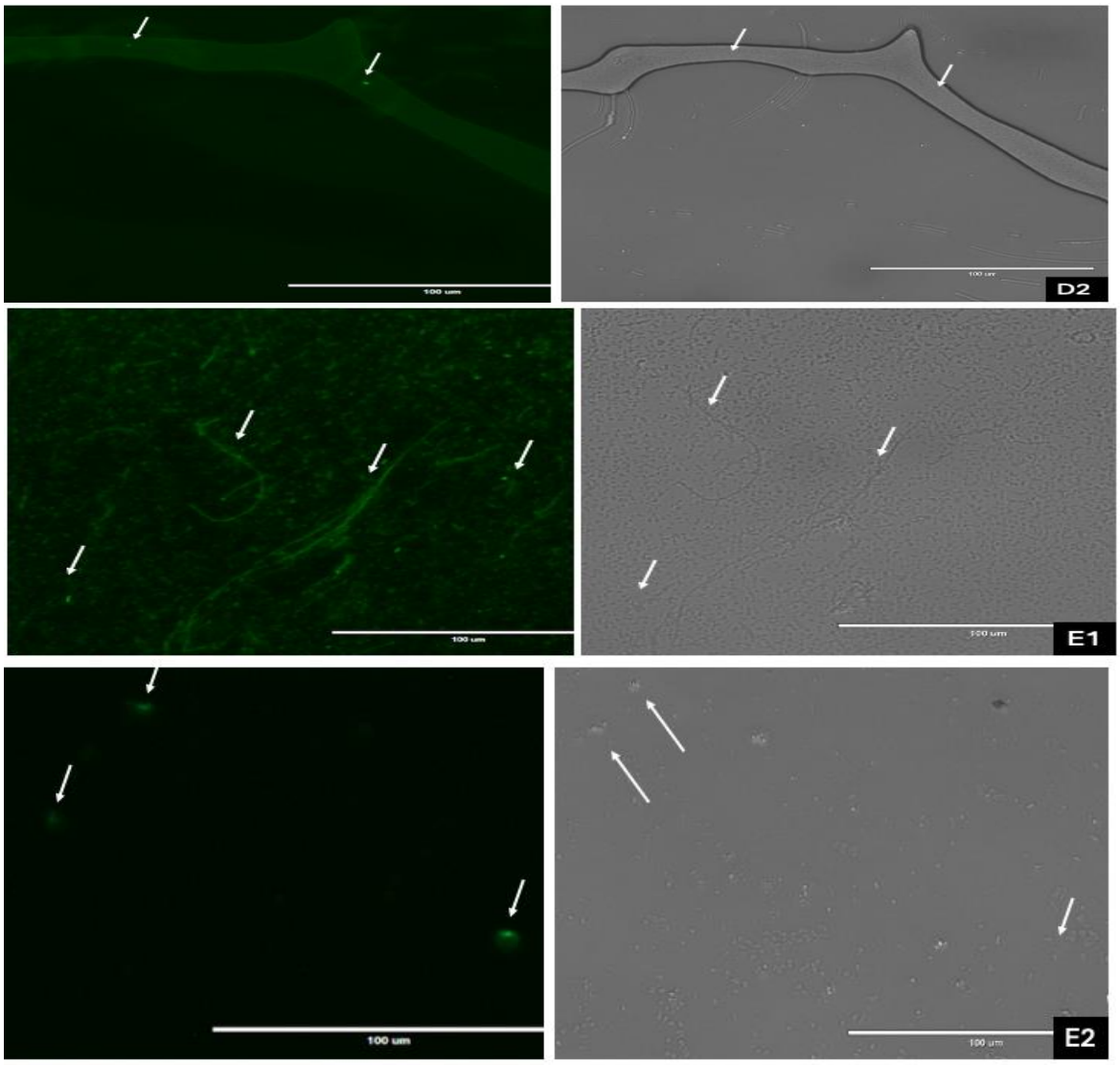


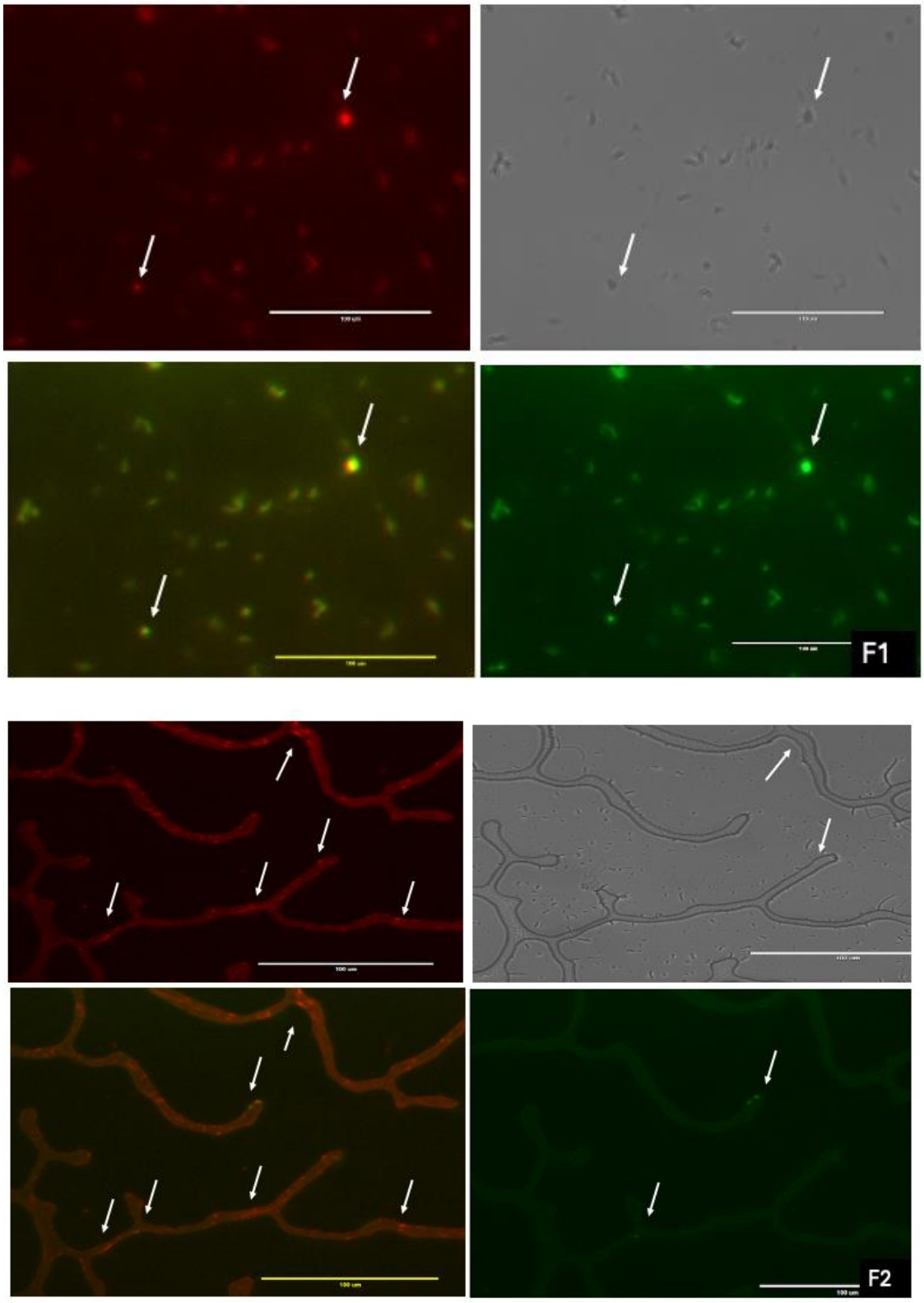
Figure 0-11. Plasmid Maps of Dual-Tagged Rex Constructs with and without linker: RexA::eGFP-RexB::RFP. Plasmid maps showing the C-terminal tagging of RexA and RexB with eGFP and RFP, respectively. The second construct used the Linker sequence between the Rex protein and the tag. Both constructs were cloned into the pPL451 backbone for expression in *E. coli* cells. The dual-tag configuration enables the simultaneous visualization of both proteins, allowing for the assessment of their interactions.

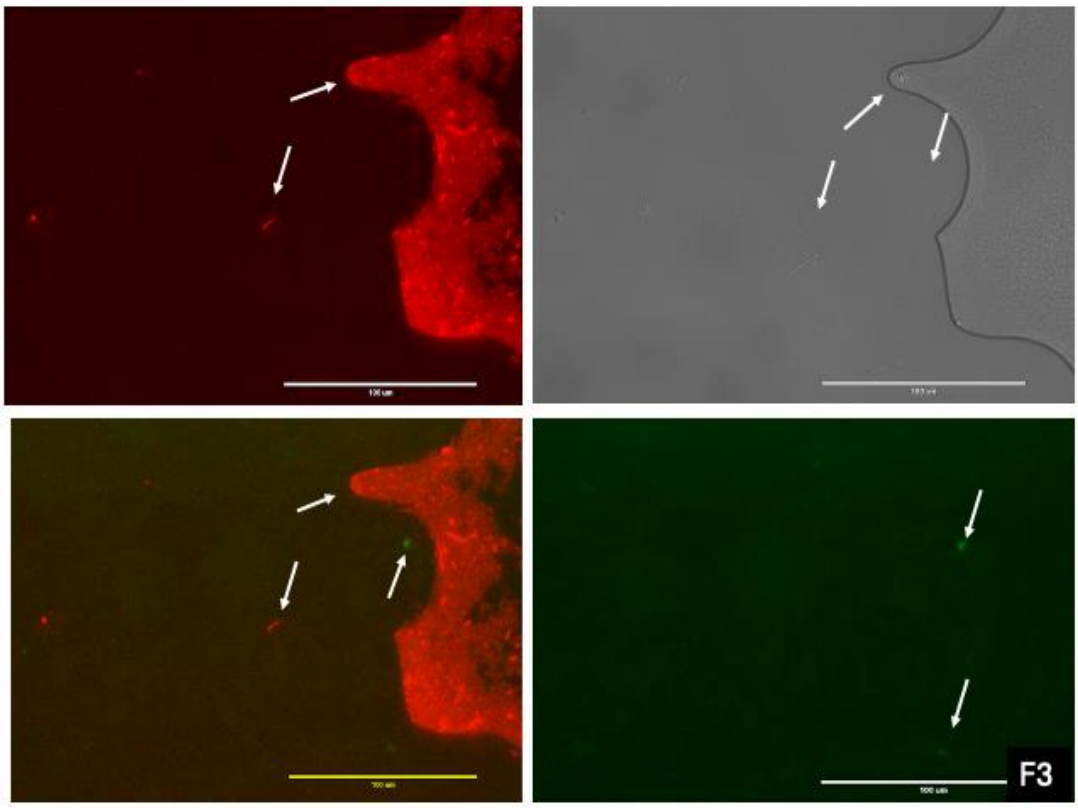
Fluorescence Microscopy of *rex::egfp/rfp* fusion constructs. Representative images showing the expression of Rex fusion proteins tagged with eGFP (green) or RFP (red). The panel includes a collection of Rex-GFP and Rex-RFP constructs expressed in *E. coli*, illustrating differences in signal intensity and distribution across constructs.




100 um
B2
100 um
C1
C2
100 um
D1


100 um
D2
100 um
E1
100 um
100 um
E2
100 um


F1
F2


F3

Appendix D

Tap Tagging and Rex proteins

The Tandem Affinity Purification (TAP tagging) system is one of the best techniques to isolate and purify functional gene product(s)/protein(s) complexes from bacterial cells since the tag addition does not affect the tagged protein function, membrane protein folding, or interfere with the molecular interaction processes and analysis.

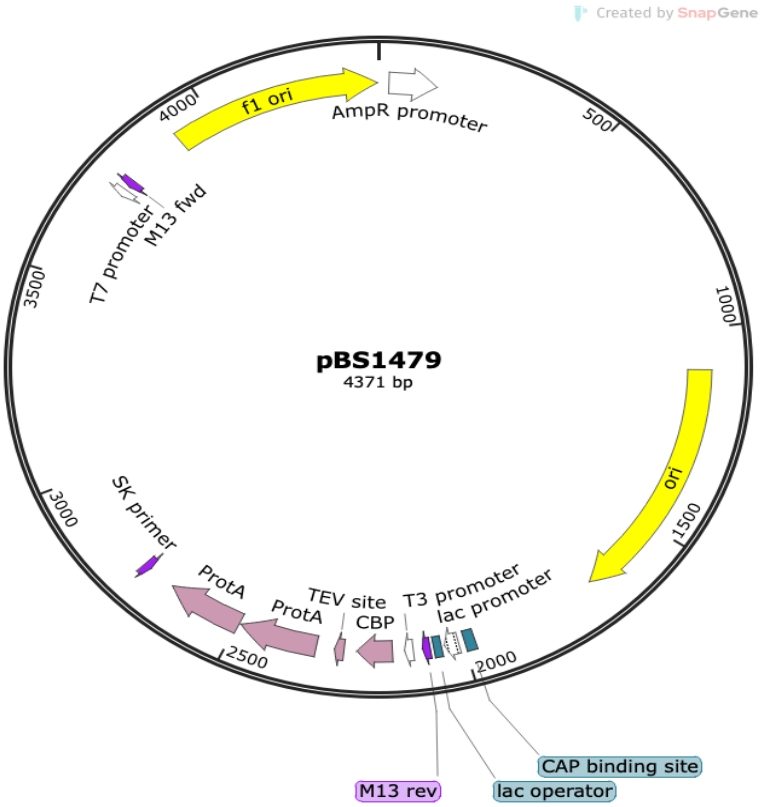


Figure 0-1. Plasmid Map Featuring C-terminal TAP Tagging Cassette. Plasmid map showing a construct designed for C-terminal TAP (Tandem Affinity Purification) tagging of target proteins. The tag consists of two IgG-binding domains from *Staphylococcus aureus* protein A (ProtA) and a calmodulin-binding peptide (CBP), separated by a TEV protease cleavage site. This configuration enables sequential affinity purification and optional proteolytic cleavage for downstream applications. The plasmid was designed using SnapGene

List of Tap-Rex Constructs:

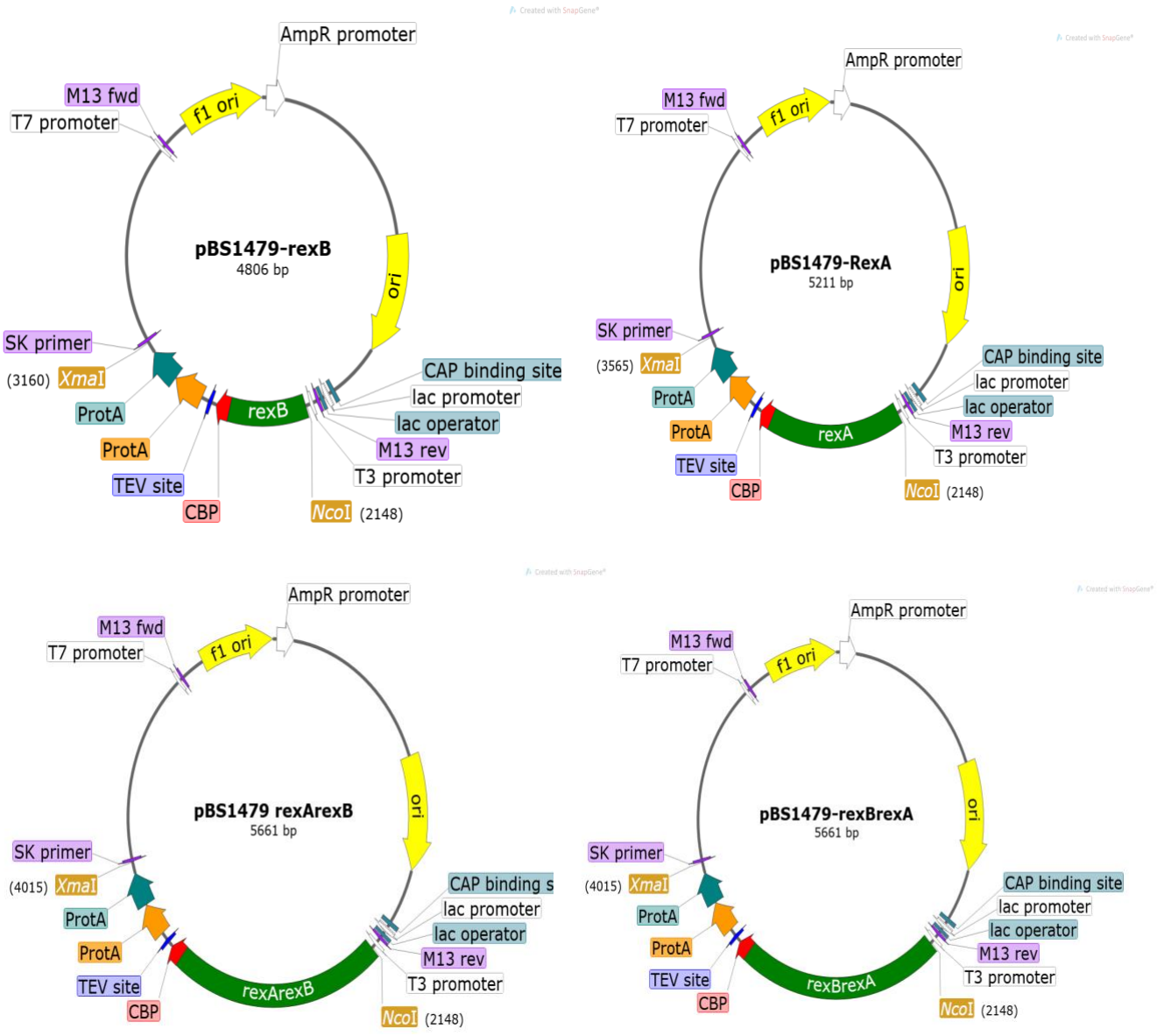


Figure 0-2. Plasmid Maps of Rex Constructs with C-terminal TAP Tags. Plasmid maps showing the design of constructs in which the TAP tag is fused to the C-terminus of various Rex protein configurations: RexA::TAP, RexB::TAP, RexA-RexB::TAP, and RexB-RexA::TAP. All plasmids were designed using SnapGene

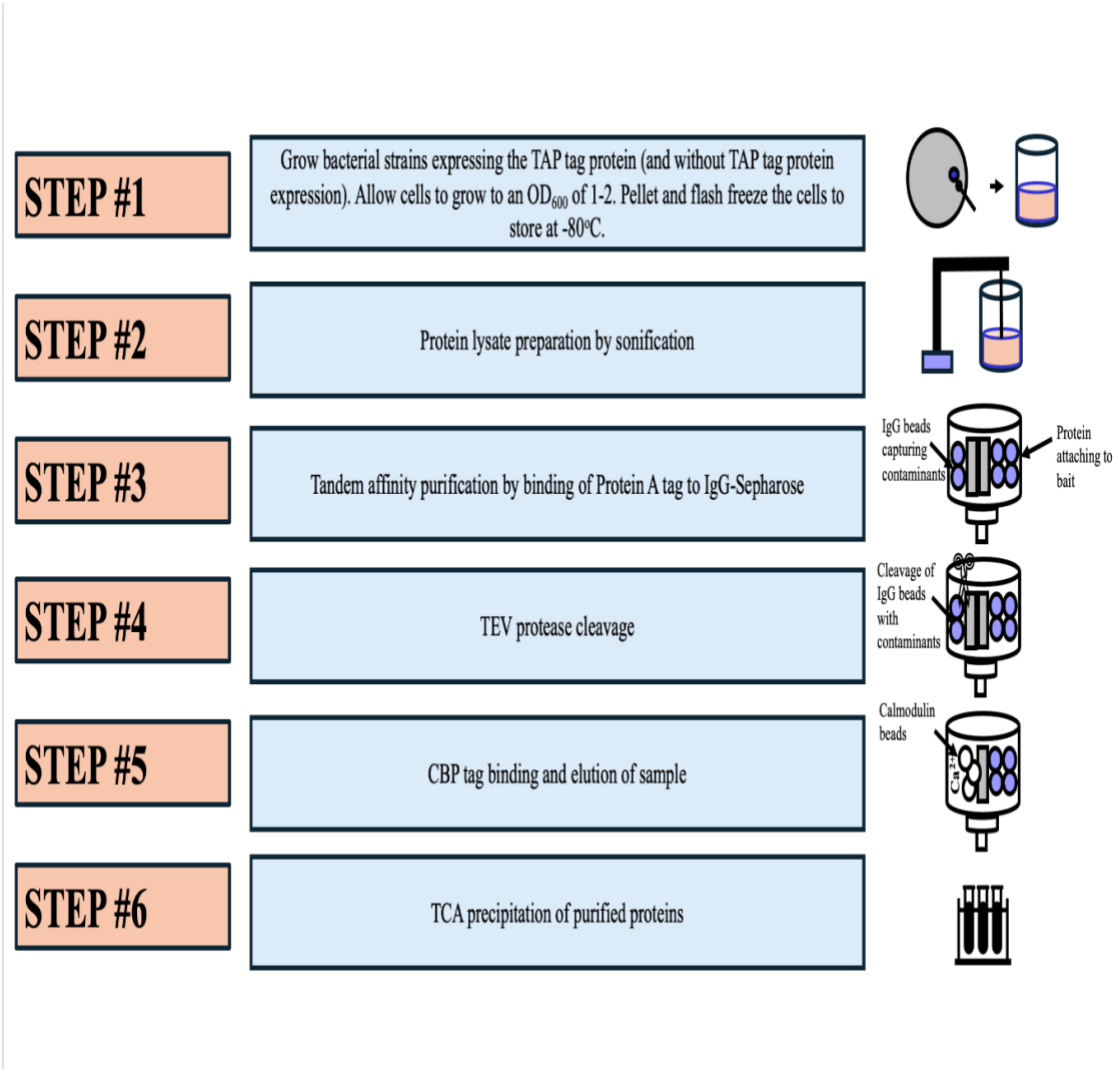
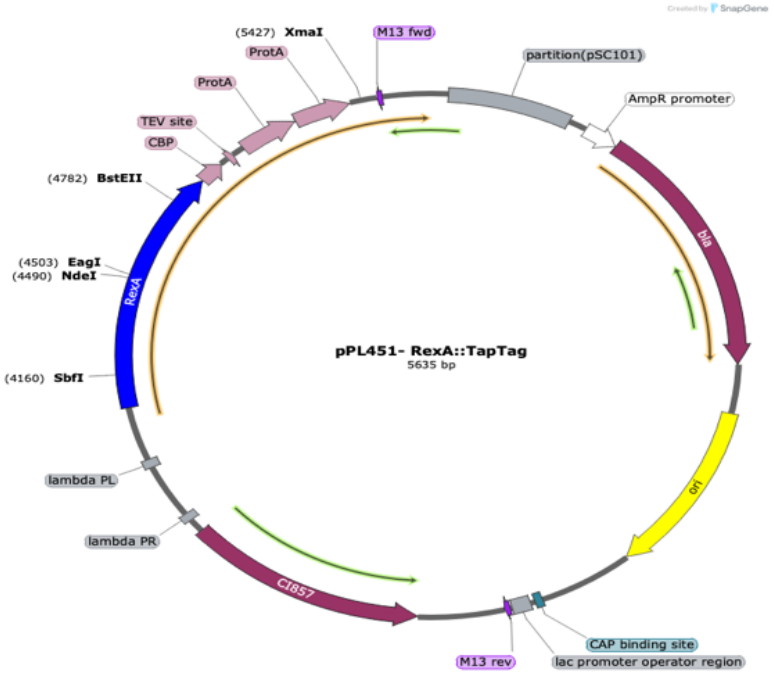
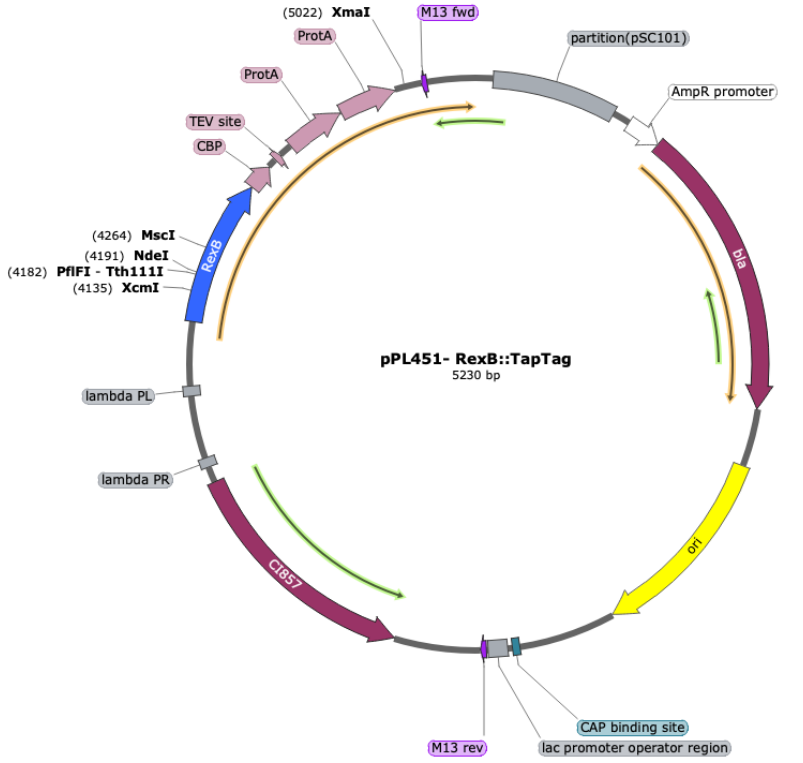


Figure 0-3. Overview of the Two-Step Tandem Affinity Purification (TAP) Process. The schematic illustrates the two-stage TAP purification strategy used to isolate a TAP-tagged protein along with its specific interacting partners. Cells will be prepared and lysed, and the Tap-tagged protein of interest will be isolated via IgG-Sepharose-coated beads. Two rounds of protein affinity washes will be performed, and the Tap-tagged protein and its interactor(s) will be released and incubated with TEV protease to be cleaved from the beads. Any protein(s) still tagged with CBP will be released and can be easily re-washed and eluted. This two-step purification significantly reduces background and enriches for specific protein complexes.

TAP-tagged Rex vectors constructed using the pPL451 expression plasmid:





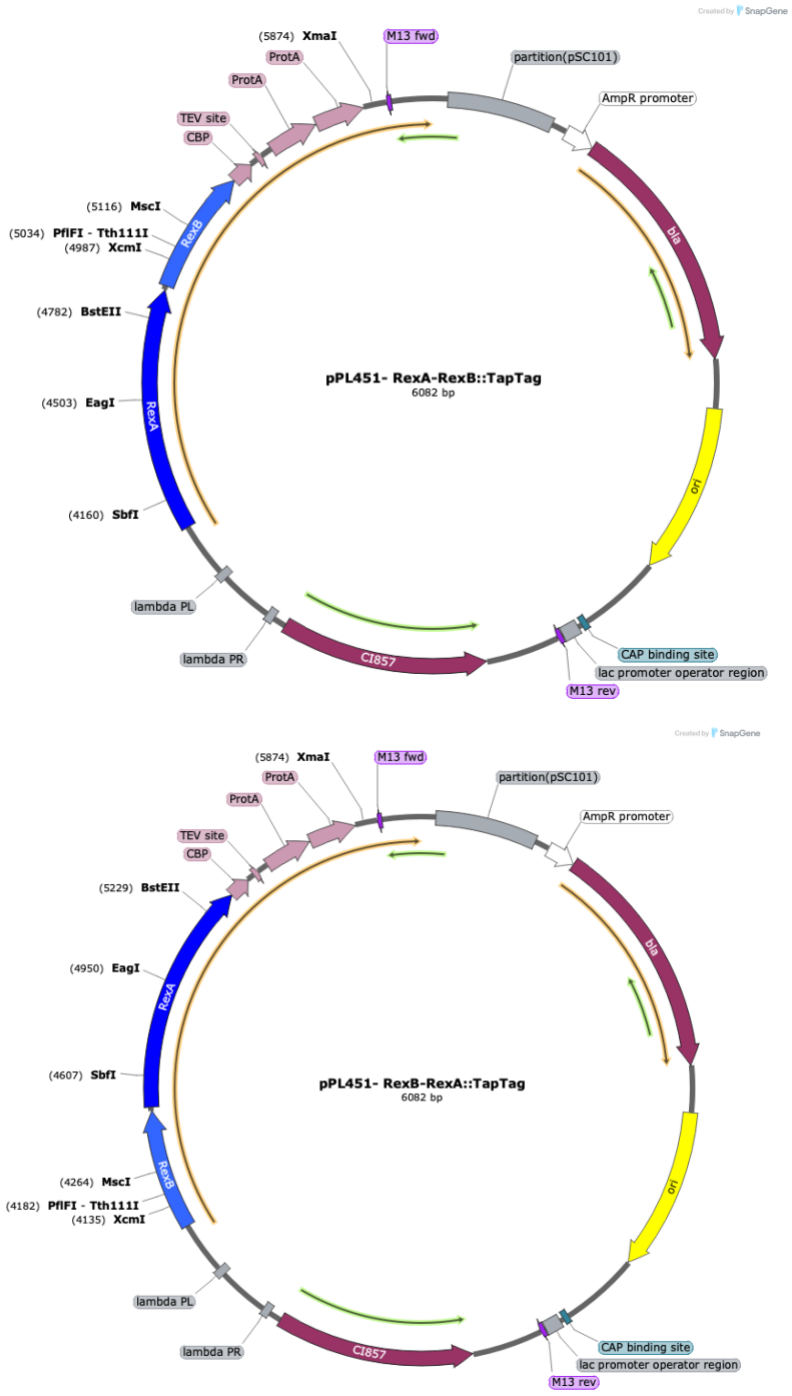


Figure 0-4. Plasmid Maps of TAP-Tagged Rex Constructs using the pPL451 Expression Vector. The Tap-tagged sequence was fused to the C-terminal of the following configurations: RexA::TAP, RexB::TAP, RexA-RexB::TAP, and RexB-RexA::TAP. These constructs enable tandem affinity purification of the tagged proteins and their potential interactors. All plasmids were designed using SnapGene